Characterization and modelling of grit chambers based on particle settling velocity distributions

Thèse

Queralt Plana Puig

Sous la direction de:

Peter A. Vanrolleghem
Paul Lessard

Resumé

Les dessableurs font partie du prétraitement de la plupart des stations de récupération des ressources de l'eau (StaRRE). Ces unités de dessablage servent à protéger les équipements et les procédés aval ainsi qu'à maintenir la performance des traitements primaire et secondaire. Même si ces unités jouent un rôle crucial, un manque criant au niveau des connaissances sur les caractéristiques des particules de « grit » sur leur comportement et sur la modélisation des dessableurs est observé. Ce manque implique une définition incorrecte des particules de « grit », l'inexistence d'un protocole standard d'échantillonnage et de caractérisation des particules autour d'un dessableur, et l'utilisation de modèles simples basés sur un % d'enlèvement constant.

Le premier objectif de la thèse est de développer une méthode de caractérisation de la vitesse de chute des particules, variable clé du processus de sédimentation. Cet objectif peut être divisé en plusieurs sous-objectifs. Un premier sous objectif est de concevoir un protocole d'échantillonnage spécifique pour les sites expérimentaux échantillonnés. Un deuxième sous-objectif est de comparer les méthodes actuellement utilisées pour caractériser les particules de «grit» de proposer une méthode de caractérisation pour les particules mentionnées autour des unités de dessablage.

Le deuxième objectif de la thèse est de développer un modèle dynamique basé sur la distribution de vitesse de chute des particules (DVCP). Le modèle est appliqué à deux différents cas d'études avec différentes conceptions de dessableur (vortex et aéré) et de capacités de traitement. Dans les deux cas, le modèle est calibré et validé avec succès. Il s'agit d'un modèle puissant permettant de prédire la concentration des solides à la sortie des dessableurs et la quantité de solides enlevés (particules de « grit ») en fonction de la dynamique des solides et du débit à l'entrée du dessableur.

Les résultats obtenus dans le cadre de ce doctorat ont permis de présenter une nouvelle approche expérimentale pour la caractérisation des particules de grit ainsi que, pour la première fois, un modèle dynamique des unités de dessablage basé sur la DVCP. Les deux nouveaux outils ont été testés avec succès.

Abstract

Grit chambers can be found at the headworks of most water resource recovery facilities (WRRFs) to protect equipment and the processes downstream and maintain the performance of primary and secondary treatments. Even though they play a crucial role, there is a lack of knowledge on grit characteristics and grit chamber behaviour and modelling. This leads to an improper grit definition, a non-existing standard protocol of sampling and characterization, a non-existing standard protocol to evaluate the performance of the system and only simple models based on a static %-removal.

Given the fact that particle settling is the governing process of grit particle removal, that a vast diversity of sampling and characterization methods is existing, and modelling has been limited to very simple static %-removal based equations, two main objectives in the context of this study are pursued.

The first objective aims for a characterization method taking into account the key parameter of the settling process, i.e. particle settling velocity. It is divided in multiple subobjectives. First, the establishment of a site-specific sampling protocol to obtain representative samples from the water around the studied grit chambers. Then, the currently used methods to characterize grit particles and wastewater are compared and adapted prior to the proposal of a characterization method.

The second objective of this study is to present a new dynamic model based on particle settling velocity distributions (PSVD). The model is tested on two different case studies with different grit chamber designs (vortex and aerated) and treatment capacities. In both cases, the model was successfully calibrated and validated showing a powerful model to predict the solids concentration at the outlet and solids removal at the underflow (i.e. grit particles) of a grit chamber depending on the inlet dynamics.

Summarizing, the results of this PhD study are a new experimental characterization and, for the first time, a dynamic model, based on PSVD. Both new tools have been successfully tested at full-scale.

Contents

List of Figures

List of Tables

List of Symbols and Abbreviations

List of symbols

A	Surface area (m^2)
a	Polygon side (m)
a, b	Coefficients of the logarithmic regression (-)
C	Concentration (g/m^3)
C_d	Drag coefficient ($-$)
D	Depth (m)
d_p	Particle diameter (mm, m)
$F_{inorganic}$	Inorganic fraction of the grit particles (-)
F_{v_s}	Fraction for a given settling velocity (-)
g	Acceleration due to gravity (m/s^2)
H	Height (cm, m)
i	Number of layer (-)
k_{high}	Constant defining how "fast" the curve approaches $F_{v_s}^{min}$
k_{low}	Constant defining how "fast" the curve approaches $F_{v_s}^{max}$
J_{down}	Downward particles flux (g/d)
J_{mix}	Particles flux due to mixing (g/d)
$J_{settling}$	Particles flux due to settling (g/d)
J_{up}	Upward particles flux (g/d)
N_R	Reynolds number ($-$)
Q	Flowrate (m^3/d)
Q_{down}	Downflow (m^3/d)
Q_{air}	Air flow (m^3/d)
Q_{in}	Inlet flow (m^3/d)
Q_{mix}	Flow due to mixing forces (m^3/d)
Q_{out}	Outlet flow (m^3/d)
$Q_{underflow}$	Underflow (m^3/d)
Q_{up}	Upflow (m^3/d)
S_{Ig}	Soluble inorganic solids (mg/L)

S_U	Soluble unbiodegradable solids (mg/L)
T_B	Organic biodegradable solids (mg/L)
T_{Ig}	Inorganic solids (mg/L)
T_U	Organic unbiodegradable solids (mg/L)
t	Time (s, min, h, d)
V	Volume (m^3)
v	Flow velocity (m/s)
v_c	Critical settling velocity (m/s)
v_{rot}	Rotation speed of the paddles (RPM)
v_s	Settling velocity (m/s, m/h)
$v_{s(t)}$	Terminal settling velocity (m/s)
$X_{Ig,Cel}$	Particulate inorganic solids associated to biomass cellular material (mg/L)
$X_{Ig,EC}$	Extracellular particulate inorganic solids (mg/L)
X_H	Substrate for biomass growth and heterotrophic biomass (mg/L)
X_U	Particulate unbiodegradable solids (mg/L)
XS_B	Soluble and particulate biodegradable organic solids (mg/L)

α_D	Dispersion factor ($(m^3/d)^{\beta_D+1}$)
β_D	Mixing behaviour (-)
γ_D	Impact factor of the induced forces (speed of the paddles rotation or air flow) on the mixing flow (-)
$\varnothing$	Diameter (cm, m)
μ	Water dynamic viscosity ($kg/(m \cdot s)$)
Ψ	Sphericity ($-$)
$\rho_{estimated}$	Estimated particle density (kg/m^3)
ρ_p	Particle density (kg/m^3)
ρ_w	Water density (kg/m^3)
υ	Water kinematic viscosity (m^2/s)

List of abbreviations

APHA	American Public Health Association
ASTM	American Society for Testing and Materials
AWWA	American Water Works Association
CCS	Cross channel pumped sampling
CFD	Computational Fluid Dynamics
COD	Chemical oxygen demand
COD_s	Soluble chemical oxygen demand

FIS	Filtered inorganic solids
FVS	Filtered volatile solids
GRS	Grit removal system
HRT	Hydraulic retention time
IS	Inorganic solids
ISS	Inorganic suspended solids
IUWS	Integrated urban wastewater system
IWA	International Water Association
MBR	Membrane bio-reactor
MBBR	Moving bed biofilm reactor
MSL	Model specification language
PSD	Particle size distribution
PSVD	Particle settling velocity distribution
PVC	Polyvinyl chloride
RMSE	Root mean squared error
RPM	Revolutions per minute
SAA	Surface active agents
SBR	Sequential batch reactor
SCADA	Supervisory control and data acquisition
SES	Sand equivalent size
SG	Specific gravity
SOR	Surface overflow rate
TS	Total solids
TSS	Total suspended solids
UFT	Umwelt- and Fluid-Technik
U.S. EPA	United States Environmental Protection Agency
UV	Ultraviolet
UV-VIS	Ultraviolet–visible spectrometry
ViCAs	Wastewater settling velocity
VISS	Vertically integrated slotted sampling
VS	Volatile solids
VSS	Volatile suspended solids
WEF	Water Environment Federation
WEFTEC	Water Environment Federation's Technical Exhibition and Conference
WRRF	Water resource recovery facility

Grit. *Noun [Uncountable]*
1. (stones) very small pieces of stone or sand;
2. (courage) passion and perseverance for long-term and meaningful goals despite difficulty.

Acknowledgements

I can still remember the day I said: "I will never do a PhD!". It was a while before I discovered what working on research actually means. And here I am, writing the acknowledgements of my PhD thesis. At this time, looking back at the long way travelled during my PhD studies, I realize that I have met a lot of interesting and encouraging people and I would like to express my sincere gratitude to all of them.

In the first place, I would like to thank my supervisor Peter A. Vanrolleghem and my co-supervisor Paul Lessard. You make a well-balanced team and I feel very fortunate to have been guided by both of you throughout this journey. Peter, thank you for your endless energy and enthusiasm; for sharing your knowledge and your passion for research; and for teaching me to never give up. Paul, thank you for your precious support based on your deep knowledge and your valuable and generous guidance; for your calmness during turbulent times; and for bringing a realistic point of view (sometimes highly needed). And last but not least, thank you very much for all *fêtes du blé d'Inde* at the Perle Noir around a fire accompanied by the gentle breeze of the St. Laurent river.

Thank you to the members of the jury: Simon Tait, Charles Bott, Majdala Mansour-Geoffrion and Geneviève Pelletier. Your comments and input have not only helped to enhance the content of this PhD Thesis, but they have nurtured me with new ideas and made me think beyond my specific research topics.

I would like to thank the industrial partner of the dessabl*EAU* project, *Veolia Water Technologies Canada*, specially to Aurélien Pauléat, Marc Béliveau, Martin Caspar and Alain Gadbois for sharing their practical knowledge and experience on grit particles characterization and grit chambers design, as well as for the interesting conversations exchanged along these years.

I also want to mention my gratitude to the wastewater treatment services of the Ville de Québec and Ville de Lévis to let me sample, characterize and study the grit chambers of their plants.

I cannot forget to thank all students who collaborated on the dessabl*EAU* project: Jessy, Françoise, Léa and Alicia. Thank you for all the help during the sampling campaigns and the countless hours spent working in the laboratory.

Additionally, I would like to thank all current and former model*EAU* colleagues: Romain, Gamze, Sovanna, Andreia, Niels, Bernard, Elena, Thomas, Cyril, Sylvie, Asma, Julia, Kamilia, Maryam, Feiyi, Jean-David, Sey-Hana, Rania, Coralie, Maxine and Céline. Thank you to the colleagues at the Civil and Water Engineering Stéphanie, Cath, Gaëlle, Greg, Boris, Catherine, Antoine, Sam, Julie, Jasson, Ana, Maxine, MJ, Gonzalo, and all others that I might forgot. To all of you, thank you for the nice shared moments inside and outside the University.

Finally, I would like to thank all my family, specially my parents and brother, for their unconditional support. Despite the thousands of kilometres that have been between us during the last years, could always feel your warmth and love very close.

To all those people (I hope that you will know who you are) who have shared a moment with me along the PhD journey - no matter at which side of the ocean -, who have supported me on this adventure or who have simply listened to me when I needed...

... Thank you. Merci. Gracias. Gràcies.

Foreword

During the PhD thesis, several national and international communications have been made to promote the work into the scientific community, including academic researchers, manufacturers and utilities. In the context of this thesis, three papers have been published to peer-reviewed journals which have been included as chapters in the dissertation. Also, seven oral communications and two poster communications have been presented in conferences. The references of the publications and communications are listed below, together with a specification of the author's contribution.

Peer-reviewed publications

- Q. Plana, J. Carpentier, F. Tardif, A. Pauléat, A. Gadbois, P. Lessard and P.A. Vanrolleghem (2018). Grit particle characterization: Influence of sample pretreatment and sieving method. *Water Science & Technology*, 78(6):1400-1406

  My contribution in this paper as a first author was my participation in the sampling campaigns, the planning and development of the characterization tests, and the evaluation and interpretation of the results. Also, I was the main author of the paper.

- Q. Plana, A. Pauléat, A. Gadbois, P. Lessard and P.A. Vanrolleghem (2019). Characterizing the settleability of grit particles. *Water Environment Research*, 92: 731–739

  For this paper, as a first author, I performed the sampling campaigns, lab tests, and the results interpretation. Also, I was the main author of the paper.

- Q. Plana, P. Lessard and P.A. Vanrolleghem (2020). Dynamic grit chamber modelling: dealing with particle settling velocity distributions. *Water Science & Technology*, 81(8): 1682–1699

  As a first author, my contribution to this paper was the collection of the data presented, and the development and application of the model. Also, I was the main author of the paper.

Conferences and symposiums

Oral communications

- Q. Plana, P. Lessard and P.A. Vanrolleghem (2019). Dynamic grit chamber modelling based on particle settling velocity distribution. In: *IWA Particle Separation Specialist Conference 2019*, Amherst, MA (USA), 13th to 15th November 2019 (accepted)

- Q. Plana, J. Carpentier, L. Gagnon, A. Pauléat, A. Gadbois, P. Lessard and P.A. Vanrolleghem (2018). Grit particle characterization: Study of the settleability. In: *91st Annual Water Environment Federation's Technical Exhibition and Conference (WEFTEC)*, New Orleans, LA (USA), 1st to 3rd October 2018

- Q. Plana, J. Carpentier, L. Gagnon, A. Pauléat, A. Gadbois, P. Lessard and P.A. Vanrolleghem (2018). Study of the settleability of grit particles. In: *32nd Eastern Canadian Symposium on Water Quality Research*, Sherbrooke, QC (Canada), 4th May 2018

- Q. Plana, J. Carpentier, F. Tardif, A. Pauléat, A. Gadbois, P. Lessard and P.A. Vanrolleghem (2017). Grit particle characterization: Influence of sampling and characterization methods. In: *Water and Development Congress & Exhibition 2017*, Buenos Aires (Argentina), 13th to 16th November 2017

- Q. Plana, J. Carpentier, F. Tardif, A. Pauléat, A. Gadbois, P. Lessard and P.A. Vanrolleghem (2017). Influence of sample pretreatment and weather conditions on grit characteristics. In: *90th Annual Water Environment Federation's Technical Exhibition and Conference (WEFTEC)*, Chicago, IL (USA), 2nd to 4th October 2017

- Q. Plana, J. Carpentier, F. Tardif, A. Pauléat, A. Gadbois, P. Lessard and P.A. Vanrolleghem (2017). Influence of sample pretreatment on analysis of grit characteristics. In: *31st Eastern Canadian Symposium on Water Quality Research*, Québec, QC (Canada), 19th May 2017

- J. Carpentier, Q. Plana, F. Tardif, A. Pauléat, A. Gadbois, P. Lessard and P.A. Vanrolleghem (2016). Caractérisation des particules retenues par les unités de dessablage. In: *Symposium sur la Gestion de l'Eau 2016*, Laval, QC (Canada), 9th to 10th November 2016. (In French)

Poster communications

- Q. Plana, P. Lessard and P.A. Vanrolleghem (2019). Dynamic grit chamber modelling: Dealing with particle settling velocity distributions. In: *10th IWA Symposium on Mod-*

elling and Integrated Assessment (Watermatex 2019), Copenhagen (Denmark), 1st to 4th September 2019

- Q. Plana, J. Carpentier, F. Tardif, A. Pauléat, A. Gadbois, P. Lessard and P.A. Vanrolleghem (2017). Propriétés des particules retenues par les unités de dessablage: Influence de la méthode de caractérisation. In: *Symposium sur la Gestion de l'Eau 2017*, Lévis, QC (Canada), 11th to 12th October 2017. (In French)

Introduction

Context of the study

Grit chambers can be found at the headworks in most water resource recovery facilities (WRRFs), between the screens and the primary treatment. Their goal is to remove all settleable grit during dry and peak wet weather flows obtaining a final product suitable for landfill disposal (Wilson et al., 2007). More importantly, they are installed to remove sand particles to avoid equipment abrasion and sand accumulation, thus to protect the equipment and processes downstream and maintain the performance of primary and secondary treatments (Wilson et al., 2007; Tchobanoglous et al., 2014).

Despite their important role, characterization and modelling studies of these units are scarce (Reddy and Pagilla, 2009; Rife and Botero, 2012). On WRRFs, most modelling studies are carried out from the primary influent onwards (e.g. Lessard and Beck (1988) and Ribes et al. (2002) on primary treatment; Henze et al. (2000) on the activated sludge process; and Takács et al. (1991) on secondary clarifiers) since grit chambers have always been considered to have a low impact on the secondary treatment. Thus, the interest for them to be studied has been lower than for other treatment units (Rife and Botero, 2012). However, with the increasing importance of integrated modelling and the optimization of energy costs (i.e. for aeration), to operate grit chambers, the interest of grit chambers is also increasing.

As a result, the characteristics of particulate pollutants at the inlet, outlet and underflow of grit chambers are rarely documented and their removal efficiency is questioned since grit is found accumulated in downstream processes (Andoh and Smisson, 1996; Pitman, 1999; Reddy and Pagilla, 2009; McNamara et al., 2012). This lack of knowledge leads to an improper grit definition, a non-existing standard protocol of sampling and characterization, and a non-existing standard protocol to evaluate the removal performance of the system (Rife and Botero, 2012). In addition, modelling has been limited to very simple static %-removal based models.

To design grit chamber units, grit has traditionally been defined as follows: *Grit particles consist of sand, gravel, cinders or other heavy materials with a diameter larger than 0.21 mm*

(65 mesh[1]) and a specific gravity (SG) of 2.65 g/cm^3 (Finger and Parrick, 1980; Tchobanoglous et al., 2003; U.S. EPA, 2004). However, recent studies have questioned whether the assumption of a 0.21 mm particle with a SG of 2.65 g/cm^3 is adequate to design grit chambers since this specific gravity only holds for clean sand. Evidently, grit patricles are not just clean sand as they contain a considerable organic fraction and are coated with grease (Barter and Sherony, 2011; Pretorius, 2012; Herrick et al., 2015).

Some authors, like Reddy and Pagilla (2009), Herrick et al. (2015) and Gerges et al. (2018), suggest the settling velocity and the clean sand equivalent size (SES) as new ways to characterize grit particles. The *Grit Sampling and Characterization* Task Force of the Water Environment Federation (WEF) recommended that: *"The definition of grit for the purpose of sampling be the settling velocity of the grit particle as it exists in the raw wastewater of the appropriate size that is intended to be removed by the system being sampled"*. This definition has been included in the *"Guidelines of Grit Sampling and Characterization"* book published by WEF (2016).

In view of the lack of research in this field, this PhD project called dessablEAU (grit chamber, "dessableur" in French), aims to meet the expectations of municipalities and industry by developing (i) a reliable characterization protocol of the water quality around a grit chamber including a sampling procedure that considers the challenge of vertical heterogeneity in pollutant flows, and (ii) a methodology for analyzing the samples for relevant variables of the system studied, such as the particle settling velocity distribution. Also, the project will develop (iii) a conceptual dynamic grit chamber model (adapted for the most used types of grit chamber: aerated and vortex systems) to model the water quality of the effluent and underflow in terms of total suspended solids (TSS).

Then, a variety of operating scenarios can be tested with the goal of unit operation optimization and design. Also, organic matter removal can be reduced so it can be recovered in the primary clarifier and be sent to digestion. In addition, modelling the whole WRRFs can be significantly improved because the inflows of the primary and secondary treatments, as well as of the sludge treatment system can be better described and predicted.

Contents of this PhD thesis

This thesis has been structured in seven main chapters. First, in Chapter 1, an overview is given of grit removal systems and the processes taking place, the characteristics of the grit particles accompanied with the methods that are currently in use to sample and characterize them and, finally, the existing models for grit chambers. This literature review leads to the

[1] The mesh size is the number of openings in one inch screen (Reddy and Pagilla, 2009).

problem statement and the specification of the objectives in the context of this PhD thesis (Chapter 2).

The methods and material used in the context of this study are presented in Chapter 3. The case studies are detailed including the main WRRF characteristics, the type of grit chamber and their dimensions and the type of sewer system. Also, the equipment used to sample, characterize and monitor the water quantity and quality around the grit chamber are described. Finally, the software used to model the grit chamber, i.e. WEST©, is presented briefly.

Chapter 4 presents the results obtained from the conducted experimental comparison of sampling equipment and the sampling strategy to implement. From these results, a sampling equipment was selected and a sampling strategy was implemented to collect samples around the studied grit chambers for further tests.

The characterization of the particles around a grit chamber unit has been divided into two different chapters. The first chapter (Chapter 5) presents the methods compared to determine the particle size distribution (PSD) from the grit particles collected at the grit bin. These methods not only have been compared in terms of particles size, but also in terms of particle composition and density. Furthermore, the impact of the weather conditions on the mentioned characteristics is shown.

The second chapter related to particle characterization (Chapter 6) consists in the comparison of two different methods to obtain the particle settling velocity distribution (PSVD) adapted specifically for fast settling particles such as grit particles. In addition, how the settling velocity distribution varies with the TSS concentration is also detailed.

The characterization of the particles around the studied unit, the study of the hydraulics into the vortex grit chamber, and the monitoring of the dynamics of the TSS, allowed developing a conceptual model to describe the vortex grit chamber behaviour as presented in Chapter 7. This model is based on PSVD and was inspired by the work of Bachis et al. (2015) on primary clarifiers. The calibration of each model parameter together with the validation tests are presented.

The conceptual model has also been adapted for the studied aerated grit chamber. The model calibration and validation results are shown in Chapter 8.

Finally, the main conclusions in the context of this PhD study together with some recommendations for future work are described in Chapter 8.7.

Chapter 1

Literature review

This chapter provides an overview of the state-of-the-art literature related to grit chamber characterization and modelling. First, a brief introduction is presented about the wastewater treatment with special focus on the grit removal step. Then, the related grit literature is presented including grit properties, characterization and sampling methods, grit removal systems, and grit chamber modelling.

1.1 Wastewater treatment

Wastewater generated by municipalities and communities is generally collected through catchments and sewer systems and transported to water resource recovery facilities (WRRFs) to be treated before discharged to the receiving environment (e.g. rivers) (see Figure 1.1). At WRRFs, wastewater is treated with unit operations (physical treatment units) and unit processes (chemical and biological treatment units) (Tchobanoglous et al., 2014). Those units can be regrouped in different levels as described by Tchobanoglous et al. (2014) and summarized in Table 1.1.

According to the classification presented in Table 1.1, grit chambers are considered as part of the preliminary treatment. They can be found in most of the WRRFs between the screens and the primary treatment (see example in Figure 1.1). The specific goal of this unit is to remove all settleable grit during dry and wet weather flows obtaining a final product suitable to landfill disposal (Wilson et al., 2007). Moreover, they have a long-term important role: protect the equipment and processes downstream and maintain the performance of primary and secondary treatments (Morales and Reinhart, 1984; Pitman, 1999; U.S. EPA, 2004; Reddy and Pagilla, 2009). For example, Bennett (1989) and Flanagan (2014) identified that grit can settle in wells, chambers and channels, harm pumps and pipelines, and accumulate in digesters reducing their efficiency and increasing their maintenance costs (see Figure 1.2).

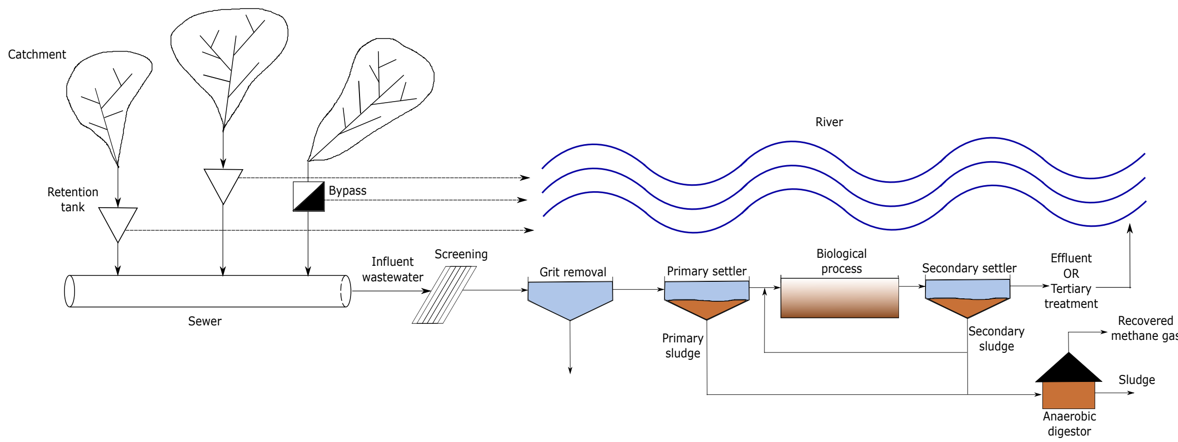

Figure 1.1: Scheme of an integrated system including the catchments, sewer system, a conventional WRRF and the river.

Table 1.1: Levels of wastewater treatment process (from Tchobanoglous et al. (2014)).

Treatment stage	**Description**
Preliminary	Gross solids removal like rags, sticks, floatables, grit, and grease that can cause maintenance or operational problems with the treatment operations, processes, and ancillary systems.
Primary treatment	Removal of a portion of the suspended solids and organic matter from the wastewater.
Advanced primary	Enhanced removal of suspended solids and organic matter from the wastewater. Typically accomplished by chemical addition or filtration.
Secondary	Removal of biodegradable organic matter (in solution or suspension) and suspended solids. Disinfection is also typically included in the definition of conventional secondary treatment.
Secondary with nutrient removal	Removal of biodegradable organics, suspended solids, and nutrients (nitrogen, phosphorus, or both nitrogen and phosphorus).
Tertiary	Removal of residual suspended solids (after secondary treatment), usually by granular medium filters, cloth filters, or microscreens. Disinfection is also typically a part of tertiary treatment. Nutrient removal is often included in this definition.
Advanced	Removal of dissolved and suspended materials remaining after normal biological treatment when required for various water reuse applications.

In addition, grit removal is becoming more crucial with the development of new advanced treatment processes like membrane bio-reactors (MBRs) or other high-intensity and high-efficiency units since they have become more sensitive to the presence of inert solids (Mansour-

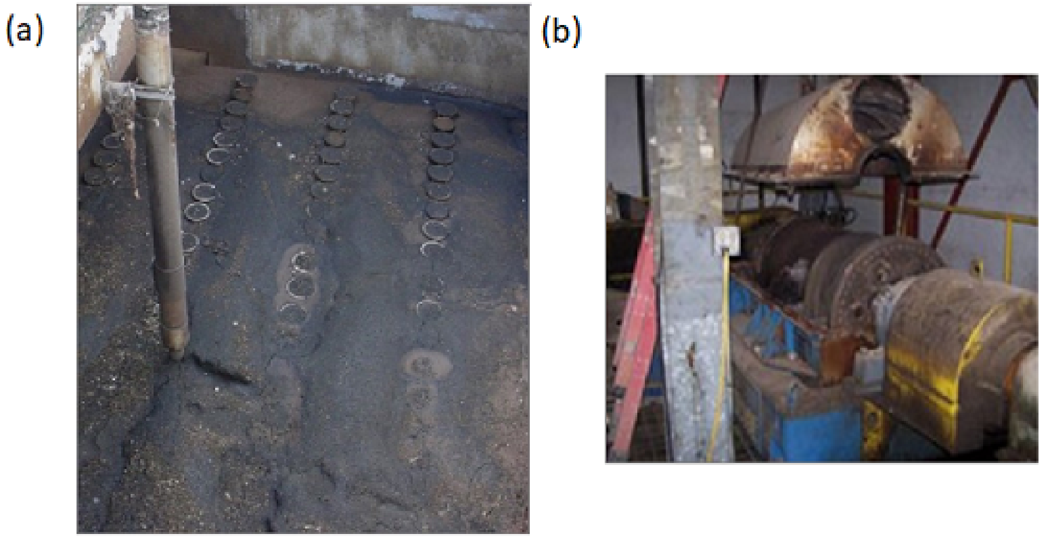

Figure 1.2: Examples of issues caused by grit: (a) grit accumulation in aerated reactors, and (b) harmed equipment due to grit abrasion (Image courtesy of Hydro International plc (2019)).

Geoffrion et al., 2010; Andoh, 2015). Thus, grit removal systems should be optimally designed and operated (WEF, 2010; Herrick and Sherony, 2017).

1.2 Grit removal systems

To better understand the grit removal process and its limitations, the components of a grit removal system and the removal principle are presented in this section.

1.2.1 Components of grit removal systems

Grit removal systems (GRSs) not only consist of grit chamber units. With the goal to obtain a final product suitable for landfill disposal, GRSs are built with three different unit processes as presented in Figure 1.3 (Wilson et al., 2007). The first step of the process is the separation of the settleable grit particles by gravity from the raw wastewater (Hendricks, 2016). This is carried out in the grit chamber and it typically removes about 5 - 10 % of the inlet TSS (Qasim, 1999). Generally, grit chambers have been designed to remove 95 % of particles larger than 0.21 mm with a density of 2650 kg/m^3 (Finger and Parrick, 1980; U.S. EPA, 2004; Andoh, 2015).

Washing and dewatering units are added to process the grit slurry retained by the grit chamber and are carried out in a classifier (see Figure 1.4). First, the slurry is washed to remove organic material collected with grit. The aim is that it reduces volatile solids from 50 % to 20 %, and

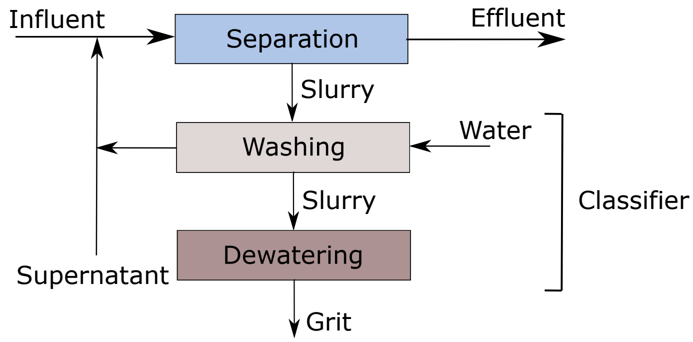

Figure 1.3: Grit removal system unit processes (adapted from Wilson et al. (2007)).

retains at least 95 % of settleable grit (Tchobanoglous et al., 2014). Second, the free water contained in the cleaned grit is removed (Wilson et al., 2007; WEF, 2010). The dewatering step has the objective to reach a total solids concentration of 60 % and retain at least 95 % of settleable grit (Wilson et al., 2007). Finally, clean grit is collected and stored in a container, and the supernatant with the recovered volatiles, is recycled to the inlet of the grit chamber. Normally, grit collected into the grit sump is transported to hydrocyclones and/or pumps to agitate the slurry sufficiently to wash the grit. Then, the grit particles are transported to a submerged rake or inclined screw that allows separation of the volatiles from the grit and also dewatering the grit (Wilson et al., 2007; Tchobanoglous et al., 2014).

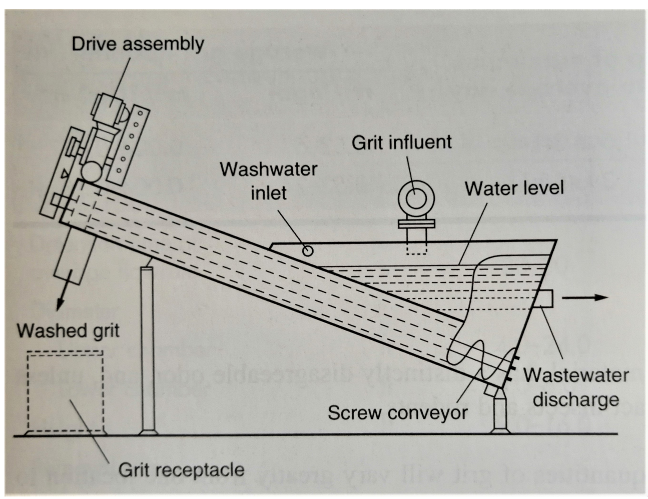

Figure 1.4: Schematic of a grit classifier unit (Tchobanoglous et al., 2003)).

1.2.2 Principle of gravity separation

In wastewater treatment, several unit processes are based on sedimentation. According to Tchobanoglous et al. (2014), four different types of settling can be found in a treatment chain:

- *Type I settling: Discrete settling.* It is the process where the particles are found at low concentrations and settle by gravity in a constant acceleration field. Also, particles settle individually without interaction with neighbouring particles.

- *Type II settling: Flocculent settling.* It is the process where particles at a low concentration, coalesce, or flocculate, during settling. Flocculation causes the particles to increase in mass and settle at a faster rate.

- *Type III settling: Hindered or zone settling.* It is the process in which at an intermediate concentration, interparticle forces are present and hinder the settling of neighbouring particles. The mass of particles tends to settle as a unit with individual particles remaining in fixed positions with respected to each other.

- *Type IV: Compression.* It is the process in which the concentration of particles is so high that settling can only occur through compression of the structure.

More precisely, because of the characteristics and the concentration of the particles to be removed in a grit chamber, two different types of settling exist in the mentioned unit: the discrete and the flocculent settling (Qasim, 1999; Tchobanoglous et al., 2014), with the former the predominant mechanism (Qasim, 1999; WEF, 2016).

For discrete settling, particle behaviour can be evaluated through the sedimentation laws of Newton and Stokes (Qasim, 1999; Tchobanoglous et al., 2014). Newton's law assumes that the terminal particle velocity equals to the gravitational force of the particle to the drag force. This law can be translated to the equation (Tchobanoglous et al., 2014):

$$v_s = \sqrt{\frac{4 \cdot g}{3 \cdot C_d} \cdot \left(\frac{\rho_p - \rho_w}{\rho_w}\right) \cdot d_p} = \sqrt{\frac{4 \cdot g}{3 \cdot C_d} \cdot (SG_p - 1) \cdot d_p} \tag{1.1}$$

where v_s is the terminal settling velocity of the particle, g the acceleration due to gravity, C_d the drag coefficient, ρ_p the density of the particle, ρ_w the density of water, d_p the diameter of the particle, and SG_p the specific gravity of the particle.

The drag coefficient varies with the characteristics of the particle and the flow regime around the particle (i.e. laminar or turbulent conditions). The coefficient can be estimated through Equation 1.2:

$$C_d = \frac{24}{N_R} + \frac{3}{\sqrt{N_R}} + 0.34 \tag{1.2}$$

where N_R is the Reynolds number, defined as:

$$N_R = \frac{v_s \cdot d_p \cdot \rho_w \cdot \Psi}{\mu} = \frac{v_s \cdot d_p \cdot \Psi}{\upsilon} \tag{1.3}$$

where μ is the water dynamic viscosity, υ the water kinematic viscosity, and Ψ the sphericity factor of the particle. The sphericity factor is defined as the ratio of the surface area of a sphere with the same volume as the particle studied itself to the surface area of the particle. Generally, the sphericity factors are between 1 for spheres and 0.7 for crushed sand.

Depending on the regime surrounding a particle, Equation 1.1 can be simplified.

Settling in the laminar regime. Laminar regime is considered when the Reynolds number is lower than 1 and the viscosity is the governing force on the settling process. Thus, the first term in Equation 1.2 dominates the others, leading to Stokes' Law (Equation 1.4).

$$v_s = \frac{g \cdot (\rho_p - \rho_w) \cdot d_p^2 \cdot \Psi}{18 \cdot \mu} = \frac{g \cdot (SG_p - 1) \cdot d_p^2 \cdot \Psi}{18 \cdot \upsilon} \tag{1.4}$$

Settling in the turbulent regime. In case of the turbulent regime ($N_R > 2000$), the predominant forces are the inertial ones. Thus, the first two terms in the Equation 1.2 have a low impact, and the drag coefficient can be considered equal to 0.4. Then, the equation derived from 1.1 can be presented as follows:

$$v_s = \sqrt{3.33 \cdot g \cdot \left(\frac{\rho_p - \rho_w}{\rho_w}\right) \cdot d_p} = \sqrt{3.33 \cdot g \cdot (SG_p - 1) \cdot d_p} \tag{1.5}$$

Settling in the transition regime. In this regime, Equation 1.2 has to be used in its complete form. Hence, to estimate the settling velocity, an iterative process has to be followed combining Equations 1.1, 1.2 and 1.3.

Furthermore, for settling tank design, a critical particle settling velocity is established as a cut-off point (Wilson et al., 2007). It means that all particles which settle at a higher settling velocity than the critical settling velocity, will settle in the basin (Sprenger et al., 2016). Moreover, this critical settling velocity depends on the flowrate of the unit as presented in equation:

$$v_c = \frac{Q}{A} \tag{1.6}$$

where v_c is the critical particle settling velocity, Q the flowrate, and A the surface of the sedimentation basin.

Hence, the critical particle settling velocity is also called the surface overflow rate (SOR) (Wilson et al., 2007). Also, this critical settling velocity can be determined through the depth (D) and the hydraulic retention time (HRT) of the basin, like:

$$v_c = \frac{D}{HRT} \tag{1.7}$$

1.3 Grit characteristics

According to Wilson et al. (2007), the main goals of a grit removal system have been set to: (i) remove all depositable grit during peak wet weather flow, and (ii) produce a final product suitable for landfill disposal. However, the characteristics of grit and the final product to be obtained are not specified and there is still no consensus.

In this section, an overview of the current literature related to the grit definition and its physical characteristics is presented.

1.3.1 Definitions

Over the years, several grit definitions have been proposed but there is still no consensus among the scientific community. However, an evolution has recently been observed together with an improvement of the knowledge on grit characteristics. An early definition was proposed by Camp (1942):

"Grit includes sand, silt, coal dust, coffee grounds, fruit seeds, etc. Much of the grit is organic, but if it is not putrescible it may be disposed of readily as fill."

Despite the early definition of Camp (1942), considering that an important fraction of grit particles is organic, late definitions considered grit as inorganic and non-putrescible. For example, Finger and Parrick (1980) and the 4^{th} edition of Metcalf & Eddy book (Tchobanoglous et al., 2003) applied the definition:

"Grit consists of sand gravel, cinders, or other heavy solid materials that have subsiding velocities or specific gravities, susbstantially greater than those of organic putrescible solids in wastewater."

From the consideration that grit is mainly inorganic, other definitions were suggested based on particle size and specific gravity (SG). For example, U.S. EPA (2004) proposed:

"Grit is traditionally defined as particles larger than 0.21 mm (65 mesh) and with a SG of greater than 2.65."

Or even a more detailed definition was included in the last edition (5^{th} edition) of the Metcalf & Eddy book (Tchobanoglous et al., 2014):

"Grit consists of inorganic settleable solids ranging in size from 0.05 to 1 mm with settling characteristics similar to clean, spherical silica sand with a SG of 2.65 and a particle size predominantly larger than 0.21 mm."

However, the same Tchobanoglous et al. (2014) questioned this definition since the expected performance did not coincide with the experimentally observed one, resulting in additional costs for maintenance and operation.

Lately, considering that grit is not only inorganic particles, and the organic fraction of the grit particles is significant, the Water Environment Federation's (WEF) Grit Task Force suggested a new definition based on the particle settling velocity concept (WEF, 2016):

"Assuming the grit system is designed to remove 100 μm grit, sampling methods must capture solids with a settling velocity of at least 100 μm clean grit, and preferably less if it is agreed that grit $\geq$ 100 μm in its raw state can have settling characteristics of less than 100 μm grit. For this reason, it is recommended that the definition of grit for the purpose of sampling be the settling velocity of the grit particle as it exists in the raw wastewater of the appropriate size that is intended to be removed by the system being sampled."

In addition to the definitions presented, when considering the importance of the particle settling velocity for grit chambers design, some authors also presented the typical settling velocity used as a cut-off point for the unit design. For example, Qasim (1999) mentioned that a typical settling velocity for a particle of 0.21mm-diameter is 72 m/h, Tchobanoglous et al. (2014) presented that for particles with a diameter of 0.21 mm the typical settling velocity is 69 m/h wherever for particles of 0.15mm-diameter it is 45 m/h. Hendricks (2016) stated that the typical settling velocity is 76 m/h for a particle with a diameter of 0.2 mm.

Seeing these definitions, in the context of this thesis, grit has been considered as particles that are a mix of inorganic and organic fractions and are characterized by high settling velocities (for example, $v_s > 70\ m/h$, which is a settling velocity similar to the ones presented by Qasim (1999) and Tchobanoglous et al. (2014)).

1.3.2 Physical characteristics

The solids concentration, flux and characteristics in sewer systems and arriving at WRRFs vary with time, mainly depending on the type of collection system, domestic and industrial discharges to the collection system and weather conditions (Tchobanoglous and Schroeder, 1985; Lessard and Beck, 1988; Ashley et al., 2005). Hence, these variations can be observed as well on the grit characteristics and their quantities.

According to the literature review, the quantities of grit collected at WRRFs are variable not only between WRRFs, but also between studies. For example, Qasim (1999) mentioned that grit quantities can vary between 0.005 and 0.2 L/m^3; WEF (2010), after a survey done on 328 U.S.A. WRRFs, presented that the collected quantities can range from 0.00037 to 0.148 L/m^3, and lately, Tchobanoglous et al. (2014) made a difference between separate and combined sewer systems: the quantity removed from separate sewer systems can vary between 0.004 and 0.037 L/m^3, and in combined sewer systems it can vary between 0.004 and 0.2 L/m^3.

As understood from the grit definitions, grit consists in particles with inorganic and organic fractions such as sand, gravel, cinders, eggshells, bone chips, coffee grounds, fruit seeds, etc. (Camp, 1942; Tchobanoglous et al., 2014). Grit travels along the collection system before it reaches the WRRF and grit particles can thus agglomerate with surface active agents (SAAs) or other organic matter, modifying this the settling characteristics (Tchobanoglous et al., 2014; WEF, 2016; Judd et al., 2017).

Settling characteristics change with particle size, density and shape (see Equation 1.3). For example, the density of grit particles depends on their composition and it varies over a wide range and, as mentioned above, it is site specific (WEF, 2010; Desai et al., 2014). Tchobanoglous et al. (2014) presented that the moisture content can vary between 13 and 65 %, and the organic content between 1 and 56 %. This leads to a wide range of particle densities. For example, WEF (2016) noticed that grit density can range between 1100 and 2650 kg/m^3 (i.e. with specific gravities between 1.10 and 2.65) and Qasim (1999) mentioned that it can be between 1500 and 2700 kg/m^3 (i.e. with SGs between 1.50 and 2.70).

Influence of the collection system

Generally, a sewer system to collect wastewater should be designed to assure flow velocities sufficient to avoid solids deposition in the sewers (Ashley et al., 2005; Rippon et al., 2010). However, solids accumulation is inevitable, because of the dynamics and variable nature of sewer system inlet flows and characteristics (Ashley et al., 2005). Thus, the accumulation and flow dynamics create an impact on the solids at the inlet of WRRFs.

The characteristics of the solids at the inlet of a WRRF depend on the characteristics of the collection system and the origin of the solid sources (Ashley et al., 2005; Reddy and Pagilla, 2009). Qasim (1999), Ashley et al. (2005), Reddy and Pagilla (2009), Rippon et al. (2010) and WEF (2016) pointed out characteristics such as the type of the collection system (i.e. separate (sanitary) or combined (sanitary and storm) systems), the size of sewer system, the age of the system, the status of the system, the number of pumping stations, the presence of in-line units (e.g. sewer grit removal, retention tanks, stormwater tanks, etc.), the topography (e.g. slope within the collection system), maintenance activities in the collection system, the characteristics of the soil, and the level of the water table.

Related to the origin of the solids, Ashley et al. (2005) identified five different sources which can have an impact on the solid characteristics:

- *The atmosphere.* The solids from the atmosphere consist in fine dust particles and aerosols from activities like incineration, automobile traffic, industry, etc. which will precipitate with the rain.
- *The surfaces of the catchment.* The solids are washed off from different surfaces on the catchment like roofs, streets or gullies.
- *Domestic sewage.* These solids mainly consist in sanitary solids, gross solids (e.g. paper, rags or other sewage litter), and kitchen sink organics.
- *Industrial and commercial activities.* The characteristics of these solids are highly variable and depend on the type of the activity carried out.
- *The environment and processes inside the sewer system.* Solids derive from infiltration and/or sewer decay or degradation and wrong connections into the sewer system.

Influence of the weather conditions

Solids variation can occur in short periods of time and is complex to predict, especially under wet weather conditions and de-icing periods (Ashley et al., 2005; He et al., 2012).

For example, in Figure 1.5a, flow variations can be observed at the inlet of a WRRF. The first four days depict the typical diurnal flows pattern under dry weather conditions with a peak early in the morning because of the morning loading increase as part of the living habits. The last five days in Figure 1.5a show higher peak flows at the inlet of the WRRF because of rain events (Verbanck, 1995). These rain events affect the conductivity and the suspended solids significantly (see Figure 1.5b). After a rain event, the observed conductivity is reduced due to dilution (Verbanck, 1995). The concentration of suspended solids increases, especially for the first rain event and this behaviour is called the first flush effect due to the solids accumulation on the catchments and in the sewer system (Gupta and Saul, 1996; Ashley et al., 2005; Verbanck, 1995).

Generally, under dry weather conditions, flow velocities may not be sufficiently high to keep all solids in suspension and carry them to the WRRF; hence, heavier solids tend to settle and accumulate in the sewers (Desai et al., 2014). Thus, under dry weather conditions, finer solids with lower settling velocities would be expected in the raw wastewater samples in comparison to samples collected under wet weather conditions (Gromaire et al., 2008; Krishnappan et al.,

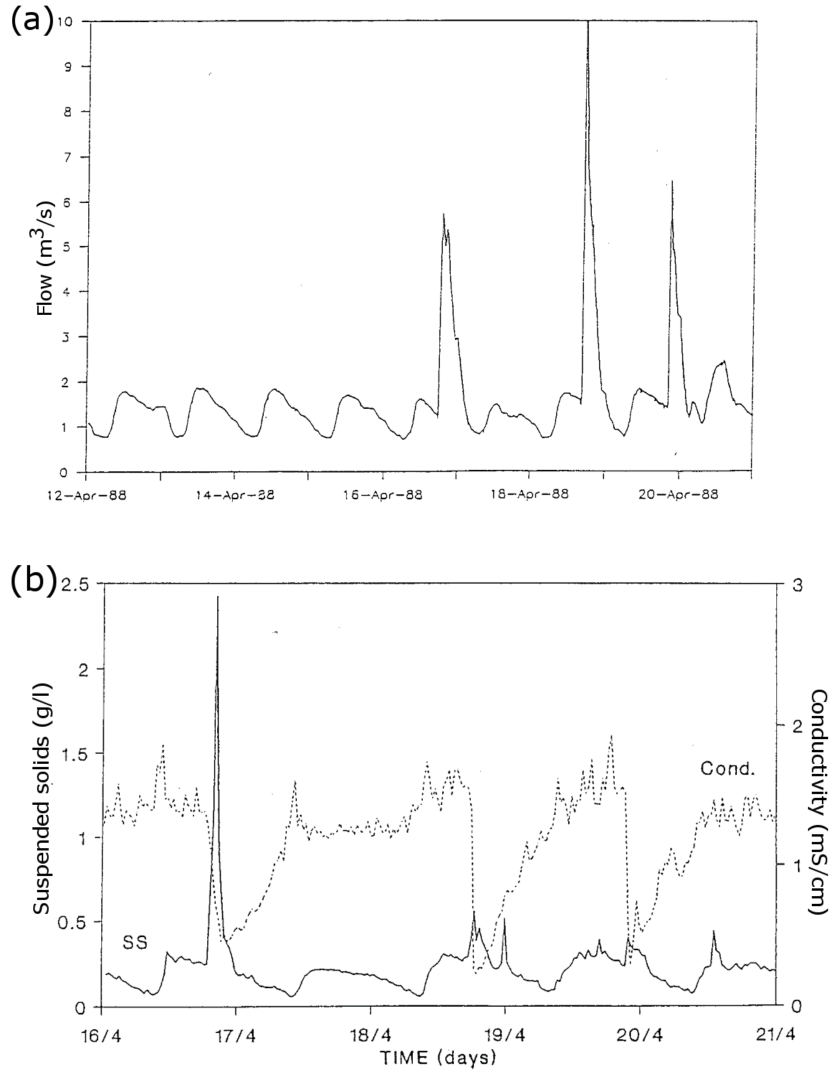

Figure 1.5: Example of (a) flow patterns at the inlet of the WRRF under dry and wet weather conditions and (b) the effect of wet weather conditions (last 5 days of the top figure) on conductivity and suspended solids (Verbanck, 1995).

2012). This can be explained because under wet weather conditions, higher flows are observed and they induce higher bed shear stresses, which makes that coarser solids with higher settling velocities can be resuspended in the sewer system and be carried to the WRRF (Krishnappan et al., 2012).

Grit loads

The fluctuations presented above influence the solids transport through a sewer system and WRRF flows, especially affecting the fastest settling particles like grit (Ashley et al., 2005). Thus, physical characteristics of the particles arriving at the WRRF also vary with time

(Maruéjouls et al., 2013). Depending on the flowrate, grit particles can travel in suspension ($v > 1.07\ m/s$), travel with the moving bed ($0.52\ m/s < v < 1.07\ m/s$), or remain deposited until a runoff or peak flow in sanitary sewers with higher velocities can transport them through the system ($v < 0.52\ m/s$) (Rippon et al., 2010). In Figure 1.6, the vertical profile of the solids transport is presented. Generally, the heavier grit particles travel along the bottom of the channel until they fall inside the grit chamber, while lighter particles travel suspended, and partly settle in the grit chamber. Osei and Andoh (2008) estimated that up to 90 % of the annual volume of grit is transported during peak flows.

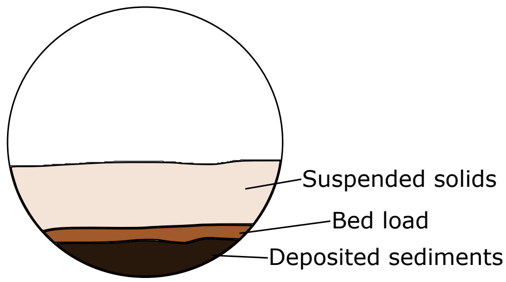

Figure 1.6: Vertical profile of solids transport in sewer systems and WRRF flumes (Adapted from Ashley et al. (2005)).

1.4 Sampling and characterization methods

Despite the importance of grit and the negative effects it may cause in a WRRF, no standard peer-reviewed methods exist to characterize and sample it (Wilson et al., 2007; Reddy and Pagilla, 2009). Moreover, accurate data about grit characteristics are scarce (Pretorius, 2012; McNamara et al., 2014). As Reddy and Pagilla (2009) pointed out, this leads to, among others, improper estimation of the performance of grit chambers.

Currently, there is still a wide diversity of grit characterization procedures and parameters characterize the grit (Reddy and Pagilla, 2009). This diversity is due to the difficulty to obtain a representative sample and the unclear grit definition (Reddy and Pagilla, 2009; Rife and Botero, 2012). In addition, most of these methods have been proposed by private companies and consultancies. They are thus continuously modified and hardly published in peer-reviewed literature (Reddy and Pagilla, 2009; Rife and Botero, 2012).

The most common methods used, or that could be adapted to be used, to characterize grit and sample the streams around a grit chamber are described in this section.

1.4.1 Sampling methods

In-situ sampling to characterize grit is complex and difficult (Reddy and Pagilla, 2009). Due to the challenges related to the heterogeneity in the wastewater and the large variations in grit properties, and the low priority given to better understand grit removal, erratic grit characteristics, and uncertain grit loads can be determined if the sample is not representative (Pretorius, 2012).

In the existing literature, only sampling methods for the liquid stream (inlet and outlet) are described. Methods to sample solid streams like the grit removed from the system are not mentioned. Gerges (2014) proposed that, for sampling methods for the liquid stream to be accurate, they should consider the following:

- Not obstruct the flow and minimize the disturbances to the flow pattern at the sampling point;
- Grit is rarely uniformly distributed;
- Pumping rates should equal the flow velocity.

Currently, several sampling methods are in use but they are often proprietary designs and none have been published in the peer-reviewed literature (Reddy and Pagilla, 2009; Gerges, 2014). According to Reddy and Pagilla (2009) and WEF (2016), the most relevant methods are:

- *Bucket sampling*: it is the simplest method used. It consists in manually collecting grab samples with a receptacle (Reddy and Pagilla, 2009).
- *Single-point pumped sampling*: the water is pumped from a single point in the channel and collected in a container. Normally the pipe is placed horizontally face to the flow at the bottom of the channel where the highest quantity of grit particles is found (Reddy and Pagilla, 2009).
- *Vertically integrated slotted sampling (VISS)*: this sampler consists of a PVC (polyvinyl chloride) pipe with a slot along the pipe and closed at one end (see Figure 1.7). The pipe is inserted vertically into the channel with the slot oriented face to the flow (Wilson et al., 2007). Then the water inside the column is withdrawn by a pump (Reddy and Pagilla, 2009). It is used to sample the entire depth of a channel.
- *Cross channel pumped sampling (CCS)*: with this sampler the water is siphoned from the channel and collected in settling basins. It consists in a 1-inch square pipe submerged

Figure 1.7: VISS sampler (Image courtesy of Black Dog Analytical Lld (2019)).

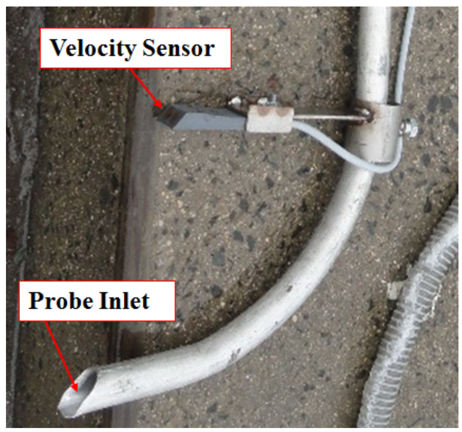

Figure 1.8: CCS sampler (Image courtesy of Grit Tech (2019)).

horizontally face to the flow (see Figure 1.8). This pipe is moved to several locations across the bottom of a section of the channel (Gerges, 2014).

- *Manifold pumped sampling*: this is a multi-point sampler installed vertically and horizontally distributed over a cross section of the channel as shown in Figure 1.9 (Reddy and Pagilla, 2009). A pump is connected to the manifold to collect the water and store it in a basin.

1.4.2 Sample pretreatment

When sampling particles around a GRS, a mixture of organic and inorganic solids together with water is obtained (See Figure 1.10). A few methods to characterize the desired characteristics of grit particles require sample pretreatment to simplify laboratory work and transport efforts (Reddy and Pagilla, 2009; WEF, 2016). The pretreatments currently in use, included and detailed in WEF (2016), are:

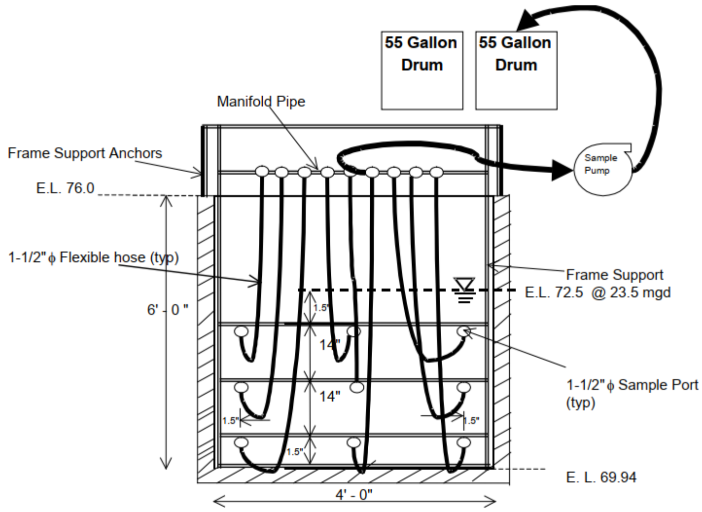

Figure 1.9: Manifold sampler (Reddy and Pagilla, 2009).

- *Reduction*: used to remove excess water and organic materials.
- *Rinsing*: used to remove collected organic material.
- *Coarse wet sieving*: used to remove large and organic particles that are not considered part of grit.

Despite the fact that the methodologies of each sample pretreatment are described in the *Guidelines of Grit Sampling and Characterization* by WEF (2016), each user (i.e. manufacturers, consultants, etc.) develops his/her own method (Reddy and Pagilla, 2009).

Figure 1.10: Pulpy material. Image taken during this PhD study of a sample from the inlet of a grit chamber (Plate dimensions 25.4 cm x 38.1 cm x 4 cm).

1.4.3 Characteristics

Despite the importance of the settling characteristics for sedimentation processes based on gravitational forces (Camp, 1936), as presented in Section 1.3.1, previous grit definitions have been focused on particle size characteristics, considering only the inorganic fraction and assuming particles to be homogeneous spheres with a SG of 2.65 (Camp, 1942; Tchobanoglous et al., 2014; U.S. EPA, 2004).

As sewage solids, however, grit particles do not have a single representative value of specific gravity and they are not only inorganic homogeneous spheres (Hedges et al., 1998). Thus, later studies, e.g. by Barter and Sherony (2011) and Herrick et al. (2015), have questioned the conventional approximations due to the heterogeneity of the particle composition. Instead, settling characteristics have been proposed to act as important particle characteristic for grit (Wilson et al., 2007; Reddy and Pagilla, 2009; Herrick et al., 2015) and are now included in the new definition of grit proposed by the Grit Sampling and Characterization Task Force of the WEF (WEF, 2016).

Due to the variability in definitions of grit particles including different variables, there is also a diversification of grit characterization methods and the characteristics that are measured (e.g. particle settling velocity, particle size and density) (Reddy and Pagilla, 2009). The methods currently used are relatively different and there is no industry consensus among the methods, thus leading to different results.

According to currently used methods, this section has been divided in subsections considering the different variables that can be studied, the sample pretreatment and the particles composition.

Solids composition

The heterogeneous solids in wastewater can be fractionated depending on their characteristics, i.e. size, volatility and biodegradability (Mansour-Geoffrion, 2013; WEF, 2016). To characterize the solids composition, *Standard Methods for the Examination of Water and Wastewater* were proposed by the American Public Health Association, American Water Works Association, Water Environment Federation (APHA, 2012). In the context of this study, the particulate fractions are of interest since grit is part of them.

According to (APHA, 2012) characterization methods, Mansour-Geoffrion et al. (2014) presented the fractionation shown in Figure 1.11. The total solids (TS) are considered the material residue left in a sample after evaporation of a sample and its subsequent drying in the oven at 103 - 105 °C. As shown in Figure 1.11, they can be fractionated further into volatile and inorganic solids (VS and IS, respectively) determined after ignition of the total solids at 550

°C (the volatilized fraction at 550 °C is VS). VS are considered as organic solids. Both VS and IS can be further fractionated depending on their size: filtered solids with a size $< 0.45\ \mu m$ (FVS and FIS) and suspended solids with a size $> 1.2\ \mu m$ (VSS and ISS). Particles ranging from 0.45 to 1.2 μm are too big to be considered as part of the filtered solids and too small to be considered as part of the suspended solids, and they are generally not considered in the wastewater solids fractionation.

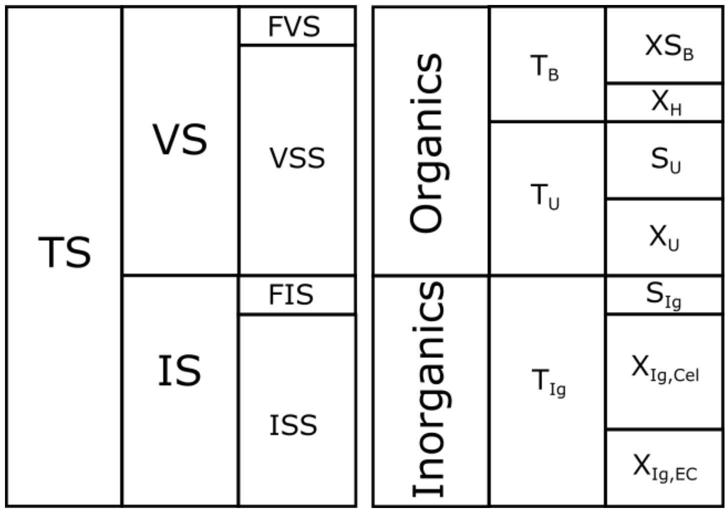

Figure 1.11: Fractionation of the solids at a WRRF inlet (adapted from Mansour-Geoffrion et al. (2014)).

Organic solids can be fractionated into biodegradable and unbiodegradable organic matter (T_B and T_U, respectively). Then, each one can be divided depending on their size into soluble and particulate biodegradable organic solids (XS_B), soluble unbiodegradable solids (S_U), and particulate unbiodegradable matter (X_U). Also, part of the biodegradable matter, heterotrophic biomass is considered (X_H).

Inorganic solids can be fractionated into soluble inorganics (S_{Ig}), particulate inorganic solids associated to biomass cellular material ($X_{Ig,Cel}$), and extracellular particulate inorganic solids ($X_{Ig,EC}$). According to the traditional (inaccurate) definition, grit particles are classified into $X_{Ig,EC}$.

Particle size and shape analysis

Grit particles are traditionally characterized by their particle size distribution (PSD) (Reddy and Pagilla, 2009; WEF, 2016). However, this characteristic does not provide information about the settling characteristics of grit particles: It has to be estimated through a mathematical equation that relate settling velocity and size such as Stokes' and Newton's laws (Tchobanoglous et al., 2014). Because of their simplicity, the most common methods used are:

- *Wet sieving* is recommended when performing settling velocity testing of grit samples, and when there is a clear indication that the grit particles being collected at a WRRF have considerable amounts of organic matter attached, possibly affecting the particle settling velocity (WEF, 2016; Gerges, 2016). For example, *Grit Solutions* or *Black Dog Analytical, LLC* use this methodology to estimate the PSD of grit particles (Reddy and Pagilla, 2009; Black Dog Analytical Lld, 2019).

- *Dry sieving* is usually performed by drying or ashing the sample in the oven (at 105 °C or 550 °C), followed by the sieve analysis. It can be used to characterize grit. For example, Finger and Parrick (1980) uses the methodology to determine the PSD of ashed grit. However, after ashing grit particles, the characteristics of the particles are changed since the organic fraction is volatilized.

Despite the fact that sieving methods are simple, fast, and provide comparable results, they only provide a two-dimensional picture of the particles. Since there is no evidence that grit particles are spherical, and the collection system type and characteristics could play an important role in this aspect of grit, particle imaging is another advanced technology that proved to be reliable and accurate (Osei et al., 2010; Gwinn et al., 2011). It could thus also be used to characterize particle size and, in addition, shape (WEF, 2016).

Density and specific gravity

Density is defined as the mass per unit volume of a material (Tchobanoglous et al., 2014). Material density is important for determination of the forces acting on particles, such as grit. For example, material density will impact gravitational and centrifugal forces affecting grit particles.

Bulk density is the mass of material studied per unit volume it occupies including "voids" or pockets of another substance, such as water. The bulk density is typically much lower than the material density (WEF, 2016). For instance, bulk density is important for determining the mass of grit in a given dumpster volume or the dumpster volume needed to hold an estimated mass of grit. Bulk density may be found by measuring the physical volume occupied by a known solid mass.

SG is the ratio of a material's density as compared to a standard value (White, 2011). Typically, for liquids and solids, the standard value used is that for water at 4 °C which has a material density of 1000 kg/m^3 (WEF, 2016) and SG would be calculated using the material density. However, the ratio of the bulk density to water is sometimes stated as SG as well, so care must be taken to note which density is being used in the calculation.

Generally, for grit chambers design, a material density of 2650 kg/m^3 (i.e. a SG of 2.65) is used to estimate the settling velocities from particle size. However, it can lead to an overestimation of the design parameter, the settling velocity (Tchobanoglous et al., 2003; Herrick et al., 2015). Some studies have shown that the density of the grit particles can vary between 1400 and 2650 kg/m^3 (i.e. a SG from 1.4 to 2.65) (McNamara et al., 2009; Kitching and Denton, 2012).

Settling velocity (including other water systems)

The particle settling velocity is the most relevant characteristic of grit particles to design grit chambers (Gromaire et al., 2008; Herrick et al., 2015; WEF, 2016). It depends on the particle size, density and shape of the particles (Aiguier et al., 1996; Marsalek et al., 2006). Despite the importance of this variable, it is not frequently measured and used to design and optimize grit chambers (Osei et al., 2012). The variable of interest is the vertical one-dimensional terminal velocity of the grit particle while settling in quiescent flow under the influence of gravitational and drag (viscous) forces.

Since grit particles are heterogeneous, the particle settling velocity distribution (PSVD) is preferably estimated experimentally (Gerges et al., 2018; Sober et al., 2018). However, there is no a universally accepted apparatus nor is there one specific for grit particles or for any wastewater solid particles (Ashley et al., 2005; WEF, 2016). Frequently, methods and/or apparatus are modified depending on the needs (Ashley et al., 2005). Generally, the methods to characterize the settling velocity of wastewater solid particles can be classified in two groups: (i) static settling devices where the liquid is under quiescent conditions, such as settling columns (Aiguier et al., 1996); and (ii) dynamic settling devices where the liquid is under dynamic conditions, e.g. elutriation devices (Krishnappan et al., 2004).

Within the class of static settling devices, several settling columns have been developed over the years. For example, the Aston column (Tyack et al., 1993), the Umwelt- and Fluid-Technik (UFT) column (Michelbach and Wöhrle, 1993), the CERGRENE protocol (Chebbo, 1992), the U.S. EPA column (O'Connor et al., 2002), and the ViCAs protocol (Chebbo and Gromaire, 2009). Depending on the setup, the height of the settling columns varies between 0.2 and 1.8 m, with sample volumes varying between 1 and 40 L. On several occasions, these methods have been compared and results show different PSVD curves (Aiguier et al., 1996; Lucas-Aiguier et al., 1998; Berrouard, 2010; Krishnappan et al., 2012). Lucas-Aiguier et al. (1998) and Berrouard (2010) pointed out that these differences are probably due to the different sizing of the columns and the fact that several pretreatments are applied before the test to preselect the particles to be studied.

Table 1.2: Summary of the characteristics of the presented settling columns to measure settling PSVD of wastewater solid particles.

	Settling column					
Characteristics	**Aston**	**UFT**	**CERGRENE**	**EPA**	**ViCAs**	**Hydro International**
Sample	5 L of wastewater	1 g of settled solids	1 g of solids > 50 μm	70 L	4.5 L of wastewater	Not specified solids mass
Settling depth	1.5 m	0.7 m	1.81 m	2.5 m	0.7 m	2.4 m
Cross section form	○	○	○	○	○	□
Cross section dimensions	$\varnothing = 0.05$ m	$\varnothing = 0.05$ m	$\varnothing = 0.05$ m	$\varnothing = 0.19$ m	$\varnothing = 0.064$ m	a = 0.3 m square
Device	Column	Column + Imhoff cone	Column	Modular column	Column	Column
Pretreatment	Solids settled within 3 h in the column	Solids settled within 2 h in an Imhoff cone	Sieving ($d_p < 50\ \mu m$)	None	Sieving ($d_p < 2\ mm$)	Not specified
Initial conditions	Well-mixed	Particles settle from the top of the column	Particles settle from the top of the column	Well-mixed	Well-mixed	Particles settle from the top of the column
Measurement	Mass(t)	Conc.(t)	Mass(t)	Conc.(t)	Mass(t)	Mass(t)
Tested v_s range	0.6 - 97.2 m/h	0.4 - 838.8 m/h	5 - 250 m/h	2.5 - 150 m/h	0.03 - 42 m/h	18 - 1165 m/h

Lately, a settling column has been developed and tested specifically to measure settling velocities of grit by Hydro International plc (Osei et al., 2012; Gwinn et al., 2013). In comparison to other settling columns, Osei et al. (2012) proposed a square settling column as final design. It has been applied and published for several case studies (Sober et al., 2018). The detailed characteristics of the all settling columns identified previously are presented in Table 1.2.

As dynamic settling devices, some systems have been proposed to study the settling velocities of wastewater particles. Two different setups can be found in the literature: (i) modified settling columns with the addition of oscillating grids to create turbulence, e.g. the Rasmussen and Larsen (1996) device; and (ii) the elutriation apparatus, firstly developed by Walling and Woodward (1993), and later updated by Krishnappan et al. (2004) and Marsalek et al. (2006). As a newer device, Gerges et al. (2018) presents a single dynamic settling column for grit particles characterization based on the same principle as the elutriation system (i.e. controlling the upflow velocity in the column, but here only the particles with a settling velocity above a threshold velocity will be collected at the bottom of the column).

Sand Equivalent Size

The settling velocity of a grit particle depends on several factors, one of them being that the particle may include organic material. This organic matter reduces the density and thus the settling velocity of the particle and also modifies the shape of the grit particle, leading to on angular particle settling slower than rounder particles (Herrick et al., 2015; WEF, 2016).

Clean silica sand is known to have a SG of 2.65. However, because grit is seldom clean or round, and may not be made of silica, settling velocities are different (Figure 1.12). The sand equivalent size (SES) concept is a way of describing the settling characteristics of municipal grit in relation to clean round silica sand. It is defined as the size of a clean sand particle, measured in microns, that has the same settling velocity of a collected grit particle, as depicted in Figure 1.12.

1.5 Grit chambers

The separation of grit is mainly carried out in grit chambers to physically separate fast settling particles (Tchobanoglous et al., 2014; WEF, 2016). Currently, there are several designs of grit chamber units (WEF, 2010; Tchobanoglous et al., 2014): horizontal flow (detritus and velocity control tanks), aerated, and vortex grit chambers. Also, in some WRRFs, grit is settled in the primary treatment and it is then separated from the primary sludge (Reddy and Pagilla, 2009).

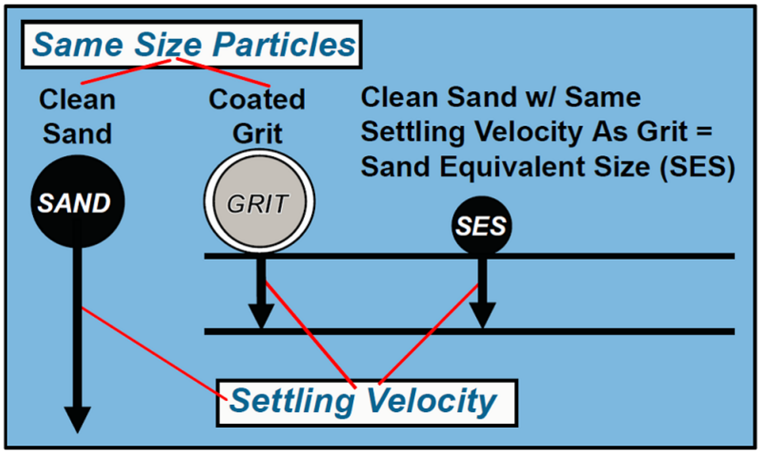

Figure 1.12: Sand equivalent size of grit (Wilson et al., 2007).

In this section, only aerated and vortex grit chambers are presented, given their popularity.

1.5.1 Aerated grit chambers

In aerated grit chambers, commonly used in Europe and in large WRRFs in the U.S.A., grit is removed by introducing air along one side of a rectangular tank causing a spiral flow pattern perpendicular to the flow through the tank, as shown in Figure 1.13 (U.S. EPA, 2004; Tchobanoglous et al., 2014). This pattern makes faster settling particles of grit settle at the bottom while slower settling particles stay suspended and pass through the tank (WEF, 2010; Hirschbeck and Günthert, 2015).

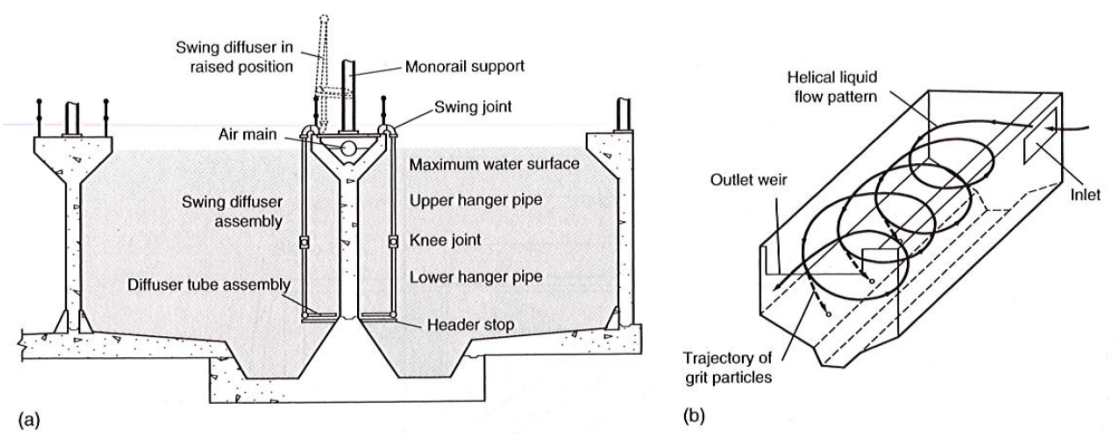

Figure 1.13: Schematic of a typical aerated grit chamber (Tchobanoglous et al., 2014). (a) Cross-section of the aerated grit chamber. (b) Schematic of the helical flow pattern through an aerated grit chamber.

Normally, they are designed with a hydraulic retention time at peak flow between 2 to 5 min (Morales and Reinhart, 1984; Qasim, 1999; Tchobanoglous et al., 2014). However, if it is desired to remove finer grit particles to control septicity at the primary clarifier, the hydraulic retention times may vary between 10 and 20 min (WEF, 2012).

The grit accumulated at the bottom of the tank is typically transported along the bottom of the tank to the grit sump using screws or travelling-bridge buckets (WEF, 2010; Tchobanoglous et al., 2014). Other methods also exist but they are less used: chain-and-bucket collectors, chain-and-flight collectors, clamshell buckets, airlifts and jet pumps (WEF, 2010; Tchobanoglous et al., 2014).

The velocity of roll or agitation can be adjusted depending on the properties of the grit to be removed (Finger and Parrick, 1980; Butler et al., 1995; Sawicki, 2004). Thus, considering an appropriate placement of the diffusers, the air source and baffles, and operating with a proper velocity, controlled by the rate of aeration, high removal efficiencies will be obtained for a wide influent flow range (Morales and Reinhart, 1984; Munoz and Young, 2009). Only a relatively low putrescible organic content will then be removed with the grit (U.S. EPA, 2004). Such high removal efficiencies may improve the performance of the downstream units by reducing the sceptic conditions in the incoming water avoiding anaerobic zones, thus reducing the production of the toxic and corrosive H_2S gas (U.S. EPA, 2004). The most critical operating conditions and a considerable reduction of the efficiency of the grit chamber occur under intense rain events, which goes together with the highest amount of grit (Sherony and Herrick, 2015). Thus, the grit chamber has to be designed and dimensioned to handle this situation (Londong, 1989). More detailed information on how to design aerated grit chambers and the recommended features are described in Londong (1989), WEF (2010) and Tchobanoglous et al. (2014).

Despite its simple mechanical design and the easy-access for maintenance (Tchobanoglous et al., 2014), the construction of this unit requires large space and considerable power for aeration, maintenance and control of the aeration system requires additional labour compared to other grit removal units (U.S. EPA, 2004; Tchobanoglous et al., 2014).

1.5.2 Vortex grit chambers

Vortex grit chambers, commonly used in North America, consist of a circular chamber where grit is removed with the force of the tangential inflow velocity which creates a vortex flow pattern as its name indicates (Tchobanoglous et al., 2014). Generally, the hydraulic retention time observed in this unit varies between 20 and 30 s (Qasim, 1999; Tchobanoglous et al., 2014).

This type of grit chambers has a consistent removal efficiency over a wide flow range and the headloss through it, is minimal (typically 6 mm) (U.S. EPA, 2004; McNamara et al., 2014). Also, they are able to remove a high percentage of fine grit (up to 73 % of 0.11 mm (140 mesh)) (U.S. EPA, 2004). However, as U.S. EPA (2004) pointed out, this type of grit chambers has often proprietary designs and it is complicated and difficult to modify and adapt them to specific needs.

The horizontal dimensions of vortex grit chambers are smaller compared to other systems but they have a deep basement (Tchobanoglous et al., 2014; Blain et al., 2018). Thus, they require a deep excavation, increasing construction costs, especially if hard rock is present (U.S. EPA, 2004). It also makes access complicated for maintenance and the grit sump has a tendency to clog. If this occurs, high pressure agitation is required using water or air to loosen grit compacted in the sump (Butler et al., 1995; U.S. EPA, 2004). On the other hand, there are no submerged bearings or other parts that often require maintenance (U.S. EPA, 2004).

Currently, three different types of vortex units exist on the market: mechanically induced vortex, hydraulically induced vortex, and multi-tray vortex. A brief description of them is presented below.

Mechanically induced vortex units use a rotating impeller to augment the vortex flow pattern caused by the tangential flow entry (See Figure 1.14) (Tchobanoglous et al., 2014; Blain et al., 2018). The velocity of the paddles can be varied according the inlet flow of the unit to obtain better separation of the grit particles from the slower settling particles. In addition, this vortex flow pattern creates a quiescent zone at the center of the tank where the grit is separated from the organics and settles by gravity to the bottom of the tank into the grit sump while organic matter remains in suspension (WEF, 2010; Tchobanoglous et al., 2014).

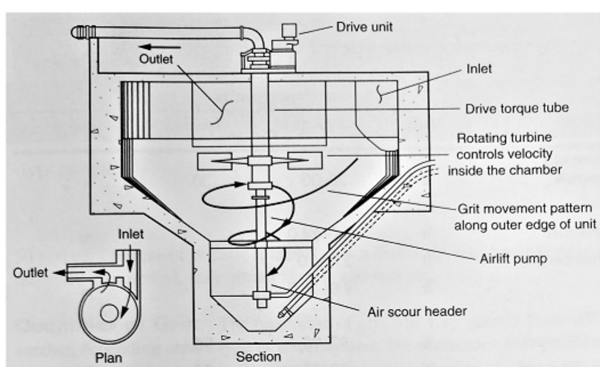

Figure 1.14: Schematic of a mechanically induced vortex grit chamber (adapted from Smith & Loveless by Tchobanoglous et al. (2003)).

In *hydraulically induced vortex* units, the vortex is only created by the inflow, i.e. there is no mechanical equipment to force it (WEF, 2010; Tchobanoglous et al., 2014). As shown in Figure 1.15, the flow enters tangentially into the cylindrical unit, letting the grit settle at the bottom, forming a spiral path to the center cone. The slower settling particles remain in suspension and leave the chamber through the outlet of the unit.

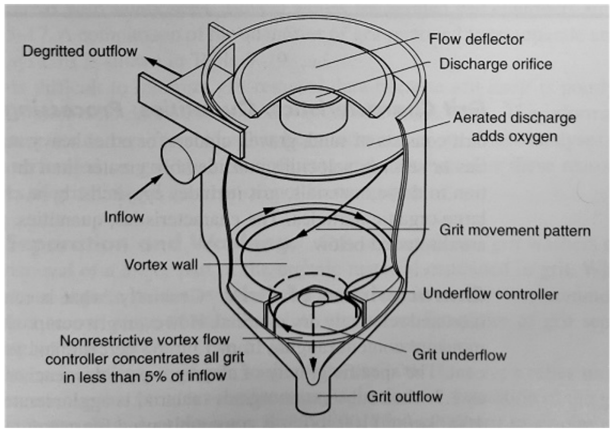

Figure 1.15: Schematic of a typical hydraulically induced vortex grit chamber (adapted from Eutek by Tchobanoglous et al. (2003)).

The *multi-tray vortex* unit is a proprietary system based on multiple stacked trays that maximize the surface area and minimize the settling area as shown in Figure 1.16 (WEF, 2010). The flow is split to the different trays by a flow-distribution header. Again, the wastewater enters the unit tangentially creating the vortex flow pattern similar to the other vortex units (WEF, 2010). Compared to the two other vortex units, this system is more compact and the headloss is lower (Tchobanoglous et al., 2014).

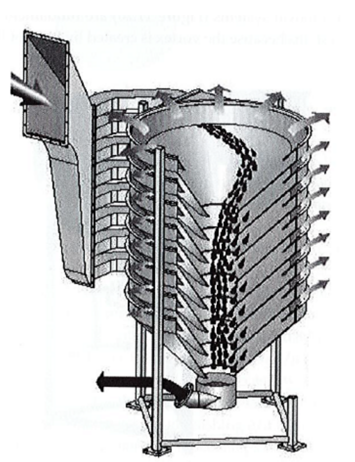

Figure 1.16: Schematic of a multi-tray vortex grit chamber (included in *Design of municipal wastewater treatment plant: Manual of Practice 8* by WEF (2010) as a courtesy of Hydro International).

1.6 Modelling – state-of-the-art

Models allow describing real complex processes and their behaviour by mathematical equations (Gujer, 2008). They are used to predict system behaviours in view of understanding, optimising and managing a system. Since wastewater systems are time-dependent, dynamic models are the best approach to describe the real behaviour of those systems (Beck, 1976; Gujer, 2008).

In the last decades, researchers have started to model the integrated urban wastewater system (IUWS) and the whole WRRF in the context of resource recovery (Bauwens et al., 1996; Benedetti et al., 2013). These integrated approaches improve the understanding of the entire system by describing their dynamics (Rauch et al., 2002). However, integrating the different existing models of each unit is complex due to the different model concepts that are typically chosen on the basis of the objective of the model's use (Rauch et al., 2002).

Despite the importance of the whole system's modelling, preliminary treatment is rarely included explicitly in these models, and preliminary treatment models are hardly available in modelling and simulation softwares. With the improvement of knowledge and the increased number of emerging new technologies, Rieger et al. (2012) have demonstrated that, to properly model secondary treatment, the fractionation of the influent of the WRRF into the different pollutant components has a large influence on the prediction of the quality at the outlet of the WRRF. Thus, as part of the preliminary treatment, grit chamber units have received increased interest in studies (WEF, 2016).

1.6.1 Grit chamber models

In the case of water quality models for grit chambers, currently two different modelling approaches exist to estimate the quantity of grit removed: simple static models and complex hydrodynamics models (WEF, 2016).

Static models

In some modelling and simulation softwares of WRRF (for example, SIMBA by ifak e.V. (Magdeburg, Germany) and GPS-X by Hydromantis (Hamilton, ON, Canada)), the model associated to grit chambers is a simple empirical model. The quantity of grit removed is directly proportional to the incoming flux in the grit chamber (Tchobanoglous et al., 2014). This removal factor consists in a % of the suspended solids removed from the influent and it is fixed by the user (WEF, 2010). Generally, an approximative value found in literature is applied and it is not adapted to daily, seasonal or weather induced changes (i.e. wet weather conditions or snowmelt period).

This approach is a simple gross approximation to estimate the quantity of grit removed. However, it presents considerable limitations (WEF, 2016). Since the quantity and characteristics of collected grit can vary from one WRRF to another and with weather conditions, an erroneous estimation of the efficiency of the grit chamber can be calculated and it can have a significant impact on the predicted performance of the overall plant (WEF, 2010; Rife and Botero, 2012).

Accordingly the static models are simply calibrated by adjusting the constant %-removal from some static information published on the literature or from some data based on previous studies carried out at the WRRF under study (WEF, 2016). Finally, the performance of the model is evaluated in terms of particle removal.

Dynamic models

In the context of the design and optimization of WRRF operation, a dynamic model would be more accurate to predict the behaviour of the system because it can cope with the variability of the characteristics of the incoming flow (Beck, 1976). However, at this moment, no such dynamic mathematical model specific for grit removal exists (WEF, 2016).

Over the last few years, computational fluid dynamics (CFD) modelling has been used as an approach for studying WRRF unit processes such as aeration tanks and settlers (Knatz et al., 2015; Wicklein et al., 2016). CFD allows to accurately study the hydrodynamic behaviour of particles in full-scale units, although specific characteristics of the particles and of the unit to be studied are required (Seifried et al., 2013). However, despite their accuracy, the calculation time is still quite long and they cannot be used in an integrated system context or be implemented in a modelling and simulation software for whole plant modelling (Le Moullec et al., 2010; Laurent et al., 2014).

Moreover, the characteristics of particles considered as input to the CFD model are the particle sizes, given a spherical coefficient and a specific gravity (McNamara et al., 2012). From these characteristics, the settling velocity is then estimated according to Stokes' Law (Equation 1.4) (Gerges, 2014).

Commonly, the CFD models are first calibrated hydraulically comparing the simulated results with measurements collected during characterization studies such as tracer tests to evaluate the hydraulic performance or acoustic Doppler current profiling to determine the flow velocity at several locations of the studied unit (McNamara et al., 2012; WEF, 2016). Then, particles are characterized and divided into several classes at the inlet and outlet of the grit chamber.

Those classes are included in the CFD model and tracked along the studied system. Finally, the performance of the model is evaluated in terms of particle removal comparing the simulated and the observed values.

In grit chambers, some CFD studies have been carried out to estimate the efficiency of the unit (e.g. Tyack and Fenner (1999), Couture et al. (2009) and McNamara et al. (2012) on vortex grit chambers), to optimize a unit (e.g. Burbano et al. (2009), Seifried et al. (2013) and Dutta et al. (2014) on aerated grit chambers, and Chien et al. (2010), McNamara et al. (2012) and Pretorius (2012) on vortex grit chambers), and also to evaluate the accuracy of sampling techniques (e.g. Gerges (2014)). However, they do not consider the real settling characteristics of grit particles since Stokes' Law is used to estimate the PSVD for different particle classes with varying particle diameter, i.e. ranging between 50 and 3200 μm, and two SG, such as 2.65 and 1.4.

1.6.2 Settling models

In sedimentation processes, the separation depends on gravity forces and wastewater settling characteristics are thus important (Andoh and Smisson, 1996; Reddy and Pagilla, 2009). Models for other settling units adjacent to grit chambers, such as primary settlers, stormwater tanks and combined sewer retention tanks, have also been considered as a source of inspiration for model grit chambers.

Primary settler models

Primary settlers are meant to remove organic settleable solids from the influent wastewater and are placed after the grit chambers (Tchobanoglous et al., 2014). The efficiency of the unit has been considered to have a direct impact on the biological and the sludge treatment units, and thus on the quality of the effluent (Otterpohl and Freund, 1992; Gernaey et al., 2001). However, it has been considered that this unit is not highly influential on the simulated results, and simplified models are often sufficient to describe the dynamics of the unit (Lessard and Beck, 1988; Otterpohl and Freund, 1992).

Earlier primary settler models were physical models and were published during the 80s and early 90s. For example, Lessard and Beck (1988) developed a simple dynamic lumped-parameter model based on settling characteristics, and Otterpohl and Freund (1992) described a simple dynamic model where the particle removal efficiency depends on the hydraulic retention time of the unit.

According to Jeppsson et al. (2013), the most common model used for settlers is the Takács et al. (1991) secondary settler model that has also been used as a basis on further studies on primary settlers modelling. For example, Gernaey et al. (2001) started from the Takács et al. (1991) model to model a reactive primary settler, or Ribes et al. (2002) extended the Takács et al. (1991) model to include compression of the particles in the lower layers of the settler. A later model for primary settlers was presented by Bachis et al. (2015) inspired by the layer approach that is the core of the Takács et al. (1991) model. It considers the heterogeneity of the wastewater solids and the corresponding range of settling velocities (i.e. PSVD curves). Thus, the solids are fractionated in different classes characterized by a settling velocity and the dynamic mass balances are built for each class and each layer.

Stormwater and retention tanks models

Stormwater tanks and retention tanks can be built in combined sewer systems to reduce the overflows and pollutant loads and thus reduce the impact of the pollutants flushed with peak flows to the receiving environments such as rivers. In both types of tanks, settling is the main process taking place (Ashley et al., 2005).

In contrast to grit chambers and primary settlers, the interest in the mentioned tanks is higher due to the large impact of high peak flows on the receiving environment. Hence, more modelling studies have been carried out on those units.

Many of the developed models for retention and stormwater tanks are physically-based models. Generally, they have been developed with the goal of optimizing the management of the sewer system (Lessard and Beck, 1991; Maruéjouls et al., 2012). The most common models were developed to represent the water and solids dynamics in 1-D, e.g. Ferrara and Hildick-Smith (1982), Lessard and Beck (1991), Frehmann et al. (2005), Wong et al. (2006), Vallet et al. (2014), Maruéjouls et al. (2012). All of them consider the settling velocity as a key parameter to determine solids removal. However, the first four models consider only an average settling velocity, while the last two presented models that considered a distribution of settling velocities.

Chapter 2

Problem statement and objectives

2.1 Problem statement

During the last few years, municipalities and industry have been suffering from a lack of knowledge regarding preliminary treatment, especially regarding grit chambers (Pitman, 1999; Rife and Botero, 2012). Thus, in recent years, efforts have been put on the study of grit removal as this process has been recognized essential in a WRRF to avoid downstream processes to be loaded with considerable amounts of grit that can negatively affect (i) the performance of energy production by anaerobic digestion due to its inorganic fraction (Rife and Botero, 2012); (ii) the resource recovery in wastewater (nitrogen, phosphorus) that are in particulate form (Tchobanoglous et al., 2014); and (iii) the negative impact of inorganic particulates on recent technologies in secondary treatment such as MBRs, moving bed biofilm reactors (MBBRs) or treatment processes with reduced sludge production (Mansour-Geoffrion et al., 2010). Moreover, the importance of preliminary treatment is expected to increase because of the impacts of climate change, which tends to increase extreme rainfall intensity (Madsen et al., 2009), resuspending more fast settling particles present on the sewer catchment and in the sewer system due to the larger shear forces, thus increasing the solid loads at the inlet of the WRRFs.

Although some studies have already been done on grit chambers, these have only been done by private companies and consultancies (without peer review) and there is a wide variety of methodologies to evaluate the performance of grit chambers. This is due to the diversification of grit characterization methods, the parameters to be studied to characterize grit, and difficulties with sampling (Reddy and Pagilla, 2009; Rife and Botero, 2012; WEF, 2016). Thus, there is a need to standardize existing sampling and characterization methods of the inlet, outlet and underflow of grit chambers.

In addition, simulation and modelling softwares are increasingly used to design and optimize WRRFs by consulting firms (Rieger et al., 2012). While most of the time the design is done under steady state, dynamic modelling is getting increasing attention, especially for wet weather performance evaluation. Currently, most simulations are carried out from the primary treatment onwards, since in these simulators no calibrated or validated dynamic model is existing for grit chambers due to the lack of quality and representative data (WEF, 2016). Grit chamber CFD models do exist but they are too complex and difficult to solve in order to be integrated in simulation and modelling softwares for design and optimization of overall WRRFs. Currently, the grit chamber models available in simulation and modelling softwares are just simple static empirical correlations calculating percentage removals of TSS and they are not able to describe the hydraulics and dynamics of water quality around a grit chamber.

2.2 Objectives

Considering the current gaps on the research around a grit removal system (GRS) as presented briefly in Section 2.1, the main objectives of this PhD project can be divided in two main parts:

1. **Development of a standard protocol to sample and characterize the water quality around a GRS.**

   This objective aims for a proper characterization of the particles around a grit chamber in view of the particle settling velocity as a parameter of interest since it is the key parameter for grit chambers design. This objective can be split in the following specific objectives:

   a) Development of a site-specific sampling protocol of the streams around a GRS, including inlet, outlet and underflow, to obtain representative samples.

   b) Critical evaluation of the current methods used to characterize the particles around a grit chamber, i.e. methods to study the particle size distribution (PSD) and the particle settling velocity distribution (PSVD).

   c) Development of a methodology to analyse the settleability of particles.

   d) Characterization and evaluation of the settleability of the particulate pollutants at the inlet, outlet and underflow of a GRS.

2. **Development of a conceptual dynamic model of grit chambers based on particle settling velocity distributions.**

   The goal of this part of the work is to provide a model that can describe the water quality dynamics at the outlet of a grit chamber taking into account the settling characteristics of the particles around a GRS and the hydraulic behaviour of the unit. The PSVD model concept for primary clarifiers proposed by Bachis et al. (2015) is the basis to build the mentioned model. This main objective can be subdivided into several specific objectives:

a) Development and application to vortex grit chambers dealing with the specificities of this type of grit chamber.

b) Development and application to aerated grit chambers dealing with the specificities of this type of grit chamber.

c) Calibration and validation of the model for vortex and aerated grit chambers with the collected data from lab tests, on-line measurements and hydraulic studies.

Chapter 3

Materials and methods

This section describes the case studies considered in the context of the dessablEAU project, and the materials and methods used to reach the presented goals of this thesis.

3.1 Case studies

In this study, both aerated and vortex full-scale grit chambers were studied. Two potential case studies in the Québec City area (Canada) were selected because of their proximity, historical work in collaboration with Université Laval, and the access agreements between the WRRF and the university.

Detailed information about both case studies is presented separately in the following sections.

3.1.1 Vortex grit chamber - Saint-Nicolas

The vortex grit chamber studied is installed at the Saint-Nicolas WRRF (municipality of Lévis) (see Figure 3.1). This WRRF was built in 1997 to treat the wastewater from Charny, Saint-Nicolas and Saint-Rédempteur neighbourhoods with a sequential batch reactor (SBR) as secondary treatment. It has the capacity to treat wastewater for 36 000 people equivalents and designed for an average flow of 18 750 m^3/d and up to 95 500 m^3/d under wet weather conditions.

The sewer system is partially combined and partially separate or pseudo-separate. The origin of the wastewater is mainly municipal and from infiltration processes. Moreover, the sewer is divided in two different parts as indicated in Figure 3.2. For the part closest to the Saint Lawrence river, the flow is pumped to the WRRF from a pumping well of 158 m^3 with 3 pumps with the capacity to pump 14 m^3/h in total. One of the pumps is activated when the well is filled up to a predefined water level and it is turned off when the well is emptied.

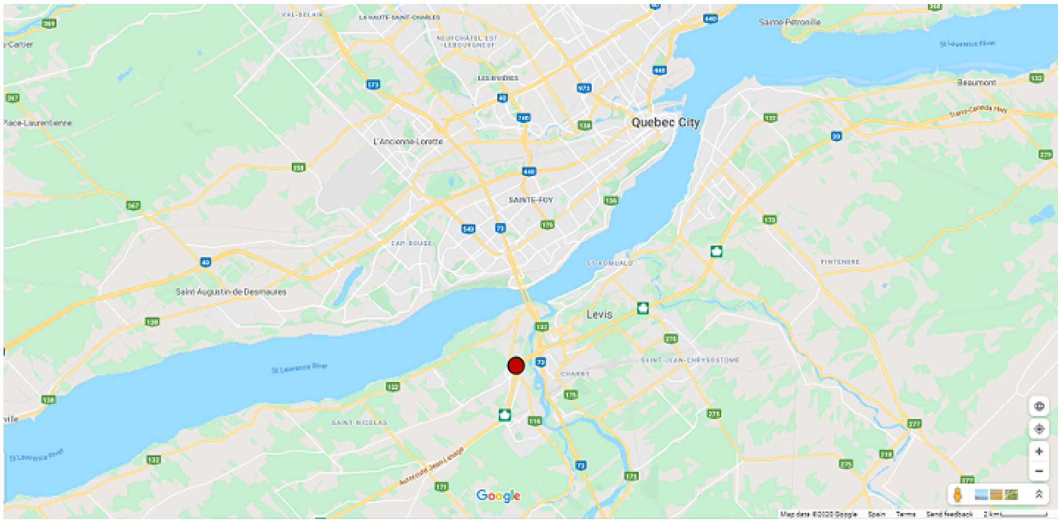

Figure 3.1: Location of the WRRF at Saint-Nicolas indicated by a red point (source *Google Maps*).

A second pump is only turned on when the water level is continuing to increase despite one pump already being on. The third pump is just used for emergency. For the inner part of the sewer, the flow is arriving at the WRRF by gravity (i.e. free flow). Since the sewer system and the WRRF are relatively small, the pump activation creates large dynamic flow variations at the inlet of the WRRF (see Figure 3.3) and will need to be modelled separately (Section 7.3.3).

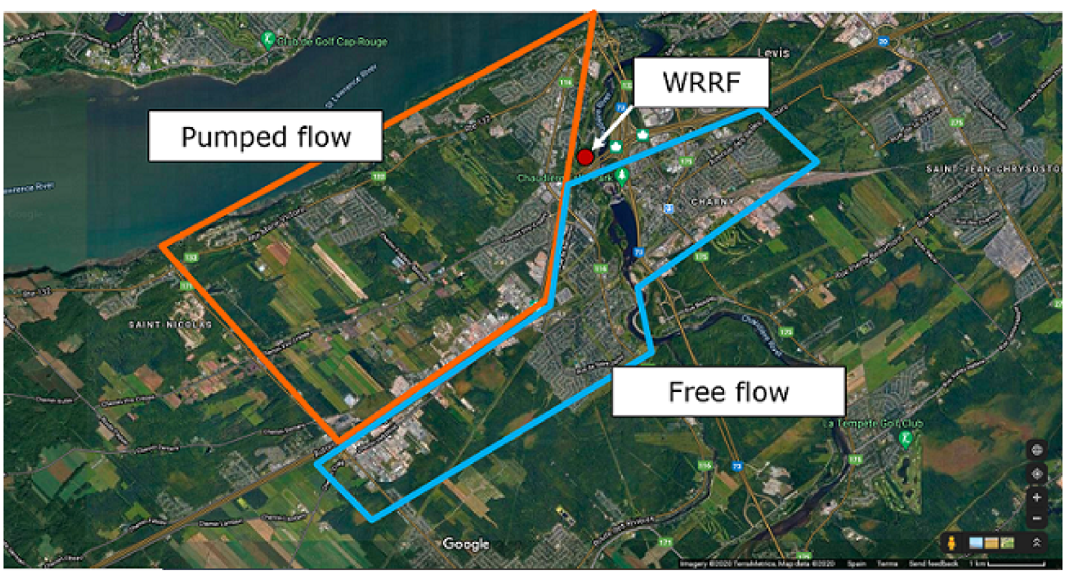

Figure 3.2: Division of the sewer system of Saint-Nicolas (source *Google Maps*).

The pretreatment of this WRRF consists in two different steps: screening and grit removal

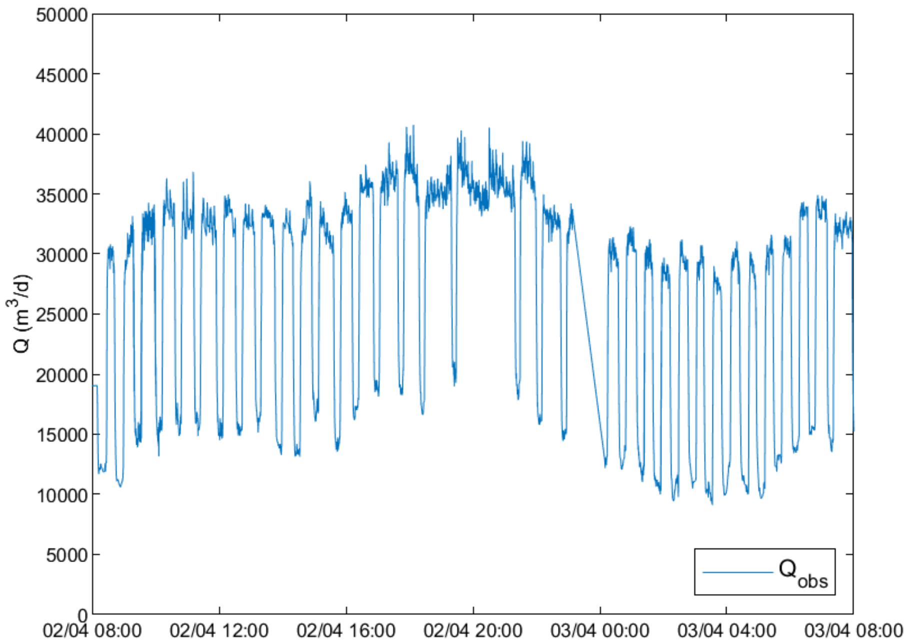

Figure 3.3: Inlet flow dynamics at Saint-Nicolas WRRF due to pump activations from April 2nd at 8 a.m. to April 3rd at 8 a.m., 2017.

(see Figures 3.4 and 3.5). There are two bar screens with a spacing of 12.7 mm which are able to remove the gross solids from the wastewater. Then, the grit removal is implemented. This part of the preliminary treatment contains two vortex grit chambers. The model of the units at Saint-Nicolas WRRF is named *Mectan*, designed by *Veolia Water Technologies Canada*. Each grit chamber has been built to treat a maximum flow of 50 950 m^3/d and remove between 0.2 and 1.0 m^3/d of grit at average flow.

The studied *Mectan* grit chambers have a diameter of 4.2 m and a lower part with a diameter of 1.5 m (see Figure 3.6). At the center of the units, two paddles are installed to induce mechanical forces and create the vortex flow rotating 15 times per minute. Also, there is a baffle installed which occupies part of the inlet channel and part of the outlet channel. The particles settled in the grit chamber are periodically extracted with an airlift pump from the bottom of the grit chamber and injecting air and recycled water. This injection creates a turbulence that can disaggregate particles (for example separate inorganic and organic fractions). The mixture is sent to a grit classifier (or washer) to remove organic particles and considerably reduce the water quantity (see Figure 3.7). The grit particles are then collected in a container and the supernatant is returned to the inlet of the grit chamber number 1.

The extraction of the settled particles at the bottom of the grit chamber is done periodically

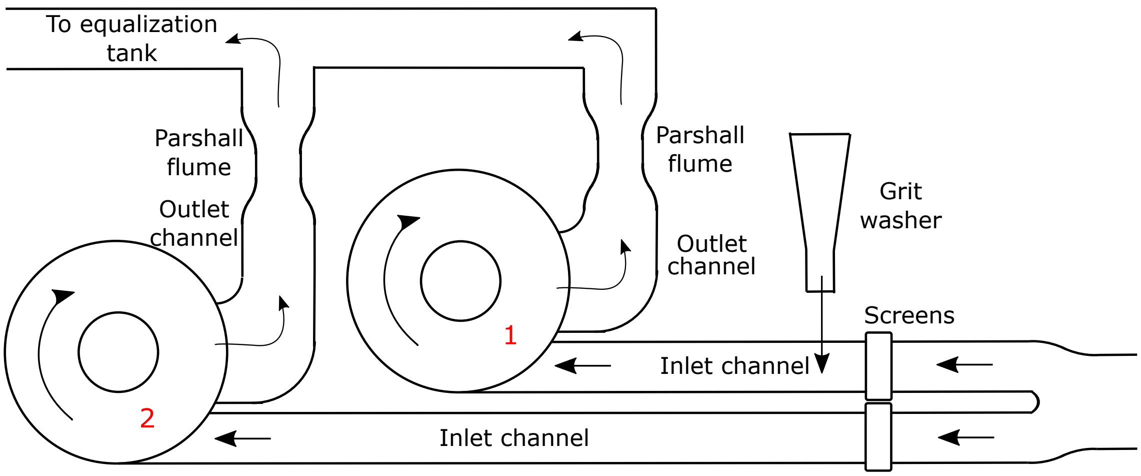

Figure 3.4: Scheme of the pretreatment at the Saint-Nicolas WRRF.

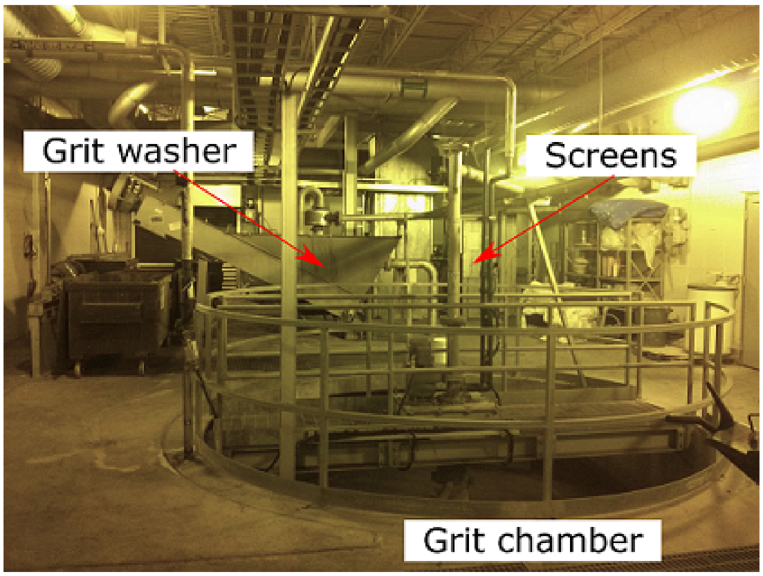

Figure 3.5: Picture of the grit chamber number 1, the grit separation and washing unit and the screens at the Saint-Nicolas WRRF.

and the frequency depends on the season. For example, during winter and summer seasons, only 2 extractions per day are done while during the snow melt period and the spring season the frequency is increased to 4 extractions per day. The extraction is set to 30 seconds and the washing step is set to 20 minutes.

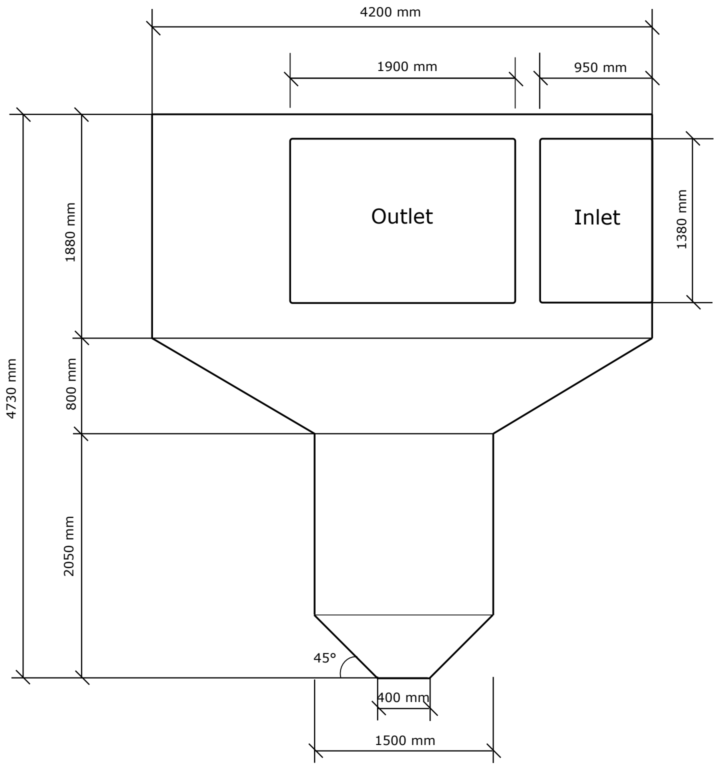

Figure 3.6: Profile of the vortex grit chamber at the Saint-Nicolas WRRF. The inlet channel is the square next to the wall and the outlet channel is the square in the middle of the upper part of the grit chamber.

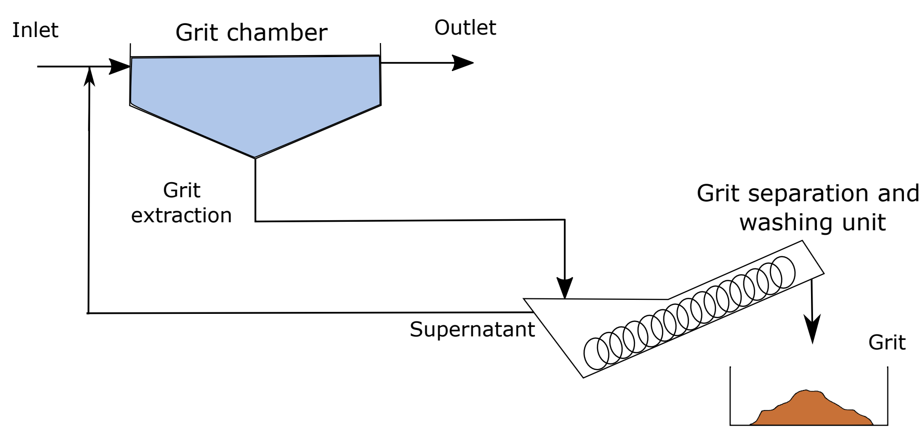

Figure 3.7: Scheme of the grit removal system.

3.1.2 Aerated grit chamber - Québec City

The aerated grit chamber studied was part of the the East WRRF of Québec City (see Figure 3.8). The wastewater is coming from the Eastern part of the city (see Figure 3.9). The treatment chain in that WRRF consists in: (i) screens and aerated grit chambers for pretreatment,

(ii) lamellar primary clarifiers, (iii) biofilters as secondary treatment, and (iv) UV desinfection as tertiary treatment (only during the summer season). It has a capacity of 270 000 people equivalents with an average flow of 230 700 m^3/d.

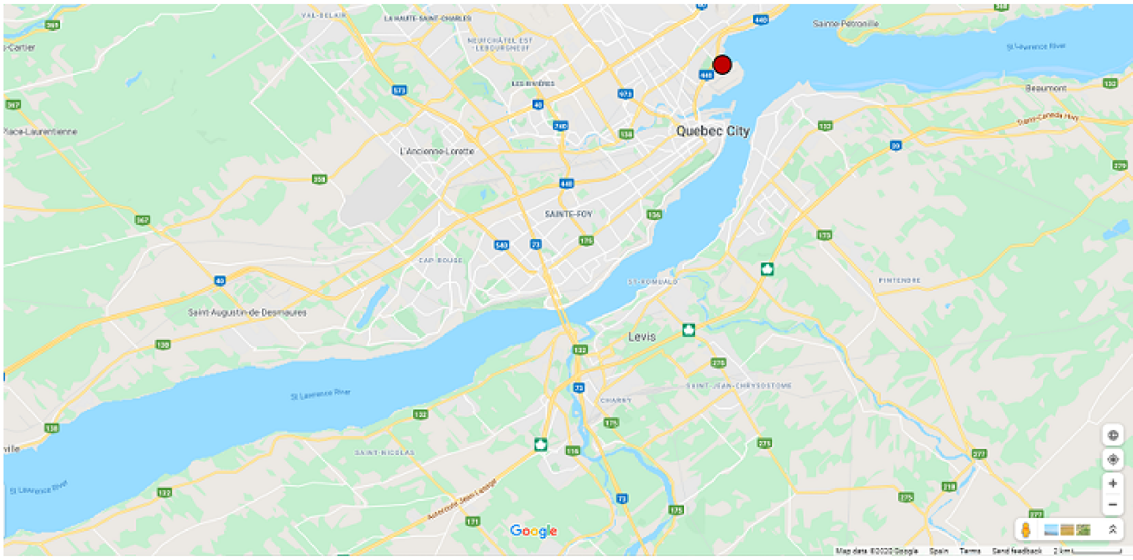

Figure 3.8: Location of the East WRRF of Québec City indicated by a red point (source *Google Maps*).

The sewer system is composed of 30 % combined sewer and 70 % of separated or pseudo separated sewer. In the sewer network, 10 retention tanks were implemented with a total volume of 111 000 m^3 (Fradet et al., 2011). These tanks allow to reduce the impacts of combined sewer overflows on the receiving environment during rain events.

The pretreatment at the East WRRF of Québec City consists in two steps: bar screens and aerated grit chambers (see Figure 3.10) . There are 4 screens with a spacing of 19 mm. They are followed by five aerated grit chambers with a length of 25 m, a width of 6 m and 4 m deep (see Figure 3.11). The maximal capacity of the pretreatment is 720 000 m^3/d leading to a maximal overflow rate of 40 $m^3/m^2/d$ and a hydraulic retention time of 6 minutes.

To remove the settled particles from the bottom of the aerated grit chamber, a scraper system is used that is travelling along the grit chamber. The grit removal is sequentially for the 5 grit chambers. The collected particles are pumped to a classifier which operates continuously. In this WRRF, approximately, 12 tons of wet grit particles are collected each day.

3.2 Sampling equipment

In this section, the equipment used to sample the liquid streams in both WRRFs is presented. The next section, i.e. Section 3.3, details how this equipment was applied.

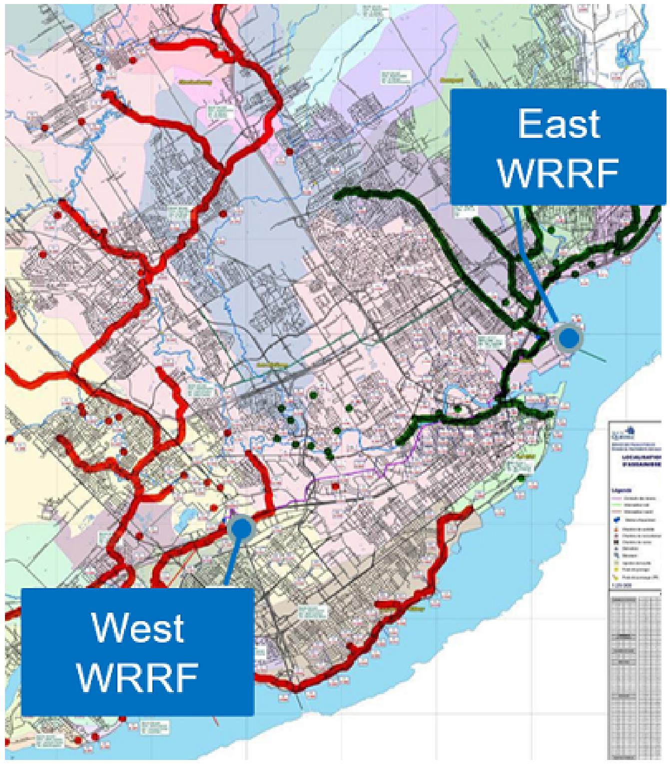

Figure 3.9: Mains pipes of the East and West parts of the sewer system of Québec City.

3.2.1 Van Dorn sampler

The *Van Dorn* equipment, normally used in rivers and lakes, comes in different sizes and the largest size available was used given the need of the particle separation tests (15 L minimum). This equipment consists in a 8.2 L bottle with two openings (see Figure 3.12). It was developed to take grab samples and it can be placed at different heights. The opening of the sample is placed face to the flow allowing to sample at the same velocity as the liquid stream.

The sampler consists in a sealed PVC cylinder of 150 mm diameter and 480 mm length, and is equipped with a 30 m nylon rope and two clippers to close the cylinder. The clipped doors are closed with a weight attached at the rope which is thrown by the user.

However, with the strength of the flow, the stability of the cylinder with the rope was poor and it was difficult to place and maintain the equipment at the desired position. Thus, some supports were fixed to control the sampler and place the sampler as desired at different heights in the channel (see Figure 3.14).

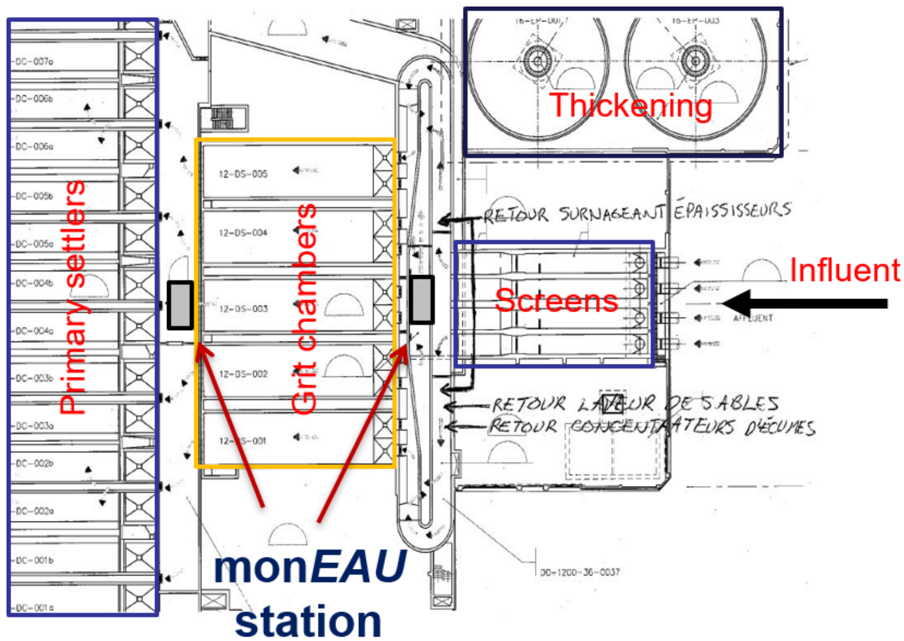

Figure 3.10: Scheme of the pretreatment and primary treatment of the East WRRF of Québec City.

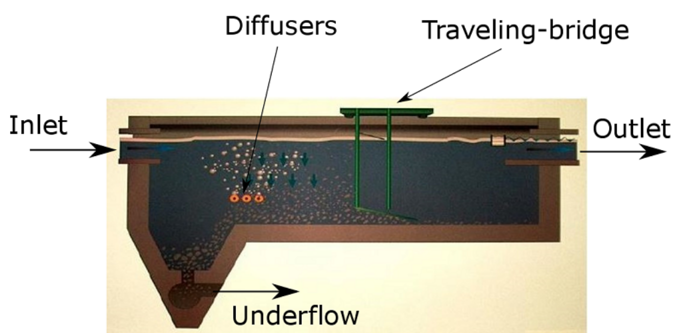

Figure 3.11: Scheme of the aerated grit chamber of the East WRRF of Québec City.

3.2.2 Multipoint sampler

The multipoint sampler consists in several points placed to cover the cross section of the channel. Then, the sample collected from the different points is homogenized. The number of points to be sampled depends on the dimensions of the channels and it will be presented in Section 3.3 specifically for each case study.

In the context of this project, two different samplers were used to sample at different points of the cross-section of the channels: manual and pumped samplers. Both of them are presented below.

Figure 3.12: *Van Dorn* sampler (Hoskin Scientific Ltd, 2019).

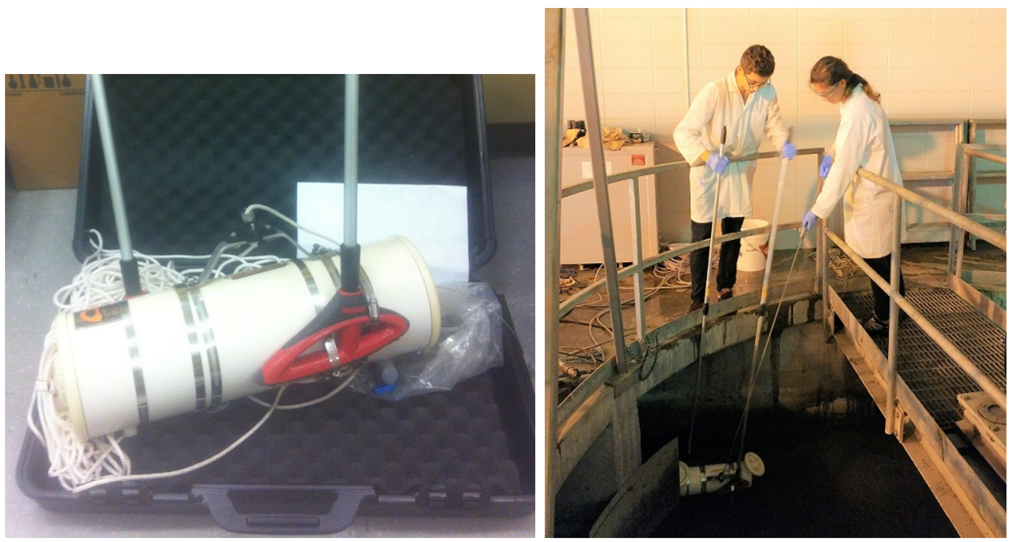

Figure 3.13: Modified *Van Dorn* sampler: (a) Fixed supports and (b) two interns (Alicia Adrović and Angel Manjarres) placing and controlling the modified *Van Dorn*.

Manual sampling

The manual sampler was built with a beaker of 500 mL attached to a rigid stick of plastic. This system allowed collecting samples at different points in the cross-section channel. Hence, particles from the entire water height in the channel, including grit particles, could be collected.

Pumped sampling

This equipment is a manifold sampler with six tubes, three multihead peristaltic pumps and two 150 L cones built by the industrial partner *Veolia Water Technologies Canada* (see Figure 3.15). With these pumps and tubes with a $\varnothing = 1$ cm, the flow velocity into the tubes was about 1900 m/h, thus allowing to also collect particles with high settling velocities such as

Figure 3.14: Manual sampler: (a) Beaker of 500 mL with its support and (b) beaker of 500 mL.

grit. This equipment was used as an alternative to sample the inlet and outlet channels of the grit chambers.

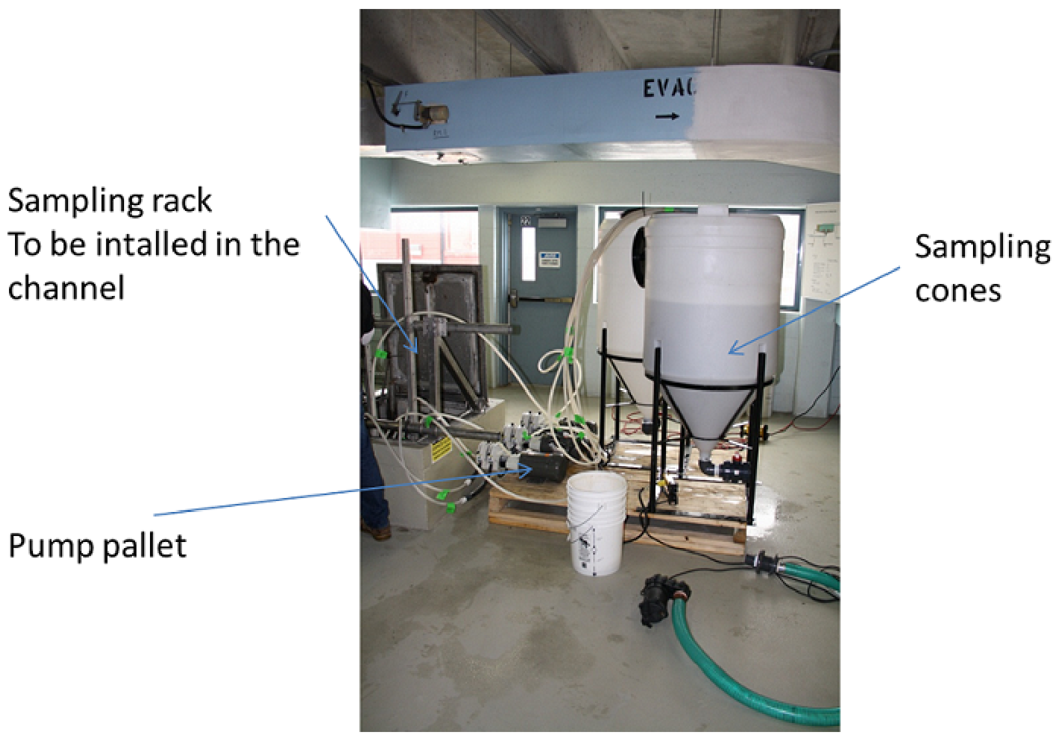

Figure 3.15: Multipoint sampler developed by Veolia Water Technologies Canada.

3.3 Sampling methods

In this section, the sampling points around the grit chamber and how the equipment presented in Section 3.2 was applied on each case study are presented.

3.3.1 Sampling points

Generally, in a GRS, five sampling points can be identified to evaluate the performance of the system (see Figure 3.16). Point 1 corresponds to the liquid stream of the influent of the GRS that is considered vertically heterogeneous because the fast settling particles may be rolling at the bottom of the channel. Point 2 is the liquid stream of the effluent of the GRS which is considered homogeneous because the fast settling particles are already removed at the grit chamber and the flow is able to keep the remain particles in suspension. Point 3 is the solid final product ready for disposal ans named grit. Point 4 is the slurry removed from the bottom of the grit chamber which is also considered homogeneous because of the turbulence of the stream. Finally, point 5 is the supernatant which contains water with organics separated from the grit in the classifier and is also considered homogeneous.

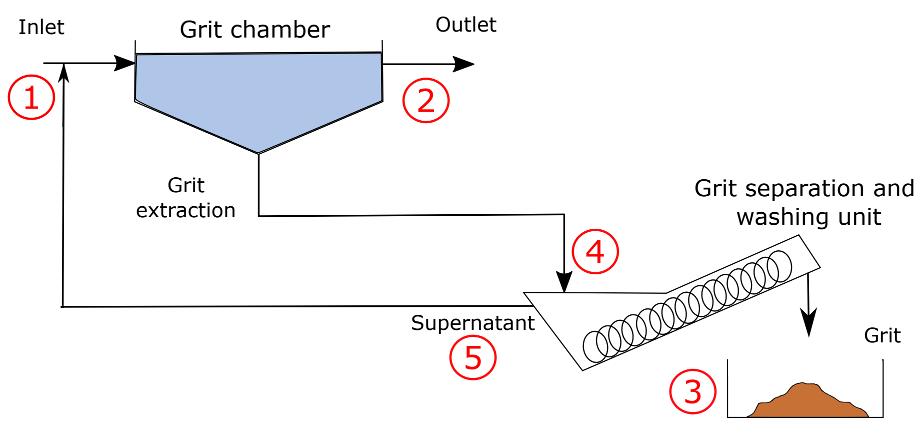

Figure 3.16: Sampling points in a grit removal system.

Only three of these sampling points were sampled to close the mass balance. Considering their relevance, sampling simplicity and human safety, the points sampled were 1, 2 and 3. Point 3 was preferred due to its simplicity compared to point 4 because the extraction system is closed without any access in both of the case studies. And point 5 has no special interest to be sampled, if point 4 cannot be sampled.

3.3.2 Sampling methods at the Saint-Nicolas WRRF

In this section, it is detailed how the inlet and outlet channels and the grit bin at the Saint-Nicolas WRRF were sampled.

Inlet and outlet channels

At the Saint-Nicolas WRRF, the inlet and the outlet of grit chamber number 2 were sampled with two different equipments: the *Van Dorn* and pumped multipoint samplers.

The *Van Dorn* sampler was lowered parallel to the bottom of the channel as presented in Figure 3.17. At the inlet, it was placed into the channel to the grit chamber. And at the outlet, it was placed at the Parshall flume as shown in Figure 3.4. These two points were selected because of their easy access. Also, in this case study, the *Van Dorn* sampler permitted to sample the entire height of the channels because of their dimensions and water height.

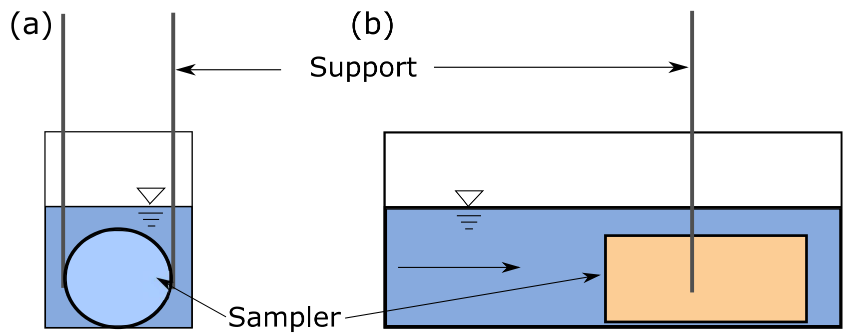

Figure 3.17: Schema of the *Van Dorn* sampler used at the Saint-Nicolas WRRF: (a) cross-section and (b) profile of the *Van Dorn* sampler as placed into the channel.

With the pumped multipoint sampler, at the inlet of the grit chamber, four sampling tubes were placed, two at the bottom (between 0 and 2 cm of height), and the other two were placed at about 10 cm height as indicated in Figure 3.18. This configuration was considered to represent the cross-section of the inlet channel. For the outlet of the grit chamber, only two tubes were installed vertically with one support similar to the inlet since this point was considered homogeneous because of the turbulence created in the grit chamber.

With both equipment, samples were collected in one or more 20L-containers depending on the volume needed for the tests. First, samples were collected at the inlet and then at the outlet, considering the hydraulic retention time. Also, at each sampled point, the sample collected with the different equipment was homogenized. For example, the 8L-samples collected with the *Van Dorn* sampler at the inlet of the grit chamber were mixed in the containers; while the four sampling tubes at the inlet of the grit chamber with the multipoint sampler were mixed

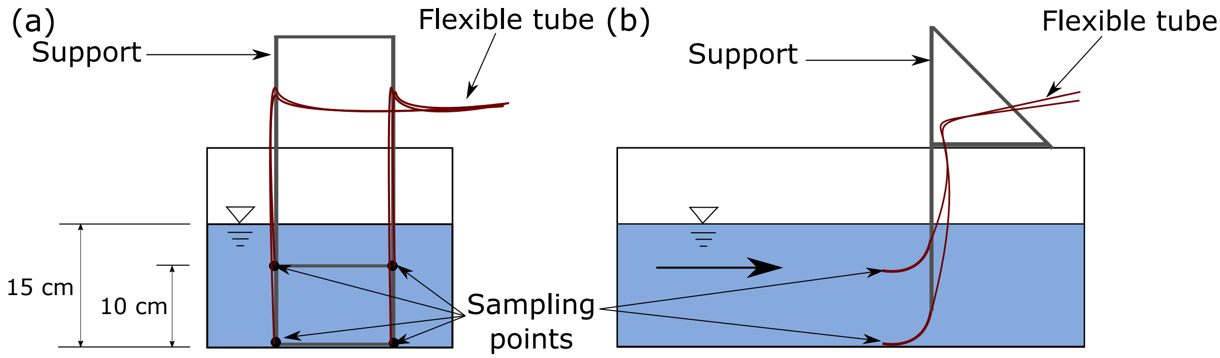

Figure 3.18: Schema of the multipoint sampler used at the Saint-Nicolas WRRF: (a) cross-section and (b) profile of the multipoint sampler as placed at the inlet channel.

in 20L-containers.

In addition, because the inlet flow dynamics depends on the pump activations upstream of the WRRF, the concentration at the inlet and at the outlet of the grit chamber at the Saint-Nicolas WRRF can vary considerably over a short period of time (e.g. between 10 - 20 minutes) (see Figure 3.3). Thus, to assure the most representative sample of the inlet and outlet of the grit chamber, two different strategies were compared: grab sample and flow proportional sample. To study both sampling strategies, the multipoint sampler was used.

Grab samples were taken during 5 minutes to fill the 20L-containers independently of the flow at the inlet of the grit chamber. The flow proportional samples were taken as follows: at high flow, every minute, 5-second samples were taken, and at low flow, every 3 minutes, also sampling during 5 seconds. The actions were repeated until the 20L-containers were filled.

A comparison was made between both equipments and the sampling strategies applied in this case study. The results are presented and discussed in detail in Chapter 4.

Grit bin

Fresh grit was collected for each grit sampling event. The extraction of the grit settled at the bottom of the grit chamber at the Saint-Nicolas WRRF can be started manually. Thus, during a sampling event, manual extraction was applied to assure the freshness of the sample. Then, with a shovel, the particles were taken from the top of the pile inside the 4 m^3 bin (see Figure 3.19) and stored in a 20L-container.

Collecting fresh grit is important because grit is a mixture of particles with inorganic and organic fractions. Hence, some degradation of the organic particles could occur in the bin before the sample was collected. To avoid any modification of the original grit particles found in the grit bin, fresh grit was preferred.

Figure 3.19: Grit bin at the Saint-Nicolas WRRF.

3.3.3 Sampling methods at the Québec City WRRF

To sample at the East WRRF of Québec City, different equipment and methods were applied. The strategies applied are presented below.

Inlet and outlet channels

The inlet and outlet channels of grit chamber number 3 (the middle one) at the East WRRF of Québec City were sampled (see Figure 3.10). The equipment used was the manual multipoint sampler presented in Section 3.2.2.

To representatively sample the inlet and outlet channels, a multipoint strategy was applied. The inlet channel was simultaneously sampled at three different points distributed horizontally in the cross-section of the channel. Then, at these three points, samples were collected along the entire height of the channel (see Figure 3.20). A certain number of beakers were filled until the desired volume was collected in 20L-container.

The outlet channel was always sampled after sampling the inlet channel considering the hydraulic retention time. Thus, the same water mass was sampled before and after the grit chamber.

The sampling strategy applied at the outlet of the grit chamber consisted in three points

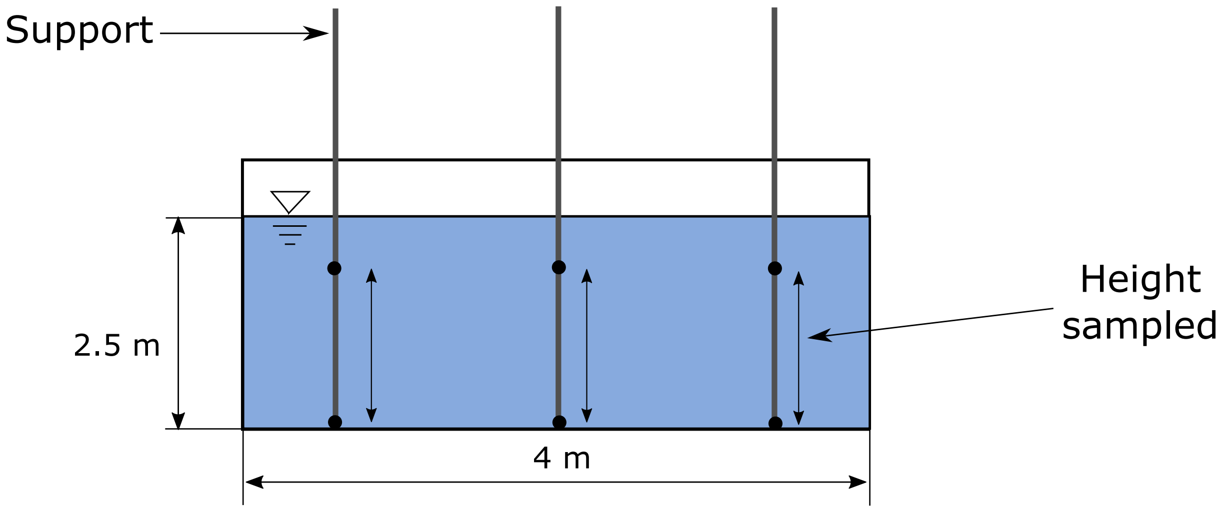

Figure 3.20: Schema of the cross-section of the inlet channel with the multipoint strategy used at the Québec City East WRRF.

distributed horizontally to sample the overflow of the outlet weirs (see Figure 3.21). Again, the three points were sampled simultaneously, considering that the outflow is homogeneous thanks to the turbulence created at the outlet. The filled beakers were also collected in containers of 20 L and the beakers were refilled as many times as needed to get the desired volume of sample.

Figure 3.21: Outlet of the aerated grit chamber at the Québec City East WRRF.

Grit bin

Similar to the Saint-Nicolas WRRF, the grit sampled was as fresh as possible. In this case, since the extraction system is operated continuously, the grit was collected directly at the top of the pile with a shovel in the operated bin (see Figure 3.22).

Figure 3.22: Grit bin at the Québec City East WRRF.

3.4 Characterization methods

Because of the diversity of methods to characterize grit and parameters to be studied as presented in Section 1.4.3, several methods were selected and adapted to study grit particles. Even though the PSVD is the preferred approach to characterize grit particles and the basic concept for the model developed, other parameters such as PSD, composition and density were also studied. All these parameters were evaluated to compare the PSVD results obtained in this study to standard grit characteristics commonly used such as as specific gravity 2.65 and $d_p > 0.21$ mm. This comparison also allowed to support the PSVD as a better approach to characterize grit with the goal to propose a new protocol to characterize grit particles based on the PSVD in view of industries to make the transition from PSD measurements and sand equivalence to PSVD measurements. The methods used in this study are summarized in Table 3.1, with more details about the methods selection provided separately in different sections.

Table 3.1: Test methods used to determine grit characteristics.

Test	Characteristics				Protocol adapted
	Particle size	**Particle settling velocity**	**Composition**	**Density**	
Dry sieving	X				ASTM (2015b)
Wet sieving	X				Reddy and Pagilla (2009)
ViCAs		X			(Chebbo and Gromaire, 2009)
Elutriation		X			(Krishnappan et al., 2004)
ISS/VSS			X		(APHA, 2012)
Pycnometer				X	(ASTM, 2015a)

Moreover, the methods presented in Table 3.1 were combined to determine the characteristics of different particle classes, for example, the study of the composition for each particle class obtained either by particle settling velocity methods or by particle size methods.

3.4.1 Sieving methods

Generally, the PSD is the most studied parameter to characterize grit particles. With this distribution, the corresponding settling velocities are subsequently estimated through the Stokes' or Newton's Laws (Equations 1.4 and 1.1, respectively) considering spherical, homogeneous particles with a specific gravity of 2.65. Despite the fact that this project is focused on PSVD characterization, the industry-standard PSD is also studied to compare these results to other studies and improve the knowledge on the particles collected in the grit bin.

In the context of this project, two different methods were used to study the particle size: dry and wet sieving. Since there is no agreement on a standard protocol to characterize grit particles by sieving, several tests were performed based on the American standard method *ASTM C136 - Standard Test Method for Sieve Analysis of Fine and Coarse Aggregates* developed by ASTM (2015b) for dry sieving and some applications presented for wet sieving in Reddy and Pagilla (2009). In both methods, fourteen stacked sieves with openings ranging from 75 μm to 13.5 mm were used: see detailed sieve sizes in Table 3.2.

Experimental sampling campaigns were also planned to study the effect of weather conditions. To evaluate these conditions, 31 samples were collected under dry and wet weather conditions and during the snow melt period, 25 at the Saint-Nicolas WRRF and 6 at the Québec City East WRRF. From the 25 samples collected at Saint-Nicolas WRRF, 16 were taken under dry weather, 6 under wet weather and 3 during the snow-melt period together with a rain event.

Table 3.2: Opening sizes of the sieves used to determine the PSD of grit particles through dry and wet sieving.

Sieve series			
Opening size ($mesh$)	**Opening size** (μm)	**Opening size** ($mesh$)	**Opening size** (μm)
0.525 inch	13 200	18	1 000
0.375 inch	9 500	30	600
3	6 700	50	300
4	4 750	70	212
6	3 350	100	150
8	2 360	140	106
14	1 400	200	75
		Plate	0

For the Québec City East WRRF, 3 of the 6 samples were collected under dry weather, and the other 3, under wet weather.

Dry sieving

As mentioned, there is no agreement on a standard protocol for dry sieving to characterize the PSD of the grit particles. Thus, the American norm *ASTM C136 - Standard Test Method for Sieve Analysis of Fine and Coarse Aggregates* developed by ASTM (2015b) was adapted to the needs of this project.

In the context of this study, between 250 and 350 g of dried sample were used to characterize the PSD of the grit particles. The sample was spread over the top sieve of the series. The stack sieve series (presented in Table 3.2) was then shaken with an automated shaker (Rotap Model B, W.S. Tyler, Mentor, OH, U.S.A.) during 15 minutes. Finally, the subsamples retained on each sieve was weighted separately and stored for further analysis to determine the composition and, occasionally, the density. The material used is presented in Figure 3.23.

To assure the quality of the results, the mass balance was calculated at the end of each test. It was compared the initial mass used for the test with the sum of the masses collected from each sieve including the bottom plate. The results were accepted as valid when the mass balance was within ± 15 %.

Wet sieving

Similar to dry sieving methods, no accepted standard protocol on wet sieving exists for grit particle characterization. In this study, a protocol was developed that was inspired by the protocol of the company *Grit Solutions* presented in Reddy and Pagilla (2009).

Figure 3.23: Dry sieving material.

After sampling the grit particles at the bin, about 100 g of wet sample was weighed prior to the wet sieving test. The sample was placed at the top of the stacked sieves series (presented in Table 3.2) as it was collected and without any pretreatment (see Figure 3.24). Then, with tap water at low pressure spread over the top sieve, the particles were rolling on each sieve allowing their classification depending on their sizes. To let the water pass through the stack of sieves, the plate was not used to recuperate the particles smaller than 75 μm. Hence, compared to the dry sieving test, the particles smaller than 75 μm were lost. The particles retained on each sieve were recovered separately, dried at 105 °C and weighed.

Figure 3.24: Wet sieving setup.

In addition, three wet samples of about 10 g were dried to determine the humidity of the sample. Then, to calculate the mass balance similar for the dry sieving test, the humidity percentage is subtracted from the fresh wet sample. This mass is then compared to the sum of the masses collected from each sieve. Again, valid results were accepted when the mass balance was less than ± 15 %. There are particles smaller than 75 μm, but this fraction represents less than 0.2 % of the total mass (see results in Chapter 5). Thus, the impact of this lost fraction on the mass balance can be neglected.

3.4.2 Settling characterization methods

As mentioned previously, the PVSD can be obtained from different methods, either under quiescent conditions or dynamic conditions (see Section 1.4.3). These methods have been indicated to be a promising new approach to characterize grit particles (Andoh and Smisson, 1996; Reddy and Pagilla, 2009). However, these methods have to be adapted to better characterize particles with high settling velocities, such as grit particles.

In the context of this study, two different methods were evaluated and compared: (i) the ViCAs protocol developed by Chebbo and Gromaire (2009) as a quiescent conditions method; and the elutriation methodology proposed by Krishnappan et al. (2004) as a dynamic conditions method. They were chosen for their large use to characterize stormwater, sewage and wastewater along the treatment chain in addition to their reliability and reproductivity, and the previous experience in the modelEAU research group (Berrouard, 2010; Maruejouls et al., 2011; Hadj, 2013).

The application of both methods in this study is described in detail in the following sections.

ViCAs

The ViCAs protocol developed by Chebbo and Gromaire (2009) is a batch settling method which has already been used to characterize stormwater and wastewater in different studies in the research group (e.g. Berrouard (2010), Maruejouls et al. (2011) and Hadj (2013)).

The original method consists in quickly (< 5 seconds) filling a settling column (H = 70 cm, ⌀ = 7 cm) with a homogenized 4.5L-sample (Figure 3.25). At determined time steps (in this case, t = 1, 3, 5, 10, 20, 35 and 60 min), the settled solids are collected at the bottom of the column; then these solids are analysed as TSS according to APHA (2012). The initial and final concentrations into the column are also measured as TSS doing triplicate filtrations.

At the end of the test, with the accumulated mass of the collected solids over the time, the PSVD is estimated. Also, the mass balance is estimated by comparing the initial mass and the mass accumulated along the test. Only tests with a mass balance error smaller than ±

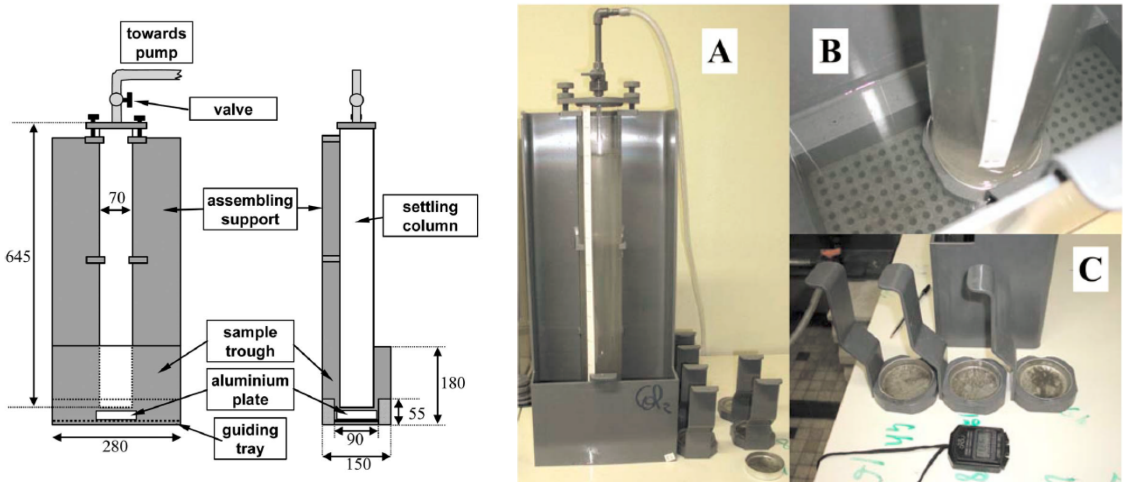

Figure 3.25: ViCAs experimental setup (Chebbo and Gromaire, 2009). (a) Diagram of the ViCAs experimental setup, and (b) Pictures of the ViCAs experimental setup: (A) settling device; (B) the bottom of the settling column; and (C) aluminium plates and plate holders to collect the particles settled. The dimensions of the column are in mm.

15 % are accepted as valid to assure the quality of the data (as Chebbo and Gromaire (2009) suggested).

With the standard ViCAs column (H = 70 cm) and the proposed time intervals, the range of settling velocities that can be studied is 35, 12, 7, 3.5, 2, 1 and 0.5 m/h, respectively. Considering that the typical critical settling velocity for grit particles, i.e. 72 m/h for a sand particle of 0.21 mm-diameter as suggested by Qasim (1999), it cannot be studied. Thus, the standard ViCAs column had to be upgraded to a higher column to better study the particles with high settling velocities like grit particles.

The new settling column was designed at model*EAU* and built by the industrial partner, *Veolia Water Technologies Canada*. It consists of a settling column with H = 2 m, and a ⌀ = 8 cm (see Figure 3.26). Then, keeping the same time intervals as for the standard 70cm-ViCAs column, the new settling velocity distribution is 120, 40, 24, 12, 6, 3.4 and 2 m/h, respectively. With this new setup, 15 L are needed instead of the original 4.5L-sample.

Elutriation device

The elutriation test allows studying the settling characteristics under dynamic conditions. Similar to ViCAs, it has also been used to study the settleability of stormwater, sewage and wastewater (Krishnappan et al., 2004; Hettler et al., 2011).

The equipment consists in a series of columns with different diameters in increasing order as presented in Figure 3.27. The sample is pulled by a pump (so as to not break the particles)

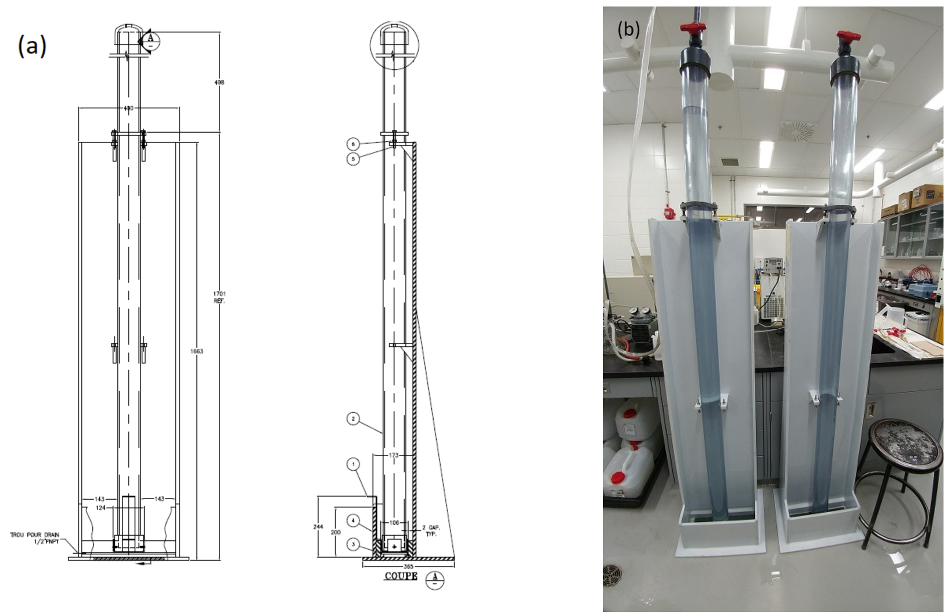

Figure 3.26: Upgraded ViCAs experimental setup. (a) Scheme of the front and side of the upgraded ViCAs column, and (b) Picture of the upgraded ViCAs column.

through each column from the bottom to the top (Krishnappan et al., 2004). Hence, the upflow velocity varies in each column and decreases as the water moves downstream. Only particles with a settling velocity higher than the upflow velocity will settle in each column. Hence, particles settled in each column can be collected separately and quantified as TSS according to APHA (2012). Note that the operating flow can be adjusted depending on the settling velocities of interest.

In this study, the elutriation protocol was adapted to study fast settling particles. The pumped flow was adjusted with two ceramic pumps, type *"Q" PUMP* from the brand CeramPump© (Fluid Metering, Inc., Soysset, NY, U.S.A.) installed in parallel giving 1.6 L/min in total. Operating only six columns with diameters of 34, 49, 70, 105, 143 and 197 mm, the upflow velocities at each column are 104, 65, 24, 11, 6 and 3 m/h, respectively (see Figure 3.28).

The volume of the samples was varied depending on the TSS concentration so as to collect sufficient particles in each column. During the tests, samples of a minimum of 20 L were used. In addition, to keep the raw sample homogeneous, a mixer was installed inside the container with a rotation velocity of 100 RPM considering that there is no impact on the particles at this rotation speed.

Before to start the test, the columns are filled with tap water, and are verified for leaks. Afterwards, the raw sample is passed through the system. Once there is no sample left, the container installed at the inlet of the elutriation system is filled with tap water again to avoid that suspended particles with low settling velocities remain in the columns. The test is run

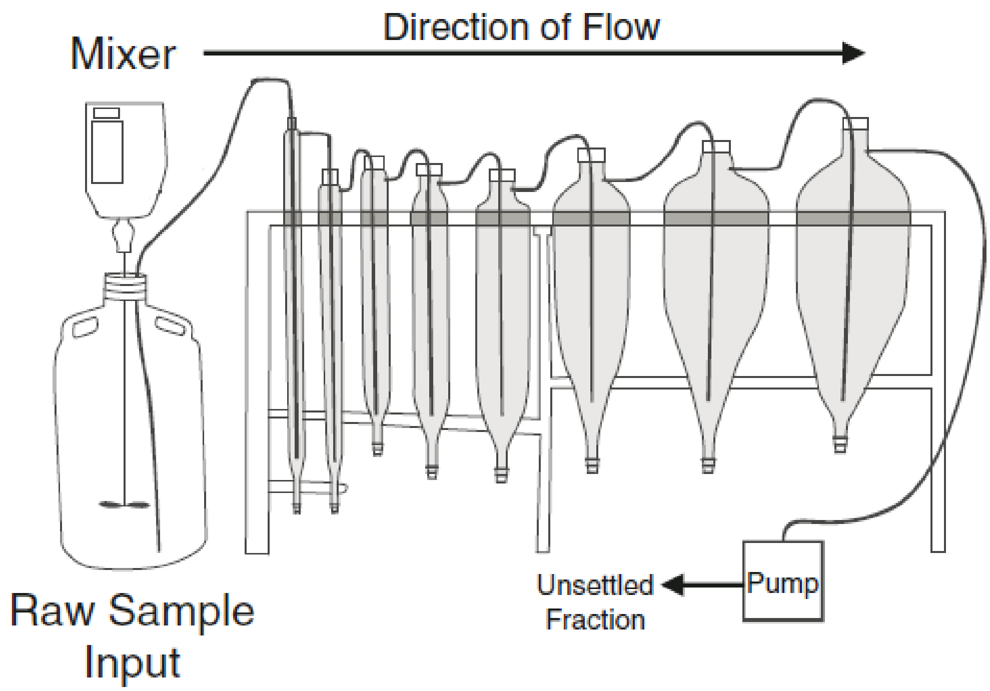

Figure 3.27: Schema of the elutriation system built by Krishnappan et al. (2012).

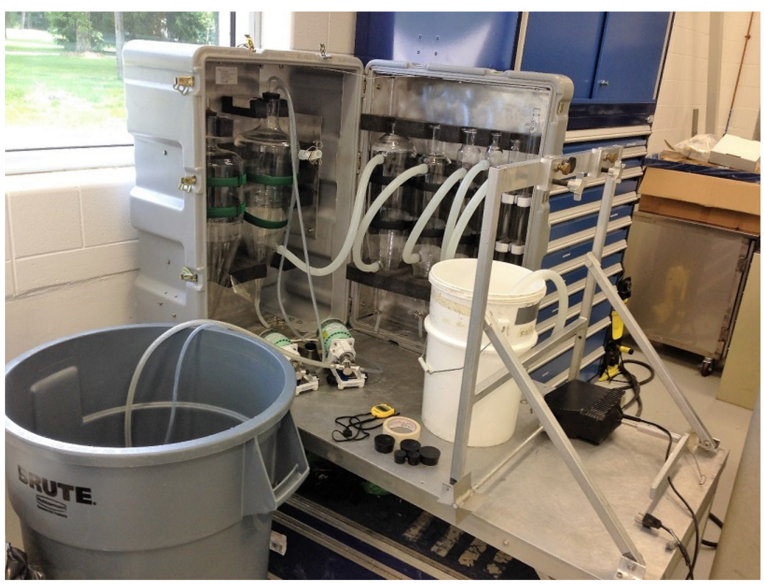

Figure 3.28: Picture of the elutriation setup used in this study.

for at least three times the hydraulic retention time of the system. In this case, since the operating flow was 1.6 L/min, the retention time was 15 minutes. Thus, the tests were run for a minimum of 45 minutes.

At the end of the tests, as mentioned above, the particles settled in each column are collected separately and measured as TSS. Also, the initial TSS concentration of the sample tested and the concentration of the sample collected at the end of the series of settling columns is also measured. These concentrations are measured as triplicates of the filtrations. Again, the mass balances are estimated by comparing the initial mass and the masses collected in each column and the effluent container. Similar to ViCAs tests, only tests with a mass balance error lower than ± 15 % are accepted as valid.

3.4.3 Analytical methods

Further to PSD and PSVD methods, other tests were done on the different particle classes classified either by their size or by their settling velocity. The goal of these analyses was to characterize the particle classes in terms of composition (i.e. inorganic and organic fractions) and density which both have an impact on the settleability of the particles.

Composition characterization

Following the standard methods of APHA (2012), the inorganic/organic ratio of the particle was studied for the different particle classes obtained by both size and settling velocity methods.

After weighing the particle fractions obtained from dry sieving, a maximum of 5 g was taken from each dry fraction and burnt at 550 °C in a muffle furnace for 1 hour. After burning each fraction, the inorganic/organic ratio can be estimated. The mass that remains in the plate was also weighed and the inorganic fraction (inorganic solids, IS, for the sieving tests and inorganic suspended solids, ISS, for the ViCAs and elutriation tests) was estimated. The difference between the initial mass and the ISS allows to determine the volatile fraction (volatile solids, VS, for de sieving tests, and volatile suspended solids, VSS, for the ViCAs and elutriation tests).

For the wet sieving, first, the entire mass collected in each sieve is dried at 105 °C in an oven for 12 hours and weighed before they are burnt at 550 °C following the same methodology as the particle classes from the dry sieving.

The particle classes obtained from the ViCAs and elutriation tests were first dried at 105 °C to determine the total TSS collected for each class. Then, to estimate the inorganic and organic fractions, they were also burnt at 550 °C. From the mass differences before and after burning the samples, the ISS and VSS are calculated.

Density

Due to the uncertainty and diversity observed in the literature regarding the density of grit particles, several density analysis were performed on different particle classes collected in dry sieving tests. Those analyses were performed with a helium pycnometer AccuPyc© II 1340 (Micromeritics, Norcross, GA, U.S.A) under American norm *D5550-14: Standard Test Method for Specific Gravity of Soil Solids by Gas Pycnometer* presented by ASTM (2015c).

For the density analysis, about 9 cm^3 of each particle class is needed. A sample is placed in a $10cm^3$-cell specifically built for the pycnometer equipment. Before the start of the helium injection into the cell to fill the voids, the samples are weighed at high precision (i.e. 0.0001 g). Finally, knowing the volume of the injected helium, it is possible to estimate the real volume of the sample, thus allowing to calculate the specific density of the particles.

3.5 Hydraulics study

The HRT of grit chambers is really low compared to other process units of a WRRF (as mentioned in Section 1.5, 2-5 minutes for aerated grit chambers and 20-30 seconds for vortex grit chambers) (Qasim, 1999; Tchobanoglous et al., 2014). Logically, it has an influence on their efficiency.

Together with the particle settling characteristics, the hydraulics in a grit chamber was also evaluated to develop a simplified conceptual model adapted for vortex and aerated grit chambers.

The basis of the hydraulics can be simply studied with non-reactive tracer substances (Levenspiel, 2012). Similar to other hydraulic studies on grit chambers (e.g. Morales and Reinhart (1984), Sawicki (2004)), in this study, pulse input tracer tests (Dirac pulse) were performed with Rhodamine WT fluorescent dye because this tracer has no influence on the hydraulic behaviour of the tank. In other terms, it does not modify the transport characteristics of water, does not change the density of the water, does not react with the solids, is highly soluble and not toxic (Gujer, 2008).

This type of tracer test is the most frequently applied method for the characterization of full-scale systems. It consists of an injection of a well-known mass at time 0 at the inlet of the reactor (in this case study, at the inlet of the studied grit chambers). The tracer has to be injected as fast as possible (Gujer, 2008), not exceeding 1% of the theoretical retention time (V/Q) (Teefy, 1996; Gujer, 2008).

Two tracer tests were performed at Saint-Nicolas WRRF at different flow conditions and following the protocol developed by the model*EAU* research group (modelEAU, 2015). Since the inlet channel of the vortex grit chambers is already split before the screens, the tracer tests were only done for grit chamber number 2 (as indicated in Figure 3.4). The tracer was injected right after the screens because it was the only accessible and open point between the screen and the grit chamber. It was assumed that the tracer was perfectly mixed and dissolved with the water mass when it reached the inlet of the grit chamber.

The duration of the tracer test was estimated as three times the theoretical HRT of the studied grit chamber. In this case study, the theoretical HRT varies between 1 and 5 minutes depending on the pump flow rate (see Section 3.1.1). Thus, the duration of the test had to be approximately 15 min. However, in both tracer tests, samples up to 20 minutes were taken.

Given the short HRT of the vortex grit chamber, a peristaltic pump was used to sample quickly and continuously the outlet of the studied vortex grit chamber. This setup allowed to collect 30 mL samples every 5 seconds during the first 5 minutes. After these 5 minutes, 30 mL samples were collected every 20 seconds.

Noteworthy during the test, there was no grit extraction. Thus, the underflow was zero. However, at the end of the test, a manual extraction was started to determine whether some tracer had accumulated in the lower part of the grit chamber during the test. Three samples were taken at point 5 (see Figure 3.16) along the 20 minutes of grit extraction.

In case of the aerated grit chambers, two tracer tests were performed in the context of other studies (Tik and Vanrolleghem, 2017). The methodology followed, the experimental conditions studied and the development of the hydraulic model are presented in the mentioned paper Tik and Vanrolleghem (2017) and detailed in the thesis of Tik (2019).

3.6 On-line data

To study the dynamics of the system, automated monitoring stations with sensors were installed at the inlet and outlet of the grit chambers. With it, long-term continuous on-line data at high frequency were collected. In these case studies, the frequency data was 10 seconds.

The automated monitoring stations used were the RSM30 stations built by Primodal (Hamilton, ON, Canada) (see Figure 3.29) (Primodal, 2019). They are a versatile design of water monitoring equipment according to Rieger and Vanrolleghem (2008). Thus, they offer flexibility to be installed wherever it is desired, and different sensors from different brands can be connected (see Figure 3.29).

In both case studies, the stations were equipped with several sensors to measure turbidity and conductivity. Turbidity sensors were installed at the inlet and outlet of the grit chamber to study the TSS dynamics around the studied units since this is the parameter of interest.

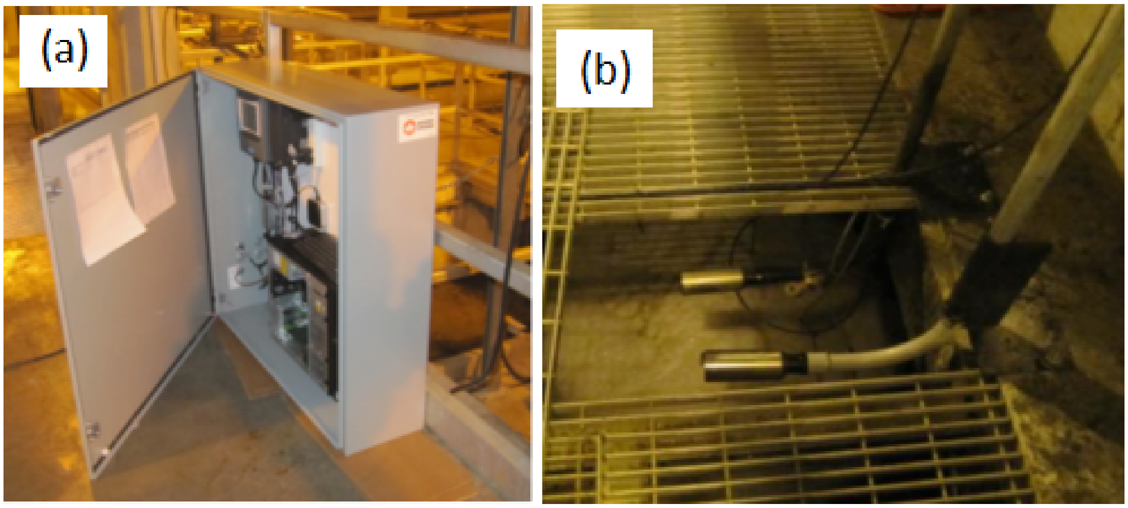

Figure 3.29: Automated monitoring station installation (Alferes et al., 2013). (a) Protection box of the data logger and the data collection system built by Primodal (2019) and (b) turbidity sensors installed at the Québec East WRRF.

Conductivity was also installed to evaluate the dilution effect of rainfall.

The methodology proposed by Plana (2015) was adapted and applied for proper maintenance of the monitoring stations as well as proper data management and treatment to obtain good quality data series on the case studies.

In the following sections, more details are provided about the deployment of the sensors on each case study and how the on-line data were processed before use for modelling.

Sensor installation at the Saint-Nicolas WRRF

At Saint-Nicolas WRRF, only one automated monitoring station was needed since the inlet and the outlet channels (points 1 and 2, respectively, in Figure 3.16) are next to each other (as presented in Figure 3.4). As mention in Section 3.3.2, grit chamber number 2 presented in Figure 3.4 was monitored.

In this case study, the automated monitoring station was equipped with five sensors: three turbidity sensors, one conductivity sensor and one UV-VIS spectrometry sensor. The turbidity and conductivity sensors were manufactured by WTW (a Xylem brand, Rye Brook, NY, U.S.A.), and the UV-VIS spectrometry sensors was manufactured by s::can (Vienna, Austria). Detailed information on the sensors and their measurement principle can be found in WTW (2019) and s::can (2019).

At the inlet, two WTW turbidity sensors and the conductivity sensor were deployed as presented in Figure 3.30. The conductivity since is temperature dependant, the correponding sensor also measures this variable. The two turbidity sensors were installed at different heights to study the heterogeneity in the vertical profile of the inlet channel. As mentioned, even though the conductivity is not a parameter of interest to model grit chambers, the conductivity sensor was installed to detect rain events and the snow melt period as explained in Section 1.3.2.

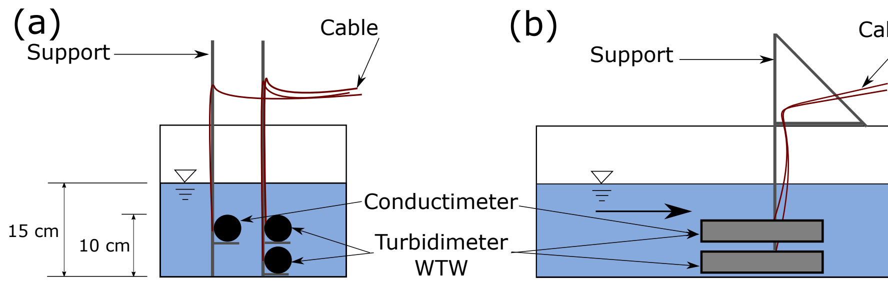

Figure 3.30: Scheme of the sensor locations at the inlet of the studied vortex grit chamber at the Saint-Nicolas WRRF.

At the outlet, one WTW turbidity sensor and the UV-VIS spectrometry sensor were installed as depicted in Figure 3.31. The UV-VIS spectrometry sensor can measure different variables depending on its application. In the case of raw wastewater application, the measured variables are TSS, total chemical oxygen demand (COD), soluble chemical oxygen demand (COD_s) and nitrate. However, for this case study, only TSS was considered.

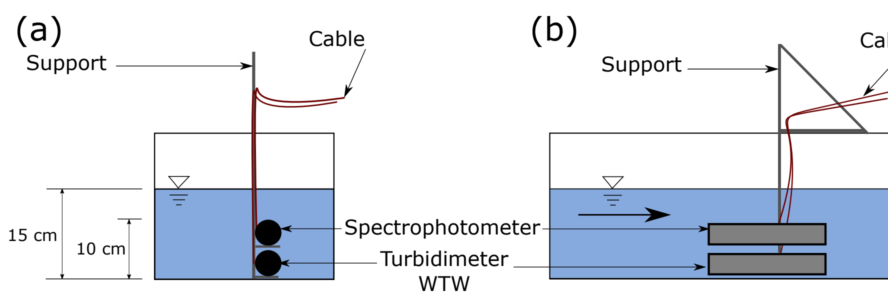

Figure 3.31: Scheme of the sensor locations at the outlet of the studied vortex grit chamber at the Saint-Nicolas WRRF.

Sensor installation at the Québec City East WRRF

At the East Québec City WRRF, two different RSM30 automated monitoring stations were installed at the inlet and outlet channels (points 1 and 2 in Figure 3.16) of aerated grit chamber number 3 (see Figure 3.10) during the summer of 2014 in the context of the PhD thesis of Tik (2019). The collected data at the inlet and outlet of the aerated grit chambers have also been used in this PhD study.

Each automated monitoring station at the East Québec City WRRF was equipped with one turbidity sensor, one conductivity sensor, one pH sensor and one UV-VIS spectrometry sensor. The turbidity, conductivity and pH sensors were manufactured by WTW and the UV-VIS probe was manufactured by s::can.

In both channels, the sensors and the setup were the same (see Figures 3.32 and 3.33). The difference between both installations was the height at which the sensors were placed into the channel. In both cases, the sensors were placed at the half height of the water level, but at the inlet the water level is higher than the outlet. Thus, the sensors at the inlet were placed at a higher height than the sensors at the outlet as can be observed in Figures 3.32 and 3.33.

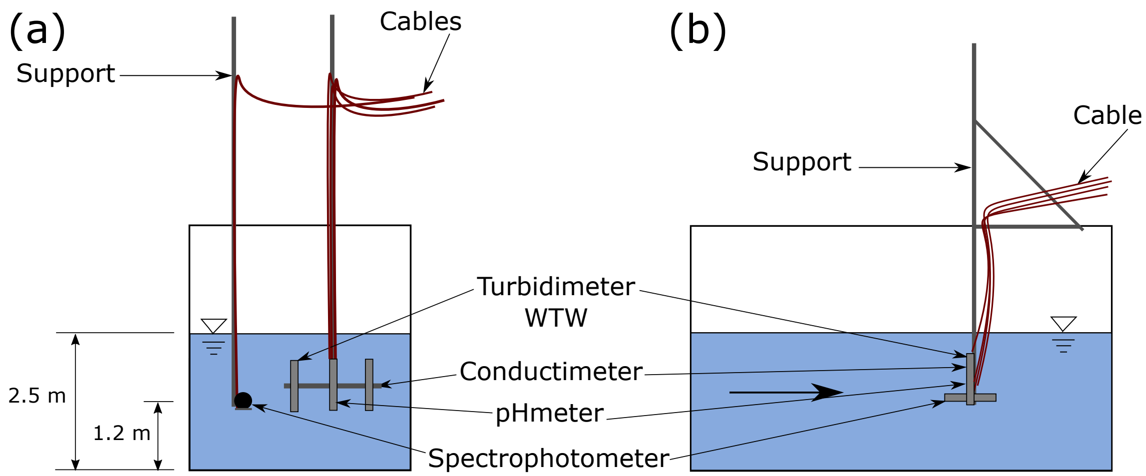

Figure 3.32: Scheme of the sensor locations at the inlet of the studied aerated grit chamber at the East Québec City WRRF.

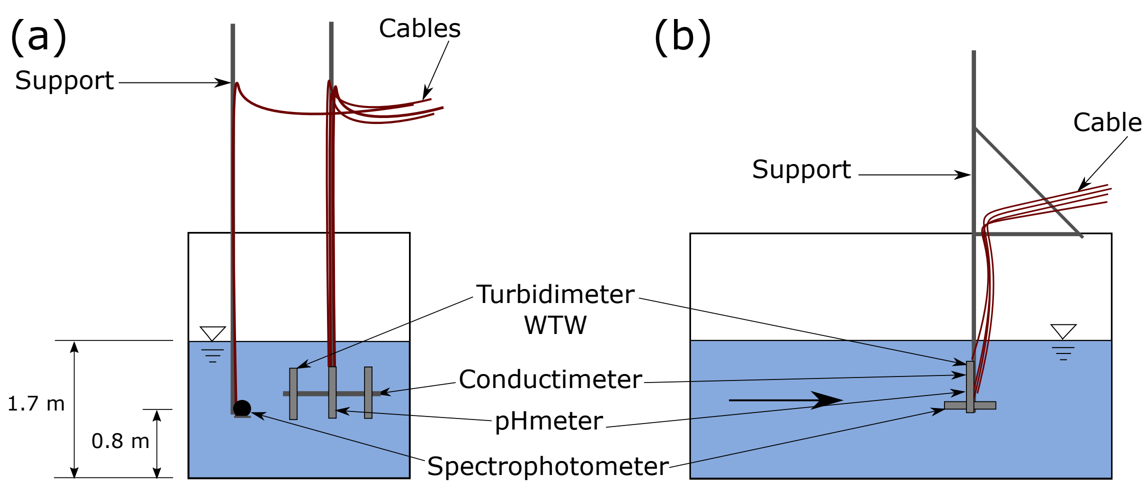

Figure 3.33: Scheme of the sensor locations at the outlet of the studied aerated grit chamber at the East Québec City WRRF.

Data treatment

The RSM30 on-line monitoring stations were used to collect data at high frequency. However, a proper procedure to assure their quality had to be applied since some issues, such as noise, missing values or systematic errors, were present because of the severe environmental conditions (Mourad and Bertrand-Krajewski, 2002; Alferes et al., 2013).

Univariate off-line and on-line methods proposed by Alferes and Vanrolleghem (2016) were combined to evaluate and validate the collected high frequency data (see Figure 3.34). Off-line methods were applied to detect bad calibration situations and systematic errors on the sensors' behaviour (Alferes et al., 2013). On-line methods were used to detect outliers, bias, or other unusual situations (Yoo et al., 2008).

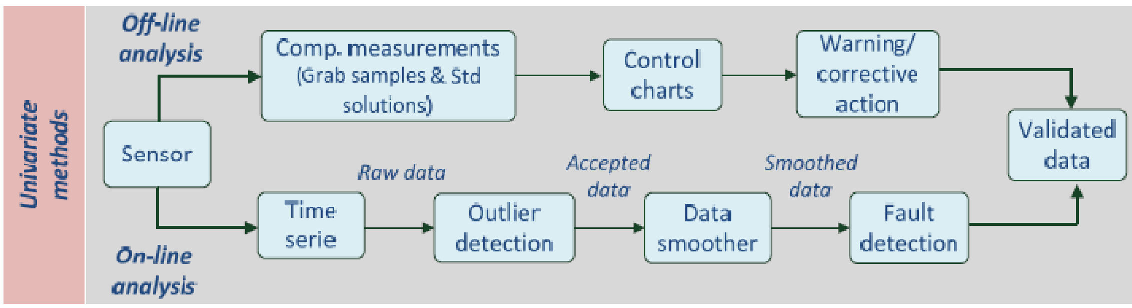

Figure 3.34: Schema of the off-line and on-line univariate methods for water quality data assessment (Alferes et al., 2013).

The off-line analyses consisted in the comparison of the on-line measurements with reference values to detect out-of-control situations by using control charts as proposed by Walter A. Shewhart (Montgomery, 2008). The detailed procedure followed was presented in Plana (2015).

The on-line analysis for fault detection permits to detect outliers and faults. The methodology applied was proposed by Alferes and Vanrolleghem (2016) and it consisted in three different consecutive steps:

1. *Outlier detection*: Autoregression models are used to predict forecast values considering historical data. Then, the forecast values are compared with the measured values. If it falls outside a confidence interval, is is considered as outlier, and is replaced by the forecast value.

2. *Data smoothing*: A Kernel smoother with a proper bandwith using a nonparametric regression is applied to remove the noisy data.

3. *Fault detection*: Some time series features, such as slope, realistic range, % forecast values to replace outliers in a time window of data, autocorrelation of the residuals,

and residuals standard deviation, are estimated together with their acceptability limits. Finally, each data value is either considered as *valid* or *not valid*.

In the context of this thesis, the goal is not to present in detail how on-line data was treated thus, only *validated data* are shown in Chapters 7 and 8. More details about the applied data treatment are presented in Alferes and Vanrolleghem (2016). Some application examples can also be found in Plana (2015).

3.7 Modelling tools

All modelling work was performed with the modelling and simulation software WEST© 2017 (MIKE powered by DHI). This software allows to model and relate dynamically most of the physical, chemical and biological processes in WRRFs, sewer systems and rivers. The main applications of the software include: evaluate a process design, monitor plant operation and troubleshooting, process optimization, develop control strategies, calibrate models, model integrated urban wastewater systems and develop, calibrate and test new models (DHI, 2019).

The software is equipped with a user-friendly interface and a model library written in MSL-USER (MSL meaning model specification language). MSL is a high-level object-oriented language which allows incorporating models with the goal to maximize knowledge re-use (Vanhooren et al., 2003).

The interest in using WEST© lies in the modelling environment, promoting the re-use of model knowledge, and the experimentation environment, to optimize accuracy and calculation performance (Vanhooren et al., 2003). In addition, since it is an open source language, there is full accessibility to the code of the model library to modify, improve and relate existing models as well as efficiently introduce new models that extend/modify existing ones.

Chapter 4

Site-specific sampling methods

4.1 Introduction

Given the importance to collect representative samples and the challenges they cause given the wastewater characteristics as presented in Section 1.4.1, this Chapter addresses the specific objective 1.a, proposing a sampling method in the context of this PhD study.

The sampling equipment presented in Section 3.2 and the sampling methods used for the Saint-Nicolas WRRF case study presented in Section 3.3.2 were compared. Results are presented in the following sections.

This Chapter has been separated in two main parts. The first one presents the comparison between the two different equipments used. In the second part two, different sampling strategies were applied for the same case study.

4.2 Comparison of the sampling equipment

First, the two sampling devices used to sample around the grit chamber at the Saint-Nicolas WRRF presented in Section 3.3.2 (i.e. the multipoint and *Van Dorn* samplers) were compared.

To compare both methods, only samples at the inlet of the grit chamber were collected since the inlet channel is more heterogeneous and thus more difficult to sample representatively. The samples collected with both devices were taken at the same time as follows: while the multipoint sampler was pumping raw wastewater from the inlet channel into the 20L-containers, samples with the *Van Dorn* sampler were collected into other 20L-containers time proportionally distributed to the sampling time with the multipoint sampler. For example, when sampling with the multpoint sampler during 20 minutes, 4 samples with the *Van Dorn* were collected: the first sample between minutes 0 and 5 after sampling started with the multipoint sampler, the second sample between minutes 5 and 10, the third sample between minutes 10 and 15, and the last sample, between minutes 15 and 20. Both sampling devices were compared in terms of PSVD using the 2m-ViCAs columns presented in Section 3.4.2.

In the context of this part of the study, five samples were collected to compare both devices. TSS concentrations of the samples collected were varying between 100 and 280 mg/L. In Figures 4.1 and 4.2, two examples are shown with measured TSS concentrations about of 255 and 185 mg/L, respectively.

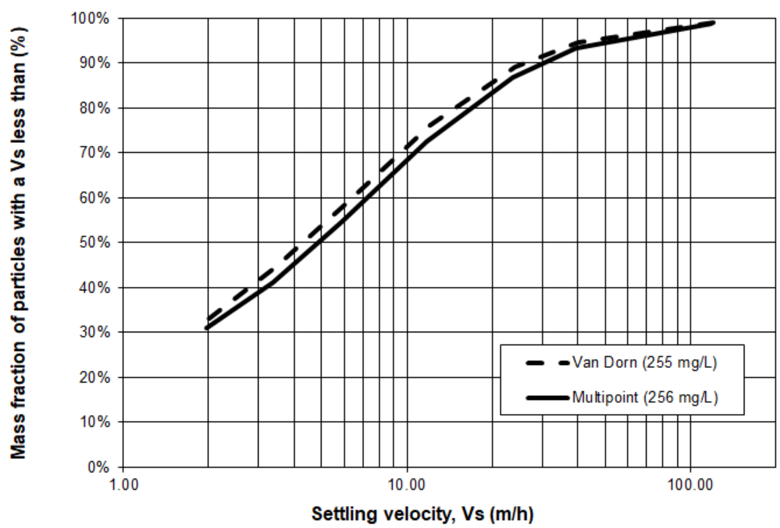

Figure 4.1: PSVD curves from samples collected with the multipoint and *Van Dorn* samplers at a TSS concentration of 255 mg/L.

The TSS concentrations in both samples obtained with both sampling devices were not significantly different (difference $\leq 10\%$). Comparing the PSVD curves, similar behaviour was also observed within the samples collected for one sampling event. In Figures 4.1 and 4.2, small differences are noticed between the two PSVD curves presented on each graph, especially for high settling velocities fractions (differences varying between 5 % and 25 % depending on the fraction). The PSVD curve obtained with samples collected with the multipoint sampler are not consistently above or below the PSVD curves obtained with samples collected with the *Van Dorn* sampler.

In case of the Saint-Nicolas WRRF, the *Van Dorn* sampler was able to sample the entire height of the inlet and outlet channel similar to the multipoint sampler (see Figure 4.3). Hence, this feature may explain the small differences between the PSVD curves obtained with both sampling devices.

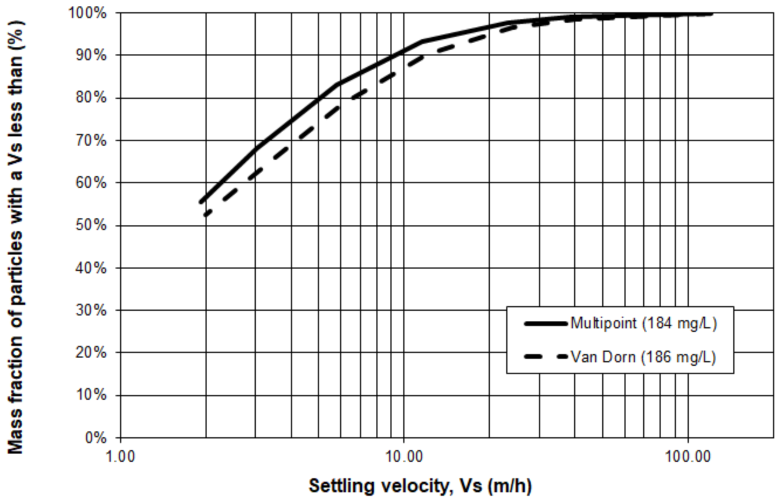

Figure 4.2: PSVD curves from samples collected with the multipoint and *Van Dorn* samplers at a TSS concentration of 185 mg/L.

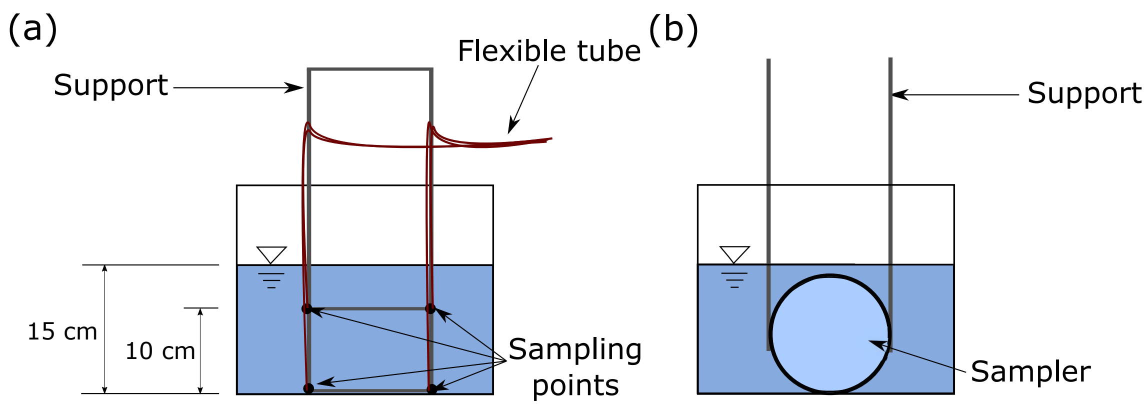

Figure 4.3: Cross-section schema of (a) the multipoint and (b) the *Van Dorn* samplers at the Saint-Nicolas WRRF.

4.3 Comparison of the sampling strategy

As presented in Section 3.1.1, in the Saint-Nicolas WRRF, part of the wastewater is pumped to the WRRF. The pump activations have a high impact on the inlet flow dynamics varying over short periods of time (e.g. between 10 - 20 minutes) (see Figure 3.3). The TSS concentrations at the inlet and at the outlet of the grit chamber could be affected by these dynamics.

To assure the most representative sample at the inlet and outlet of the grit chamber, two different strategies were compared: grab sampling and flow proportional composite sampling. Both strategies were compared using the multipoint sampler to collect the sample and the

2m-ViCAs column to characterize the sample in terms of PSVD.

The flow proportional samples were obtained by sampling during 5 seconds every minute at high flows and during 5 seconds every 3 minutes at low flows. Sampling was continued until sufficient volume was collected for the lab tests (e.g. samples collected for 1h - 1h30). The grab samples were collected by quickly filling the 20L-containers after the flow proportional samples had been collected. In addition, the inlet and outlet channels were sampled simultaneously using both sampling strategies.

For this part of the study, three samples were collected to compare the sampling strategies. The TSS concentrations from these samples were ranging between 200 and 320 mg/L for the inlet and 220 and 320 mg/L for the outlet. Figures 4.4 and 4.5 present examples of PSVD curves from the inlet and outlet channel, respectively.

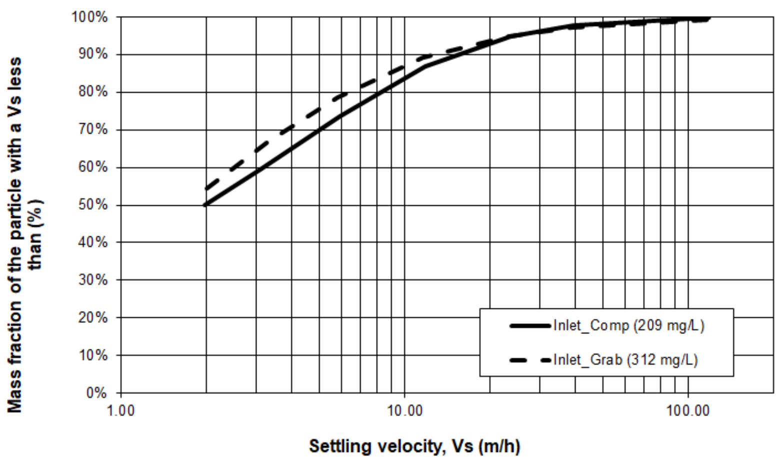

Figure 4.4: PSVD curves from grab and flow proportional samples collected with the multi-point sampler at the inlet of the Saint-Nicolas WRRF.

Comparing the TSS concentrations between grab and composite samples, large differences were observed. Due to the important dynamics, the TSS concentration of a grab sample can be higher or lower than the TSS concentration of a composite sample. In the results presented (Figures 4.4 and 4.5), the TSS concentration of the grab sample is higher than the TSS concentration of the composite sample for both inlet and outlet. This difference can be explained by the possibility that at the moment that the grab sample was collected, the TSS concentration in the inlet or outlet was particularly high.

Despite the fact that the TSS concentrations observed in the two samples collected with the two different sampling strategies are significantly different, the PSVD curves are similar for both the inlet and the outlet samples. This can be due to the fact that the composite samples were collected in only about 1h - 1h30 and given this short sampling time, the settling

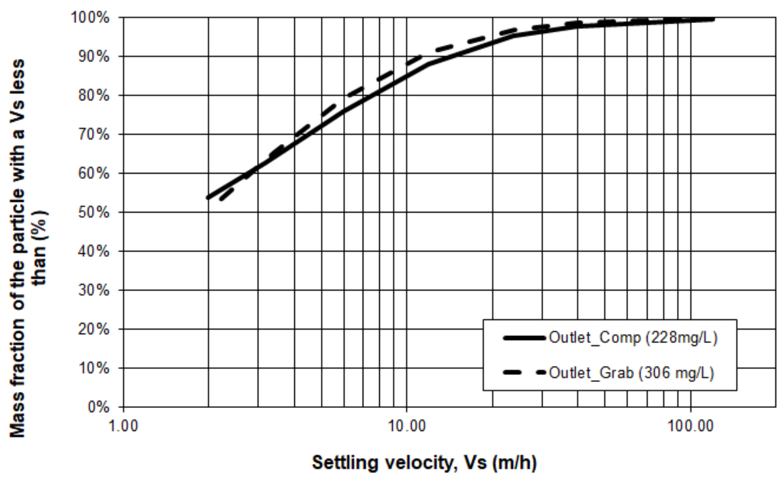

Figure 4.5: PSVD curves from grab and flow proportional samples collected with the multi-point sampler at the outlet of the Saint-Nicolas WRRF.

characteristics between samples do not change even though the TSS concentrations do differ.

In terms of characterization of settling of the particles collected with the two sampling strategies, both strategies were considered acceptable (differences $\leq 5\%$, see Section 6.2.3 for more details) to obtain representative samples of the inlet and outlet channels. However, one sampling strategy, *in casu*, the grab sampling strategy was selected for the entire sampling campaign because of the low sampling time required (between 5 - 10 minutes).

4.4 Conclusions

In this case study, both sampling devices can be used indifferently to sample the inlet and outlet channels at the Saint-Nicolas WRRF since both devices allow sampling the entire water height of the channels, thus representing the cross-section.

Moreover, it was observed that grab and composite samples can largely differ on the TSS concentrations but not significantly on the particle settling characteristics. Thus, the grab sampling strategy was chosen because of the similarity of the PSVD curves and the time-consuming collection of composite samples. Being consistent on the sampling strategy allowed comparing PSVD curves in the further studies.

After comparison of the sampling equipment and strategies at the Saint-Nicolas WRRF, it has been concluded that both sampling devices and both sampling strategies can be applied indifferently. However, further studies should be performed at other WRRF to compare both sampling devices and sampling strategies to determine whether the sampling device and strategy to be applied are site-specific and to evaluate the importance of representing the cross-section of the channel to be sampled.

Chapter 5

Particle size characterization methods

5.1 Introduction

This chapter addresses specific objective 1.b related to the study of the current methods used to characterize the particles around a grit chamber. The most common methods used to characterize the particles around a GRS are sieving methods. Thus, a critical evaluation of these methods used to characterize grit particles is presented. These methods are compared in terms of particle sizes, composition and density. Also, the impact of weather conditions on the characteristics of the grit particles is shown.

The results obtained in this part of the PhD thesis have already been published in a peer-reviewed journal:

- Q. Plana, J. Carpentier, F. Tardif, A. Pauléat, A. Gadbois, P. Lessard and P.A. Vanrolleghem (2018). Grit particle characterization: Influence of sample pretreatment and sieving method. *Water Science & Technology*, 78(6):1400-1406

In addition, the results related to the impact of weather conditions which were published in conference proceedings, have also been included in this chapter:

- Q. Plana, J. Carpentier, F. Tardif, A. Pauléat, A. Gadbois, P. Lessard and P.A. Vanrolleghem (2017). Influence of sample pretreatment and weather conditions on grit characteristics. In: *90th Annual Water Environment Federation's Technical Exhibition and Conference; WEFTEC2017*, Chicago, IL (USA), 2nd to 4th October 2017

5.2 Grit particle characterization: influence of sample pretreatment, sieving method and weather conditions

Abstract

Grit causes problems in water resource recovery facilities (WRRFs): clogging pipes, damaging pumps, and reducing the active volume of aeration tanks and anaerobic digesters by grit accumulation. Grit chambers are built to remove these particles. However, no standardized methodology exists to characterize grit particles for grit chamber design and operation despite the large observed variability in grit composition. Therefore, this paper proposes a combination and adaptation of existing methods to sample and characterize grit particles in view of proper grit chamber design and its modelling to ultimately optimize the efficiency of this important WRRF unit process. Characteristics evaluated included particle size distribution from sieving after different sample pretreatments, organic/inorganic fractions, and density.

5.2.1 Introduction

Grit accumulation and grit-induced damage can be reduced by installing a grit chamber at the headworks of a water resource recovery facility (WRRF). However, for this treatment to be successful, grit chambers should be designed and operated properly (WEF, 2010). Commonly, for grit chamber design, grit is defined as inorganic settleable particles larger than 0.21 mm with a specific gravity of 2.65 or higher such as sand, gravel, cinders or other heavy materials (U.S. EPA, 2004). Moreover, since a discrete settling process is observed in a grit chamber and the settling velocity is thus the key parameter, this last parameter is generally estimated through Newton's or Stokes' Laws (Tchobanoglous et al., 2014; WEF, 2016). Despite the fact that Newton's Law is more accurate to estimate the settling velocity of a grit particle taking into account the shape and the turbulent flow conditions, Stokes' Law is presented for an easier interpretation of the results presented in this paper:

$$v_s = \frac{g \cdot (\rho_p - \rho_w) \cdot d_p^2}{18 \cdot \mu} \tag{5.1}$$

where v_s is the settling velocity (m/s), g the acceleration due to gravity (m/s^2), ρ_p the particles' specific gravity (kg/m^3), ρ_w the specific gravity of water (kg/m^3), d_p the diameter of the particles (m), and μ the water viscosity $(kg/(m \cdot s))$.

Recent studies start to question whether the definition of grit based on particle sizes (bigger than 0.21 mm) and the sand specific gravity (bigger than 2.65) is correct to estimate the settling velocity of grit particles, and subsequently, for grit chamber design (Barter and Sherony, 2011;

Herrick et al., 2015). For example, Barter and Sherony (2011) conclude that grit settles at a lower rate because of the organic matter attached to the inorganic particles. Thus, the settleability of grit particles (and consequently the efficiency of the grit chamber) varies with the density, depending on the particle's composition.

Hence, for proper design and operation of grit chambers, grit particles should be well-characterized and representatively sampled. Currently, there is a wide diversity of grit characterization procedures and of variables to be determined to characterize grit (WEF, 2016). Surprisingly, however, no standard peer-reviewed characterization and sampling protocols exist yet (WEF, 2016). The diversity in procedures can be explained by the difficulty in obtaining a representative sample and the unclear grit definition (Reddy and Pagilla, 2009; Rife and Botero, 2012).

Added to the lack of standard characterization and sampling protocols, the characteristics of the particulate pollutants at the streams around a grit chamber (inlet, outlet and underflow) are hardly documented and the efficiency of grit removal is uncertain since grit particles are still found in the downstream processes where they cause long-term problems (Andoh and Smisson, 1996; McNamara et al., 2014).

Recently, the Water Environment Federation's grit task force suggested a new definition of grit based on the settling velocity of the particle as it exists in the raw wastewater (WEF, 2016). Also, WEF (2010) added that specific gravities can lie between 1.1 and 2.65. Thus, a wide heterogeneity of the particles is observed, and it creates a vertical stratification in the raw wastewater arriving at the grit chamber, inducing sampling problems (Ashley et al., 2005; WEF, 2016).

Due to the diversity of grit definitions and the concepts included in those definitions, i.e. particle size, specific gravity and settling velocity, a wide diversity of characterization methods exists (WEF, 2016). For example, to characterize the particles' sizes, generally two different tests are used: dry and wet sieving. For dry sieving tests, the sample is dried at 105 °C before the test. In the case of wet sieving, the sample is fresh. Also, several sieving methodologies are used, for example stacked sieves and individual sieves, as well as different sample pretreatments, such as removing the excess water of the sample, washing the sample to remove small particles and burning the sample to remove the organic fraction (Reddy and Pagilla, 2009; WEF, 2016).

The objective of this study was to evaluate the performance of the different sieving methods and the different sample pretreatment approaches that are currently in use to characterize grit particles, while keeping in mind that a good sieving test should be safe, repeatable, and allow sample storage for some time in order to facilitate the analysis of many samples at the same time. As well, the impact of the weather conditions on the particle characteristics was studied. This study has been based on the particles settling and retained in grit chambers, accepting the fact that some grit particles will have escaped from the treatment unit.

5.2.2 Material and methods

In this study, fresh grit particles removed by two different types of grit chambers (an aerated and a vortex grit chamber) at two different WRRFs in the Québec City area treating combined sewage have been sampled and characterized. The particles studied were collected at the outlet of the grit classification unit, before they fell into the grit bin, providing a representative sample of settled grit under known conditions.

To evaluate the influence of the sample pretreatment on the characteristics of the grit particles, three parameters were studied: the particle size distribution (PSD), the composition (in terms of organic/inorganic fractions) and the density.

Particle size distribution

The PSD of the collected particles was studied by using the two basic sieving methods that are currently in use: dry and wet sieving (Reddy and Pagilla, 2009; WEF, 2016). In both sieving tests, the indications suggested by WEF (2016) were followed. Fourteen stacked sieves with openings between 75 μm and 13.5 mm were used. The collected grit particles were distributed on the top of the sieve series and the sample passed through all of them. For dry sieving tests, to favour the particle size separation, the sieves were shaken with an automated shaker (Ro-tap Model B) for 15 minutes. For the wet sieving, the collected sample was also placed on the top of the sieve series. However, water at low pressure was sprayed over the sieves for particle classification, forcing the particles rolling on each sieve. After the particle classification, the mass retained on each sieve was collected separately, weighted and further characterized by ashing.

Composition

The composition of the classified grit particles was determined in terms of inorganic (IS) and organic (volatile solids, VS) fractions. This estimation was done following the Standard Methods presented by APHA (2012) drying the solids at 105 °C for the total solids estimation and burning them at 550 °C for the IS and VS fractions estimation.

Density

The third parameter studied, the density, was determined for three selected particle classes with a helium pycnometer based on the ASTM (2014) norm. The classes were selected to reflect the variety of composition and size.

Sample pretreatment

Several sample pretreatments were compared to evaluate how they can influence the grit characteristics in terms of the PSD, the composition of the particles and their density. Different combinations of washing the sample were applied to remove the particles smaller than 75 μm, drying the sample at 105 °C, and/or burning the sample at 550 °C to remove the organic fraction. An overview of the experimental plan that was used to study these pretreatments is presented in Figure 5.1. For the comparison, the wet sieving was considered as the reference method since the impact on the particles is lower compared to other pretreatments.

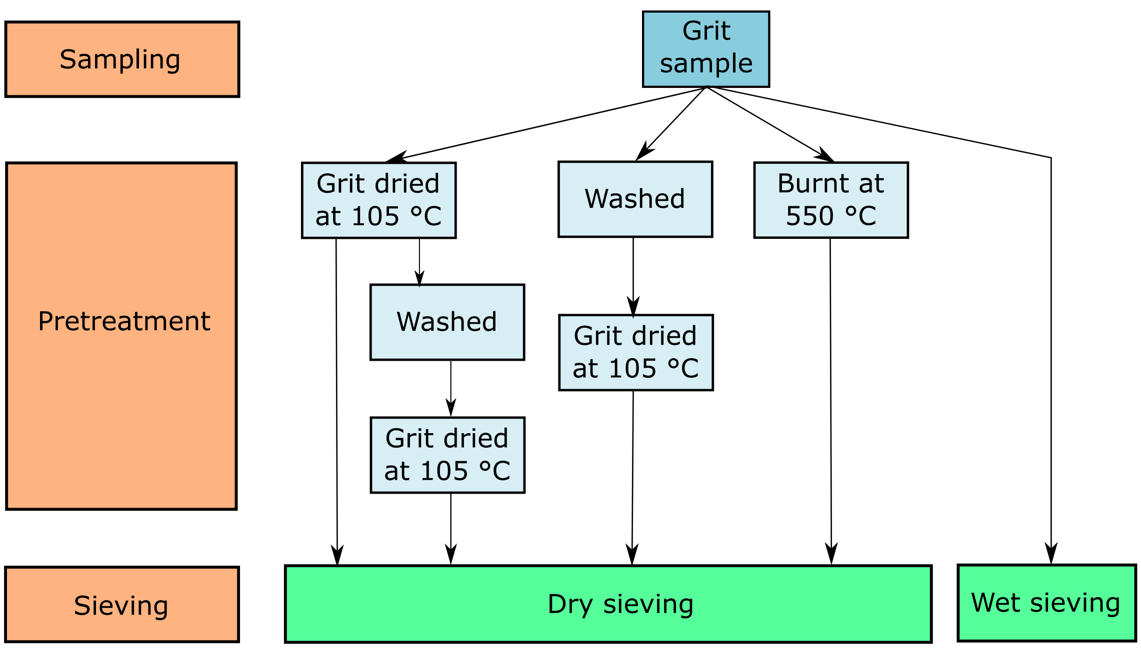

Figure 5.1: Experimental plan to determine the influence of the sample pretreatments to characterize the particle size distribution of the final grit product by sieving tests.

After the sieving tests, the IS fraction and the density were characterized for each particle class. This experimental plan was repeated for 10 samples collected under dry weather conditions (seven samples collected on a vortex grit chamber and three samples on an aerated grit chamber). Moreover, on three different occasions triplicates for the different tests were performed to assess the uncertainty of the methods.

Impact of weather conditions

The influence of rain and snowmelt events on the studied parameters has also been studied. Several samples were taken under dry weather conditions (7 samples), under wet weather (3 samples) and, also, a snowmelting period (1 sample) at the studied vortex grit chamber. Only the following sieving methodology was applied: fresh grit was washed and dried at 105 °C before the dry sieving test. Again, for each particle class obtained from the sieving test, the IS fraction and the density have been studied.

5.2.3 Results

Particle size distribution

Two examples of PSD curves obtained with the different pretreatment protocols for dry weather samples are shown in Figures 5.2 and 5.3 (vortex and aerated grit chambers respectively).

For the vortex grit chamber case (Figure 5.2), clear differences on the PSD are observed between the pretreatments studied. Particles are markedly smaller when the sample is burnt ('ashed grit'), since the organic fraction is removed and particles disaggregate. When the sample is not washed, bigger particles are observed. This is possibly due to aggregation of particles. No significant differences were observed for dry sieving of dry washed grit and non-washed grit. With dry sieving of wet washed grit and wet sieving, the results obtained are between the PSD curves of ashed grit and dry sieving of dried and non-washed grit. This can be due to the effect of washing the sample, which removes smaller particles and might break up some aggregates.

However, the effect observed is less severe than the effect of burning the grit particles before the dry sieving (ashed grit). Moreover, the results indicate that, generally, the effect of drying the sample at 105 °C facilitates aggregation that was not present in the original sample.

Comparing the differences between the curves, they are about a factor 5 on a logarithmic scale. Thus, if the PSD curve obtained is used to calculate the settling velocity of the grit particles through Stokes' Law (Equation 5.1), the results obtained can differ by a factor of up to 25 (since the diameter appears in Stokes' Law at the power of 2).

The second example presented in Figure 5.3 corresponds to the studied aerated grit chamber. In this case, it was again observed that the PSD curve of ashed grit is significantly different from the rest of the PSD curves: particles are considerably smaller after removing the organic fraction. For the rest of the sieving tests, fewer differences are observed. The particles observed on a dry sieving test without previously washing the grit are still bigger than the ones in the

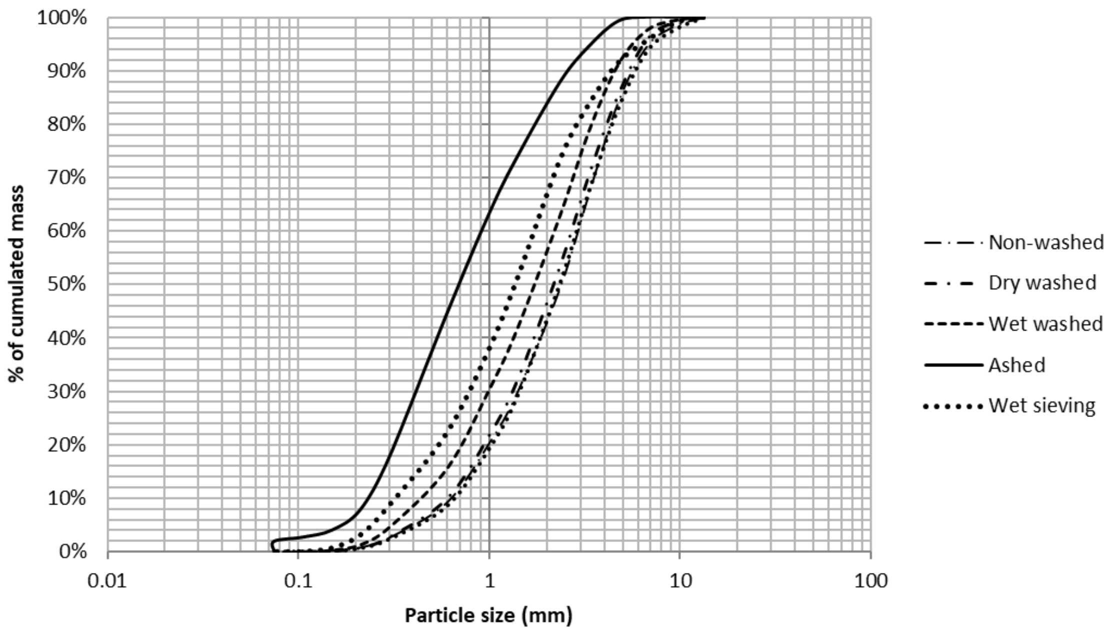

Figure 5.2: Granulometric curves for different pretreatments at the studied vortex grit chamber under dry weather conditions.

other tests, possibly because of aggregation of particles. The PSD curve after wet sieving is found between the PSD curves of ashed grit and dry sieving of non-washed grit. However, it is closer to the latter. The PSD curves of dry sieving of wet and dry washed grit are between the wet sieving and the dry sieving of non-washed grit and mostly overlap.

In this case, the differences between the curves in Figure 5.3 are about a factor of 9. Thus, the estimation of the settling velocity through Stokes' Law can be up to a factor of 81. This can lead to large uncertainties in the design of a grit chamber.

Composition

The sieving tests have also been evaluated through the composition of the particles in terms of the inorganic and organic fractions of each particle size class. Figures 5.4 and 5.5 show the results for vortex and aerated grit chambers respectively. The dry sieving test of ashed grit was not included in the comparison since the organic fraction was previously removed.

First of all, for any of the sieving tests (except for the ashed grit) it was observed that small particles (except for the smallest class) were more inorganic than large particles. This inorganic fraction represented more than 50% for the small particle classes, whereas for the bigger particles, it represented less than 20%. However, the inorganic fraction of the smaller particles was significantly higher for the aerated grit chamber than the vortex girt chamber.

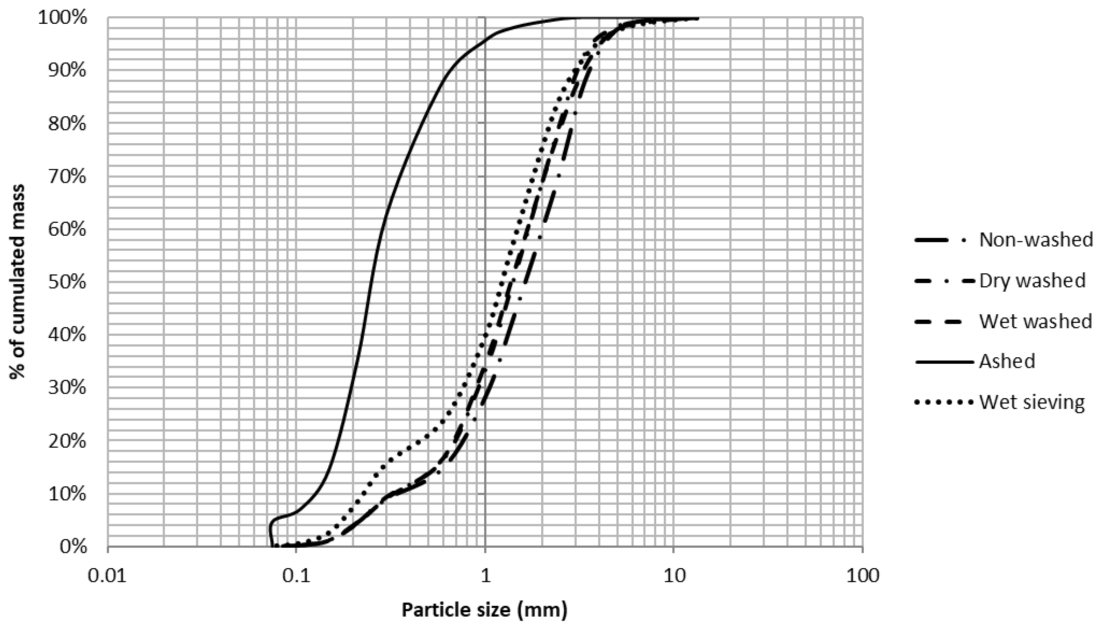

Figure 5.3: Granulometric curves for different pretreatments at the studied aerated grit chamber under dry weather conditions.

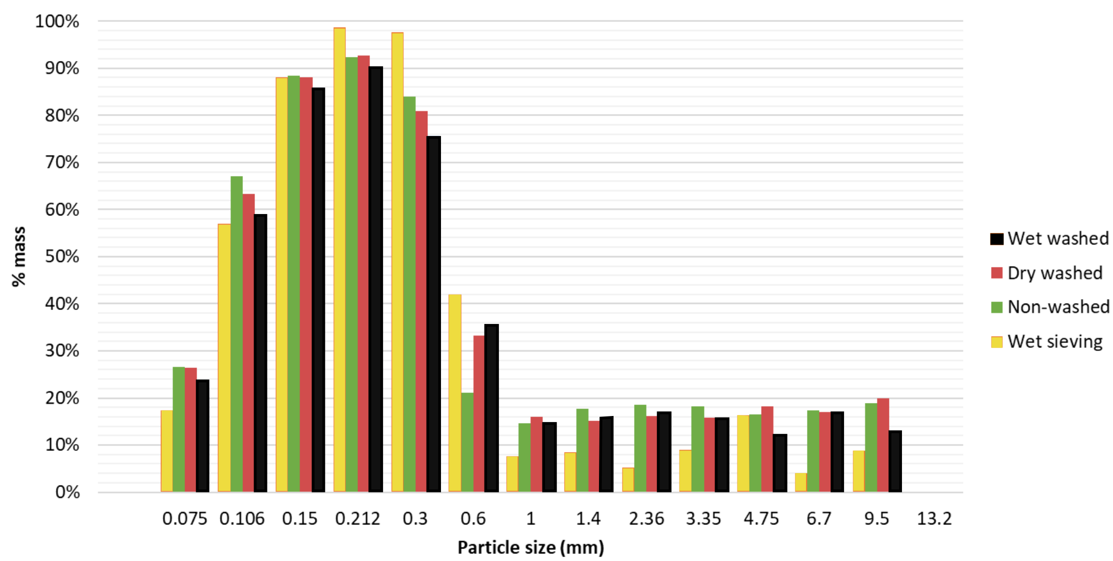

Figure 5.4: Inorganic fractions for different pretreatments of dry sieving and a wet sieving from the samples at the studied vortex grit chamber under dry weather conditions.

This fraction was ranging between 80 and 90%.

Comparing the results for each particle size class after dry sieving of the vortex grit chamber samples, small differences were found between the different pretreatments (i.e. non-washed

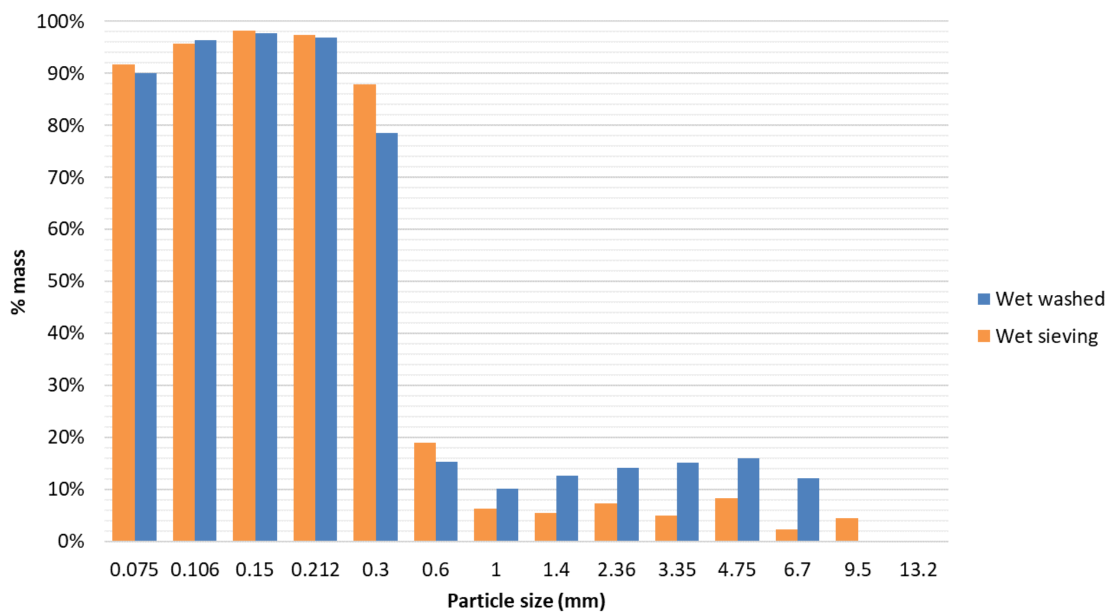

Figure 5.5: Inorganic fractions for dry sieving of wet washed grit and wet sieving from the samples at the studied aerated grit chamber under dry weather conditions.

grit particles, dry washed and wet washed grit) (See Figure 5.4).

However, when comparing wet sieving (considered as the reference test) with dry sieving of wet washed grit (test with the PSD closest to the one of the wet sieving) for the vortex grit chamber, the observed differences are more marked (Figure 5.4). Generally, small particles are a bit more inorganic for the wet sieving than for the dry sieving of wet washed grit. For the bigger particles, it was observed that they are a bit more inorganic for the dry sieving. In this case, these differences vary between 2% and 20%.

Similarly, in the case of the aerated grit chamber, no significant differences in the composition were observed between the different pretreatments (results not shown). However, the differences between wet and dry sieving observed are smaller than for the case of the vortex grit chamber (Figure 5.5). For the smaller particles, almost no differences were observed between both sieving tests, varying between 1% and 5%. For the bigger particles, bigger differences were observed ranging between 4% and 10%.

Density

The density of three different particle classes was determined with the helium pycnometer for the two studied grit chambers. The results obtained are presented in Table 5.1. It was observed that small inorganic particles can have a density above 2.50, whereas big organic particles have a density around 1.50 for the vortex grit chamber and around 1.30 for the aerated grit chamber. The inorganic fraction is different for each grit chamber and they cannot be compared.

Table 5.1: Densities measured, the inorganic fraction, density estimated and the difference between the densities for three different particles classes at the studied vortex and aerated grit chambers.

	Vortex grit chamber				**Aerated grit chamber**			
Particle size (mm)	**Density measured** (g/cm^3)	**%IS**	**Density estimated** (g/cm^3)	**Difference (%)**	**Density measured** (g/cm^3)	**%IS**	**Density estimated** (g/cm^3)	**Difference (%)**
4.75	1.51	26%	1.50	1	1.28	12%	1.29	-1
1.4	1.50	26%	1.50	0	1.33	13%	1.30	3
0.212	2.57	97%	2.60	-3	2.65	97%	2.60	5

From the results presented, a simple relation was developed to estimate the density for the grit particles depending on their composition:

$$\rho_{estimated} = F_{inorganic} \cdot 2.65 - (1 - F_{inorganic}) \cdot 1.10 \tag{5.2}$$

where $\rho_{estimated}$ is the estimated specific gravity of the grit particles, and $F_{inorganic}$ is the inorganic fraction of the grit particles studied. The value of 1.1 was estimated on the basis of the data in Table 5.1. It is noteworthy that the specific density found for the inorganic and organic fractions coincides with the range of densities mentioned by WEF (2016).

The densities of the three particle classes characterized previously with the pycnometer were estimated according to Equation 5.2. The results are shown in Table 5.1. It is observed that it is possible to estimate the density of the grit particles within ±5%. With this, the density was estimated for all particle classes to compare the influence on the density of the wet sieving and the dry sieving of wet washed grit tests.

Regarding the estimated density values for the different sieving tests; generally, the small inorganic particles have a density higher than 2.40 while large organic particles have a density below 1.40 (Figure 5.6).

Impact of weather conditions

The average PSD curves obtained under different weather conditions (dry weather, rain events, snowmelt) at the vortex grit chamber are presented in Figure 5.7. Under dry weather conditions, the grit particles retained in the vortex grit chamber were larger than those retained after rain events or a snowmelt period. The smallest particles were observed during the snowmelt period. This can be caused by the runoff of sand that is used in winter road maintenance

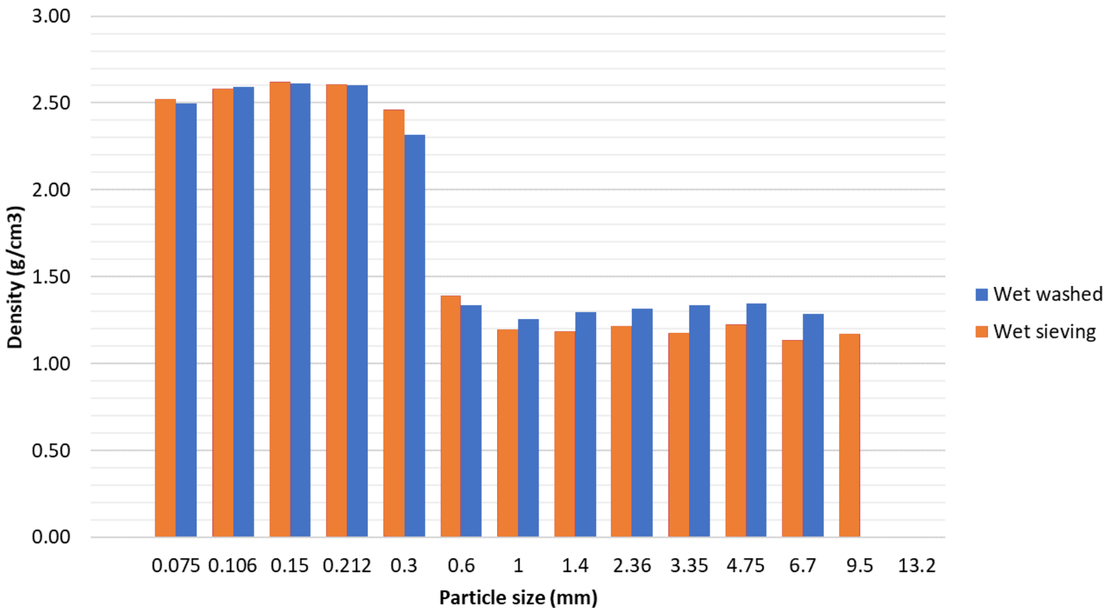

Figure 5.6: Inorganic estimated densities for dry sieving of wet washed grit and wet sieving from the samples at the studied aerated grit chamber under dry weather conditions.

to improve traction. Also, it was observed that during rain events and especially snowmelt periods, the grit retained in the grit chamber contains a substantially higher inorganic fraction than the grit collected under dry weather conditions (see Figures 5.8 and 5.9).

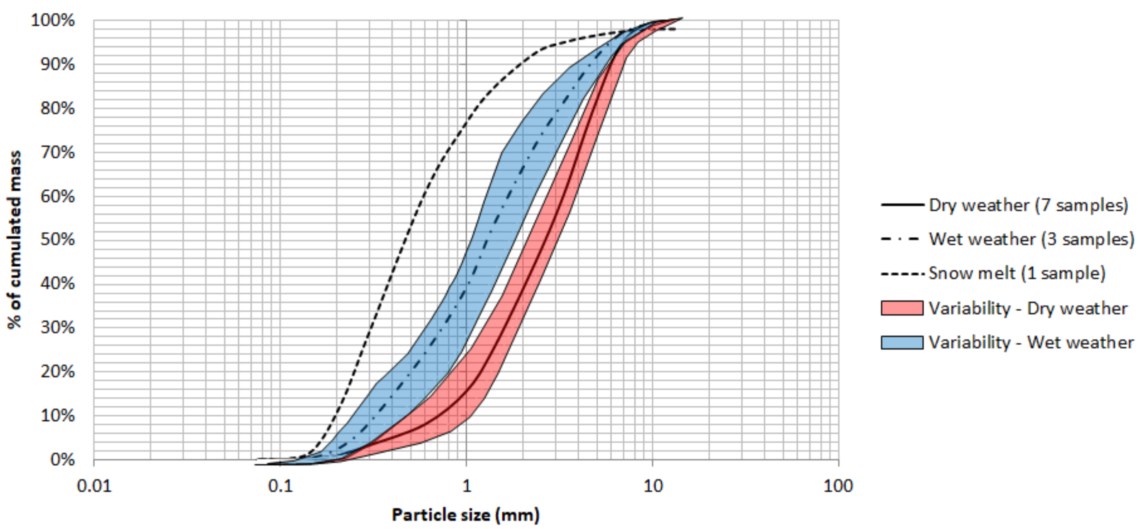

Figure 5.7: Average and variability of the PSD curves under the different weather conditions of Saint-Nicolas WRRF. In case of the snow melt period, since only one sample was collected, there is no variability presented.

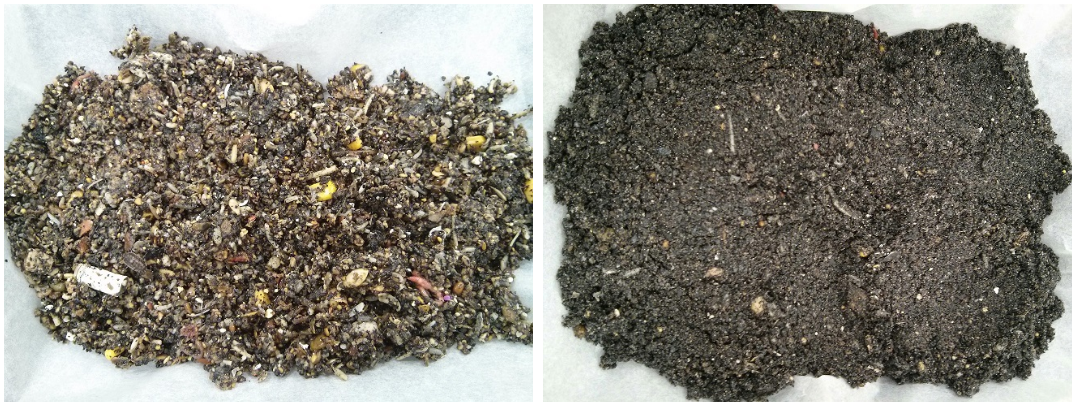

Figure 5.8: Grit particles under dry weather conditions (left) and during the snowmelt period after a rain event (right). Images taken during this PhD study from grit collected at Saint-Nicolas WRRF.

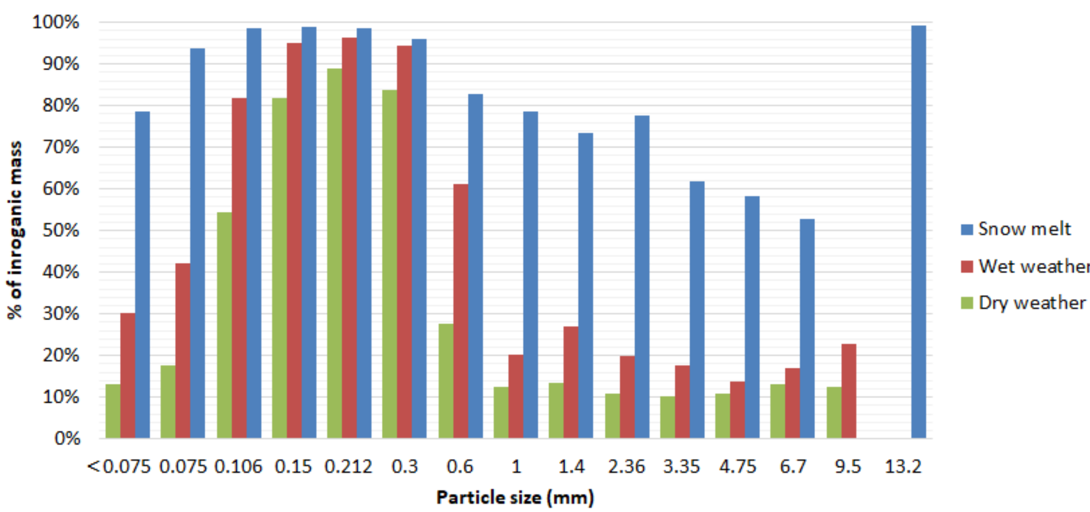

Figure 5.9: Average of the inorganic fraction under different weather conditions at the studied vortex grit chamber.

The combination of small size and high-density particles thus confirm the earlier observation on the relation between these grit characteristics and their retention in grit chambers. Ultimately, it is the settling velocity that determines whether a particle is retained or not.

5.2.4 Conclusions

The characteristics of the grit particles removed in grit chambers can be influenced by the type of sieving method used and the sample pretreatment applied.

When the grit particles are not washed prior to sieving, the particles are larger, probably due to aggregations, and when grit is burnt, smaller particles are observed because the organic fraction is removed and thus particles disaggregate.

Wet sieving can be considered the reference method since particles are not modified by sample pretreatment. However, this test is less repeatable, less safe (since grit is considered as a biorisk) and a sample cannot be stored for later analysis (the test has to be done within 24 h after sampling). Also, more personnel are needed to perform the test and it requires more time than the dry sieving tests. Thus, dry sieving of washed wet grit is suggested as the preferred method to characterize the PSD because it is safe, repeatable and allows sample storage.

The study of the PSD and grit composition for each particle class showed that smaller grit particles are more inorganic in nature whereas bigger aggregates are more organic. Density measurements of different particle classes illustrated that these differences in composition have an important effect on the particles' density. This will be reflected in the settling velocity.

An empirical equation was developed to more accurately estimate the density of a particle based on its composition in terms of inorganic and organic fractions. This would help to more accurately estimate the settling velocities of the grit particles. Thus, the type of particles that settle in a grit chamber can be better described.

Grit characteristics also depend on the weather conditions, e.g. dry weather, wet weather, and snowmelt periods. During wet weather and snowmelt periods, smaller and more inorganic particles were found to be retained in the grit chamber.

Comparing both WRRFs studied, some differences have been observed. However, it is not possible to associate these differences only to the type of grit chamber since they could also be due to other influences such as the type and size of the sewer system, land use in the catchment studies, wastewater composition (e.g. industry), etc.

Chapter 6

Particle settling velocity characterization methods

6.1 Introduction

The specific objective 1.c related to the development of a methodology to analyse the settleability of particles is addressed in this chapter. Two relevant methods that have been successfully used to characterize the settleability of particles in wastewater and stormwater were selected for evaluation. Before comparing these methods, they were adapted to reliably characterize fast settling particles such as grit particles.

The results obtained in the context of this part of the PhD thesis have been compiled and included in a peer-reviewed paper:

- Q. Plana, A. Pauléat, A. Gadbois, P. Lessard and P.A. Vanrolleghem (2019). Characterizing the settleability of grit particles. *Water Environment Research.* 92(5):731-739

The material included into this accepted manuscript describes the study of the reproducibility of both studied methods, an experimental comparison between both methods, the observed relation between TSS concentrations and PSVD curves, and the impact of the weather conditions on the PSVD curves.

6.2 Characterizing the settleability of grit particles

Abstract

Grit chambers are installed at the headworks of a water resource recovery facility (WRRF) to reduce the impact of grit particles to the equipment and processes downstream. This settling process should thus be designed and operated in an efficient way. Despite the importance of knowing settling characteristics for design and operation of grit chambers, previous grit definitions have been based only on particle size characteristics, and not on settling velocities. Thus, this study presents an evaluation of the performance of two promising settling velocity characterization methods, ViCAs and elutriation, to characterize wastewater particles in view of the design and the optimization of the efficiency of the grit removal unit.

6.2.1 Introduction

Background

Grit chambers, which can be found at the headworks of most water resource recovery facilities (WRRFs), are meant to reduce grit accumulation and grit-induced damage in processes downstream of the unit (Tchobanoglous et al., 2014; Wilson et al., 2007). However, despite their important role in a wastewater treatment chain, the interest to study these units has been lower than for any other unit because it has been considered that grit chambers have a low influence on the secondary treatment (WEF, 2016). Thus, the characteristics of particulate pollutants at the inlet, outlet, and underflow streams of grit chambers are rarely documented, and their removal efficiency is often questioned (WEF, 2016; Reddy and Pagilla, 2009).

Grit particles removal is not simply achieved by installing a grit chamber at the headworks of the WRRFs. It must also be designed and operated in a highly efficient way (WEF, 2010). Thus, grit particles should be well-characterized and representatively sampled. Surprisingly, no standard peer-reviewed characterization and sample protocols exist yet (WEF, 2016; Reddy and Pagilla, 2009).

Grit characteristics

Grit removal is a sedimentation process induced by gravity, helical flow, or centrifugal forces (Tchobanoglous et al., 2014). Hence, the governing characteristic for this process is the particle settling velocity. Tchobanoglous et al. (2014) suggests a settling velocity of 70 m/h for typical grit chamber design, which means that particles with a settling velocity of 70 m/h and more are removed at 100 %.

Regardless of the importance of the settling characteristics for sedimentation based on gravitational forces (Camp, 1936), previous grit definitions have focused on particle size characteristics considering only the inorganic fraction and assuming that particles are homogeneous spheres with a specific gravity of 2.65 (U.S. EPA, 2004). Then, according to this definition, the settling velocity of the grit particles is estimated from particle size analysis and applying Stokes' Law:

$$v_s = \frac{g \cdot (\rho_p - \rho_w) \cdot d_p^2}{18 \cdot \mu} \tag{6.1}$$

where v_s is the settling velocity (m/s), g gravitational acceleration (m/s^2), ρ_p the particles' specific gravity (kg/m^3), ρ_w the specific gravity of water (kg/m^3), d_p the diameter of the particles (m), and μ the water viscosity $(kg/(m \cdot s))$.

However, in reality, grit particles are heterogeneous particles that do not have a single representative value of specific gravity and should not be considered inorganic homogeneous spheres (Herrick et al., 2015; Plana et al., 2018).

An increasing number of studies question whether the conventional definition of grit is a proper approximation (Barter and Sherony, 2011). Thus, the Water Environment Federation's Grit Task Force has suggested a definition that considers the settling velocity of the grit particle as it exists in the raw wastewater (WEF, 2016). In addition, it is now recognized that the organic fraction of the grit particles is significant, and the specific gravity is variable and lies between 1.1 and 2.65 (WEF, 2016; Plana et al., 2018).

Measurement of particle settling velocity distribution

Thus, there is a necessity to improve the knowledge on particle settling velocities, especially considering that this characteristic depends on the particle's size, density and shape (Aiguier et al., 1996; Marsalek et al., 2006). Several methods are currently in use to determine particle settling velocities by trying to deduce them from other properties. For example, sieving methods study particle sizes from which settling velocities are estimated presuming homogeneous particle specific density and shape.

With the increasing interest in characterizing the settleability of grit particles, two devices have been proposed and tested for fast settling particles. The first device consists in a square settling column presented by Hydro International plc (Osei et al., 2012) which has been tested separately with several sand and grit particle sizes. The second device, presented by Gerges et al. (2018), is based on a single dynamic settling column allowing separating particles depending on the upflow velocity into the column. Thus, particles are classified according one settling velocity per test.

True settling characterization methods experimentally fractionate the total suspended solids (TSS) in different settling velocity classes, where each fraction is characterized by a settling velocity vs. Hence, as a result, a particle settling velocity distribution (PSVD) is obtained. These methods can be classified in: (1) static settling devices in which the liquid is under quiescent conditions, such as settling columns (Aiguier et al., 1996); and, (2) dynamic settling devices in which the liquid is flowing, like elutriation devices (Krishnappan et al., 2004).

Over the years, several static settling columns have been developed, e.g. Aston column (Tyack et al., 1993), Umwelt- and Fluid-Technik (UFT) column (Michelbach and Wöhrle, 1993), CERGRENE protocol (Chebbo, 1992), U.S. EPA column (O'Connor et al., 2002), and the newer ViCAs protocol (Chebbo and Gromaire, 2009). The height of these settling columns varies between 0.2 and 1.8 m, with sample volumes ranging between 1 and 40 L. Also, some protocols include a sample preparation step applying a pretreatment such as sieving or settleable solids preselection (Aiguier et al., 1996; Lucas-Aiguier et al., 1998). In addition, on several occasions, these methods have been compared and the results show different PSVD curves (Aiguier et al., 1996; Lucas-Aiguier et al., 1998; Krishnappan et al., 2012). Lucas-Aiguier et al. (1998) pointed out that these differences are probably due to the different sizing of the columns.

As dynamic settling devices, several systems have been proposed. Mainly, two different setups can be found in literature: (i) modified settling columns with the addition of oscillating grids to create turbulence, e.g. Rasmussen and Larsen (1996) device; and (ii) the elutriation apparatus, firstly developed by Walling and Woodward (1993), and later updated by Krishnappan et al. (2004) and Marsalek et al. (2006).

Objective of the study

Given the importance of the settling velocity for grit particle characterization and for grit chamber design, and the lack of standard and accepted methods for this characterization, the objective of this study was to evaluate the performance of two settling velocity characterization methods in use today to characterize wastewater particles.

6.2.2 Methodology

Case studies

The inlet of a grit chamber at two different WRRFs were sampled and characterized on several occasions. Both WRRFs located nearby Québec City treat combined sewage: one, with a treatment capacity of 270,000 people with an average design flow of 230,700 m^3/d, and the other one, with a capacity of 36,000 people for an average design flow of 18,800 m^3/d.

Sampling methods

For sampling, a multipoint sampler was used in both cases. Considered as a representative method to sample the inlet channel (WEF, 2016), different sampling intakes were installed at several points distributed uniformly over the cross-section of the channel. Then, the samples from each intake were homogenized. For example, at the small WRRF studied, four sampling intakes were placed with the openings oriented against the incoming flow as presented in Figure 6.1. In case of the large WRRF studied, nine intakes were placed to cover the cross-section of the sampled channel.

points.png

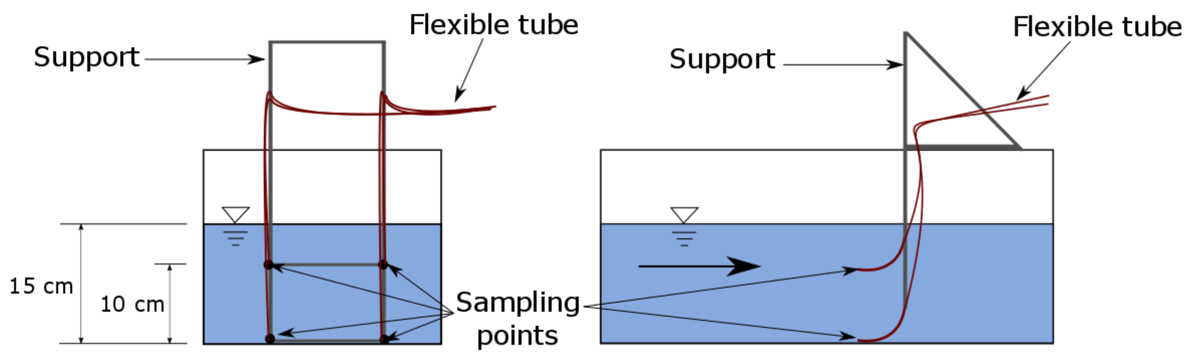

Figure 6.1: Schema of the multipoint sampler used at the small studied WRRF. (a) Cross-section of the section channel; (b) Profile of the channel.

The samples were collected during 10 minutes with multihead peristaltic pumps and collected into 20 L-containers for easy management and transport. With these pumps and tubes with a $\varnothing = 1$ cm, the flow velocity into the tubes was about 1900 m/h, thus allowing to collect particles with high settling velocities such as grit. In addition, while sampling, 3 backwashes were performed for 20 seconds to avoid clogging the openings of the tubes.

Measurement of the particle settling velocity distribution

The particle settling velocity distribution (PSVD) was assessed with two peer-reviewed methods currently in use for raw wastewater samples (e.g. at the inlet of WRRFs and in sewer systems): the experimental protocol ViCAs (a French acronym for settling velocity in wastewater) developed by Chebbo and Gromaire (2009) as a static settling device, and the elutriation method (Krishnappan et al., 2012) as a dynamic settling device. Both methods have been extensively used and applied to characterize stormwater, sewage and wastewater along the WRRFs treatment chain. Moreover, their reliability and reproducibility have been proven (Berrouard, 2010; Maruéjouls et al., 2014; Bachis et al., 2015). In this case, no sample pretreatment was applied to not modify the raw sample and to not loose any particles.

The ViCAs batch settling protocol consists in quickly filling a settling column (H = 70 cm, ⌀= 7 cm) with a homogenized sample (Figure 6.2.a). Settling solids are recovered in cups at the bottom of the column at different time intervals (t = 1, 3, 5, 10, 20, 35 and 60 min) and analysed for TSS ($d_p \geq 1.2\mu m$). Then, with the cumulated mass of settled particles over the experiment time, it is possible to estimate the distribution of the settling velocities. In this study, according to the time intervals over which cups are accumulating TSS, this distribution corresponds to velocities of 42, 14, 8.4, 4.2, 2.1, 1.2, and 0.7 m/h, respectively.

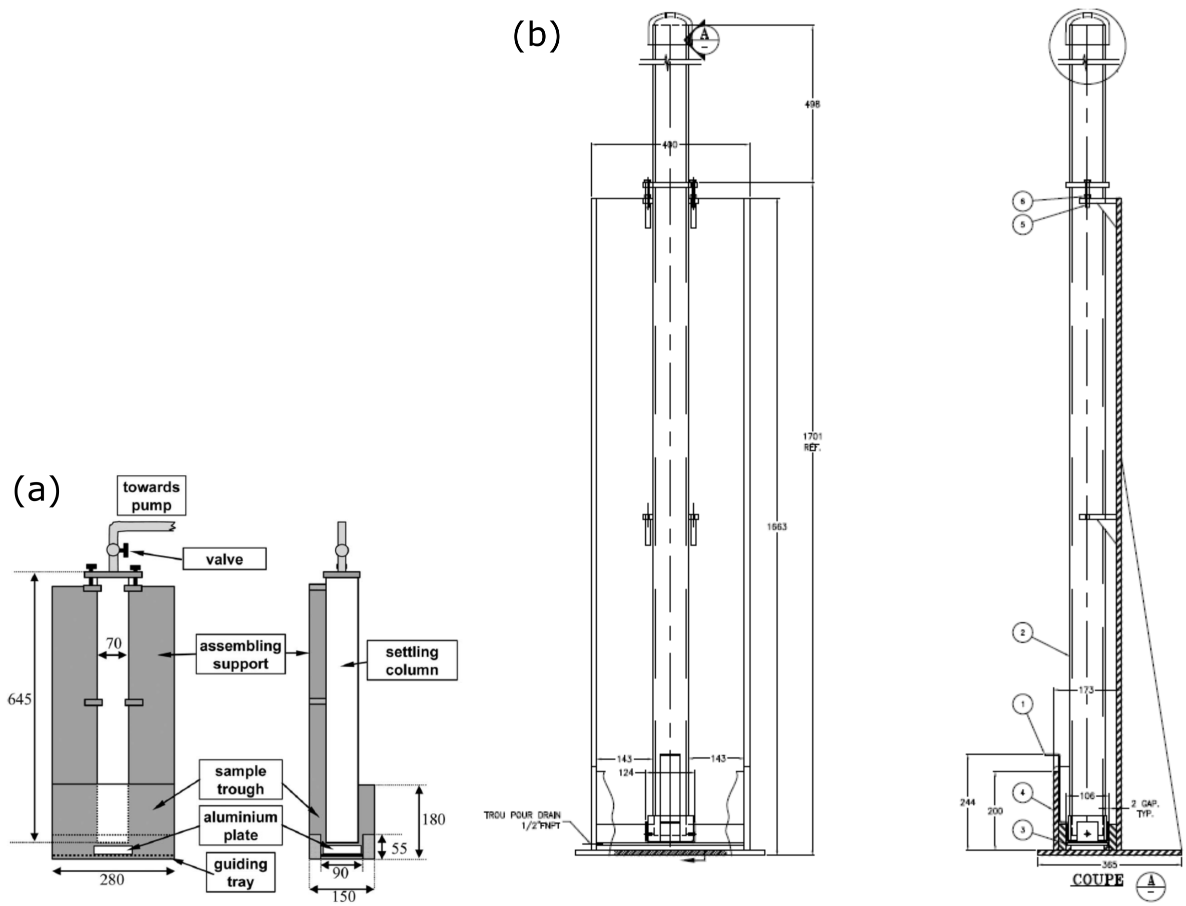

Figure 6.2: Schema of the ViCAs experimental setup. (a) original 70 cm ViCAs column (Chebbo and Gromaire, 2009); (b) adapted 2m-ViCAs column. All dimensions are indicated in mm.

However, while the ViCAs settling column has been applied before to study the PSVD of wastewater particles in sewer systems and in WRRFs, the 70cm-ViCAs column did not allow studying settling velocities above 40 m/h. Thus, the standard design was modified and upgraded to a 2m-column with a ⌀= 8 cm to better study fast settling particles such as grit particles (Figure 6.2.b). The time intervals used to collect the settled solids were kept the same as for the 70cm-column test leading to the corresponding distribution of settling velocities of 120, 40, 24, 12, 6, 3.4, and 2 m/h, respectively. For this updated ViCAs setup, 15 L rather than 4 L of sample are needed.

The elutriation system is built as a series of columns with increasing diameters (⌀= 3.4, 4.3, 7, 10.5, 14.3 and 19.7 cm) (Figure 6.3). The sample enters close to the bottom of each column going upward and leaves the column close to the top (Krishnappan et al., 2004). Thus, the upflow velocity decreases as the water moves downstream along the set of the columns, allowing the particles with a settling velocity higher than the upflow velocity to remain at the bottom of the column. Then, the particles settled in each column are collected separately and quantified as TSS. In this study, the elutriation protocol was adapted adjusting the pumped flow for fast settling velocities. Thus, the test was operated at 1.6 L/min with six columns with upflow velocities of 104, 65, 24, 11, 6, and 3 m/h. The volume of the samples was variable depending on the samples' TSS concentration to obtain sufficient particles in each column. In this study, samples of a minimum of 20 L were used for the test.

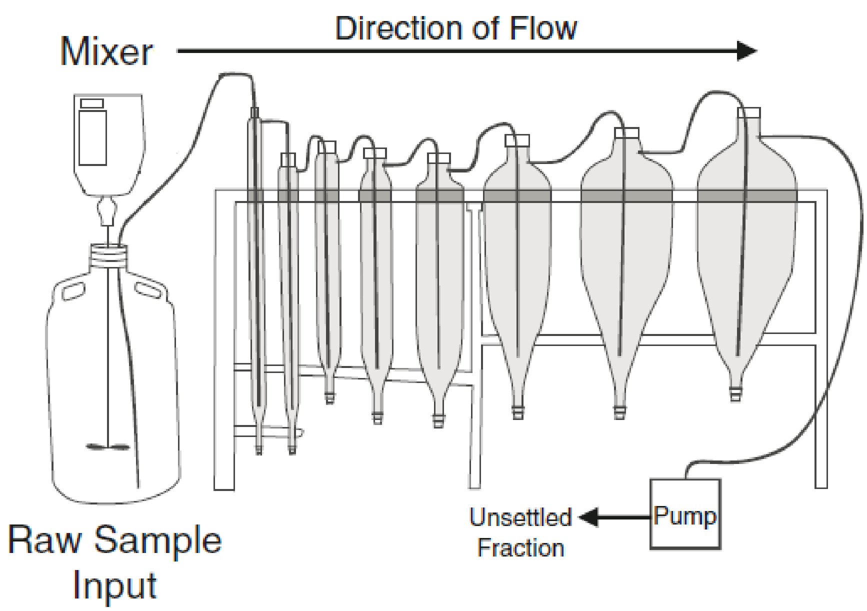

Figure 6.3: Schema of the elutriation system used (Krishnappan et al., 2012).

Quality control of the results

To assure the reliability of the obtained results, quality control was implemented. Fortunately, for both methods, a mass balance check can be performed after the test. Only tests with an error on the mass balance lower than 15 % have been considered as suggested by Chebbo and Gromaire (2009) for the 70cm-ViCAs columns. For new operators, such good results can easily be achieved after 2 or 3 tests.

6.2.3 Results and discussion

Reproducibility

First, since the standard methods have been modified and adapted for grit characterization, the reproducibility of the upgraded ViCAs column and the elutriation device with the adjusted flow were evaluated. To evaluate the method precision, triplicate samples were analysed by each method separately.

To evaluate the reproducibility of the ViCAs test, two samples of 45 L were taken and evaluated on two different days under dry weather conditions the samples collected between 8 a.m. and 10 a.m. under different flow conditions and with corresponding TSS concentrations of 200 and 300 mg/L. Each sample was split in three subsamples of 15 L. Then, the particles' fractionation according to their settling velocity was performed following the ViCAs protocol adapted for the 2m-column. The results obtained in both tests were very similar and are considered valid with a mass balance error lower than 15 % for the three tests. Figure 6.4 depicts the average of the results for the 300 mg/L sample together with the 95 % confidence interval over the triplicates. It is observed that the variability of the results is lower for high settling velocities (i.e. lower than 1 %) than for low settling velocities (i.e. lower than 5 %).

As for the ViCAs test, to evaluate the reproducibility of the elutriation device, a sample of 60 L was also taken under dry weather conditions between 8 a.m. and 10 a.m. with a TSS concentration of 240 mg/L. This sample was split in 3 subsamples of 20 L and the particles' fractionation for each sample was performed following the elutriation protocol adapted for fast settling particles. The results obtained with a mass balance error lower than 15 % for the three tests are presented in Figure 6.5. It is observed that the elutriation setup is reproducible since the variation in the results is minimal. However, again, for low settling velocities, the variability of the results appears higher, i.e. lower than 10 %.

Comparison between 2m-ViCAs and elutriation device

Ten 60L-samples with TSS concentrations ranging between 60 and 360 mg/L were collected at the studied WRRFs. For each test, the samples were well-mixed and split: 15 L for the 2m-ViCAs test and 30 L for the elutriation test. The time each test took, considering the time to prepare the sample, to run the test and to clean the equipment, was 1.5 h for each ViCAs test and 4 h for each elutriation test.

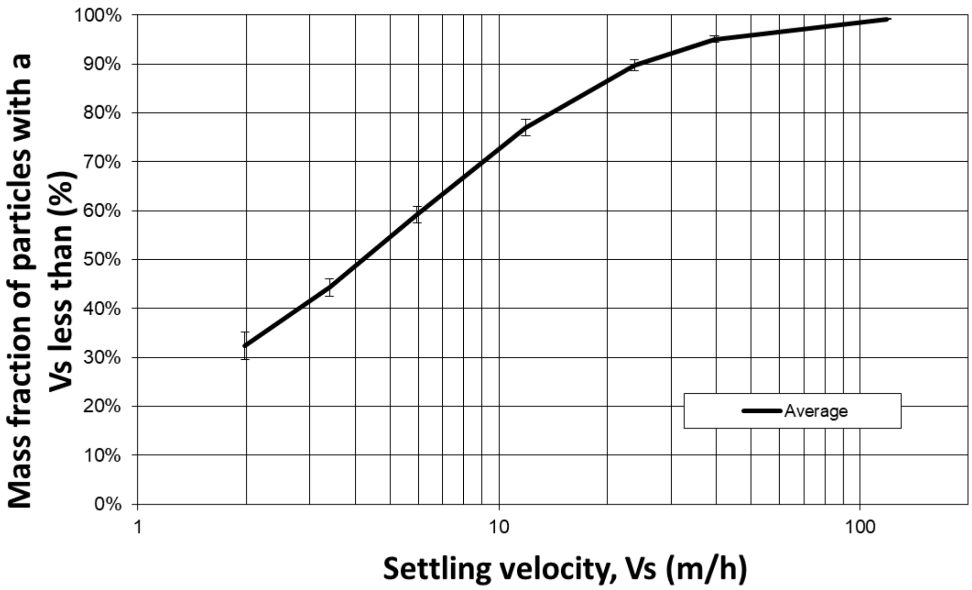

Figure 6.4: Average of the ViCAs triplicate test with bars representing the 2σ (95 %) confidence interval over the triplicates.

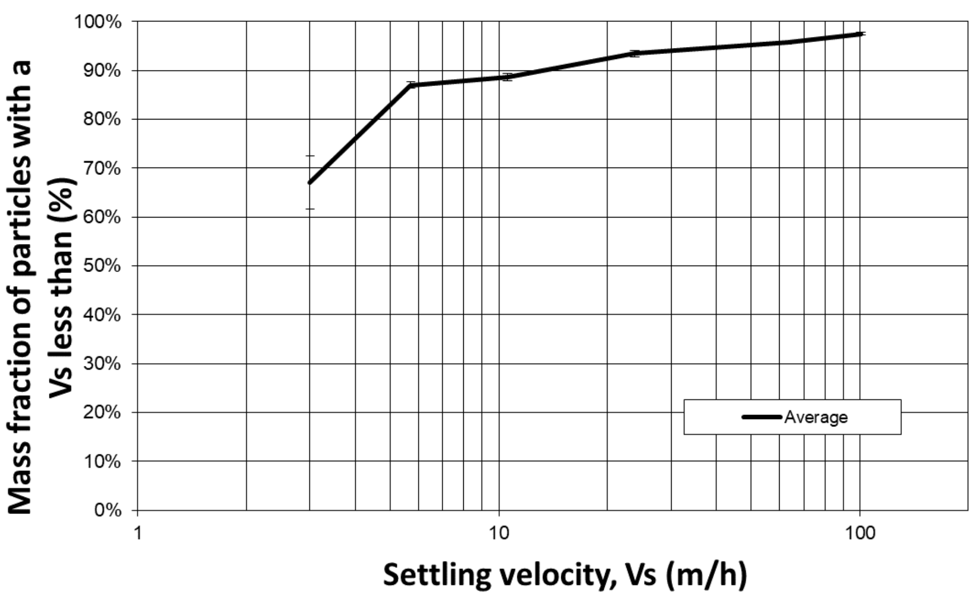

Figure 6.5: Average of the elutriation triplicate test with bars representing the 2σ (95 %) confidence interval over the triplicates.

Figure 6.6 shows three examples of results obtained at the small WRRF studied with concentrations of 60, 250 and 310 mg/L, respectively, from the 2m ViCAs column together with the elutriation results. As mentioned, thanks to the changes of equipment used, the PSVD studied ranges between 2 and 120 m/h. Thus, both setups allow studying the settling velocities of interest for grit particles (considering the typical design overflow rate of 70 m/h as depicted in red on Figure 6.6).

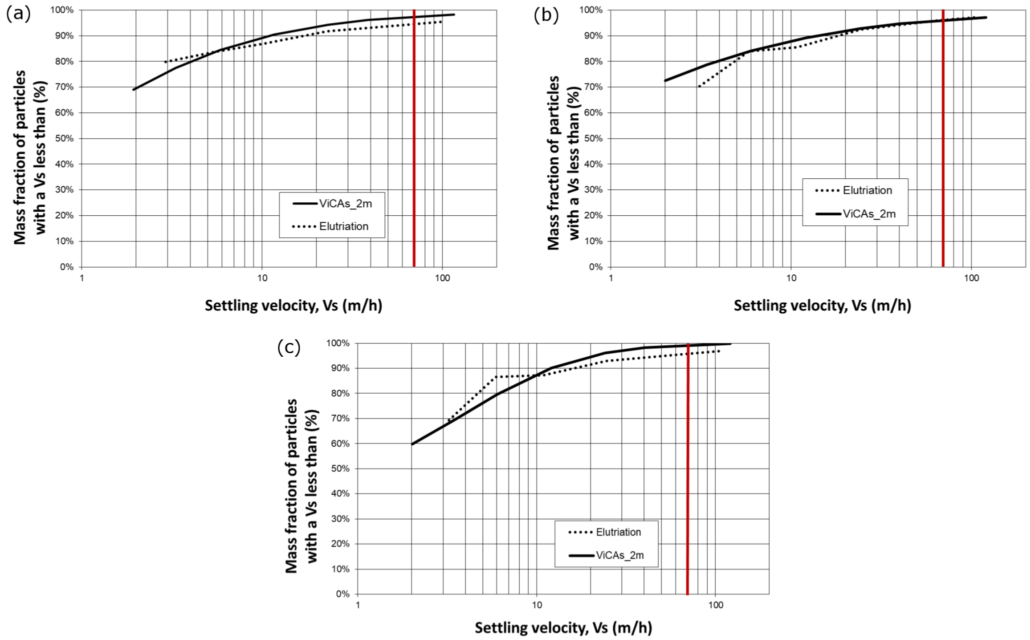

Figure 6.6: PSVD curves obtained with the ViCAs column and the elutriation system with a sample at the inlet of the grit chamber of the small WRRF studied with a TSS concentration of (a) 60 mg/L, (b) 250 mg/L, and (c) 310 mg/L. The vertical line represents the design overflow rate of 70 m/h.

The 2m-ViCAs column and the elutriation method gave very similar results. The small differences can be explained by the fact that for the ViCAs protocol, the PSVD curve is obtained after numerical adjustment of a smooth continuous function whereas for the elutriation method, the curve is not smoothed.

For the samples collected at the large WRRF studied, similar results were again observed at different concentrations (Figure 6.7). Despite the observation that the particles collected at the inlet of the large WRRF studied are settling faster than those of the small one, the PSVD curves from the 2m-ViCAs and the elutriation device, behave similarly. Again, the differences between both methods are mainly due to the mathematical adjustment to obtain the ViCAs curve, making it much smoother than the elutriation result.

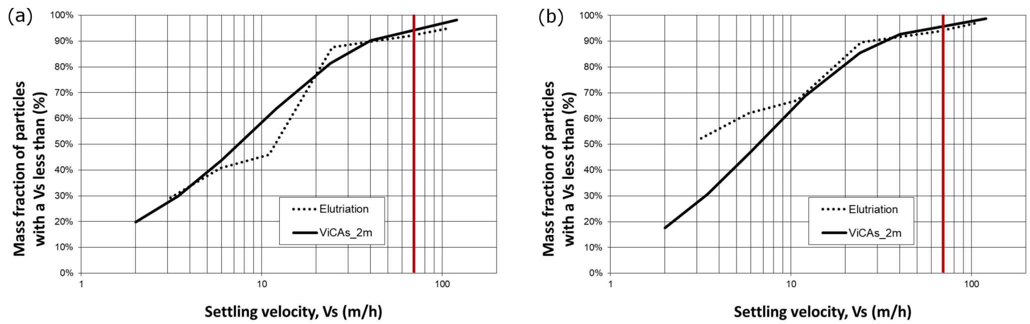

Figure 6.7: PSVD curves obtained with the ViCAs column and the elutriation system with a sample collected at the inlet of the grit chamber of the large WRRF studied with a TSS concentration of (a) 300 mg/L, and (b) 360 mg/L. The vertical line represents the design overflow rate of 70 m/h.

Observed relation between TSS concentrations and PSVD curves

Over time, TSS concentrations vary, as do the PSVD curves. A relation between both variables was observed and is discussed here. Considering the above conclusion that both setups provide similar results, only the ViCAs protocol was applied because it is faster and requires less sample.

Samples at different TSS concentrations were collected under dry weather conditions. In this case, 16 tests were accepted as valid and considered for the evaluation. The results obtained are presented in Figure 6.8. It is noticed that most of the PSVD curves follow a similar shape. However, the fractions at each settling velocity vary. Generally, at low TSS concentrations, the PSVD curves are located in the upper part of the curves in the graph, and on the contrary, at high TSS concentrations, the PSVD curves are lower in the graph. This means that at high TSS concentrations, the fraction of fast settling particles is higher. For example, from a TSS variation from 100 to 330 mg/L, the fraction fast settling particle may increase 5 %, whereas the fraction of low settling particles may increase up to 30 %. A possible explanation for this observation is that, at higher flows, more particles are transported into the WRRF (higher TSS), and that generally these particles are characterized by higher settling velocities because these higher flows have more energy, allowing to resuspend these faster settling particles.

Given these variations, the relationship between TSS concentrations and PSVD curves was further studied. The interest to relate TSS to PSVD is that TSS concentrations are easy to measure (even on-line) whereas PSVD curves are not. Having a relationship thus allows for calculating a PSVD curve from the set of collected PSVD curves.

To determine how the PSVD varies with the TSS concentrations, the settling class fractions were plotted together with the TSS concentration of the collected sample. For example, in

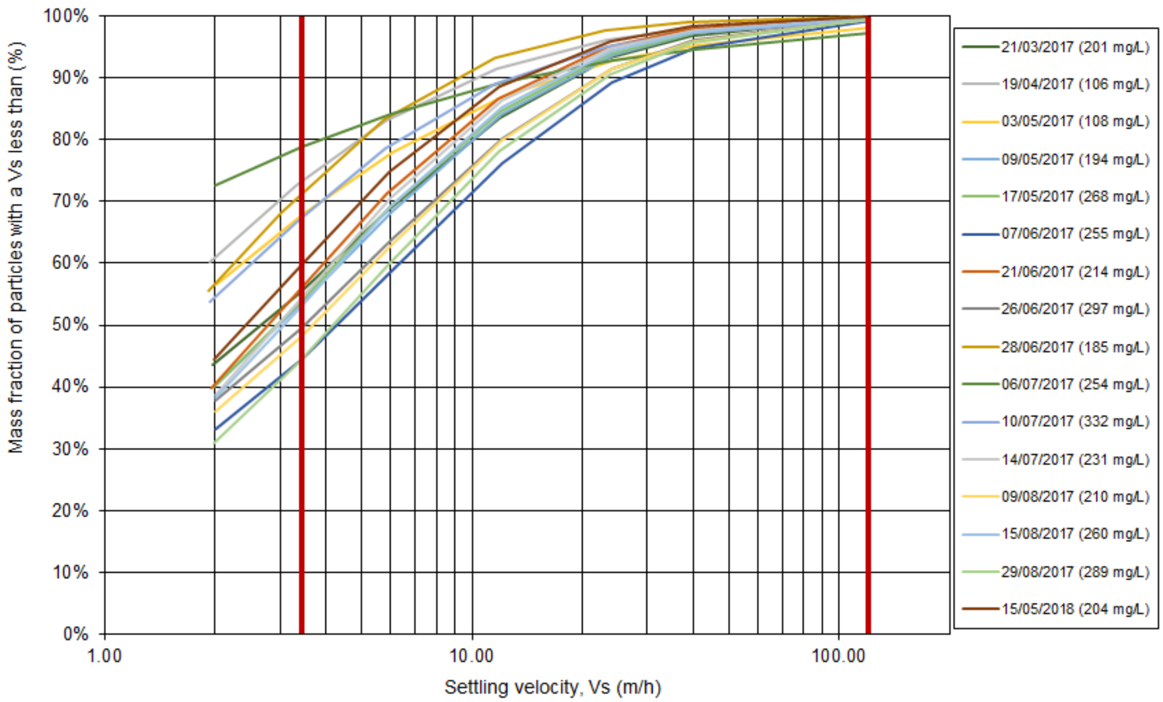

Figure 6.8: Ensemble of PSVD curves obtained with the ViCAs column from 16 samples collected under dry weather at the inlet of the grit chamber of the small WRRF studied. Vertical lines indicate the settling velocities of 3.4 and 120 m/h, respectively.

Figures 6.9 and 6.10, the PSVD fractions are depicted versus the TSS concentrations for the settling velocities of 120 and 3.4 m/h, respectively. In both cases, a linear tendency can be observed similar to the relations observed in previous studies (e.g. Maruéjouls et al. (2015) and Bachis et al. (2015)). This tendency also confirms that at higher TSS concentrations, the fraction of fast settling particles is higher (i.e. lower PSVD curves).

Impact of the weather conditions on the PSVD curves

The PSVD curves were also studied for samples collected under other weather conditions than the dry weather conditions reported so far. In this part of the study, and considering that both setups provide similar results, only the ViCAs protocol was applied because it is faster and requires less sample. Several samples were collected under different weather conditions. In this case, 22 tests with a mass balance error less than 15 % were considered: 16 under dry weather, 4 under wet weather and 2 under snowmelt conditions. In Figure 6.11, all of the obtained PSVD curves are presented. The lines are the average PSVD curves for each of the weather conditions. The coloured zones represent the distribution of all obtained curves for

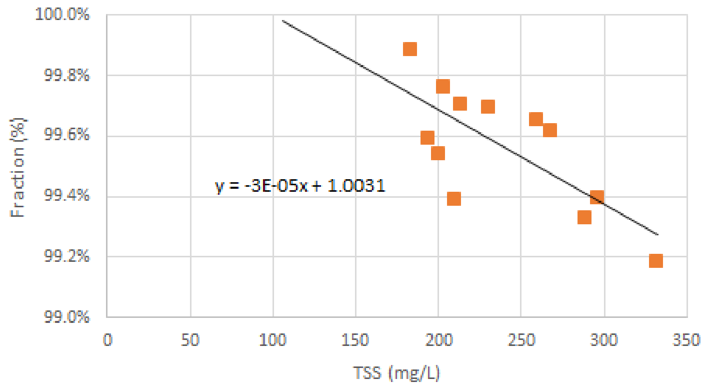

Figure 6.9: Mass fractions of particles with a settling velocity less than 120 m/h as function of the TSS concentration of the collected sample under dry weather.

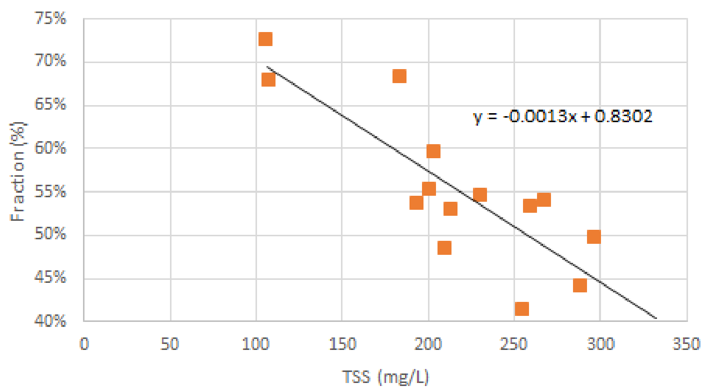

Figure 6.10: Mass fractions of particles with a settling velocity less than 3.4 m/h as function of the TSS concentration of the collected sample dry weather.

each condition. For the samples under snowmelt conditions, both results have been depicted individually.

Under dry weather conditions it has been noticed that PSVD curves vary within the day. And, as observed in other studies, e.g. Bachis et al. (2015) and Maruéjouls et al. (2015), this variation is correlated with the TSS. At low TSS concentrations, there are less particles that settle at high settling velocities. On the contrary, at high TSS concentrations, there is a higher fraction of particles that settle at high settling velocities. This phenomenon can be explained by the diurnal flowrate variation in the sewer system, with higher flowrates leading to the advection of resuspended faster settling particles compared to low flow conditions.

Generally, it is observed that on average, the particles are settling faster under wet weather conditions than under dry weather conditions. However, comparing the range of the PSVD

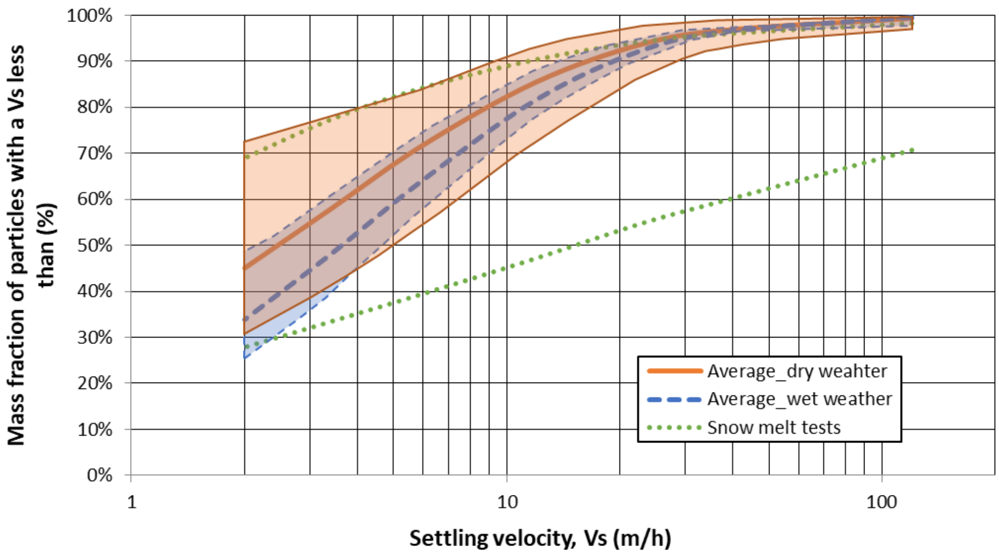

Figure 6.11: PSVD curves under different weather conditions: Solid lines represent the average and the boundaries under dry weather conditions; dashed lines represent the average and the boundaries under wet weather conditions; and the dotted lines represent the two curves obtained under snowmelt conditions with rain.

curves, the range of the PSVD curves under dry weather is larger than under wet weather, and the range of the wet weather samples is mostly included into the dry weather range. This, however, may be due to the fact that less samples were obtained under wet weather conditions.

During the snowmelt period, the percentage of particles that are settling fast is higher than under dry and wet weather conditions. This coincides with the increasing quantity of grit particles collected at the bin during the spring period when the snow melts in the Québec area. Moreover, the PSVD curve obtained can be very variable depending not only on the snowmelt conditions (i.e. the temperature), but also on rain events occurring during the snow melt period (see Figure 6.11). When occurring together with the snowmelt, a rain event can mobilise the particles used in winter road maintenance to improve traction and transport them to the WRRF. Despite the considerable differences that have been observed between the snowmelt period with rain, the dry and the wet weather conditions, only two samples were collected for the snowmelt period. One should therefore be careful when drawing general conclusions. The effect of the dry, wet and snowmelt conditions was already observed on the particle size distribution in a previous study (Plana et al., 2017).

6.2.4 Conclusions

In conclusion, since grit is highly heterogeneous, the study of the PSVD provides key information on the settleability of the particles as they exist in raw wastewater, and thus, provides a better knowledge of the particle characteristics and a better estimation of the grit chamber performance. However, existing PSVD methods, such as the ViCAs, have to be adapted for fast settling particles, like grit particles.

More importantly, since the organic fraction of removed grit is significant and variable (Plana et al., 2018), and since the density of the particles is thus variable, direct measurement of the governing characteristic, particle settling velocity, should be pursued, rather than using particle sizing that cannot easily be translated into settling characteristics (See also Chapter 5). Hence, the study of the PSVD allows better estimation of the grit chamber performance, and, consequently, has the potential of promoting better designs.

Both methods, the 2m-ViCAs test and the elutriation test, are reproducible methods and allow obtaining the same PSVD (i.e. lower than 5 % variation for the ViCAs tests and lower than 10 % variation for the elutriation tests, in the worst cases). However, the ViCAs requires less sample volume and experimentation time, and it therefore the preferred method.

Finally, it was observed that the dynamic characteristics of the wastewater and weather conditions have an important impact on the PSVD curves. First, at high TSS concentrations, there are more particles that settle fast compared to low TSS concentration samples (e.g. fractions possibly being 5 % lower for fast settling particles and up to 30 % lower for slow settling particles for TSS concentrations varying from 100 to 330 mg/L). Then, generally, particles are settling slower under dry weather conditions. The fraction of fast settling particles increases under wet weather, and this fraction might even increase further under snowmelt conditions combined with rain event. However, further studies should be performed to confirm the weather conditions' impact.

Chapter 7

Vortex grit chamber modelling

7.1 Introduction

This chapter tackles the specific objectives 2.a and 2.c related to the development of the conceptual model applied to vortex grit chambers, its calibration and validation. The chapter consists in two main parts.

The first part describes the data available from the vortex grit chamber case study, such as the inflow data, inlet and outlet data, the settling characteristics of the particles around the grit chamber, hydraulic data, and physical and operational information.

The second part consists in the model development applied to the vortex grit chamber case study. The structure of this second part is based on the published paper:

- Q. Plana, P. Lessard and P.A. Vanrolleghem (2020). Dynamic grit chamber modelling: dealing with particle settling velocity distributions. *Water Science & Technology*, 81(8): 1682–1699

The model concept and the results section of this conference paper have been extended for a proper understanding of the model development as well as to present the steps followed to reach the model proposed in this PhD thesis.

7.2 Data available

For the vortex grit chamber case study, the data available and data used to develop the conceptual model and its application are presented in this section. The data have been grouped in three main categories: performance data, hydraulic data and physical and operational data. Detailed explanations and data examples are provided in the following sections.

7.2.1 Performance data

In this section, water quantity and quality data from the Saint-Nicolas WRRF are presented. The data set includes flowrate dynamics, inlet and outlet dynamics, and settling characteristics of the inlet and outlet channels collected at different points around the studied vortex grit chamber.

Inlet flow data

At the Saint-Nicolas WRRF case study, different inlet flow dynamics are observed: seasonal, diurnal and an even shorter time scale (5 minutes) due to pump activations. The latter, short-term, variations have been studied in detail since they influence the HRT of the vortex grit chamber (e.g. ranging between 1 and 5 minutes), thus its efficiency.

The inlet flow data of the Saint-Nicolas WRRF were provided by the facility. The supervisory control and data acquisition (SCADA) system installed at the Saint-Nicolas WRRF stores average hourly flow data from a flowmeter installed between the grit chambers and the equalization tanks. The hourly inflow from the end of March until the beginning of December 2017 is depicted in Figure 7.1. Also, the daily rain data observed on the nearby weather station installed at the Québec City Jean Lesage International Airport by Environment Canada are shown in Figure 7.1 for the same period (Environment Canada, 2019). The rain data has only been used for a better understanding of the inlet dynamics. The weather station is located on the other side of the river and the rain data might differ from the rain event on the studied catchment.

As observed in Figure 7.1, considerable variations can be observed along the year. During spring and autumn, higher flows are observed compared to the summer season. In April, the high flows are due to snowmelt together with some rain events. Between the end of October and the beginning of November, intense rain events also occurred and created high inlet flows at the WRRF. However, they are neither as high as nor as long as during the snowmelt period.

From the inflow data from years 2016 and 2017, a typical daily profile was determined under dry weather conditions (see Figure 7.2). This has been used to understand the inlet dynamics

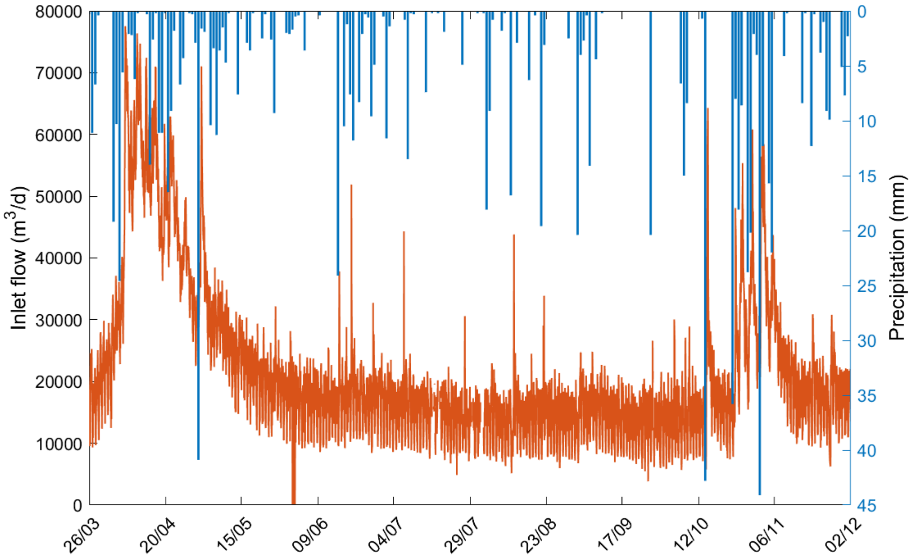

Figure 7.1: Inlet hourly flow at the Saint-Nicolas WRRF and daily precipitation from the weather station at the Québec City Jean Lesage International Airport from March 26th, 2017 to December 2nd, 2017.

at the WRRF and also to plan sampling campaigns. The average flow for dry weather was estimated considering only data collected at least two days after a rain event. The snowmelt period from the two years was not considered for the daily profile estimation due to the high flows and different dynamics observed.

In Figure 7.2, the typical daily dynamics under dry weather can be observed. Along the day, two different peaks are observed due to inhabitants activity. The first one is the morning peak when people generally wake up, and the second one, is the evening peak when people come back home. At night, the lowest flows are observed because of the low activity of the inhabitants.

After rain events, an impact can be observed at the inlet flow at the WRRF. As shown in Figure 7.3, after a rain event, the inlet flow may increase by up to three times the inlet flow under dry weather (see daily profile under dry weather conditions in Figure 7.2).

Inlet and outlet data

Considerable variations in the studied water quality variables, i.e. turbidity, conductivity and temperature, can be observed. As explained in Section 3.6, in this section only treated data is presented.

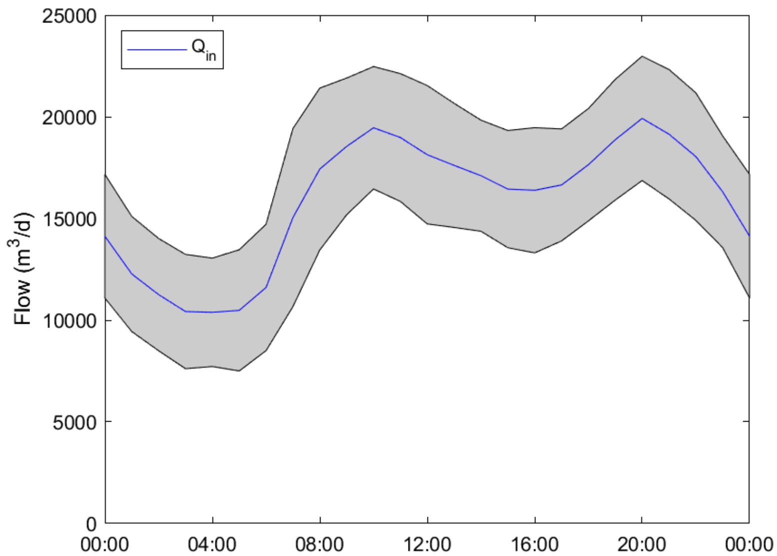

Figure 7.2: Average inlet flow with bands representing the 1σ (68 %) confidence interval for the dry weather days at the Saint-Nicolas WRRF.

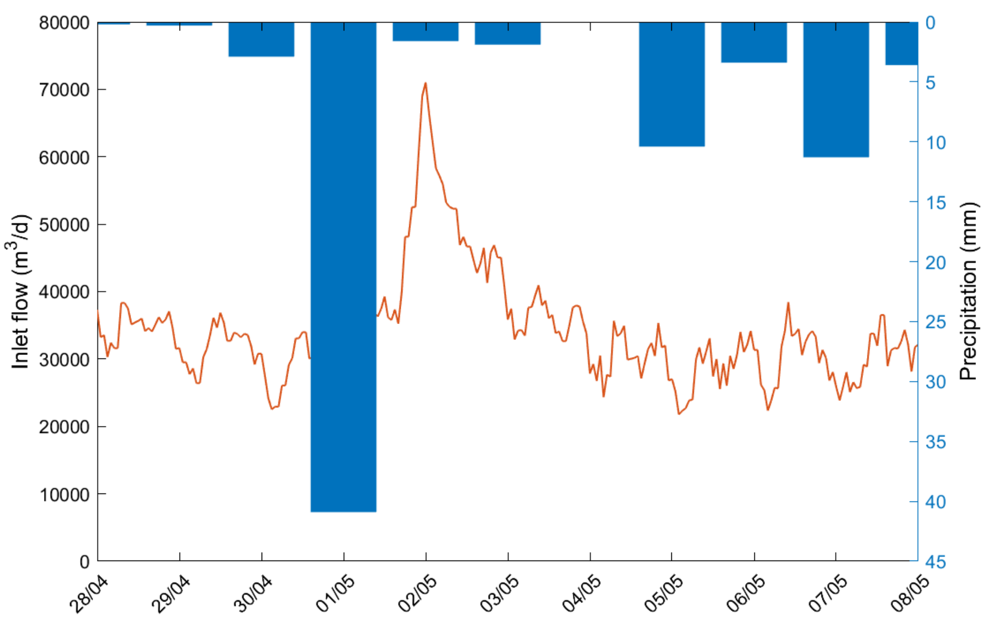

Figure 7.3: Inlet hourly flow dynamics after a rain event at the Saint-Nicolas WRRF from April 28th, 2017 to May 8th, 2017.

As mentioned, the variable of interest for grit chambers modelling is the TSS concentration. However, the sensors installed are measuring turbidity (see Figure 7.4). Thus, the turbidity measurements have to be converted to TSS concentration values. To this end, a linear turbidity-TSS relationship was built for each sensor (as suggested in other studies such as Lemieux and Lessard (1993)) (see Figure 7.5). For each sample, the TSS concentration was measured in the lab following the Standard Methods procedure (APHA, 2012). Then, these values were compared to the on-line turbidity sensor output while sampling. In case of flow proportional samples, the equivalent turbidity was also estimated flow-proportionally. For the same period as presented in Figure 7.4, the TSS concentrations estimated are depicted in Figure 7.6.

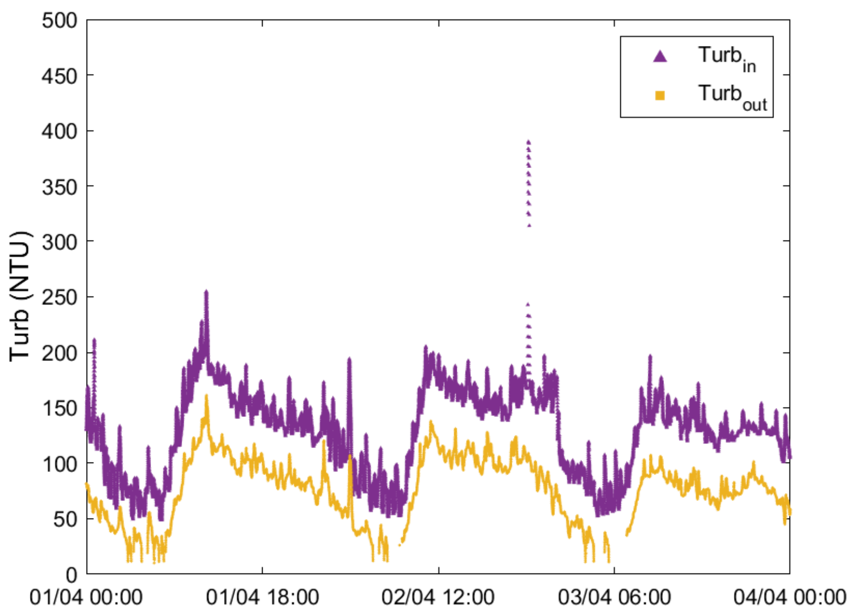

Figure 7.4: Three days of validated inlet and outlet turbidity data for the grit chamber at the Saint-Nicolas WRRF from April 1st, 2017 to April 4th, 2017.

Comparing the dynamics of the TSS concentrations at the inlet and at the outlet, in Figure 7.6 it is noticed that they are following the same pattern. However, the TSS concentrations at the inlet and outlet are different, as expected. Logically, the TSS concentrations at the outlet of the grit chamber are lower than the inlet since a % of particles is removed by the grit chamber. Despite the fact that two turbidity sensors were installed at the inlet of the grit chamber to study the vertical heterogeneity, no significant differences were observed at the two heights: the four sampling points installed at the inlet were collected separately at one occasion and the TSS concentrations obtained were varying between 185 and 197 mg/L. Hence, the most reliable TSS data at the inlet of the grit chamber were used on further studies.

In Figure 7.6, the daily dynamics in TSS can also be observed. Coinciding with the inlet flow dynamics, low TSS concentrations are observed during the night and there is a TSS peak in

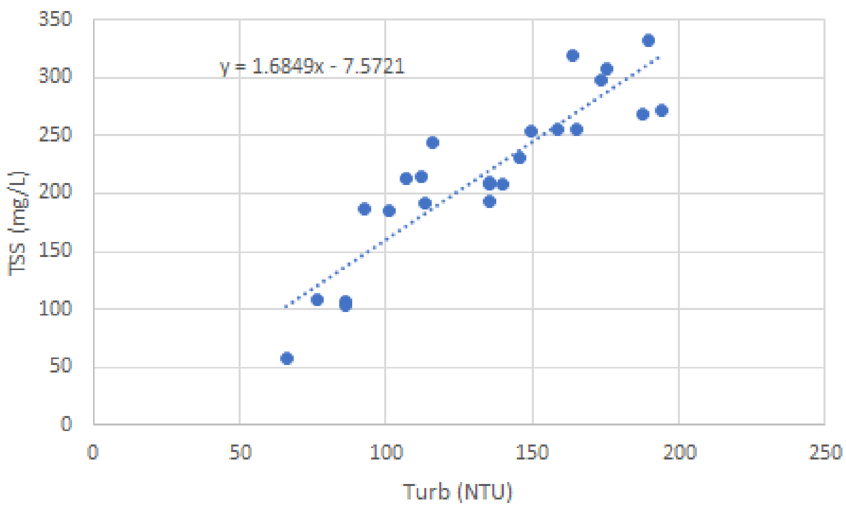

Figure 7.5: Example of turbidity - TSS concentration linear relationship for a sensor at the inlet of the vortex grit chamber at the Saint-Nicolas WRRF.

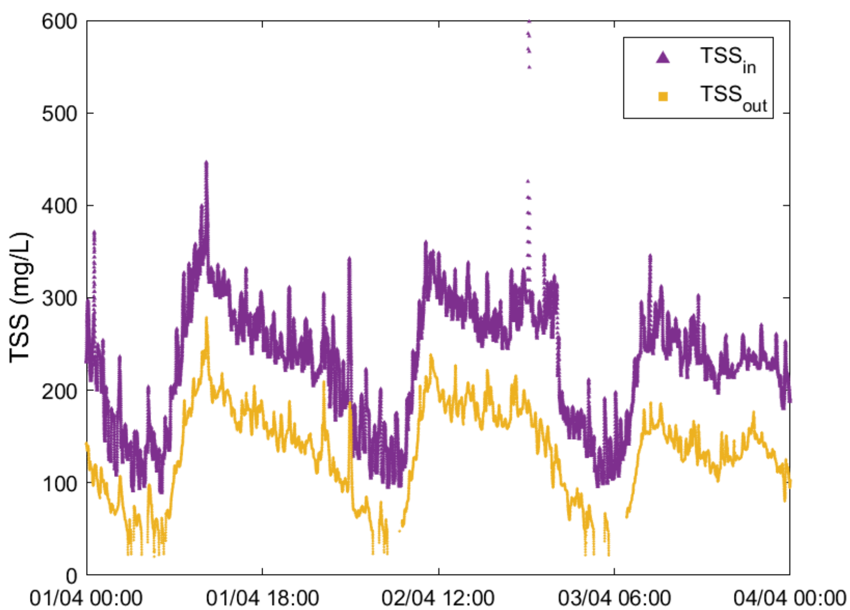

Figure 7.6: Three days of converted inlet and outlet TSS data at the Saint-Nicolas WRRF from April 1st, 2017 to April 4th, 2017.

the morning. The quick variations over a short period of time (subhourly) can be related to the pump activations presented in Section 3.1.1 (see Figure 7.7). Comparing the inlet flow and the TSS concentrations, a certain correlation between the inlet flow and the TSS concentration can be deduced. So far, it has not been possible to deduce a consistent relationship between these parameters, and the behaviour seems to vary between pump activations. In Figure 7.7, only the TSS measurements at the inlet are depicted but the TSS concentrations at the outlet follow a similar pattern.

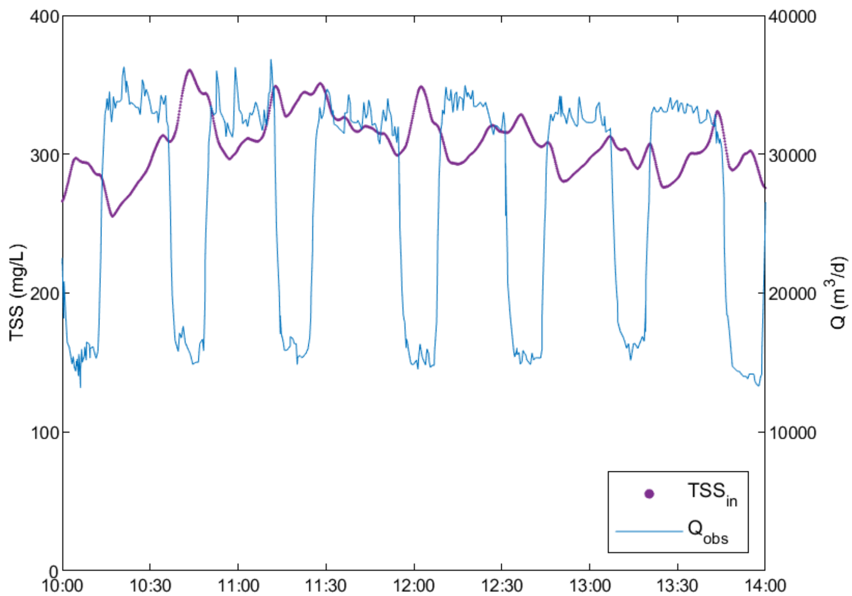

Figure 7.7: Four hours of TSS data from the inlet turbidity sensor and observed inlet flow at the Saint-Nicolas WRRF during April 2nd, 2017.

Similar to the inlet flow dynamics, after a rain event, the TSS concentrations have been observed to also increase considerably. In Figure 7.8, an increase compared to dry weather TSS dynamics is noticed. This peak coincides with the inlet flow increase shown in Figure 7.3.

The conductivity sensor, which also measures the temperature, installed at the inlet of the grit chamber, also shows daily dynamics as depicted in Figure 7.9. During the night, a temperature decrease is observed, whereas it rises during the day showing a peak in the morning and another one in the evening. On the contrary, the conductivity increases during the night and decreases during the day.

Similar to the TSS measurements, conductivity and temperature vary with the pump activations (see Figures 7.10 and 7.11). However, in contrast to the TSS dynamics, the correlation between the inlet flow and these quality parameters, i.e. conductivity and temperature, is clearer. A big step and an instantaneous change are observed when the flow wave arrives at the WRRF. During winter time, conductivity and temperature increase when the pump turns on. During summer time, temperature increases when the pump turns on, while the conductivity decreases.

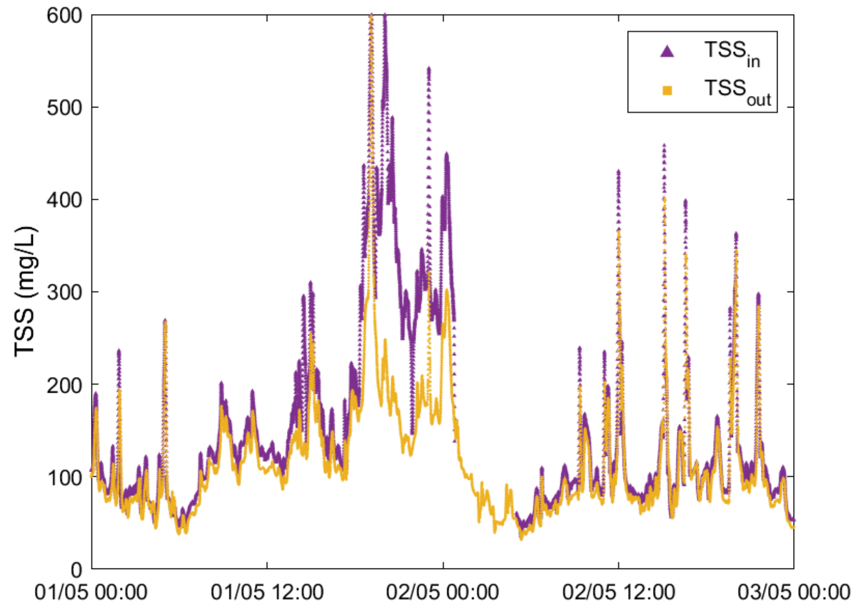

Figure 7.8: Inlet and outlet TSS dynamics after a rain event at the Saint-Nicolas WRRF from May 1st, 2017 to May 3rd, 2017 (corresponding flow rates depicted in Figure 7.3). Most of the TSS measurements at the bottom of the inlet channel were removed because of their poor quality.

After a rain event, a conductivity decrease is observed in Figure 7.12. Conversely, there is no a remarkable change in the temperature measurements. The conductivity reduction coincides with the peak flow after the rain event presented in Figure 7.3.

PSVD data

As presented in Section 6.2.3, PSVD curves can be related to TSS concentrations. From all the tests carried out at the Saint-Nicolas WRRF, a range of PSVD curves could be determined.

At the inlet of the grit chamber at Saint-Nicolas WRRF, 22 ViCAs tests were accepted as valid. From these tests, 16 samples were collected under dry weather conditions, 4 samples under wet weather conditions and 2 samples during a snowmelt period with a rain event. The range of the PSVD curves observed has been presented in Section 6.2.3. The TSS boundaries of the PSVD curves presented in Figure 7.13 have been delimited only considering the curves obtained under dry weather conditions.

At the outlet of the studied vortex grit chamber, 12 valid ViCAs tests with a mass balance below ± 15 % were obtained. Seven of them were collected under dry weather conditions, three under wet weather conditions and two during the snowmelt period. Similarly to the

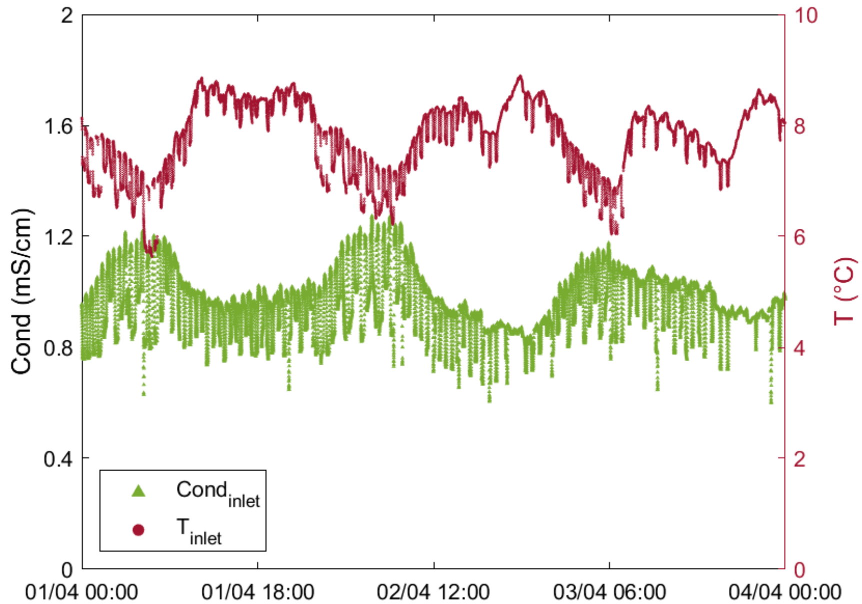

Figure 7.9: Three days of treated conductivity data at the Saint-Nicolas WRRF from April 1st, 2017 to April 4th, 2017.

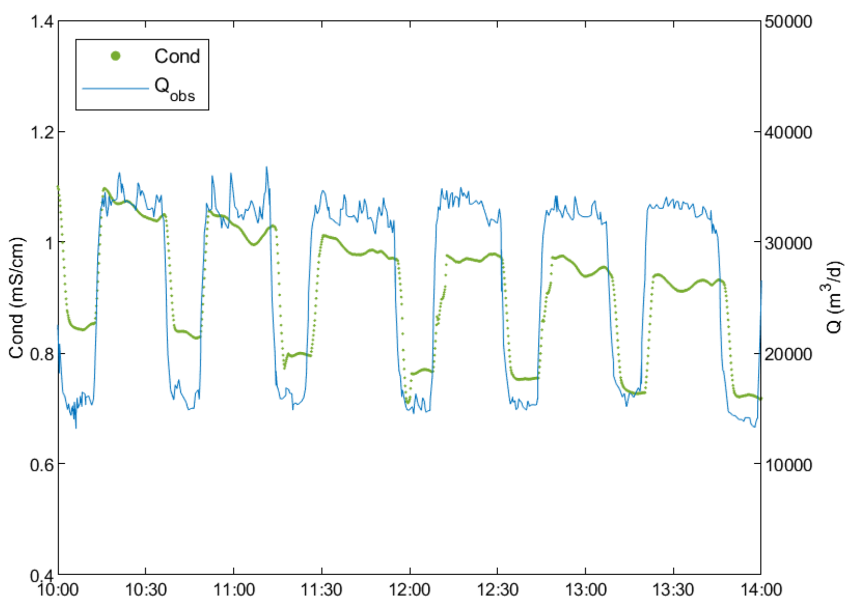

Figure 7.10: Four hours of conductivity data and observed inlet flow at the Saint-Nicolas WRRF during April 2nd, 2017.

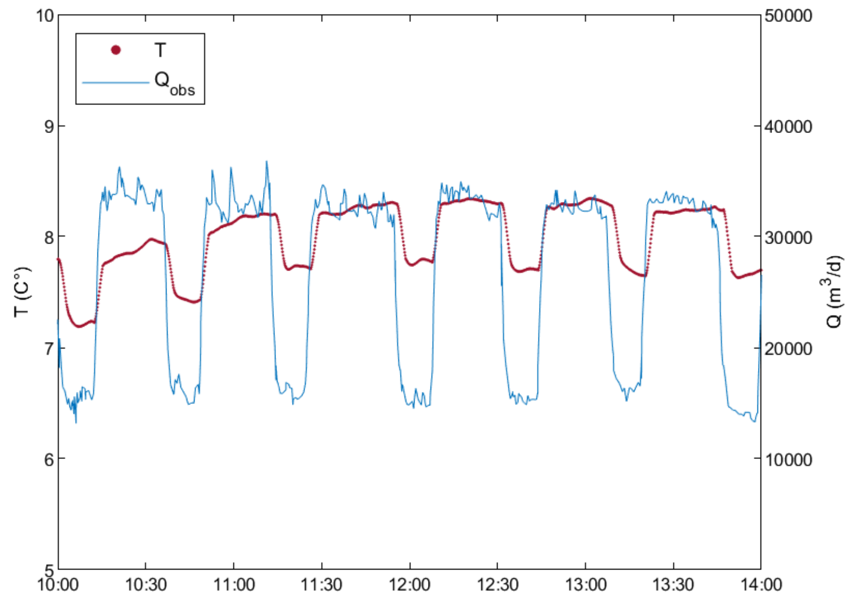

Figure 7.11: Four hours of temperature data and observed inlet flow at the Saint-Nicolas WRRF during April 2nd, 2017.

determination of the inlet boundaries, the outlet boundaries have been estimated through the PSVD curves obtained from the samples collected under dry weather conditions (see Figure 7.14).

Comparing the boundaries of the inlet and the outlet, small differences can be observed. The particles at the inlet settle slightly faster than the particles at the outlet. This small difference may be explained by the small percentage of particles removed at the grit chamber (according to Qasim (1999), between 5 - 10 %), the number of samples collected from both sampling locations do not coincide (less samples were collected at the outlet), and the range of TSS concentrations studied for both sampling points do not coincide (the TSS concentration range at the outlet is narrower than at the inlet).

7.2.2 Hydraulic data

To better understand the hydraulics into the vortex grit chamber, two tracer tests were performed following the indications mentioned in Section 3.5. Both tests were carried out at the grit chamber number 2 between 8 and 9 a.m..

The first tracer test took place in November 2016. At that time, the impact of the pump activations on the inlet flow dynamics was unknown. Thus, the inlet flow per grit chamber

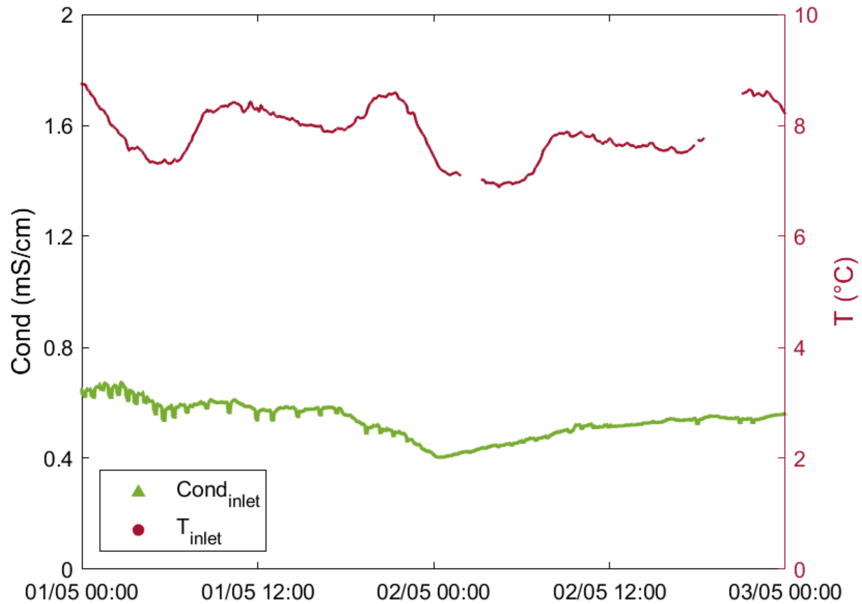

Figure 7.12: Conductivity and temperature dynamics after a rain event at the Saint-Nicolas WRRF from May 1st, 2017 to May 3rd, 2017 (corresponding flow rates depicted in Figure 7.3).

was only measured at the Parshall flume with a ruler at the beginning and at the end of the tracer test: approximately 4,000 and 16,000 m^3/d, respectively. Thus, at the beginning of the test, the pump was off, and at the end of the test, the pump was on. As a result, the HRT in the grit chamber can be expected to be between 5.3 and 1.4 min, from the beginning to the end of the test.

The tracer concentration evolution at the outlet of the studied grit chamber is depicted in Figure 7.15. Note that the HRT of the inlet channel (15 seconds under the studied conditions) between the injection point and the inlet of the grit chamber has not been considered to model the hydraulics of the grit chamber since the channel has not been part of the water quality study and the model of the vortex grit chamber. In addition, since the flow varied throughout the test, and the time instant when the pump was turned on is unknown, the mass of the recuperated tracer could not be estimated accurately. Thus, the mass balance could not be properly estimated to decide whether the test was valid.

On Figure 7.15, an early peak is observed. This means that there is a short-circuit path between inlet and outlet. Also, there is a slow response representing that part of the water that stays sufficiently long in the grit chamber to completely mix the tracer with the water.

The second tracer test was performed in July 2018. Now being aware of the impact of the

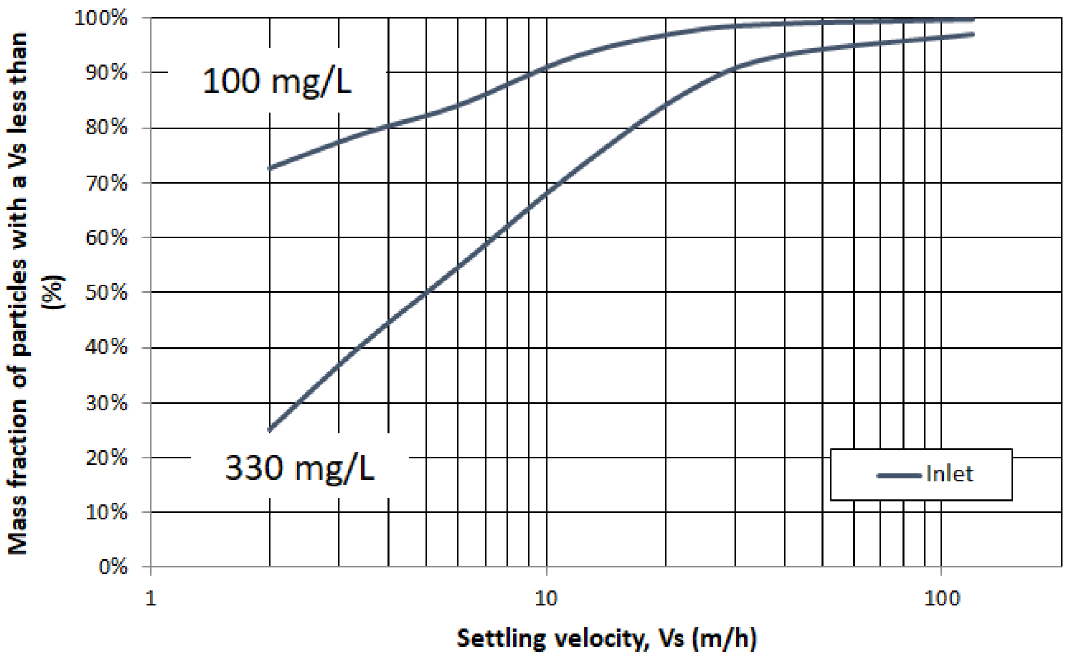

Figure 7.13: PSVD boundaries at the inlet of the vortex grit chamber at the Saint-Nicolas WRRF. The boundary at low TSS concentration corresponds to the experimental PSVD curve at 100 mg/L, and the boundary at high TSS concentration corresponds to the experimental curve at 330 mg/L.

pumping activations on the inlet flow, the flow was recorded during the test using the flowmeter installed after the grit chambers. For post-processing of the data and the hydraulic model, the inlet flow of the WRRF was considered to be distributed equally over both grit chambers.

This second tracer test was started when the pump was on, and it was finished when the pump was off. The detailed inlet flow per grit chamber during the test is shown in Figure 7.16. Thus, under these flow conditions the HRT in the grit chamber varied from 1.8 to 4.2 min.

The tracer concentration evolution observed at the outlet of the grit chamber for the second tracer test is presented in Figure 7.17. Similarly to the first tracer test, the HRT of the inlet channel has not been considered for the hydraulic model.

Similar to the first tracer test, a peak appears quickly because of the short-circuited part of the flow. Afterwards, a slow response is again noticed for that part of the tracer that resides longer in the grit chamber and is well-mixed.

Considering the flow variations, the mass balance of the tracer could be determined. Sixty % of the mass prepared for the test was recovered at the outlet of the grit chamber. This low % may be explained by the fact that part of it was lost during the injection, i.e. some tracer

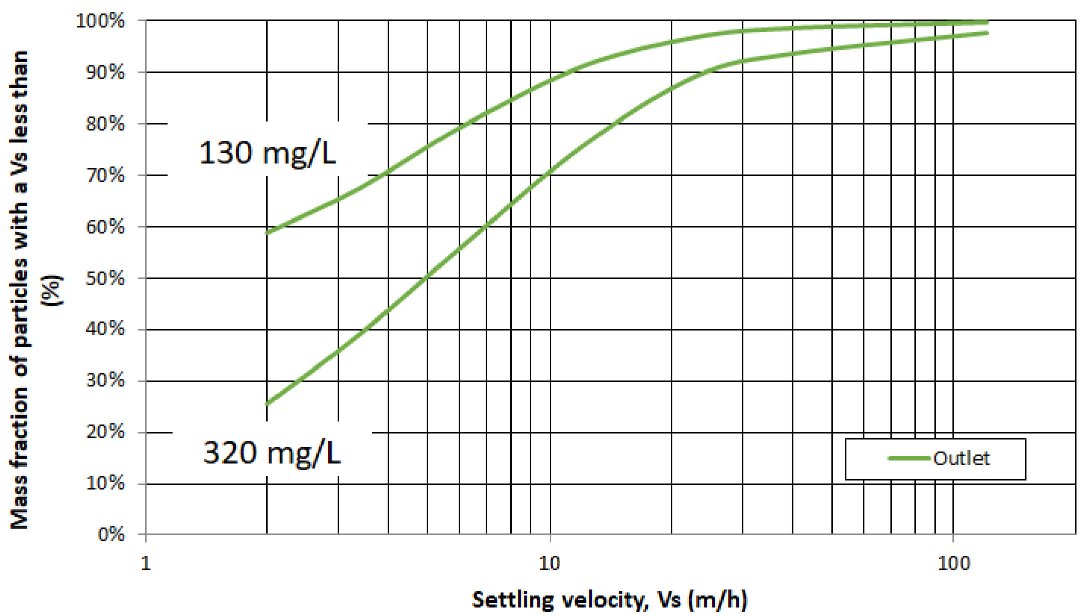

Figure 7.14: PSVD boundaries at the outlet of the vortex grit chamber at the Saint-Nicolas WRRF. The boundary at low TSS concentration corresponds to the experimental PSVD curve at 130 mg/L, and the boundary at high TSS concentration corresponds to the experimental curve at 320 mg/L.

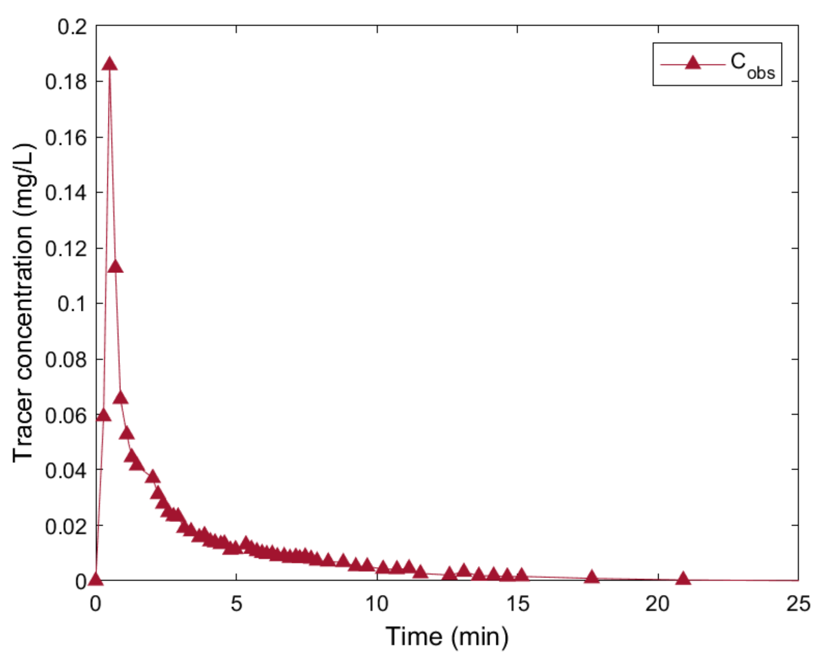

Figure 7.15: Tracer concentrations observed at the outlet of the studied vortex grit chamber.

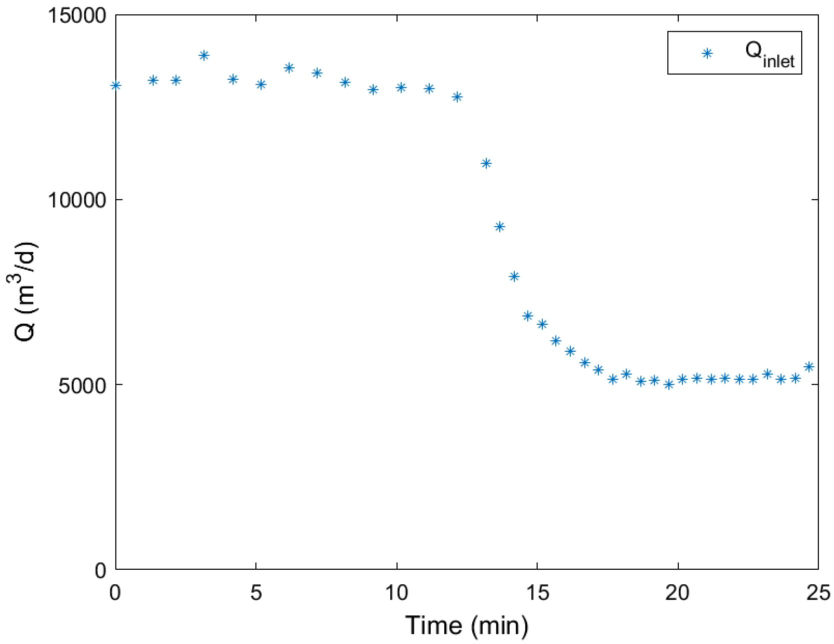

Figure 7.16: Inlet flow per grit chamber during the tracer test.

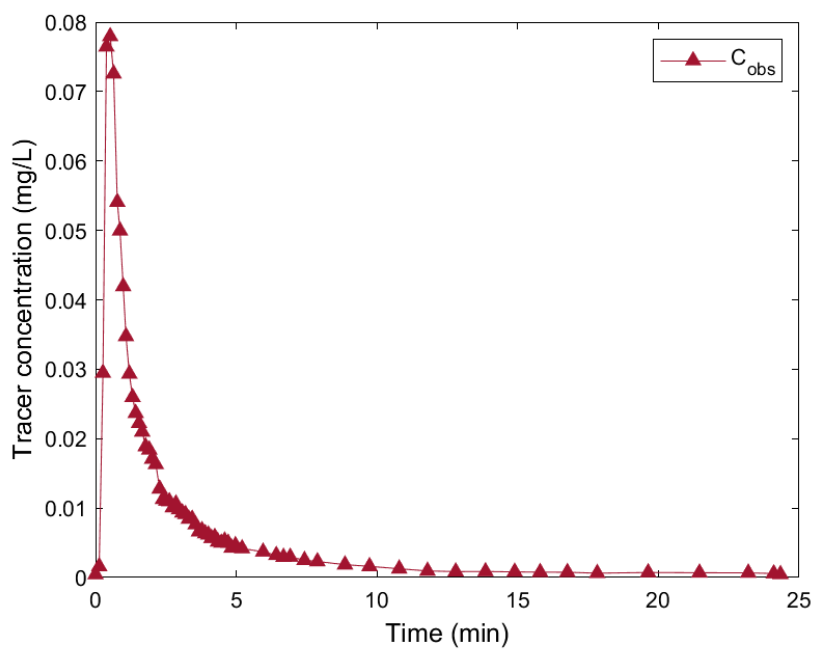

Figure 7.17: Tracer concentrations observed at the outlet of the studied vortex grit chamber.

remained in the bottle used to transport it, in the funnel and in the tube used for the injection or adsorption on solids. Hence, this tracer recovery has been considered acceptable to further develop the hydraulic model of the studied grit chamber.

The hydraulic model developed is presented in Section 7.3.3 as one of the steps followed to develop the vortex grit chamber model.

7.2.3 Physical and operational data

Physical dimensions of the studied vortex grit chamber and operational information about the extraction of settled particles and the paddles rotation were already presented in Section 3.1.1. This information has been considered for the model parameters as such (i.e. no further calibration has been proceeded).

7.3 Vortex dynamic grit chamber modelling: Dealing with particle settling velocity distributions

This section follows a journal paper structure since it has been submitted as such to *Water Science and Technology*.

7.3.1 Introduction

Grit chambers can be found at the headworks of most water resource recovery facilities (WRRFs) to protect the equipment and processes downstream and maintain the performance of primary and secondary treatments (WEF, 2016). Despite their important role, characterization and modelling studies of these process units are scarce because they have always been considered to have a low influence on secondary treatment and studies often start from primary effluent. Importantly, grit removal efficiency is increasingly questioned by utilities since grit is still found to accumulate in downstream processes (McNamara et al., 2009). In addition, only a low % of particles found in wastewater are grit particles, i.e. 5-10 %, which makes them difficult to measure under typical sampling and analysis situations (Qasim, 1999; WEF, 2016).

The characteristics of particulate pollutants at the inlet, outlet and underflow of grit chambers are rarely documented (Rife and Botero, 2012). This lack of knowledge leads to an improper grit definition, a non-existing standard protocol for sampling and characterization, and a non-existing standard protocol to evaluate the removal performance of grit chambers (WEF, 2016). Moreover, modelling has been limited to very simple static models for % TSS removal or complex hydrodynamic models focusing on flow patterns (i.e. computational fluid dynamic (CFD) models) (WEF, 2016).

Since a grit chamber is a sedimentation process, the particles' separation depends on the gravity force and wastewater particle settling characteristics (WEF, 2016). Thus, the goal of this study is to properly characterize the influent in view of grit chamber modelling and to propose a new dynamic model based on the particle settling velocity distribution (PSVD) approach inspired by the work of Bachis et al. (2015) on primary clarifiers.

7.3.2 Materials and methods

In this study, full-scale grit chambers of a combined sewage WRRF in the Québec City area (Canada) were evaluated. The WRRF has a capacity of 36,000 people equivalent and an average design flow of 18,760 m^3/d. The system studied consists in two vortex grit chambers with a diameter of 4.2 m, with a maximum capacity of 50,940 m^3/d each. With the current operational conditions, the hydraulic retention time varies between 1 and 4 minutes.

First, to characterize the particles around the grit chamber, the ViCAs protocol (Chebbo and Gromaire, 2009) was used. However, the standard 70cm-ViCAs column had to be upgraded to a 2m-column to better estimate the high settling velocities of the particles of interest (see Chapter 6). Several samples were collected at different flow and total suspended solids (TSS) conditions to evaluate how the PSVD varies.

To study the solids dynamics around the grit chamber, RSM-30 automated monitoring stations (Primodal, Hamilton, ON, Canada) were installed to collect long-term continuous on-line data at high frequency. The stations were equipped with several sensors to measure TSS at the inlet and outlet. In addition, to assure the quality of the data series, a rigorous maintenance protocol was applied together with state-of-the-art data management and treatment (Alferes et al., 2013).

Also, to build the hydraulic model of the grit chamber, two tracer tests at different flow conditions were performed. The tests consisted in a pulse input with the Rhodamine WT fluorescent dye. This tracer was chosen because it has no influence on the hydraulics behaviour of the tank (i.e. same transport characteristics as water, no modification of the water density, no reactions with nor absorption onto solids, highly soluble and not toxic).

Then, the PSVD model, based on mass balances and particle settling velocity distributions, has been developed to reproduce the TSS dynamics at the outlet and underflow of the grit chamber. It consists of the fractionation of the TSS in a determined number of particle classes, each class being characterized by a mean settling velocity extracted from the experimental PSVD curves (see Figure 7.18) (Maruéjouls et al., 2015; Bachis et al., 2015).

The 1-D layered model was implemented in WEST (mikebydhi.com), dividing the tank in a limited number of homogeneous layers. For example, in Figure 7.19, the hydraulic diagram

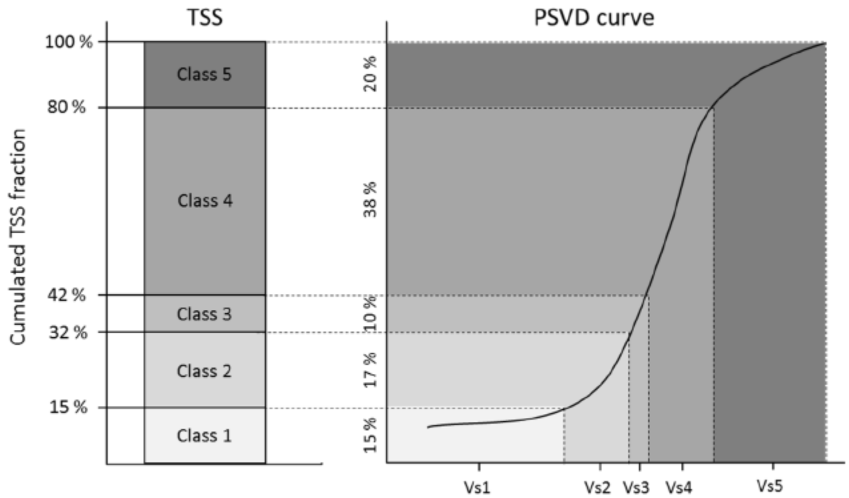

Figure 7.18: Concept of TSS fractionation from a measured PSVD curve needed to calibrate the PSVD model in this case with 5 classes each with their settling velocity Vs (Maruéjouls et al., 2015).

of the PSVD model for primary clarifiers is presented (Bachis et al., 2015). The tank is fed through the fifth layer with a flow Q_{in}. The flow at the outlet (Q_{out}) is modelled to flow out of the first layer while the underflow ($Q_{underflow}$) is modelled as the outlet of the tenth layer. Between layers, Q_{up} is the flow transported to layers above, Q_{down} is the flow transported to layers below (Bachis et al., 2015). Also, a particle flux is observed between layers of the tank; $J^*_{up}(i)$ and $J^*_{down}(i)$ are the mass of particulate pollutant transported up and down (depending on the layer), hence the "*" to indicate its optional presence above or below the feeding layer by advection. $J_{settling}$ is the mass of particulate pollutant settling from the layer above. Then, for each layer i with a height H, a dynamic mass balance is constructed for the individual particle class n to predict the evolution of its concentration (Tik et al., 2014; Bachis et al., 2015):

$$\begin{aligned}\frac{d\,C_n(i)}{d\,t} =& \frac{1}{H_{layer}}(J^*_{up,n}(i+1) - J^*_{up,n}(i) + J^*_{down,n}(i-1) - J^*_{down,n}(i) \\ &+ J_{settling,n}(i-1) - J_{settling,n}(i))\end{aligned} \tag{7.1}$$

In contrast to the PSVD model proposed for primary clarifiers by Bachis et al. (2015), a mixing flow between layers was added to better represent the induced vortex forces in the grit chamber. This was inspired by the work of Vallet et al. (2014) (see Figure 7.19). The mass balance including the mixing fluxes (J_{mix}) for layer i and particle class n becomes:

$$\frac{d\, C_n(i)}{d\, t} = \frac{1}{H_{layer}} (J^*_{up,n}(i+1) - J^*_{up,n}(i) + J^*_{down,n}(i-1) - J^*_{down,n}(i) + J_{settling,n}(i-1) - J_{settling,n}(i) + J_{mix,n}(i+1) + J_{mix,n}(i-1) - 2 \cdot J_{mix,n}(i)) \tag{7.2}$$

where the J_{mix} is calculated as follows:

$$J_{mix,n}(i+1) = \frac{Q_{mix}}{A} \cdot C_n(i) \tag{7.3}$$

where Q_{mix} is the mixing flow between layers due to the vortex forces (m^3/d), and A is the surface of the grit chamber (m^2).

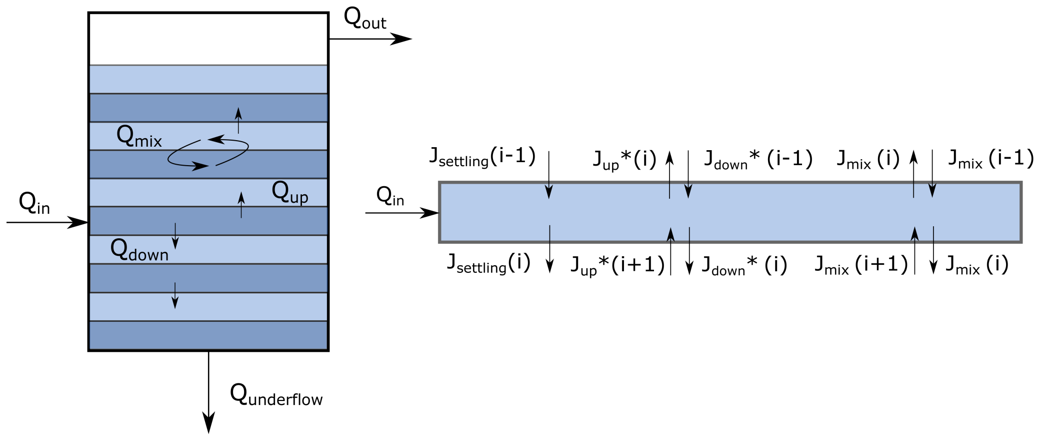

Figure 7.19: Diagram of the hydraulic model with the representation of the different variables included in the model including the Q_{mix} (a) and the pollutants flux on the feed layer, including the flux due to mixing (J_{mix}) (b). The "*" indicates the optional presence above or below the feed layer.

7.3.3 Results and discussion

PSVD fractionation

First, at the inlet of the grit chamber, the settling characteristics were determined using 16 samples collected under different flow conditions during dry weather conditions. As mentioned in Section 6.2.3, when analysing the ensemble of the 16 measured PSVD curves, it was observed that they show a relationship with the inlet TSS concentration of the sample, i.e. at a higher concentration, the PSVD curve is located in the lower region, as indicated in Figure 7.13 and presented again in Figure 7.20 (this relation was also found in the studies of Bachis et al. (2015) and Maruejouls et al. (2011)).

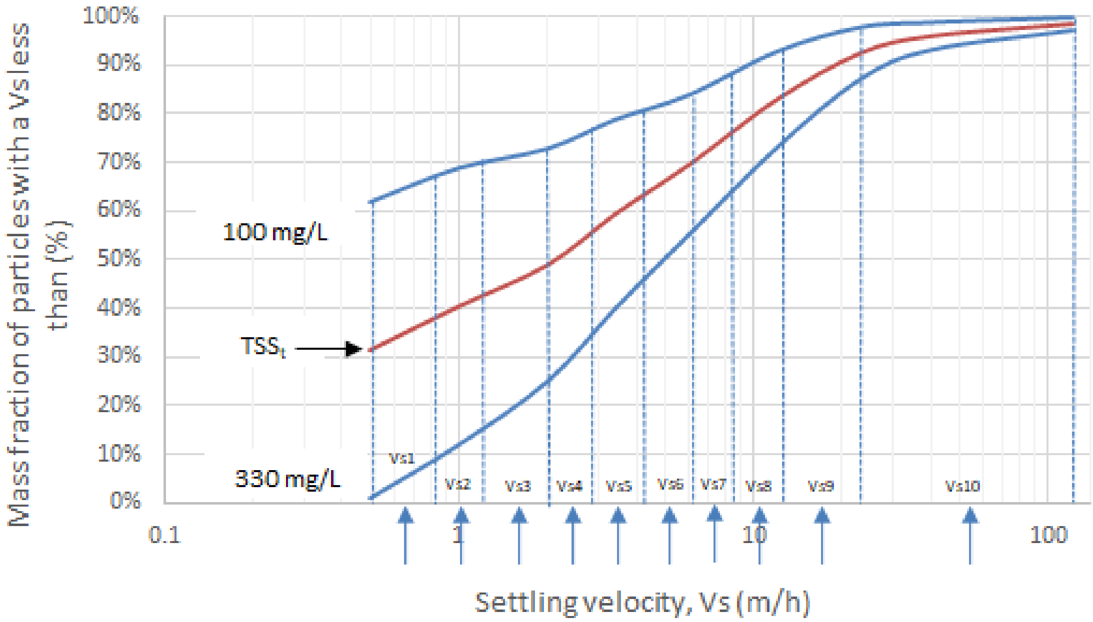

Figure 7.20: Inlet PSVD settling velocity class boundaries for a fractionation into 10 particle classes. The arrows indicate the settling velocity that characterizes each class, calculated as the geometrical mean of the boundaries of each class.

Furthermore, the minimum settling velocity measured with the 2m-ViCAs columns as shown in Figure 7.13 was 2 m/h. To better represent more particle classes it has been extrapolated down to 0.5 m/h as depicted in Figure 7.20. Each boundary was extrapolated following the equation:

$$F_{v_s} = b \cdot ln(v_s) + a \tag{7.4}$$

where F_{v_s} (-) is the estimated fraction for a given settling velocity, v_s settling velocity (m/h), and a and b coefficients of the logarithmic regression. First, a and b coefficients were adjusted to the experimental curves. Then, the two equations for each boundary were used to estimate the settling velocities down to 0.5 m/h.

In addition, the PSVD curves obtained with the 2m-ViCAs column were described by ten particle classes. This number of classes was selected because it was concluded in other studies, i.e. Tik (2019), that the PSVD model performs the best predictions without excessive calculation time. Each particle class is characterized by a mean settling velocity (see Figure 7.20). The boundaries of the 10 classes were chosen considering ten equal fractions of the average PSVD curve. Then, from the established boundaries, the geometrical mean of the boundaries was determined and set as the class' settling velocity. For this study, the particle classes with their settling velocity are presented in Table 7.1.

Table 7.1: Particle classes characterized by their settling velocity determined for the studied vortex grit chamber.

Particle class	**Settling velocity (m/h)**
Class 1	0.67
Class 2	1.04
Class 3	1.63
Class 4	2.35
Class 5	3.44
Class 6	5.21
Class 7	7.50
Class 8	10.63
Class 9	17.71
Class 10	71.46

Since the TSS concentration at the inlet of the grit chamber is varying continuously as presented in Section 7.2.1, the PSVD curve corresponding to a given TSS concentration is estimated at each time step. To estimate the PSVD given a TSS concentration between the boundaries (i.e between 100 and 330 mg/L), the cumulated fraction for each particle class is determined by linearly interpolating the following equation (Tik, 2019):

$$F_{v_s}(TSS) = F_{v_s}^{high} + \left(\frac{F_{v_s}^{low} - F_{v_s}^{high}}{TSS_{low} - TSS_{high}} \right) \cdot (TSS - TSS_{high}) \tag{7.5}$$

where $F_{v_s}(TSS)$ (-) is the cumulated fraction for each particle class given a TSS (mg/L), the $F_{v_s}^{low}$ (-) is the cumulated fraction for the lowest TSS concentration boundary for each particle class, $F_{v_s}^{high}$ (-) is the cumulated fraction of the highest TSS concentration boundary for each particle class, TSS_{low} is the lowest concentration boundary observed from the ViCAs tests (mg/L), TSS_{high} is the highest concentration boundary observed from the ViCAs tests (mg/L), and TSS is the concentration under study (mg/L).

In case the inlet TSS concentration is outside the boundaries, the PSVD curve is determined by exponentially extrapolating the cumulated fraction for each particle class (Equations 7.6 and 7.8). For example, when the TSS concentration is below the lowest concentration boundary (i.e. 100 mg/L for this case study), the cumulated fractions for each particle class to obtain the PSVD curve is calculated following the equation:

$$F_{v_s}(TSS) = F_{v_s}^{max} + \left(F_{v_s}^{low} - F_{v_s}^{max} \right) \cdot e^{-k_{low} \cdot (TSS_{low} - TSS)} \tag{7.6}$$

where $F_{v_s}^{max}$ (-) is the maximum cumulated fraction for each particle class, and k_{low} (L/mg) is the constant defining how "fast" the curve approaches $F_{v_s}^{max}$.

Considering that the $F_{v_s}^{max}$ is 1 and $TSS_{low} = 100\ mg/L$ in this case study, Equation 7.6 can be simplified to:

$$F_{v_s}(TSS) = 1 + \left(F_{v_s}^{low} - 1\right) \cdot e^{-k_{low} \cdot (100 - TSS)} \tag{7.7}$$

To estimate k_{low}, it has been considered that the fraction limit of 1 should be reached at 1/3 of the TSS limits. Thus, $k_{low} = 1/\left(100 - TSS\right)$. For $TSS_{min} = 0\ mg/L$, k_{low} becomes 1/100 L/mg.

On the contrary, when the TSS concentration is above that highest concentration observed within the ViCAs tests (i.e. 330 mg/L for this case study), the cumulated fraction for each particle class above this limit TSS concentration is estimated with the equation:

$$F_{v_s}(TSS) = F_{v_s}^{min} + \left(F_{v_s}^{high} - F_{v_s}^{min}\right) \cdot e^{-k_{high} \cdot \left(TSS - TSS_{high}\right)} \tag{7.8}$$

where $F_{v_s}^{min}$ (-) is the minimum cumulated fraction for each particle class, and k_{high} (L/mg) is the constant defining how "fast" the curve approaches $F_{v_s}^{min}$.

For higher concentrations, considering $F_{v_s}^{min} = 0$ and $TSS_{high} = 330\ mg/L$, Equation 7.8 becomes:

$$F_{v_s}(TSS) = F_{v_s}^{high} \cdot e^{-k_{high} \cdot (TSS - 330)} \tag{7.9}$$

Similar to the case of TSS concentrations lower than 100 mg/L, for TSS concentrations higher than 330 mg/L, k_{high} can be estimated considering that the fraction limit is reached at 1/3 of the TSS limits. Then, $k_{high} = 1/(TSS - 330)$ L/mg. If a large TSS concentration is set as a TSS limit for security (for example $TSS_{max} = 10,000\ mg/L$), k_{high} becomes 1/9,670 L/mg.

The extrapolated curves considering minimum and maximum TSS concentrations as 0 and 10,000 mg/L, respectively are presented in Figure 7.21 for this case study. The PSVD curves for modelling can of course be estimated for an even wider range of TSS concentrations at the inlet.

Flow reconstruction model

Monitoring the inlet and the outlet of the grit chamber, the solids dynamics were tracked as presented in Section 7.2.1. Remarkably, the sudden inlet flow variations (see Figure 3.3), due

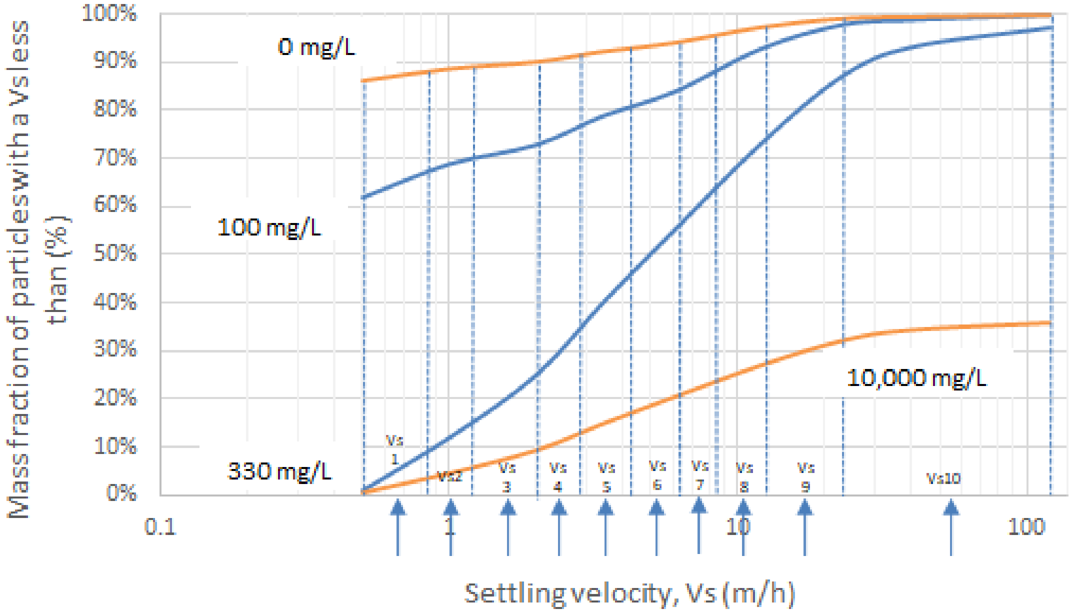

Figure 7.21: Inlet PSVD settling velocity class boundaries (in blue) and extrapolated boundaries (in orange) for a particle class fractionation into 10 classes. The arrows indicate the settling velocity that characterizes each class, calculated as the geometrical mean of the boundaries of each class.

to pumping sequences, have an impact on the TSS concentrations, both at the inlet and outlet (see Figures 7.6 and 7.7). They also affect the retention time of the grit chamber (varying between 1 and 5 min, as presented in Section 7.2.2) and, thus, the removal efficiency.

Despite the fact that the flow and pumping sequences are important for the grit chamber performance, only hourly flow rate data were available from the facility. Hence, a physical model had to be developed to reconstruct the flow at a higher frequency (i.e. Δt = 10 sec, similar to the data collected with the RSM-30 monitoring station) only considering the data available.

Fortunately, two days of detailed inflow data were available (see Figure 3.3 with one day of detailed inflow data). From these data, it was noticed that conductivity and temperature are highly correlated to the inlet flow as presented in Figures 7.10 and 7.11. From their signal, the on and off switching of the pump could be determined: when there is a sudden increase of the temperature/conductivity, the pump turns on, and when there is a sudden decrease, the pump turns off. To determine these changes, the slope of both variables has been estimated and the local maxima and minima have been located by fixing upper and lower limits of the derivation of each variable to not consider peaks due to noise. For example, in Figure 7.22, the temperature and its slope are depicted together with the detection limits.

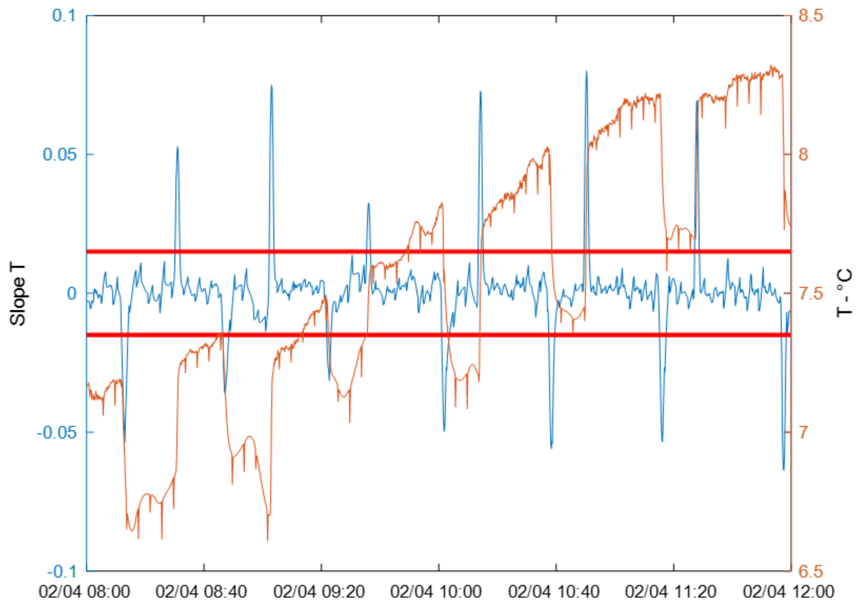

Figure 7.22: Temperature measurements and the slope of the temperature signal. The horizontal red lines indicate the limits set to estimate when the pump switches on and off.

In addition, from the signal, the period of time when the pump is on or off can also be calculated. Knowing the water volume of the pump pit and the pump capacity (see Section 3.1.1 for details), from the hourly flow, the fraction of the pumped flow and the fraction of the free flow can be determined.

Finally, the high frequency flow can be reconstructed at $\Delta t = 10$ sec as presented in Figure 7.23. Comparing the observed detailed flow for one of the two days where these data were available and the simulated flow at high frequency, a good performance of the physical model is observed.

Furthermore, to assure that the simulated flow agrees with the hourly flow provided by the utility in terms of the total water quantity, the average flow was estimated from the simulated flow. Comparing the calculated and the measured hourly flow the good performance of the physical model is confirmed (see Figure 7.24).

To sum up the model structure for flow reconstruction is presented in Figure 7.25. For more detail, the Matlab© code developed for flow reconstruction is provided in Appendix A.

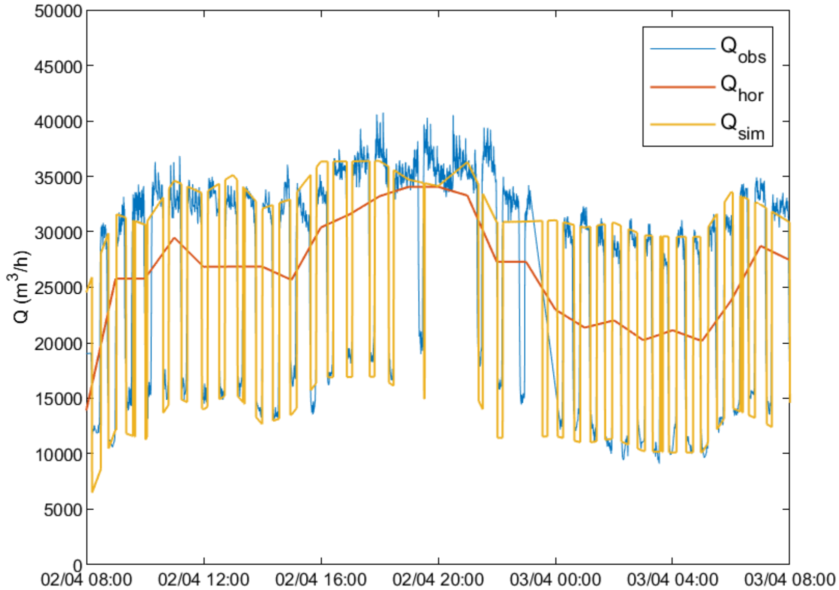

Figure 7.23: High frequency and hourly flow data at the Saint-Nicolas WRRF during April 2nd and 3rd, 2017.

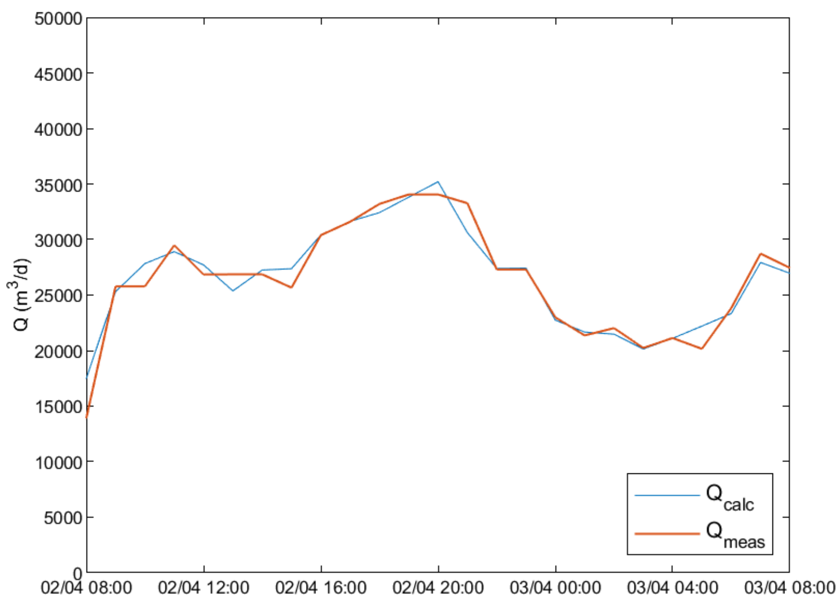

Figure 7.24: Hourly flow provided by the utility and average hourly flow calculated from the simulated flow.

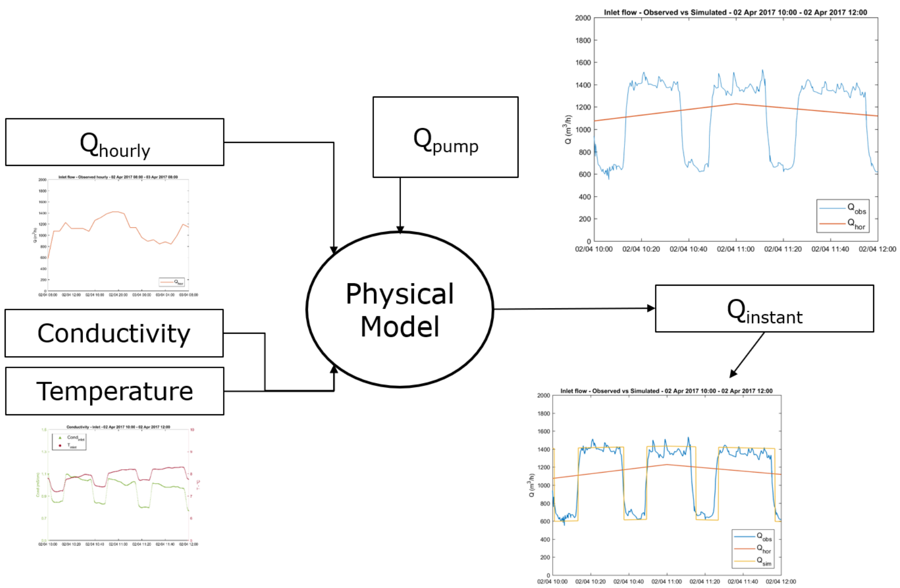

Figure 7.25: Scheme of the flow reconstruction model. For details see text.

Hydraulic model

From the two tracer tests (see Section 7.2.2), a hydraulic model of the grit chamber was built. The tracer dynamics show that part of the flow short-circuited very quickly through the grit chamber. This fraction of the flow was adjusted and the optimal was found to be one third. The other two thirds were considered passing through a settler section (see Figure 7.26).

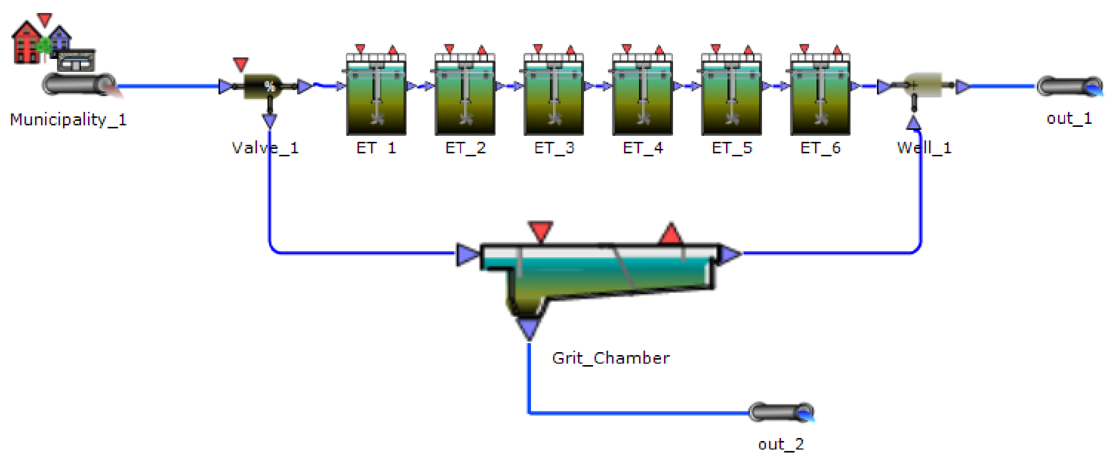

Figure 7.26: Scheme of the hydraulic model for the vortex grit chamber. One third of the flow is short-circuited to the outlet through the six tanks in series and the settler section is presented by the settler icon.

To represent the short-circuited flow, several configurations were tested. The best fit for both tracer tests was six tanks in series of 0.3 m^3 each as depicted in Figure 7.26. This volume corresponds to a layer of 13 cm at the top of the occupied volume of the grit chamber which corresponds to the water height at the inlet channel. In addition, the tracer test suggested three vertical layers (two between inlet and outlet, and one sediment layer to the underflow) to represent the hydraulic behaviour of the settling tank part as presented in Figure 7.27. Given the occupied real volume of about 16 m^3, knowing that the surface of the grit chamber is 13.85 m^2 and considering that the occupied volume of the settler is 16 m^3, the volume per layer coincides with the volume of the lower part of the grit chamber presented in Figure 3.6. The height of the settler was calculated as 1.16 m. Thus, the height of each layer is 0.39 m. The depicted arrows in Figure 7.27 represent the flow behaviour in the settler. As mentioned previously, the Q_{mix} represents the vortex forces inside the real grit chamber.

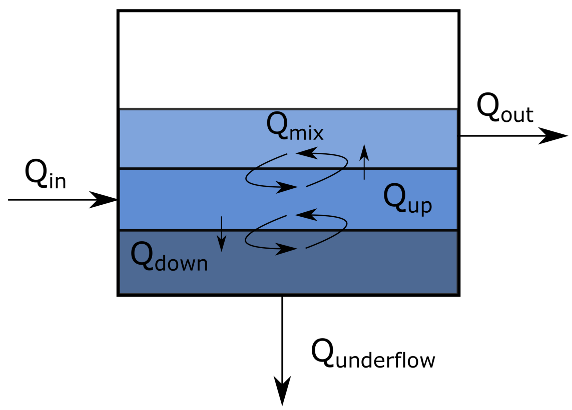

Figure 7.27: Three-layers PSVD model with the flow behaviour into the vortex grit chamber.

As a result of the adjustments presented above to represent the hydraulics of the grit chamber, experimental and simulated results for the second tracer test are compared (see Figure 7.28). Considering that only 60 % of the tracer prepared in the lab was injected into the grit chamber, a good fit of the hydraulic model can be noticed with a root mean squared error (RMSE) of 0.0017 mg/L of tracer.

Importantly, this hydraulic model agrees with the behaviour observed in CFD studies performed by the industrial partner, *Veolia Water Technologies Canada*, on a vortex grit chamber with the same configuration as the studied unit (see Figure 7.29) (Couture et al., 2009).

Details on the steps followed to develop the basic hydraulic model and simulated results for both tracer tests are presented in Appendix B.

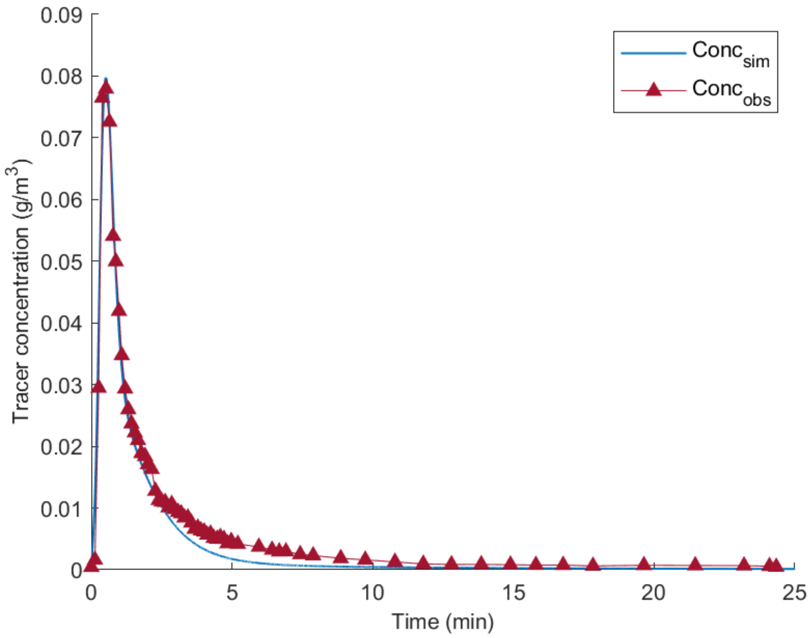

Figure 7.28: Simulated and observed results of the second test.

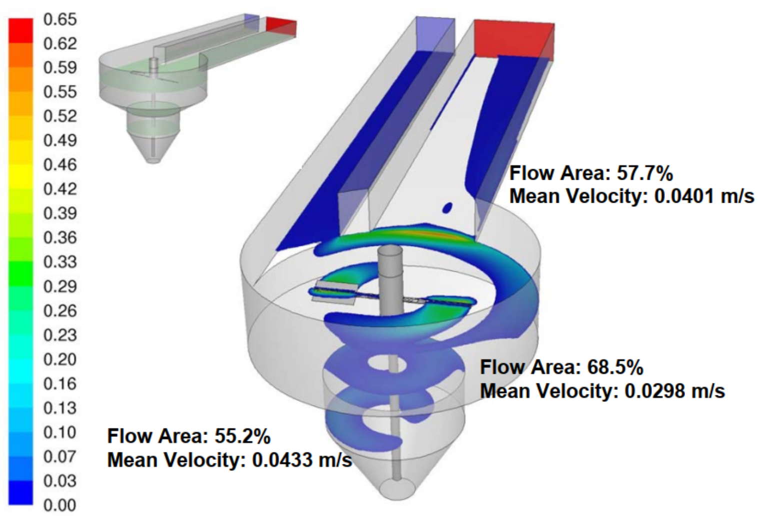

Figure 7.29: Particle velocity tracked in three horizontal CFD model sections of a vortex grit chamber (Couture et al., 2009).

Calibration of PSVD model

The removal performance of the ten particle-class model can now be calibrated through comparing the proposed model with a one-day on-line TSS data set. The data set used for model calibration was obtained under dry weather conditions (see Figure 7.30). The high frequency flow (Δt = 10 sec) calculated as explained previously and the on-line TSS concentrations are presented in Figure 7.31.

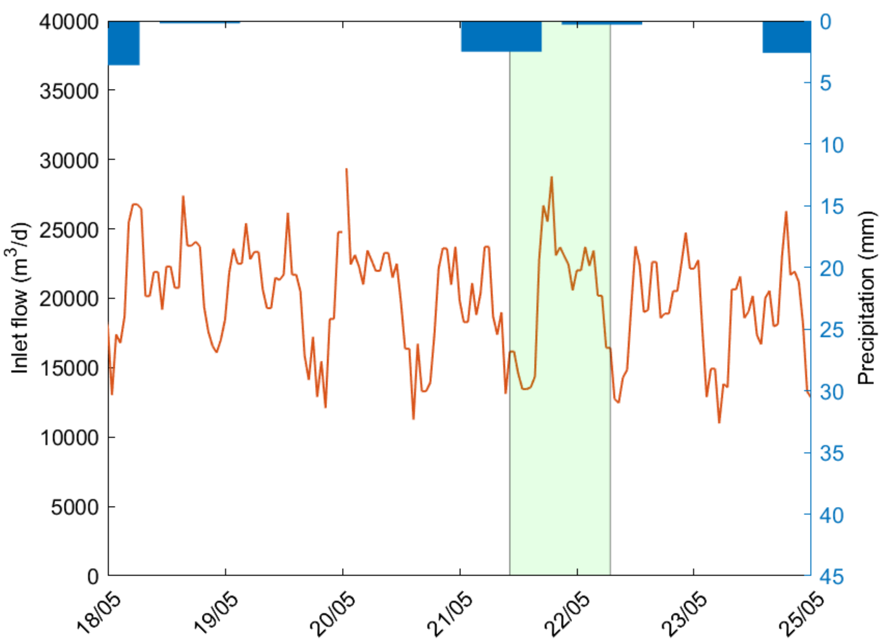

Figure 7.30: Inlet hourly flow and precipitation from May 18th to May 26th, 2017. The green square indicates the period of the calibration data set.

First, the physical model parameters of the hydraulic model (i.e. surface area and height of the grit chamber) were set to the physical characteristics and operation conditions. Despite the fact that the grit removal is performed at discrete times from the bottom of the grit chamber, the underflow was assumed constant at a low flow rate so that it does not affect the grit chamber hydraulics. This assumption could be made because the height of the particles accumulated at the bottom of the grit chamber does not overpass the 80 % of the height of the lower part as shown in Figure 3.6. The volume of that part coincides with the volume of the lower layer of the settler which is considered only as a settling zone.

Not calibrating any model parameter further and only using the ViCAs-derived settling velocity parameters (see previous Section on PSVD fractionation), a promising fit to the data was obtained, albeit with a slightly overestimated removal performance. To improve the fit, the backmixing parameters (i.e. Q_{mix}) were considered a good handle to reduce the removal efficiency. The mixing flow between the layers, leading to a resuspension of particles, was therefore augmented.

The removal efficiency of the grit chamber obviously varies with flow conditions: At low flow, due to the higher retention time, the removal is higher and particles with low settling

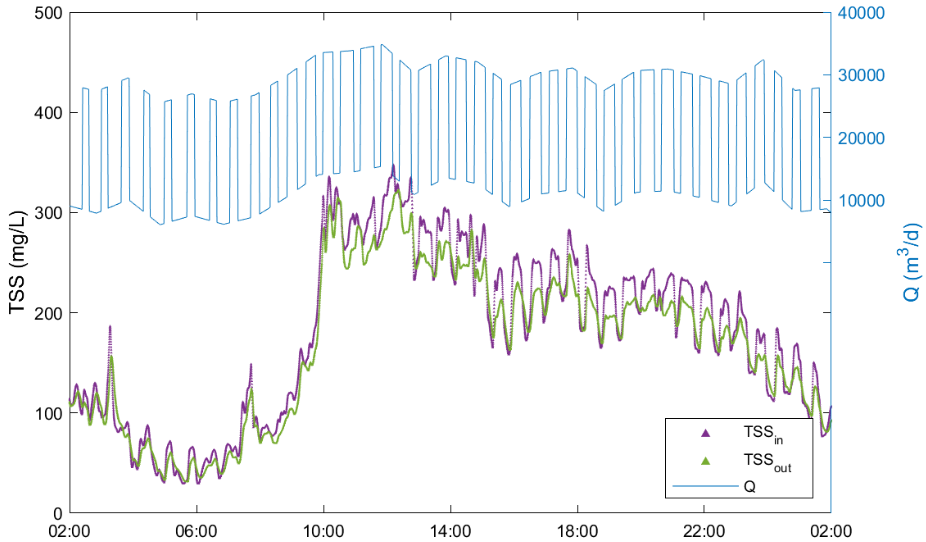

Figure 7.31: On-line TSS measurements for calibration at the inlet and outlet of the studied system, together with the simulated inlet flow.

velocities can be removed to some extent. Conversely, at high flow conditions, the retention time is reduced, leading to a lower removal and most of the particles that are removed, are the ones that settle fast.

However, when a fixed Q_{mix} was used, it was found that the removal efficiency was overpredicted at low flow conditions and underpredicted at high flow. To accommodate for this, the Q_{mix} was made dependent on the inflow. In fact, backmixing, or dispersion, is higher at low flow conditions ("there is more time for dispersion"), as for instance, expressed in the models of Chambers and Jones (1988) and Gujer (2008). A turbulent dispersion mixing flow (Q_{mix}), inversely proportional to the inlet flow (Q_{in}), was proposed and its parameters estimated from Equation 7.10.

$$Q_{mix} = \frac{\alpha_D}{Q_{in}^{\beta_D}} \tag{7.10}$$

The parameters related to this mixing flow (dispersion factor, α_D ($(m^3/d)^{\beta_D+1}$) and mixing behaviour, β_D (-)) between the model layers, were determined by fitting the model to the selected data set for calibration. The goodness-of-fit of the model was statistically estimated with the RMSE, bias and difference on the % removal criterion. The results of the scenario analysis performed to select the best set of parameters are presented in Figure 7.32.

The results of the calibrated model show a good approximation of the outlet TSS and their

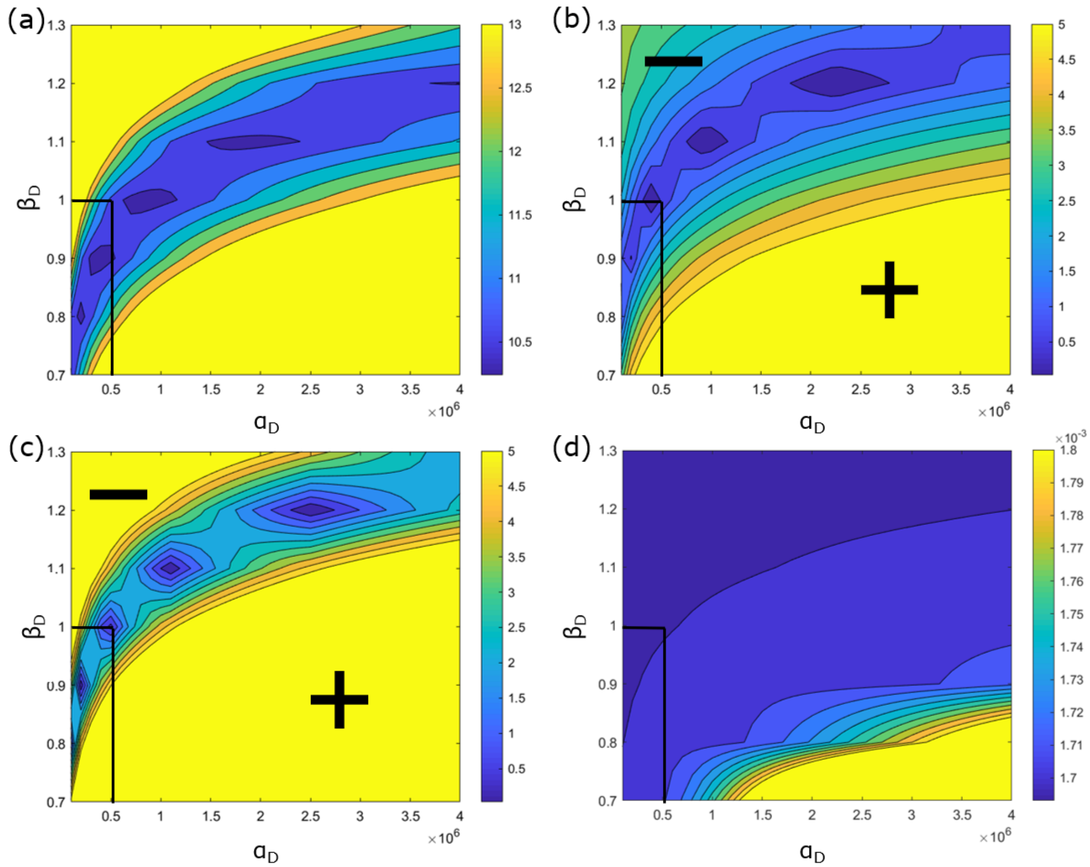

Figure 7.32: Scenario analysis results for the vortex model calibration. (a) RMSE results of the PSVD model for a range of α_D and β_D values, (b) absolute value of the difference between the observed and simulated % removal, (c) absolute values of the bias, and (d) RMSE results of the hydraulic model. The + and − symbols represent the positive and negative zone values. The crossing black lines indicate the set of parameters selected.

dynamics (see Figure 7.33 and Figure 7.34 for detailed results at low and high flows). The simulated removal efficiency of 8.7 % was similar to the measured removal of 8.5 %. The estimated RMSE was 10.9 mg/L, which represents 6 % of the average TSS concentration and is in the same order of magnitude as the measurement errors of the TSS sensors. Finally, the estimated bias was 0.31 mg/L, which is very close to 0.

In Table 7.2, the overall impact of the inlet flow on the percentage removal can be observed for each particle class during the calibration test. A key feature of the model is, of course, that it is capable to capture the more efficient removal of the particles with higher settling velocities (i.e. classes 8-10). This behaviour is also noticed when comparing the overall PSVD curves from the inlet, outlet and underflow (see Figure 7.35). It can be observed that the particles at the outlet are settling slower than at the inlet. Also, the particles at the underflow are settling much faster than those at the inlet. Hence, the percentage of fast settling particles is higher

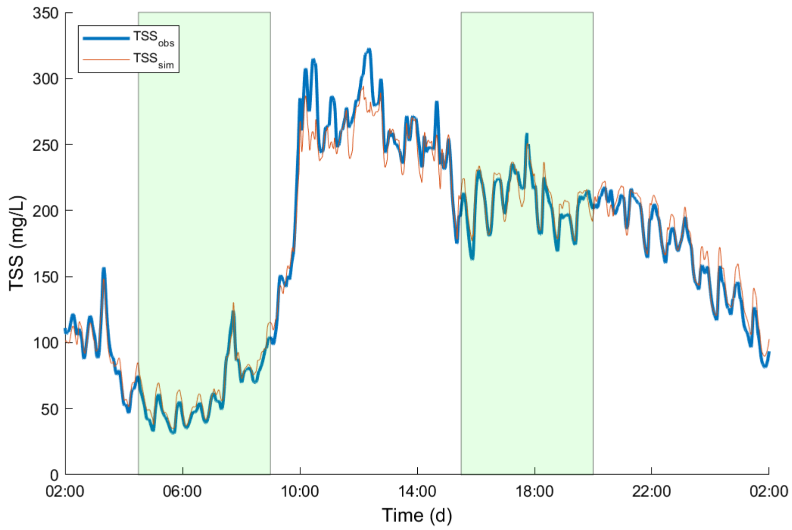

Figure 7.33: Observed and simulated results at the outlet of the grit chamber for the calibration test under dry weather conditions: during the low flow period (left patch) with high backmixing conditions and during the high flow period (right patch) with low backmixing conditions.

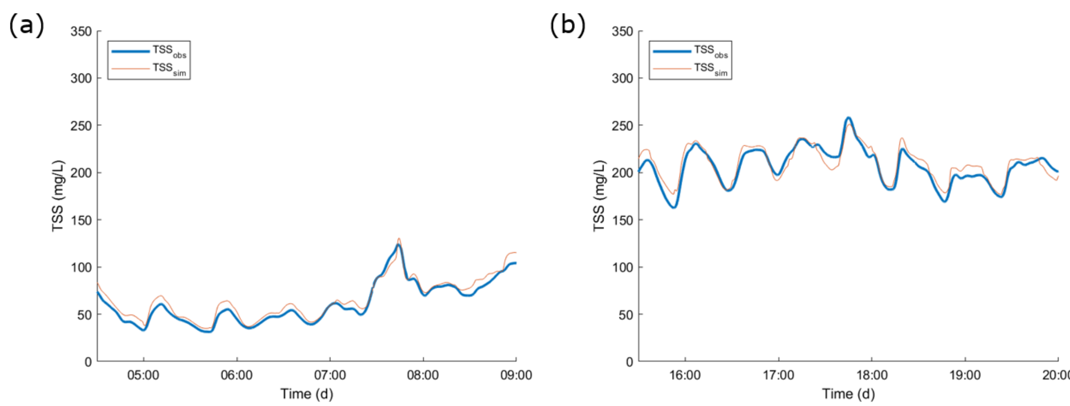

Figure 7.34: Zoom of the observed and simulated TSS concentrations of Figure 7.33 at low flow (a) and high flow (b).

at the underflow which means that they are mostly removed by the grit chamber.

Following the model calibration, an analysis of the residuals was also performed to evaluate whether the model provides a good description of the data (Dochain and Vanrolleghem, 2001; Box et al., 2005). The difference between the time series of observed and simulated data shows that there is no tendency of the particles' removal over time. The residuals have also been plotted versus two variables of interest, i.e. the TSS concentration and the inlet flow. The residuals versus TSS concentration plot suggests a certain tendency: at low TSS concentrations, generally the particles' removal is underestimated, while at higher TSS concentrations,

Table 7.2: % removal of each particle class characterized by their settling velocity for the calibration test.

Particle class	**Settling velocity (m/h)**	**Concentration (mg/L)**	**% mass**	**% removal**
Class 1	0.67	67.6	38 %	9 %
Class 2	1.04	9.6	5 %	8 %
Class 3	1.63	14.5	8 %	1 %
Class 4	2.35	11.1	6 %	2 %
Class 5	3.44	17.1	10 %	3 %
Class 6	5.21	16.2	9 %	5 %
Class 7	7.50	12.5	7 %	10 %
Class 8	10.63	9.5	5 %	15 %
Class 9	17.71	11.1	6 %	23 %
Class 10	71.46	10.8	6 %	57 %
Total		180.1		8.5 %

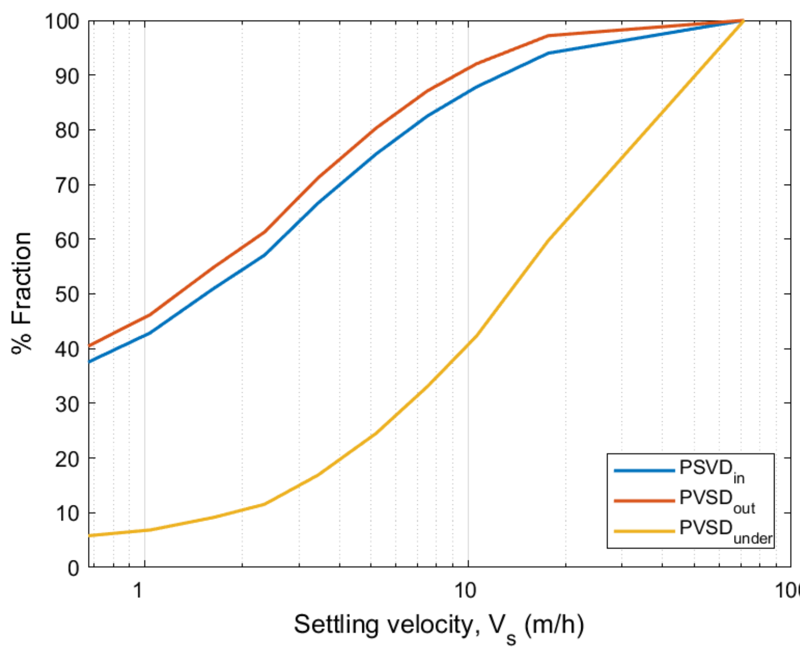

Figure 7.35: Fractions estimated for each particle class from the one-day data set for the inlet, outlet and underflow.

the particles' removal seems to be mostly overestimated. Regarding the residuals versus inlet flow plot, no clear tendency could be detected. The plots obtained from the residuals analysis are presented in Figure 7.36.

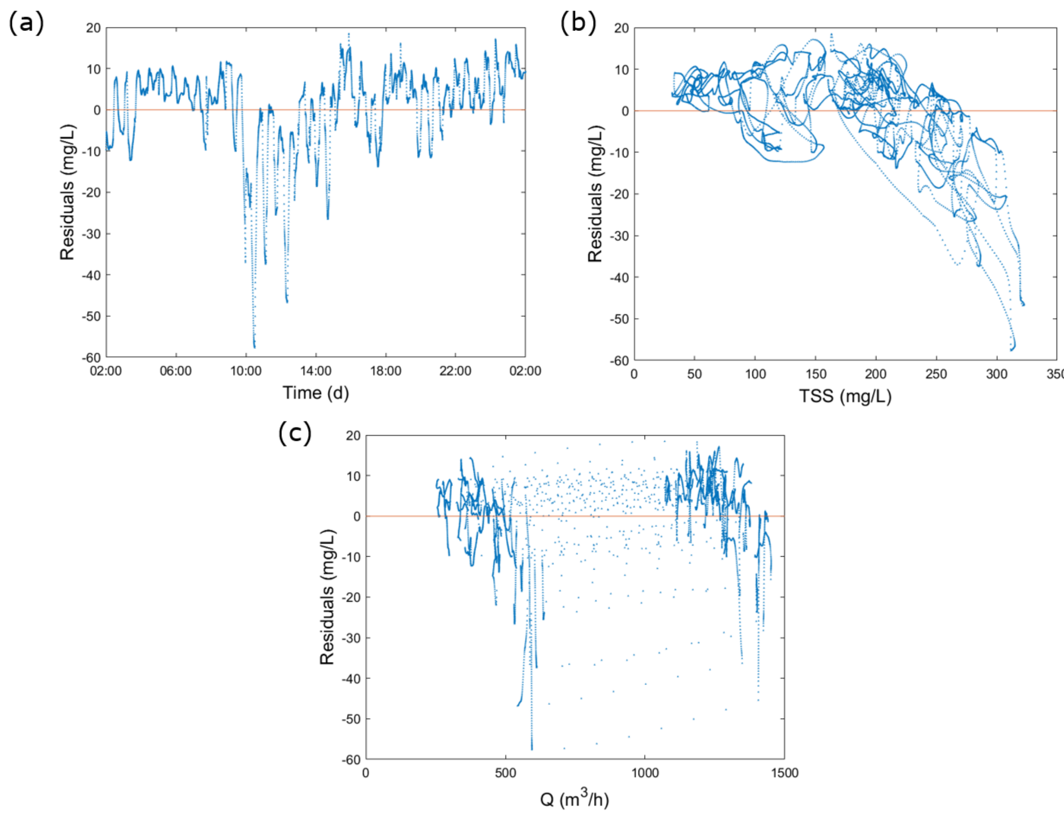

Figure 7.36: Analysis of the residuals of the calibration test for the vortex grit chamber. (a) Residuals in time sequence, (b) residuals versus TSS concentration, and (c) residuals versus inlet flow.

Validation of PSVD model

The model was validated by testing it under different conditions; with two other data sets collected under different weather conditions: first, during winter time (see Figure 7.37) and, second, under wet weather conditions during summer time (see Figure 7.38).

The validation of the winter time data set was considered to be conducted under dry weather conditions since the snowfall did not affect the inflow as depicted in Figure 7.37. The TSS data set used is presented in Figure 7.39 with the simulated inlet flow at high frequency.

The results obtained confirmed the good performance of the model, reproducing the outlet TSS concentrations and their dynamics (see Figure 7.40). This time, the % removal simulated was 7 % which is slightly different than the 11 % observed, although both are in the same order of magnitude. The RMSE was 16.8 mg/L which represents a 10 % of the average TSS concentration along the data set. The bias estimated for the validation equals 10 mg/L. Thus, the model is mostly underpredicting the particle removal since the estimated TSS is overall 10 mg/L above the observed TSS. By comparing the obtained validation RMSE with the

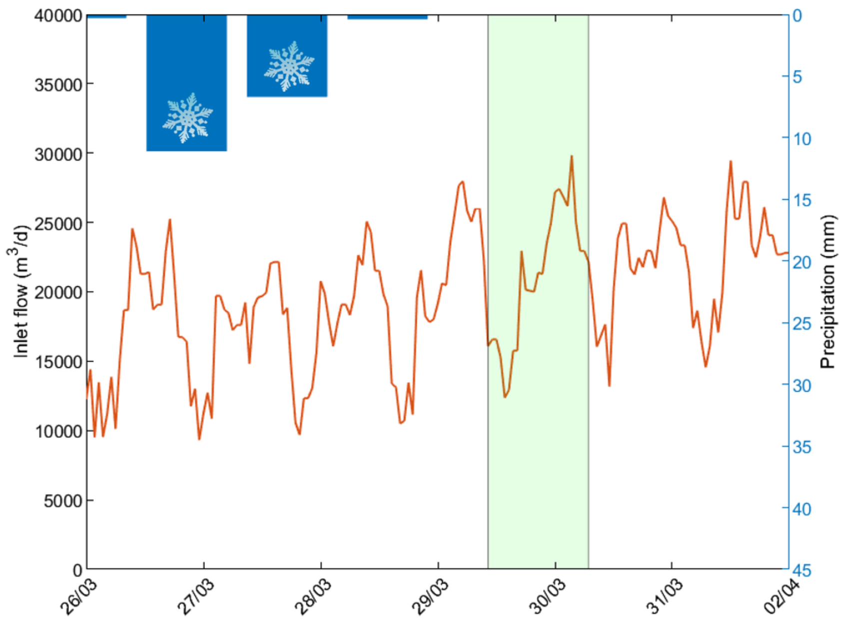

Figure 7.37: Inlet hourly flow and precipitation from March 26th to April 2nd, 2017. The green square indicates the period of the validation data set during winter time.

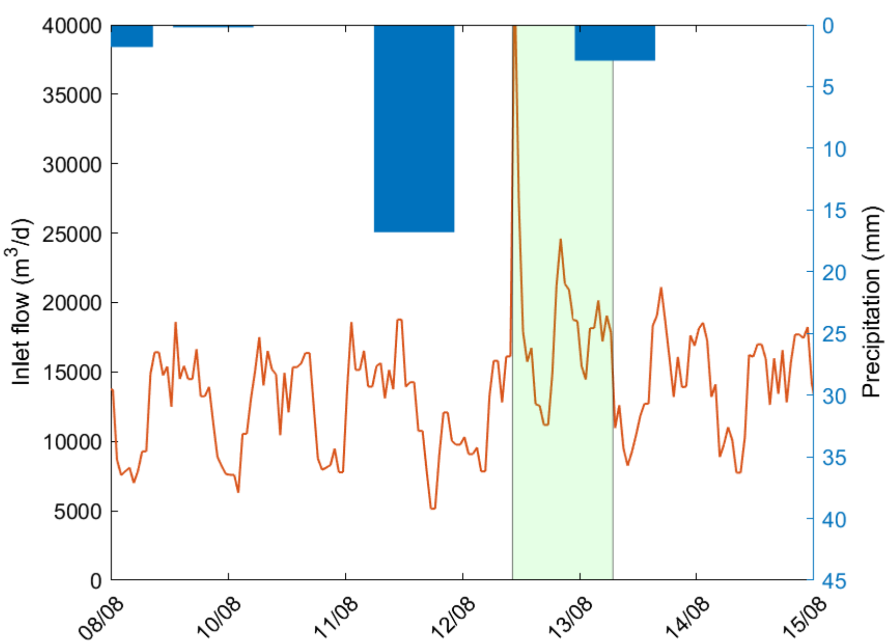

Figure 7.38: Inlet hourly flow and precipitation from August 9th to August 15th, 2017. The green square indicates the period of the validation data set under wet weather conditions.

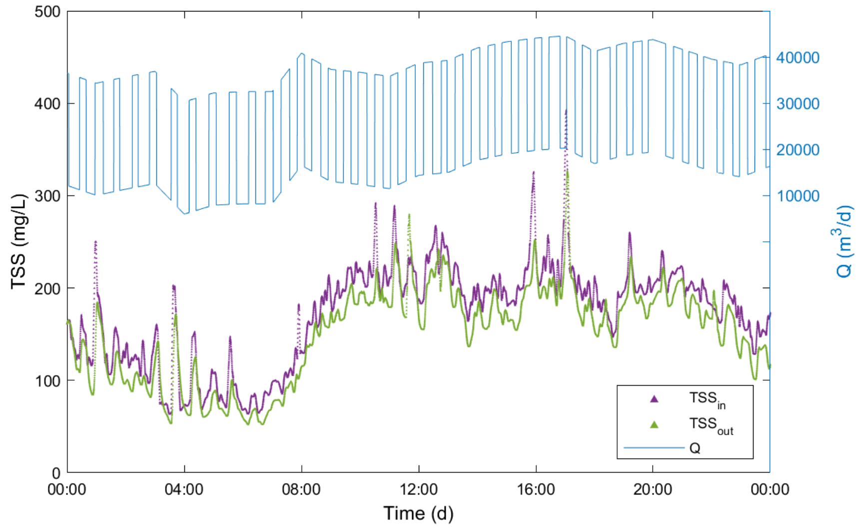

Figure 7.39: On-line TSS measurements for model validation under dry weather winter conditions at the inlet and outlet of the grit chamber with the simulated inlet flow.

calibration RMSE, the Janus coefficient could be estimated, and it was equal to 1.5 (Sin et al., 2008; Rieger et al., 2012). Thus, this validation was successful (Janus coefficient $<$2).

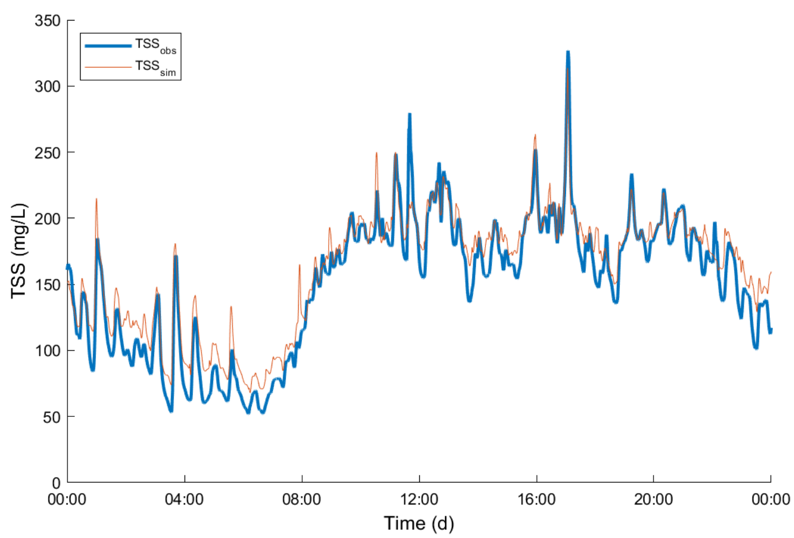

Figure 7.40: Observed and simulated results dry weather winter conditions at the outlet of the grit chamber for the validation test.

Regarding the % removal of each fraction, results similar to the calibration results were observed (Table 7.3). Again, the % removal is higher for fractions with a higher settling velocity (i.e. classes 8-10).

Table 7.3: % removal of each particle class characterized by their settling velocity for the validation test under dry weather conditions.

Particle class	**Settling velocity (m/h)**	**Concentration (mg/L)**	**% mass**	**% removal**
Class 1	0.67	79.7	47 %	1 %
Class 2	1.04	8.3	5 %	2 %
Class 3	1.63	12.6	7 %	2 %
Class 4	2.35	9.7	6 %	3 %
Class 5	3.44	14.9	9 %	5 %
Class 6	5.21	14.1	8 %	7 %
Class 7	7.50	10.8	6 %	11 %
Class 8	10.63	7.1	4 %	15 %
Class 9	17.71	7.5	4 %	25 %
Class 10	71.46	7.3	4 %	58 %
Total		171.9		6.9 %

To complete the evaluation of the first validation test, an analysis of the residuals was again performed. In Figure 7.41, a bias is observed on the three plots of the residuals versus time, TSS concentration and inlet flow similar to Figure 7.40. This may be explained by the water temperature that is lower during winter, leading to a higher water viscosity. With the increase of viscosity, the settling velocity of the particles decreases leading to lower particles' removal. Despite the bias (10 mg/L), the residuals are distributed randomly for the three variables.

The second validation test was performed with data collected under wet weather conditions as mentioned above and shown in Figure 7.38. The high peak flowrate had an impact on the TSS concentrations at the inlet and at the outlet as depicted in Figure 7.42, where it can be noticed that the pump activations are longer at high flow than under dry weather conditions for the same time during the day.

The results obtained from the second validation confirmed the good performance of the model. The model was able to reproduce the outlet TSS concentrations and their dynamics, even under wet weather conditions (see Figure 7.40).

The % removal simulated was 10 %. Compared to the 13 % observed, the simulated removal is slightly lower, but the order of magnitude is again the same. The estimated RMSE was 16.7 mg/L. Despite the similar RMSE on both validation tests, in this case, it only represents a 7 % of the average TSS concentration given the higher inlet concentration during this rain event. The bias estimated for this validation is 6 mg/L. Again, the model is slightly underestimating the particles' removal. However, the obtained bias is lower than the bias for the first validation. Finally, comparing the RMSE for the calibration and this validation, the Janus coefficient is also 1.5. Thus, the second validation test was also successful (Janus coefficient < 2).

Similar to the results presented above, the % removal of each particle class show that fast

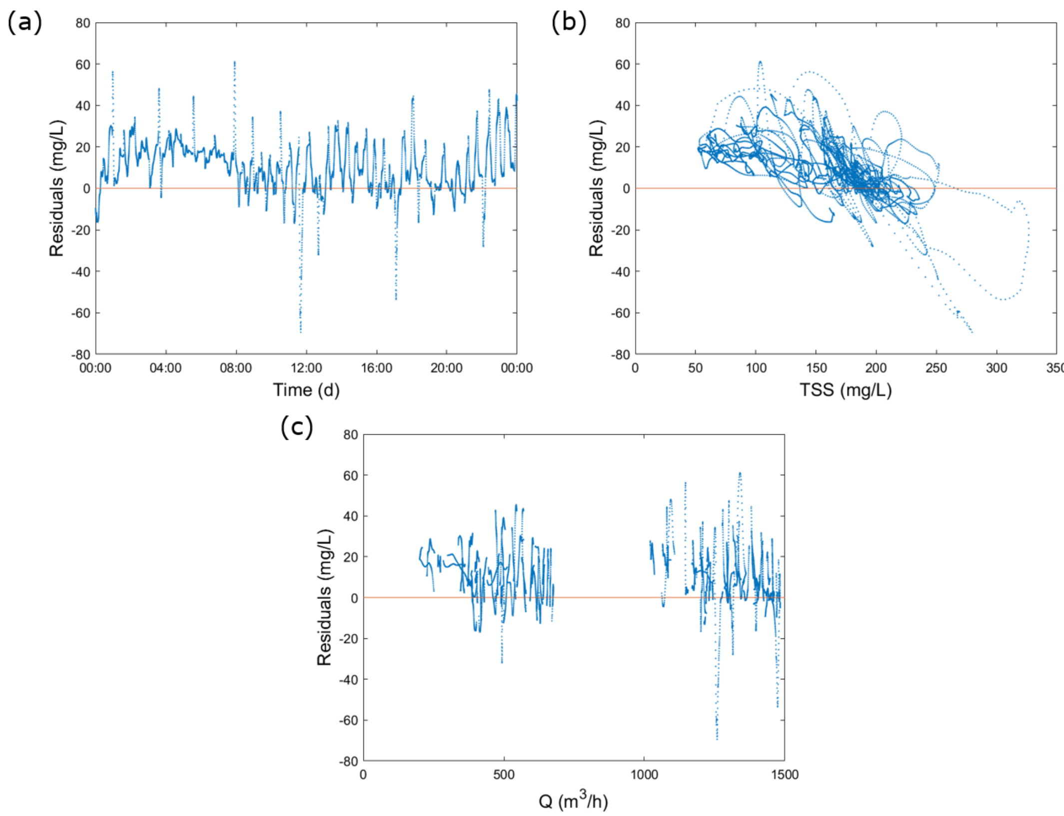

Figure 7.41: Analysis of the residuals of the validation test under dry weather winter time conditions for the vortex grit chamber. (a) Residuals in time sequence, (b) residuals versus TSS concentration, and (c) residuals versus inlet flow.

settling particles are removed better (see Table 7.4). In contrast to the previous data sets under dry weather conditions, the percentage of fast settling particles is higher under wet weather conditions due to the high flow that is able to resuspend particles accumulated in the sewer system.

Furthermore, as for the calibration test and the first validation test, to better understand the simulated results, the residuals were also studied for this validation test. In contrast to the previous validation test, no bias was observed on the residuals (see Figure 7.44). The residuals in the time sequence are distributed randomly around 0. However, the residuals show an underestimation of the TSS removal at higher TSS concentration and inlet flow.

7.3.4 Conclusions

Grit chambers need to be properly characterized in view of whole WRRF modelling, settling characteristics and hydraulic dynamics being the key characteristics. A new experimental characterization and modelling approach based on PSVD has been proposed and the new model

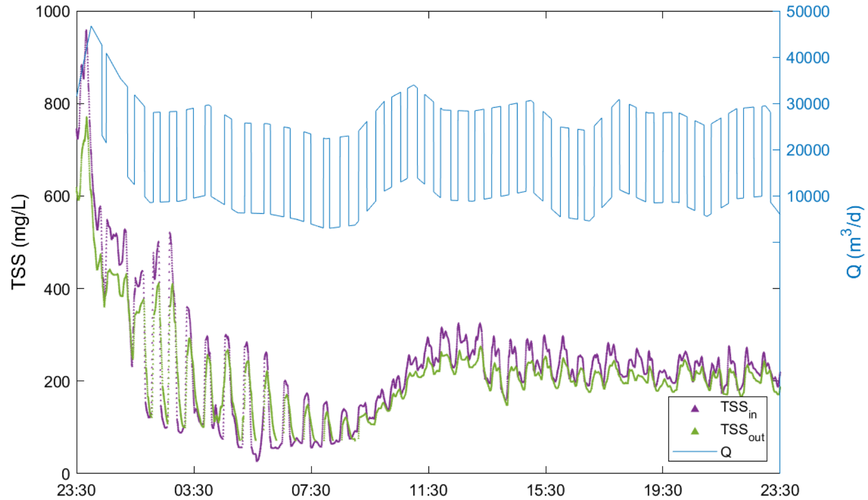

Figure 7.42: On-line TSS measurements for model validation under wet weather summer conditions at the inlet and outlet of the grit chamber with the simulated inlet flow.

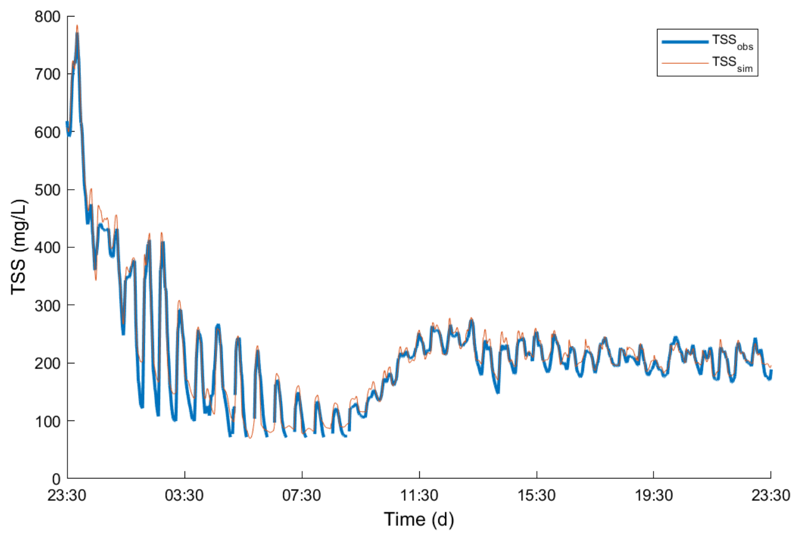

Figure 7.43: Observed and simulated TSS data under wet weather summer conditions at the outlet of the grit chamber for the validation test.

was successfully calibrated and especially validated even under quite different operation conditions. Compared to the existing (static) grit chamber models, the proposed dynamic model allows remarkably good dynamic predictions of effluent TSS and overall removal performance, including under wet weather conditions.

Table 7.4: % removal of each particle class characterized by their settling velocity for the validation test under wet weather conditions.

Particle class	**Settling velocity (m/h)**	**Concentration (mg/L)**	**% mass**	**% removal**
Class 1	0.67	67.1	28 %	1 %
Class 2	1.04	13.8	6 %	1 %
Class 3	1.63	20.9	9 %	2 %
Class 4	2.35	15.9	7 %	2 %
Class 5	3.44	24.6	10 %	4 %
Class 6	5.21	23.3	10 %	6 %
Class 7	7.50	18.0	8 %	9 %
Class 8	10.63	15.1	6 %	12 %
Class 9	17.71	18.7	8 %	21 %
Class 10	71.46	18.2	8 %	56 %
Total		235.5		9.2 %

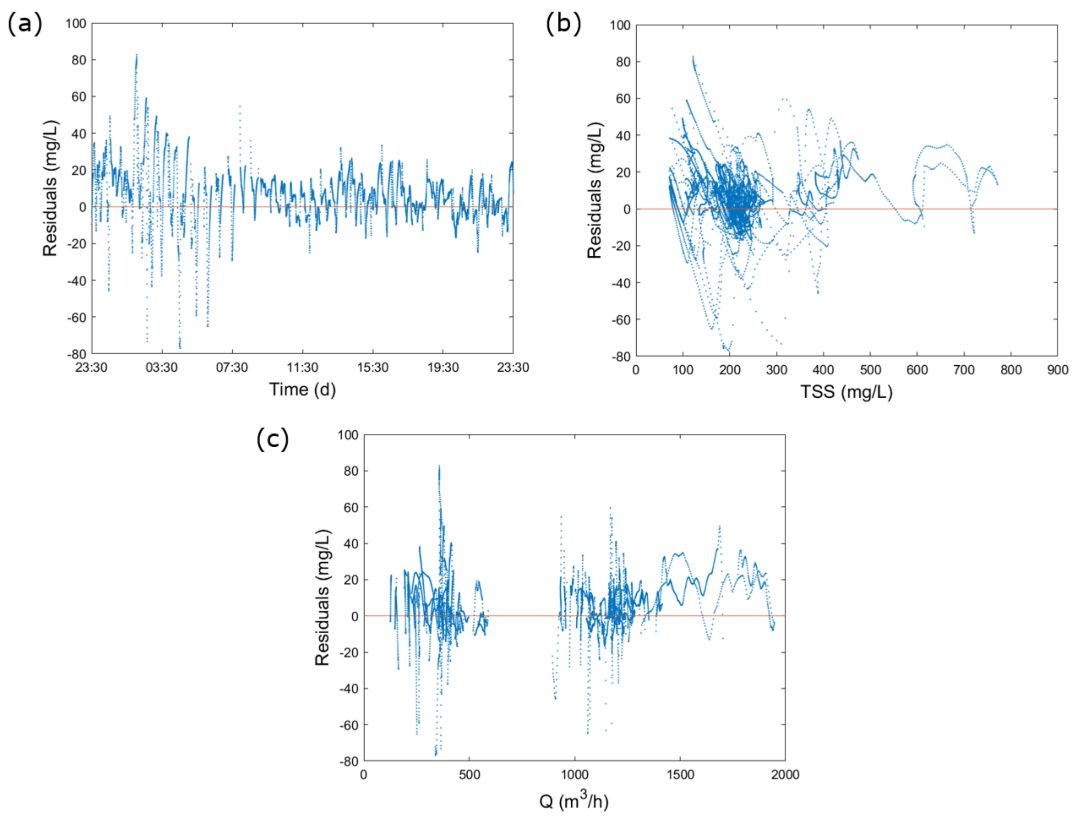

Figure 7.44: Analysis of the residuals of the validation test under wet weather conditions for the vortex grit chamber. (a) Residuals in time sequence, (b) residuals versus TSS concentration, and (c) residuals versus inlet flow.

Chapter 8

Aerated grit chamber modelling

8.1 Introduction

This chapter presents the work related to specific objectives 2.b and 2.c. It consists in a first application of the conceptual model developed and presented in Chapter 7 to the studied aerated grit chamber, including model calibration and validation.

This chapter has been structured similar to Chapter 7. First, the data available from the aerated grit chamber case study are presented. This includes inlet flow data, solids concentration from the inlet and outlet, the settling characteristics, hydraulic data, and physical and operational information.

Afterwards, the model application is described as follows: the PSVD fractionation, the hydraulic model development, the model calibration and validation, and finally, the specific conclusions related to the aerated grit chamber modelling.

8.2 Data available

The data available and used for the application of the conceptual model to the aerated grit chamber case study, was mostly collected during the summer of 2014 in the context of the PhD thesis of Tik (2019). The only data collected in the context of this PhD thesis are the PSVD data from samples collected during the summer of 2018 and characterized with the 2m-ViCAs columns. Thus, in this section, the data from 2014 are only presented briefly since they are included and detailed in the PhD thesis of Tik (2019). Details are only provided for the PSVD curves collected in the context of this PhD thesis.

8.2.1 Performance data

In this section, water quantity and quality data from the East Québec City WRRF are provided. Flowrate dynamics, inlet and outlet solids dynamics and particle settling characteristics around the aerated grit chamber are shown.

Inlet flow data

The presented inlet flow data of the East Québec City WRRF was provided by the facility. The SCADA system installed at this WRRF is storing the flow data at intervals of 15 seconds at different points of the wastewater treatment chain. For this study, the inlet flow measured at the screens was used for the modelling work. To better understand the flow data, these data were interpreted together with daily precipitation information collected at the weather station installed at the Québec City Jean Lesage International Airport by Environment Canada (Environment Canada, 2019). Both inlet flow and daily precipitation data are presented in Figure 8.1 for two months and a half coinciding with the period in which the 2014 sampling campaign was carried out.

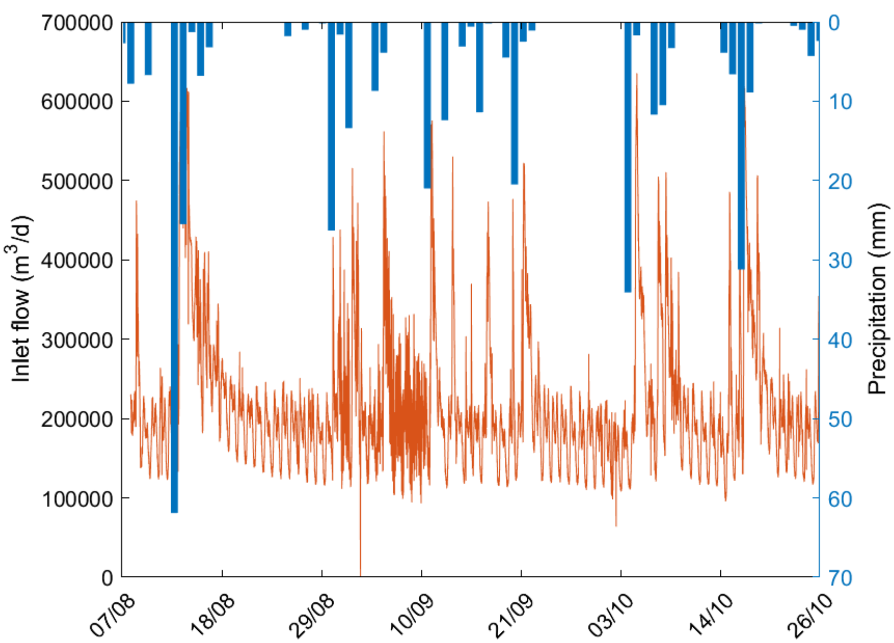

Figure 8.1: Inlet flow at the East Québec City WRRF and daily precipitation from the weather station at the Québec City Jean Lesage International Airport from August 11th to October 24th, 2014.

In Figure 8.1 it is observed that, after rain events, the flow increases considerably with peak flows that can go up to three times the average dry weather flow. In more detail, in Figure 8.2, on September 16th and 19th, typical daily profiles under dry weather are observed. Similar to the Saint-Nicolas WRRF, there are two peak flows along the day. The first one corresponds to the peak flow in the morning and the second one to the peak flow in the evening. Both can be related to typical inhabitant activity. Then, as a result of the rain event, on September 17^{th} and between September 20^{th} and 22^{nd}, three peak flows can be observed that are two times higher than the average dry weather flow. After the rain event, patterns different from the daily profile under dry weather, are observed.

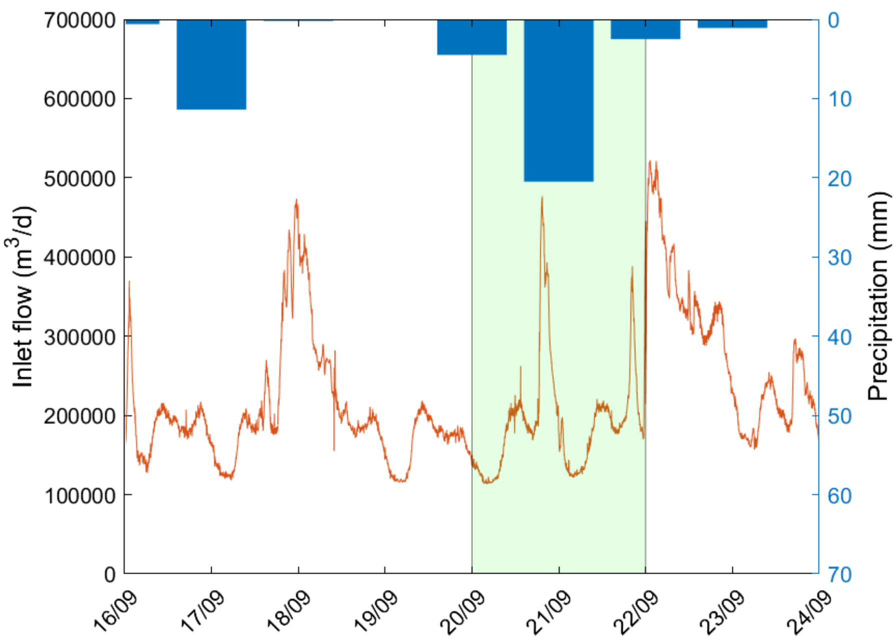

Figure 8.2: Detailed inlet flow dynamics at the East Québec City WRRF during dry and wet weather conditions from September 16^{th} to 24^{th}, 2014. The green patch indicates a wet weather period.

Inlet and outlet solids concentration data

Around the aerated grit chamber at the East Québec City WRRF, the water quality was monitored as described in Section 3.6. Even though several water quality variables were measured at high frequency during the sampling campaign in 2014 (e.g. turbidity, conductivity, temperature, pH and COD), in the context of this study, the only variable of interest is the TSS concentration. Hence, this section focuses on this variable.

Similar to the Saint-Nicolas WRRF, on-line turbidity measurements were collected at the inlet and outlet of the grit chamber to monitor the solids dynamics (see Figure 8.3). Thus, the turbidity validated data were again converted into TSS concentration data set with a linear relationship built from TSS lab measurements and on-line turbidity sensor output while sampling in the same way as the Saint-Nicolas WRRF case study.

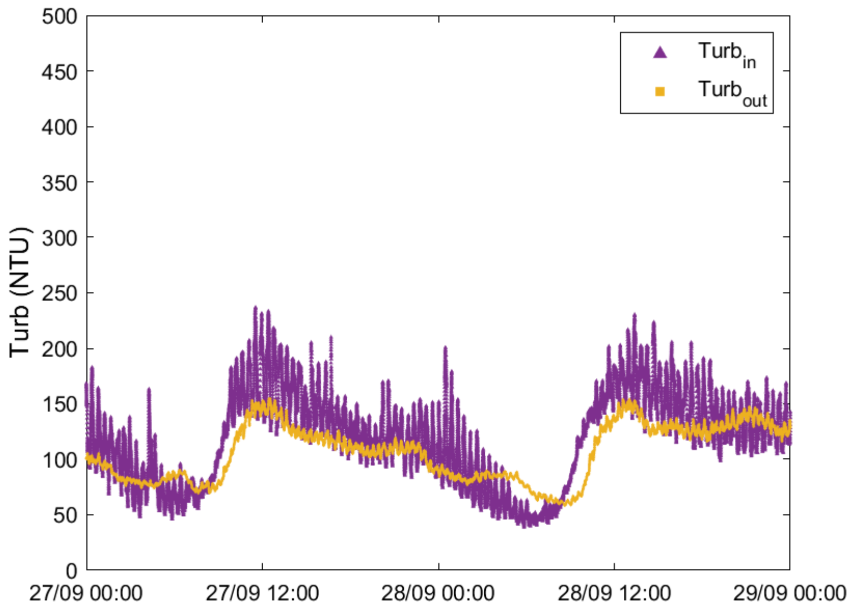

Figure 8.3: Two days of validated turbidity collected data at the inlet and at the outlet of the aerated grit chamber at the East Québec City WRRF from September 27^{th} to 29^{th}, 2014.

In Figure 8.4, inlet and outlet TSS concentrations follow a pattern similar to the inlet flow presented in Figure 8.2. TSS concentrations increase in the morning while they decrease at night. During the evening a small peak is again observed. As the inlet flow, these variations are due to the activity of the inhabitants and/or flow induced resuspension. Comparing the inlet and outlet TSS concentrations, both are following a similar pattern. Logically, inlet TSS concentrations are higher than outlet TSS concentrations. However, at night, higher TSS concentrations are observed in the outlet which can be due to the grit chamber behaviour. Also, more important dynamics are observed at the inlet of the grit chamber caused by the screens cleaning sequences scheduled every 10 min unless the inlet flow exceeds 288 000 m^3/d which makes them operate continuously. These dynamics are not observed at the outlet due to the damping effect of the unit.

Under wet weather conditions, with the increase of the flow presented in 8.2 between September 20^{th} and 22^{nd}, different patterns of the TSS concentrations than the dry weather patterns are observed (see Figure 8.5). In contrast to the dynamics at the Saint-Nicolas WRRF, there is no clear first flush peak of the TSS concentration exceeding the highest TSS concentrations under dry weather conditions.

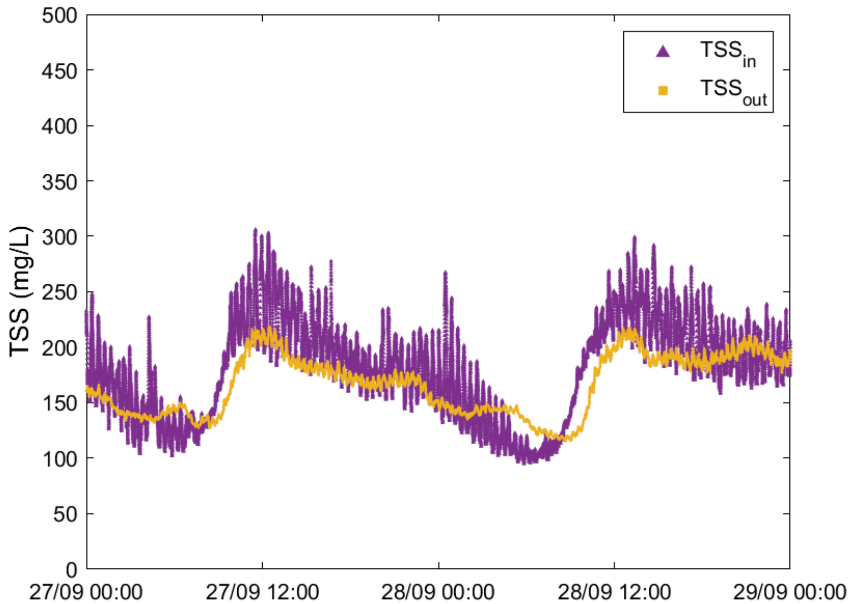

Figure 8.4: Two days of converted inlet and outlet TSS data of the aerated grit chamber at the East Québec City WRRF from September 27^{th} to 29^{th}, 2014.

PSVD data

As mentioned previously in Section 6.2.3, a relationship is again observed between the TSS concentrations and the collected PSVD curves. However, at the East Québec City WRRF, only six ViCAs tests could be carried out at the inlet and outlet of the grit chamber: four samples were collected under dry weather conditions and the other two under wet weather conditions. Due to the lack of curves under wet weather conditions, only the PSVD curves collected under dry weather conditions are considered to study the range of the PSVD curves at the inlet and outlet of the studied aerated grit chamber.

The mass balances of the four ViCAs tests carried out with samples collected at the inlet and the four tests performed with samples collected at the outlet, were all below ± 15 %. Thus, all of them were accepted as valid. The TSS concentrations of the inlet samples vary between 220 and 350 mg/L, and at the outlet, they vary between 160 and 250 mg/L (see Figures 8.6 and 8.7, respectively). In both cases, the range of PSVD curves is quite narrow compared to the range of PSVD curves from samples collected at the Saint-Nicolas WRRF (i.e. the ranges presented in Figures 7.13 and 7.14).

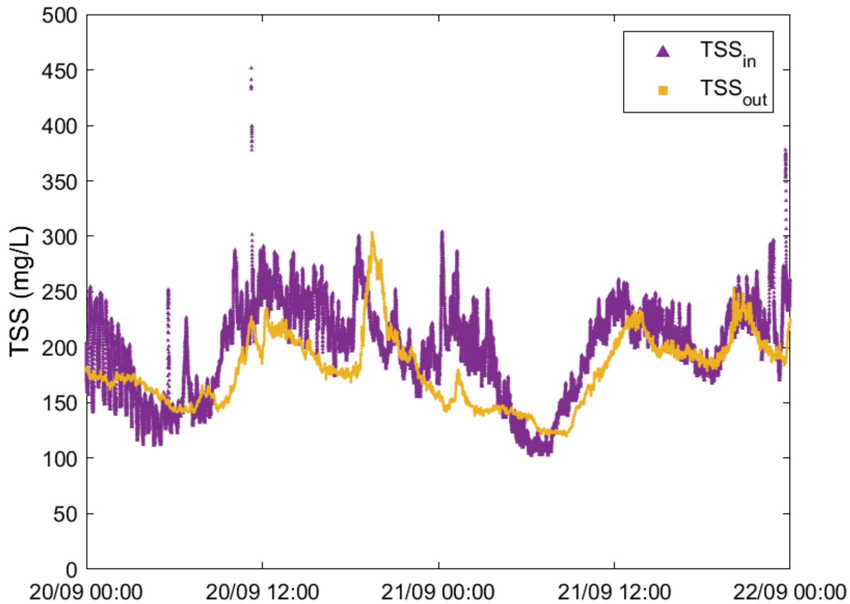

Figure 8.5: Two days of converted TSS data collected at the inlet and at the outlet of the aerated grit chamber at the East Québec City WRRF from September 20^{th} to 22^{nd}, 2014. Remarked period in Figure 8.2.

8.2.2 Hydraulic data

To better understand the hydraulics of the aerated grit chamber at the East Québec City WRRF, two tracer tests were carried out in the context of the PhD thesis of Tik (2019) the results of which have already been published in a peer-reviewed paper (Tik and Vanrolleghem, 2017). For both tests, the tracer was injected at the inlet channel and it was distributed to the five aerated grit chambers. Samples were collected during the test at the outlet of each grit chamber. In the context of this thesis, as an example and because of the similarity between the results of each grit chamber, only the tracer concentrations observed at the outlet of the aerated grit chamber number 3 in Figure 3.10, are presented (see Figure 8.8). The global mass balance for this tracer test was 80 %, which was considered as acceptable.

In Figure 8.8, the tracer concentration evolution shows a smooth response which indicates that there is no short-circuited flow through the grit chamber. During the tracer tests, the inlet flow was monitored. The inlet flow variations were not significant during the test and for this study, an averaged inlet flow of 188,000 m^3/d has been used. Under these flow conditions, the HRT of the grit chamber was 16 min. Further details are given in Tik and Vanrolleghem (2017) and Tik (2019).

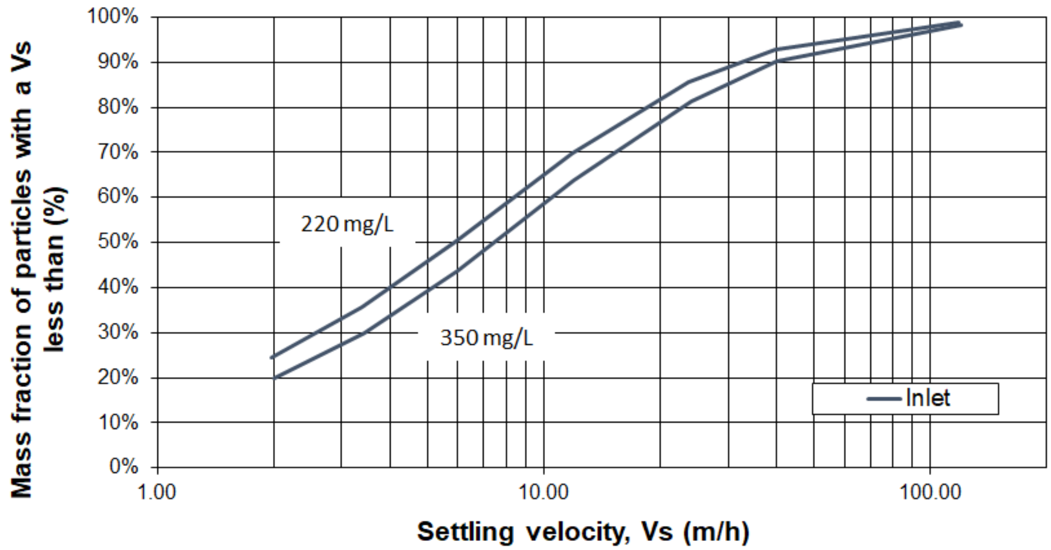

Figure 8.6: PSVD boundaries at the inlet of the aerated grit chamber at the East Québec City WRRF. The boundary at low TSS concentration corresponds to the experimental PSVD curve at 220 mg/L and the boundary at high TSS concentration corresponds to the experimental curve at 350 mg/L.

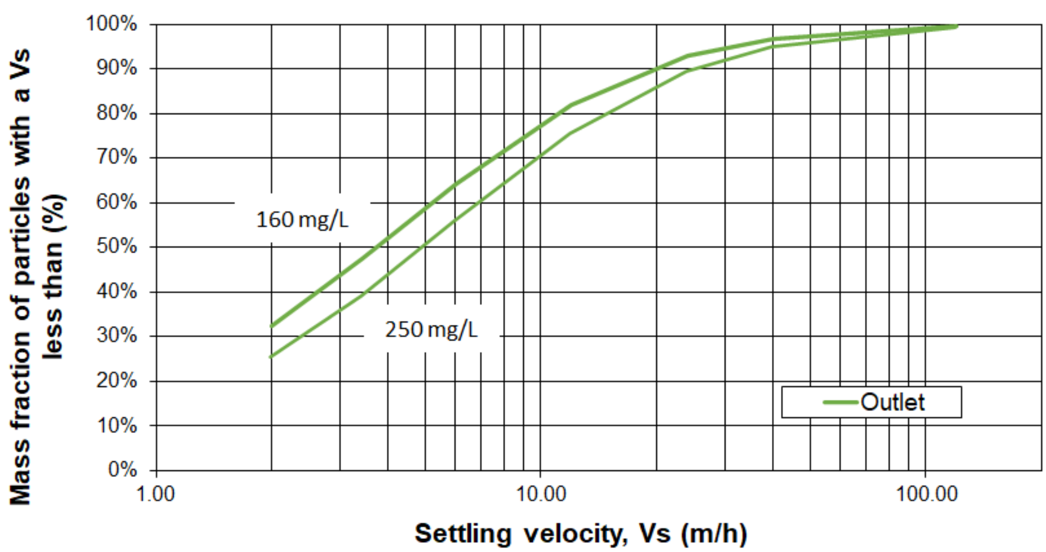

Figure 8.7: PSVD boundaries at the outlet of the aerated grit chamber at the East Québec City WRRF. The boundary at low TSS concentration corresponds to the experimental PSVD curve at 160 mg/L and the boundary at high TSS concentration corresponds to the experimental curve at 250 mg/L.

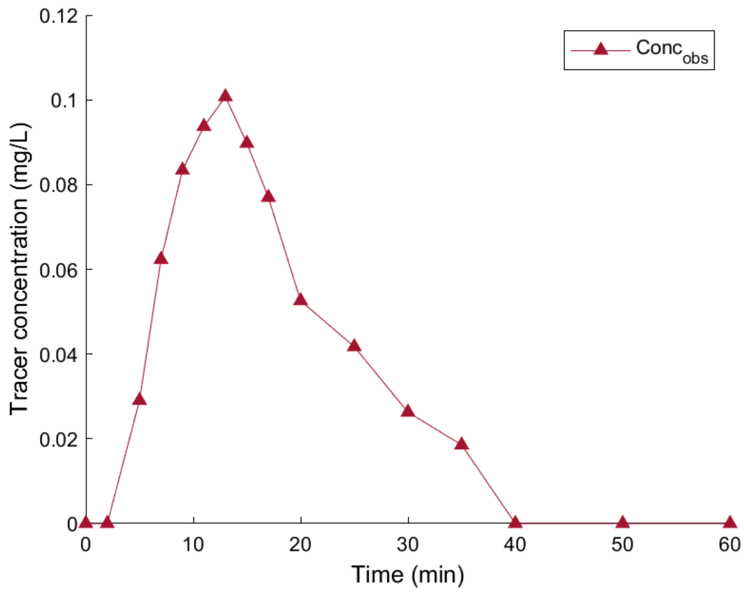

Figure 8.8: Tracer concentrations observed at the outlet of the aerated grit chamber number 3 at the East Québec City WRRF.

8.2.3 Physical and operational data

Physical dimensions and operational information for the studied aerated grit chambers have already been presented in Section 3.1.2. The provided data have been used as such to model the grit chamber. No further adjustments have been made for model calibration.

8.3 PSVD fractionation

First, the settling characteristics at the inlet of the grit chamber were determined following the procedure presented in Section 7.3.3. Given the observed relationship between the TSS concentrations and the PSVD curves presented in Section 6.2.3 and the limited number of samples collected for this case study, the same relationship was applied at the inlet of the aerated grit chamber under dry weather conditions: at higher TSS concentrations, the PSVD curve is placed in the lower region, as presented in Figure 8.6.

In Figure 8.9, the PSVD boundaries presented in Figure 8.6 have been extended from the minimum settling velocity measured of 2 m/h down to 0.5 m/h following Equation 7.4. Thus, a better representation of the particles classes' velocity distribution can be achieved.

Furthermore, the presented PSVD curves were divided into ten particle classes characterized by a mean settling velocity following the same procedure presented in Section 7.3.3 (see Figure

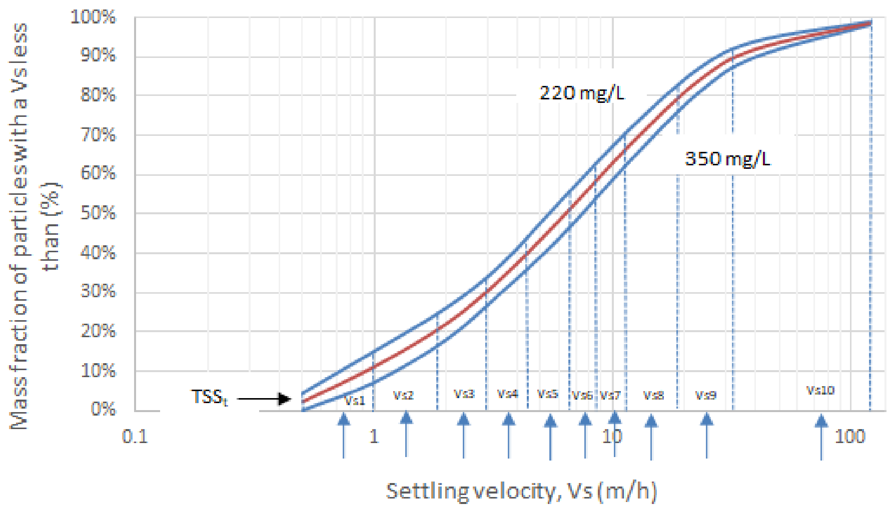

Figure 8.9: Inlet PSVD settling velocity boundaries for particle fractionation into 10 particle classes for the aerated grit chamber at the East Québec City WRRF. The arrows indicate the settling velocity that characterizes each class, calculated as the geometrical mean of the boundaries of each class.

8.9). The boundaries of the ten classes were again chosen as ten equal fractions of the average PSVD curve. Then, the geometrical means of the boundaries were calculated and were set as each class' settling velocity. The settling velocities characterizing each particle class for this case study are presented in Table 8.1.

Table 8.1: Particle classes characterized by their settling velocity determined for the studied aerated grit chamber.

Particle class	Settling velocity (m/h)
Class 1	0.75
Class 2	1.44
Class 3	2.44
Class 4	3.79
Class 5	5.62
Class 6	7.71
Class 7	10.62
Class 8	15.62
Class 9	25.00
Class 10	75.62

Once again, since a relationship was observed between the PSVD curves and the TSS concentrations, and the TSS concentrations vary continuously (see Figures 8.3 - 8.5), the PSVD curve for a given TSS concentration between 220 and 350 mg/L is determined at any time following Equation 7.5 (Tik, 2019).

In case the inlet TSS concentration lies outside the boundaries, the PSVD curve is estimated by exponentially extrapolating the cumulated fraction for each particle class following Equation 7.6 for concentrations below 220 mg/L and Equation 7.8 for concentrations above 350 mg/L.

For TSS concentrations below 220 mg/L, the $F_{v_s}^{max}$ that can be reached is 1. For this case study, Equation 7.6 becomes:

$$F_{v_s}(TSS) = 1 + \left(F_{v_s}^{low} - 1\right) \cdot e^{-k_{low} \cdot (220 - TSS)} \tag{8.1}$$

Considering that the fraction limit of 1 should be achieved at 1/3 of the TSS limit, $k_{low} = 1/\left(220 - TSS\right)$. For $TSS_{min} = 0\ mg/L$, k_{low} becomes 1/220.

When TSS concentrations exceed 350 mg/L, the $F_{v_s}^{min}$ that can be reached is 0. Then, for this case study, Equation 7.8 can be simplified to:

$$F_{v_s}(TSS) = F_{v_s}^{high} \cdot e^{-k_{high} \cdot (TSS - 350)} \tag{8.2}$$

Similar to the estimation of the k_{low}, considering that 1/3 of the TSS limit can be reached, k_{high} can be calculated from $k_{high} = 1/(TSS - 350)$. For example, given a $TSS_{max} = 10\ 000\ mg/L$, k_{high} becomes 1/9 650.

With Equations 8.1 and 8.2, the extrapolated curves with minimum and maximum TSS concentrations of 0 and 10 000 mg/L, can be estimated (see Figure 8.10). Then, a larger range of PSVD curves can be used for the grit chamber model.

8.4 Hydraulic model

From the tracer tests performed at the aerated grit chambers (see Section 8.2.2), Tik and Vanrolleghem (2017) proposed to model them by four tanks in series. This configuration was considered to build the hydraulic model presented in Figure 8.11. The four tanks in series were translated into four vertical layers between the inlet and outlet of the PSVD model (see Figure 8.12). A fifth layer was added as a settling zone.

In this case study, the hydraulic model considers the five aerated chambers as one. The total volume of the five units is 3 000 m^3, 600 m^3 per grit chamber. The total surface is 750 m^2, and the depth of each unit is 4 m. To keep the actual depth of the units, it has been considered that the height of each layer is 1 m.

With the above adjustments to integrate the hydraulics behaviour (including the turbulence mixing, Q_{mix}) into the PSVD-based grit chamber model, the experimental results presented

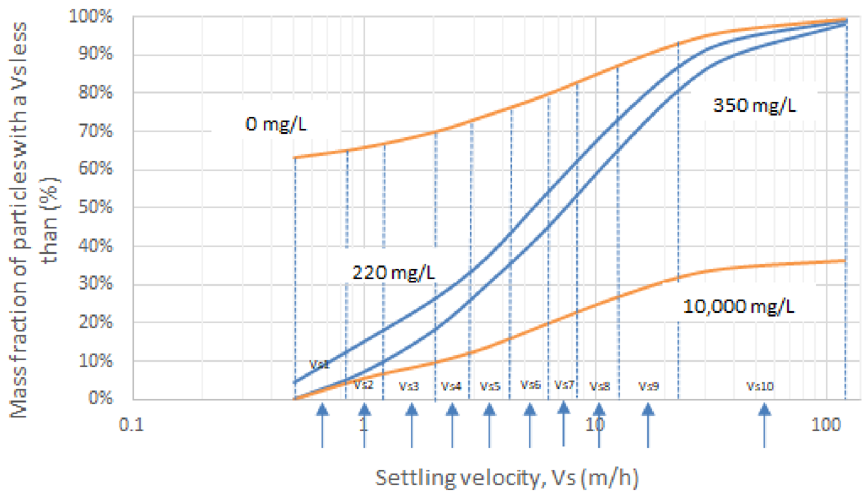

Figure 8.10: Inlet PSVD settling velocity class boundaries (in blue) and extrapolated boundaries (in orange) for a particle class fractionation into 10 classes for the East Québec City WRRF. The arrows indicate the settling velocity that characterizes each class, calculated as the geometrical mean of the boundaries of each class.

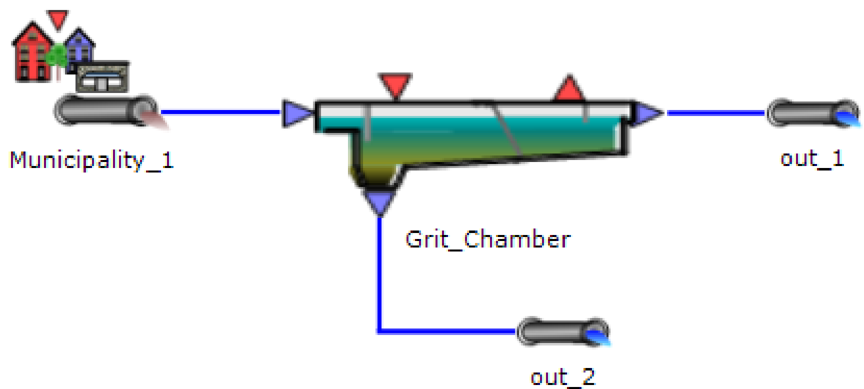

Figure 8.11: Scheme of the hydraulic model for the aerated grit chamber.

in Section 8.2.2 could be compared to the simulated results. In Figure 8.13, despite the underestimation of the tracer concentration, a good fit of the hydraulic model is observed with a RMSE of 0.0074 mg/L.

Further details of the hydraulic model are provided in Tik and Vanrolleghem (2017) and Tik (2019).

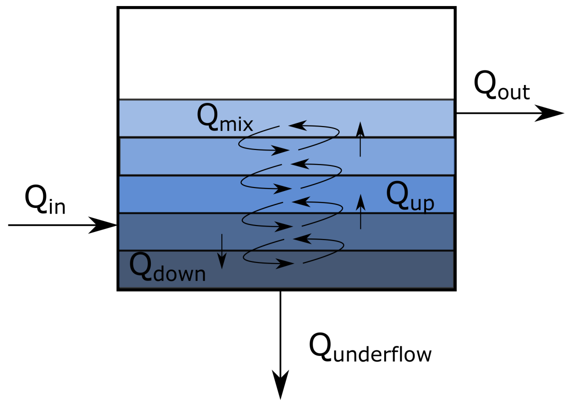

Figure 8.12: Five-layers PSVD model with the flow behaviour into the aerated grit chamber.

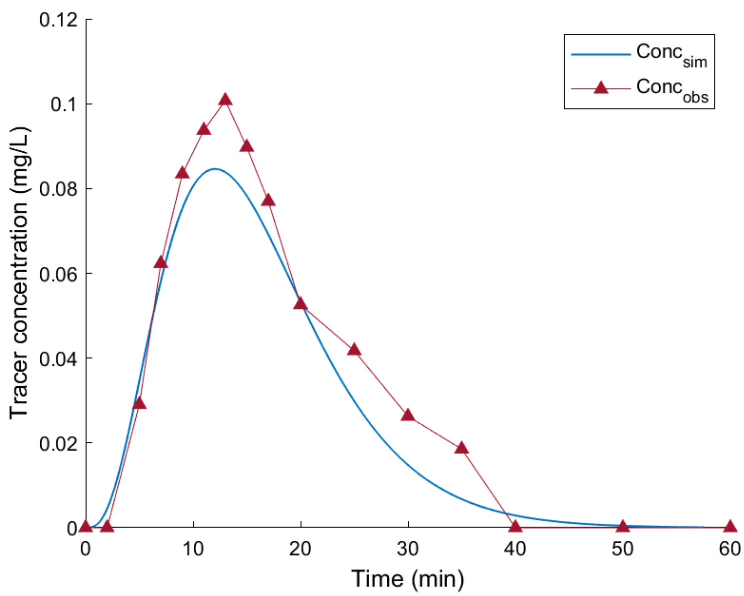

Figure 8.13: Simulated and observed tracer concentrations at the outlet of the aerated grit chamber number 3 at the East Québec City WRRF.

8.5 Model calibration

After the adjustment of the fractionation of the ten particle classes, including its relation to inlet TSS concentrations and the hydraulic model, the model proposed in Section 7.3 was calibrated with a two-day on-line TSS data set. The data set selected was collected under dry weather conditions since no rain event occurred on the previous 4 days and similar flow patterns were observed (see Figure 8.14). The detailed inlet flow and TSS concentrations at the inlet and outlet of the grit chambers during the two selected days are shown in Figure

8.15.

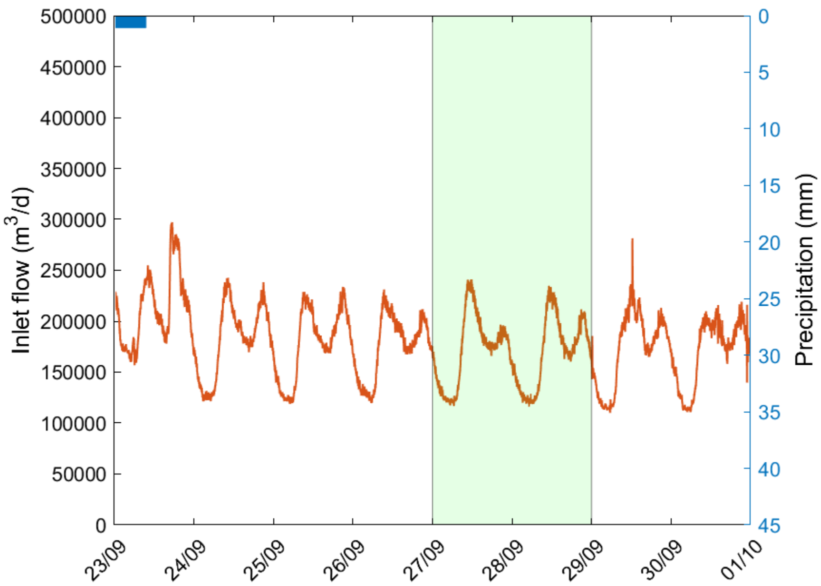

Figure 8.14: Inlet flow and precipitation from September 23rd to October 1st, 2014. The green square indicates the period used for the model calibration.

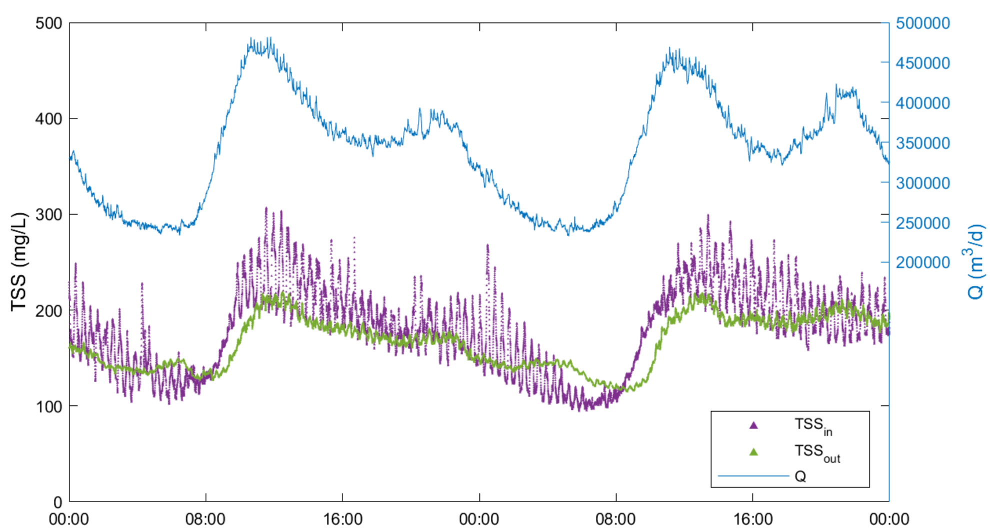

Figure 8.15: On-line TSS measurements for model calibration at the inlet and outlet of the studied aerated grit chambers.

First, the physical characteristics as surface area and height of the grit chamber were set to the actual ones. The underflow was approximated to the real operating conditions considering that the alternated grit removal from the 5 units is a constant flow.

Without further calibration of the other model parameters, the simulated results were showing a promising performance of the model despite the fact that, this time, the forces inducing recirculation into the grit chamber are caused by the air flow. Thus, the effect of the dispersion was again translated into the Q_{mix} calculated with Equation 7.10.

The parameters related to the mixing flow (i.e. α_D and β_D) were calibrated performing a scenario analysis to find the best model fit (see Figure 8.16). Again, the goodness-of-fit was statistically estimated with the RMSE, bias and difference on the % removal criteria.

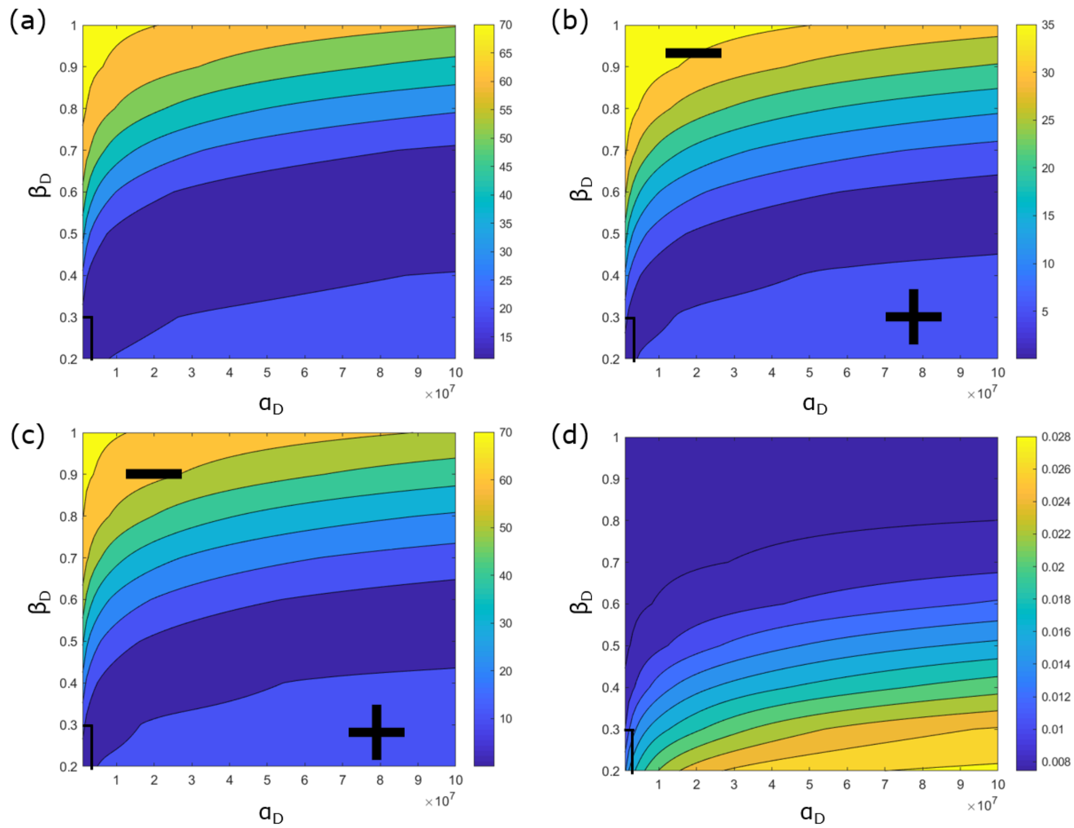

Figure 8.16: Scenario analysis results for different α_D and β_D values for the aerated grit chamber model. (a) RMSE results of the PSVD model, (b) sum of the absolute values of the difference between the observed and simulated % removal of the PSVD model, (c) absolute values of the bias of the PSVD model, and (d) RMSE results of the hydraulic model. The + and - symbols represent the positive and negative zone values.

The results presented a good approximation of the outlet TSS concentration and the overall dynamics are followed even though the simulated results are smoother than the observations (see Figure 8.17). For the two days data set, the simulated removal efficiency was 10 % which is similar to the 9 % of the observed one. The calculated RMSE was 11.1 mg/L, i.e. 6 % of the average TSS concentration. This % is in the same order of magnitude as the measurement error of TSS sensors. Finally, the bias was -2.3 mg/L, which is low and indicates a general overestimation of the TSS removal.

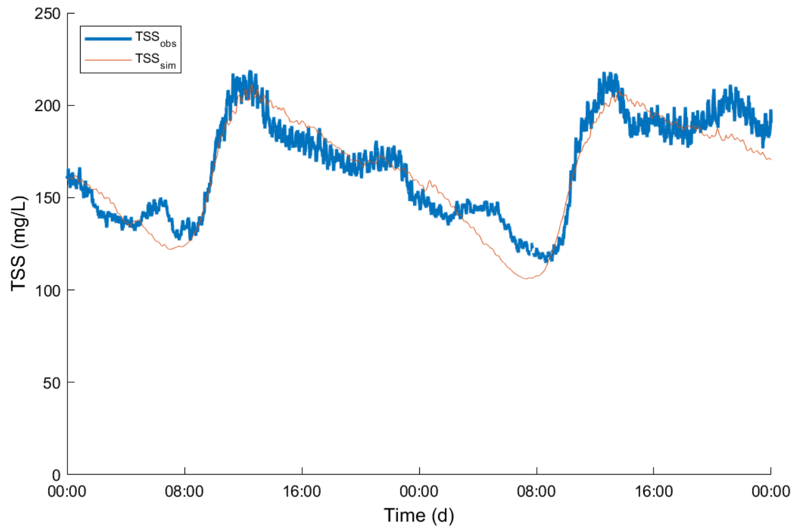

Figure 8.17: Observed and simulated results at the outlet of the aerated grit chamber for the calibration test under dry weather conditions.

In Table 8.2, the overall particle fractionation at the inlet of the grit chamber and the percentage removal of each particle class for the calibration test are presented. As expected, the model is able to describe the fact that a higher percentage of particles with high settling velocities is captured by a grit chamber(i.e. classes 9-10), reaching a retention of 90 % of the particles with a settling velocity of 75 m/h (i.e. class 10).

Table 8.2: % removal of each particle class characterized by their settling velocity after calibration of the aerated grit chamber model.

Particle class	**Settling velocity (m/h)**	**Concentration (mg/L)**	**% mass**	**% removal**
Class 1	0.75	43.3	24 %	0.3 %
Class 2	1.44	16.6	9 %	0.5 %
Class 3	2.44	17.1	9 %	0.6 %
Class 4	3.79	18.1	10 %	0.8 %
Class 5	5.62	16.8	9 %	1.2 %
Class 6	7.71	11.9	7 %	1.7 %
Class 7	10.62	14.2	8 %	2.9 %
Class 8	15.62	13.4	8 %	6.0 %
Class 9	25.00	12.8	7 %	16.8 %
Class 10	75.62	15.8	9 %	90.4 %
Total		180.3		10 %

The behaviour presented in Table 8.2 can also be noted on the PSVD curves estimated at the inlet, outlet and underflow (see Figure 8.18). It can be observed that mainly fast settling particles are removed since at the outlet, the fraction of these particles is close to 0, and at the underflow, the % of these particles is five times higher than the % at the inlet.

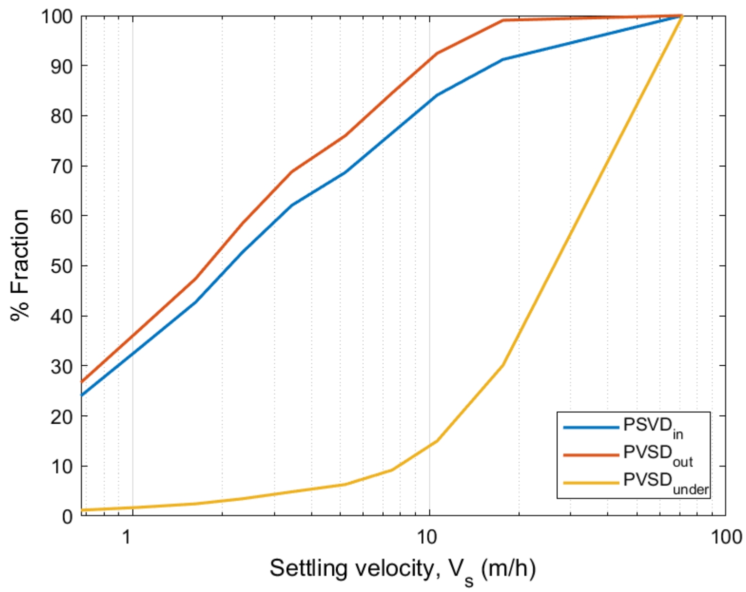

Figure 8.18: Estimated PSVD curves from 2-days data set of the inlet, outlet and underflow.

After model calibration, an analysis of the residuals was made to determine how good the model describes the data (Dochain and Vanrolleghem, 2001). First, it was observed that there is no tendency of the particles' removal over time (see Figure 8.19). The residuals have also been plotted versus the TSS concentrations and the inlet flow as both of them are variables of interest. For both variables, no real tendency is noticed. The residuals plotted versus the three mentioned variables are presented in Figure 8.19.

8.6 Model validation

This time, the model was validated with a 2-day data set collected under wet weather conditions (see Figure 8.20). In Figure 8.21, inlet and outlet TSS concentrations are depicted together with the inlet flow. During the rain event, the dilution of the TSS concentration is observed: a peak of TSS concentration appears only a few hours after the inlet flow rise because of the characteristics of the sewer system (see Section 3.1.2).

The results obtained show that the model is able to represent the overall dynamics of the TSS concentrations at the outlet of the grit chamber, including the peak of TSS concentration after the rain event (see Figure 8.22). However, similar to the calibration results, the model does not describe the detailed TSS variations over short periods of time.

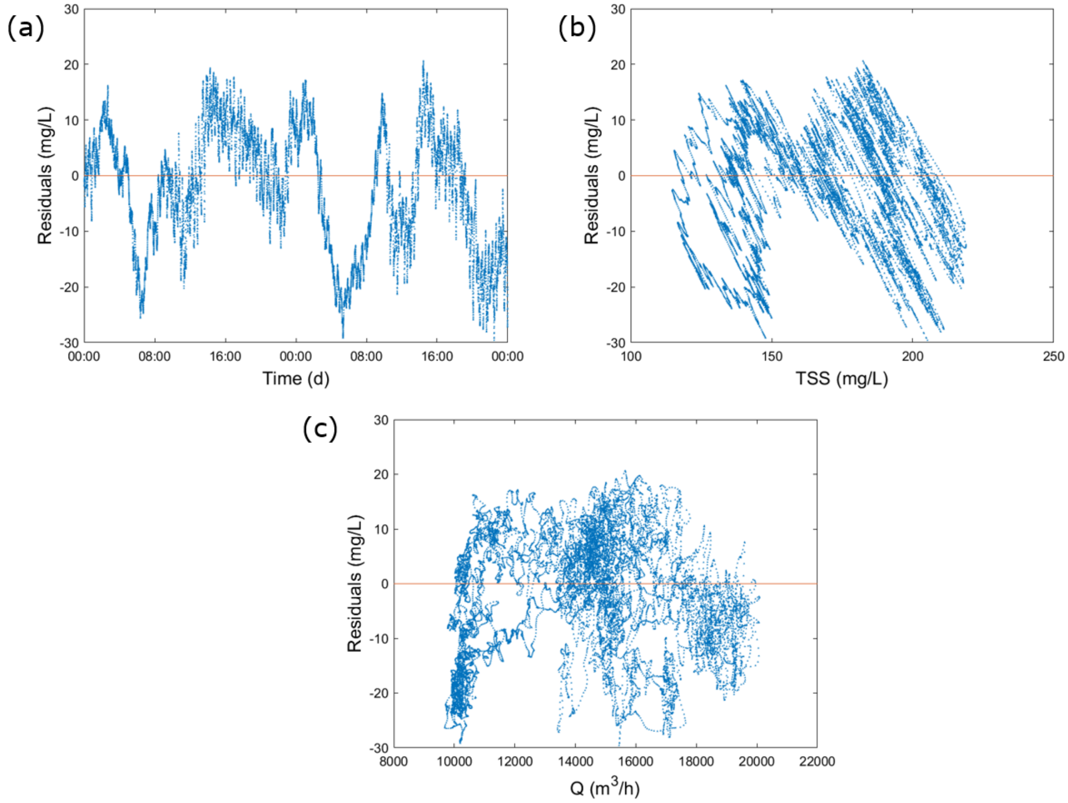

Figure 8.19: Analysis of the residuals after calibration of the aerated grit chamber model. (a) Residuals in time sequence, (b) residuals versus TSS concentration, and (c) residuals versus inlet flow.

Under these wet weather conditions, the % removal simulated was 9.5 %. Compared to the observed 8.3 %, the simulated % is higher but both values are close to each other and the difference is the same as what could be attained in calibration.

The calculated RMSE was 22.8 mg/L which corresponds to 10 % of the average TSS concentration over the 2-day data set. Surprisingly, the bias for this data set is only 0.5 mg/L which is lower, thus better, than the bias obtained in calibration. Finally, comparing the RMSE values of calibration and validation, a Janus coefficient of 2.05 could be calculated. Considering that the data set used for the model validation was collected under wet weather conditions, the small exceedance over the Janus limit of 2 allows concluding that the model is valid.

The % removal of each particle class was again calculated (see Table 8.3). Compared to the calibration results, similar percentages of each fraction are observed in the inlet. However, a lower % removal is noticed, especially for the fast settling particles. This is expected because the inlet flow is two times higher than the inlet flow under dry weather conditions. The HRT of the grit chamber is thus lower and particles have less time to settle into the unit.

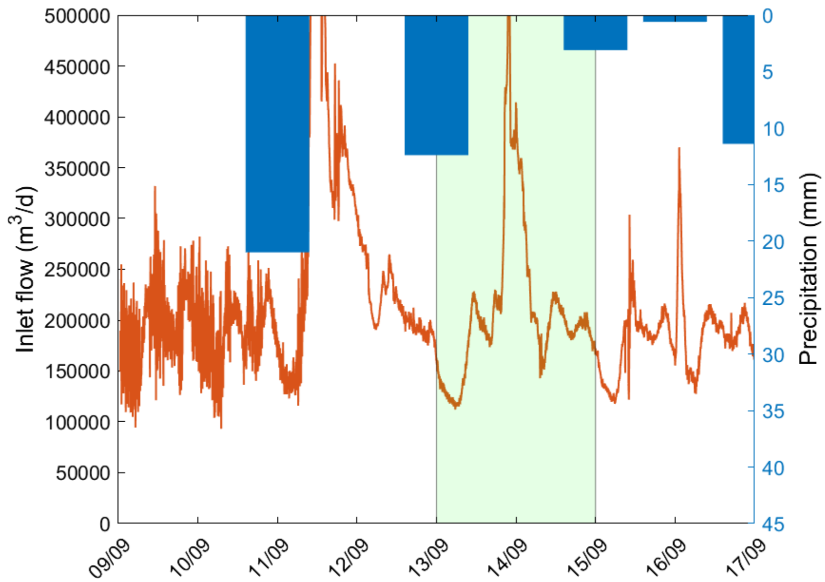

Figure 8.20: Inlet flow and precipitation from September 9^{th} to 17^{th}, 2014. The green square indicates the period of the validation data set under wet weather conditions.

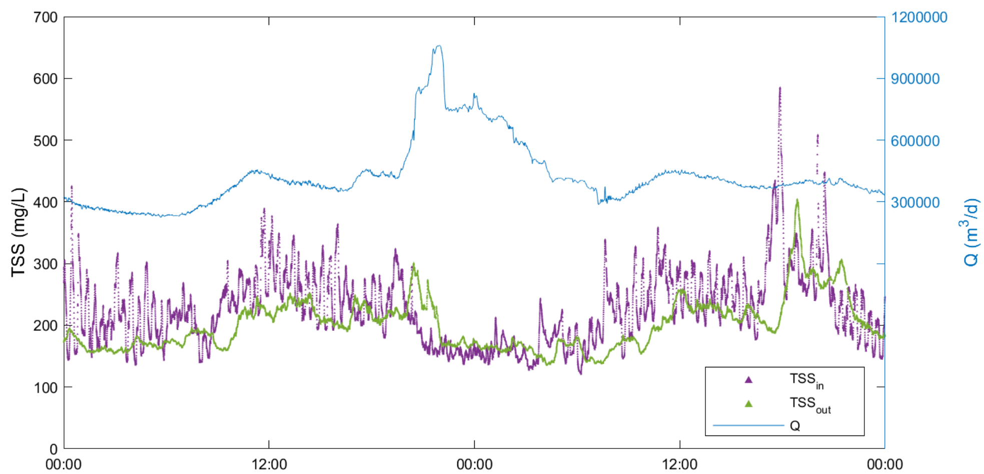

Figure 8.21: On-line TSS measurements for model validation under wet weather conditions at the inlet and outlet of the aerated grit chamber with the inlet flow.

Finally, an analysis of the residuals was again performed (see Figure 8.23). The residuals in time sequence does not show any tendency since they are distributed quite randomly around 0. However, the residuals versus TSS concentration and inlet flow present an overestimation of the % removal for high TSS concentrations and high inlet flows.

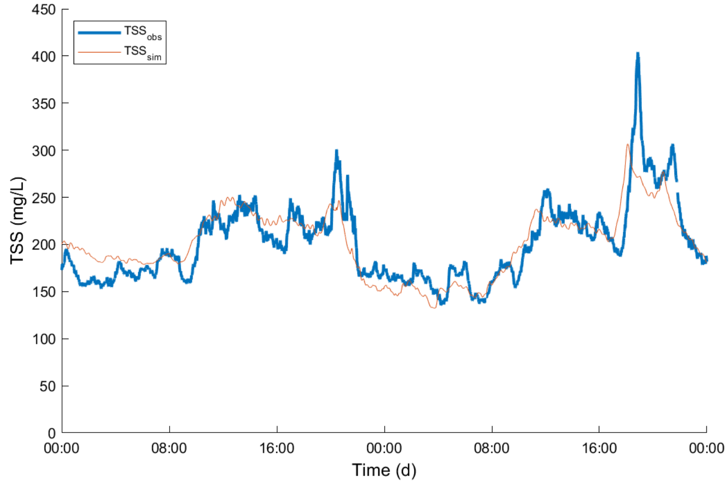

Figure 8.22: Observed and simulated results at the outlet of the aerated grit chamber for the validation test under wet weather conditions.

Table 8.3: % removal of each particle class characterized by their settling velocity for the validation test for the aerated grit chamber.

Particle class	**Settling velocity (m/h)**	**Concentration (mg/L)**	**% mass**	**% removal**
Class 1	0.75	44.5	20 %	0.3 %
Class 2	1.44	21.4	9 %	0.1 %
Class 3	2.44	22.2	10 %	0.2 %
Class 4	3.79	23.6	10 %	0.3 %
Class 5	5.62	22.1	10 %	0.5 %
Class 6	7.71	15.8	7 %	0.8 %
Class 7	10.62	19.1	8 %	1.4 %
Class 8	15.62	18.5	8 %	3.5 %
Class 9	25.00	17.6	8 %	11.4 %
Class 10	75.62	22.6	10 %	82.6 %
Total		227.3		9.5 %

8.7 Conclusions

Once again, a proper study of the settling characteristics and the hydraulics of a grit chamber showed that it is the key success factor for good grit chamber modelling. The application of the new experimental characterization and modelling approach based on the PSVD to an aerated grit chamber confirms the good performance of the model, with good calibration quality and strong validation, given that it was performed under wet weather conditions.

As a first test of the model developed for vortex grit chambers, it shows a good overall

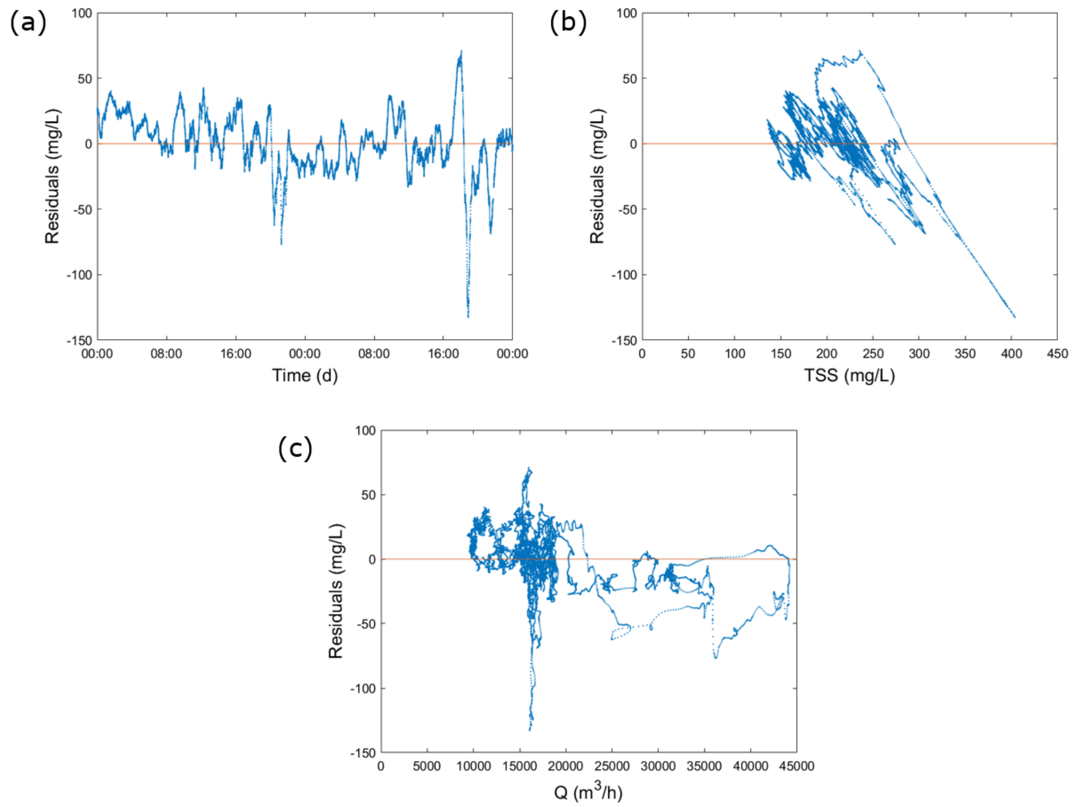

Figure 8.23: Analysis of the residuals of the validation test under wet weather conditions for the aerated grit chamber. (a) Residuals in time sequence, (b) residuals versus TSS concentration, and (c) residuals versus inlet flow.

performance for other grit chamber designs. However, the detailed dynamics over a short period of time may require further study. Despite the fact that the data available was limited, the model was able to describe the overall outlet TSS concentration dynamics under both dry and wet weather conditions.

Without including the aeration processes in the aerated grit chamber model, more particles would settle. The air flow injected into the grit chamber could not be considered as a parameter as such since the tests were performed under only one operating condition. Thus, the dispersion into the grit chamber was only determined on the basis of the inlet flow. However, in further studies, the air flow could be included into the mixing forces.

Conclusions and perspectives

Conclusions

The work presented in this thesis was realized to accomplish the following main objective: develop a conceptual dynamic model of grit chambers to describe the solids concentration at the outlet and its properties. To achieve this main objective, two specific objectives were defined in the context of the study:

1. Characterize the water quality around a grit removal system (GRS) in terms of total suspended solids and their characteristics.
2. Develop and apply a dynamic model based on particle settling velocity distribution (PSVD) to describe the particle dynamics at the outlet of the grit chamber and the particles removed by the GRS.

According to these objectives, this section has been divided in three subsections: (i) the main conclusions of the grit sampling and characterization study, (ii) the main conclusions of the proposed grit chamber model ans how it was applied on a vortex and an aerated grit chamber, and (iii) practical recommendations deduced from the PhD study.

8.7.1 Grit sampling and characterization

The presented literature review demonstrated that there is a wide diversity of grit definitions, and sampling and characterization methods. Due to this variety and to achieve the first objective, different sampling approaches and characterization methods were chosen and compared to establish sampling and characterization protocols in the context of this study. This objective is covered in Chapter 4 related to the development of a site-specific sampling protocol, and in Chapters 5 and 6 related to the particle characterization methods.

The results presented in Chapter 4 demonstrated that both equipments and the presented sampling strategies can be used indifferently for the Saint-Nicolas WRRF case study. However, the tests performed were limited to a few samples per comparison test, i.e. five samples to compare the sampling method and three samples to compare the sampling strategy. Also, they were only sampled around the same time (between 8 a.m. and 9 a.m., significant flow and particle concentration differences might be due to the pump activations). Thus, the results do not represent the inlet dynamics along the whole day.

The presented sampling methods and strategies have only been compared on samples collected at the Saint-Nicolas WRRF where the inlet channel is 95 cm large and the water height varies between 10 and 20 cm under dry weather conditions. When while applying them at other WRRFs, the observed results might be different. Other equipment, operating strategies and WRRFs should be evaluated prior to a protocol proposal. In any case, to get a representative sample remains difficult due to the spatial heterogeneity, particularly at the inlet channel. In brief, the equipment and the sampling strategy has to be adapted to the characteristics of the inlet and outlet channels of the grit chamber to be studied, and more importantly to well represent the cross section of the channels.

In Chapter 5, the results demonstrated experimentally that depending on the sieving method and the sample pretreatment, different PSDs can be obtained. Wet sieving can be considered as the reference method since particles are not preteated, thus not modified. For reasons of safety and health, time consumption and sample storage period, dry sieving of washed wet grit is chosen as an alternative method to characterize the PSD.

The study of the grit composition showed that smaller particles retained in a grit chamber are more inorganic whereas bigger aggregate particles are more organic. These results accompanied by the density measurements demonstrate that the composition variation has an impact on the particles' density, thus on the settling velocity. An equation was proposed to estimate the density of a particle depending on its organic/inorganic composition.

The importance of the study of the settling characteristics was demonstrated in Chapter 6. The results showed that the upgraded 2m-ViCAs method and adapted elutriation device allow studying settling velocities up to 120 m/h, which is of interest for grit particles. Moreover, the PSVD curves obtained from the ViCAs column and the elutriation device were not significantly different. However, it must be recognized that both methods have not been tested on synthetic and known samples, which would have allowed them to be properly verified.

PSVD curves were again found to depend on the TSS concentration of the sample as in the earlier works of Bachis et al. (2015) and Maruéjouls et al. (2015). For this study, particle settling velocities were determined as they exist in raw wastewater. Thus, the characterization of the settleability can be considered more accurate compared to the PSD-based settling velocity estimates.

All studied PSD and PSVD methods are reproducible methods (i.e. lower than 5 % variation, except for elutriation that has variation up to 10 %). However, PSVD methods are preferred over PSD methods because of the more accurate estimation of the particle settling velocities.

Moreover, while studying PSD and PSVD characterization methods, an effect of different weather conditions, i.e. dry weather, wet weather and snowmelt on the grit characteristics, was observed. On the whole, the particles from samples collected under dry weather are bigger, more organic and settle slower compared to particles collected under wet weather. These differences can be explained by the higher flows occurring under wet weather conditions that are able to resuspend and carry particles with a higher settling velocity that were deposited in the sewer system and on the surfaces of the catchment. During the snowmelt period induced by a rain even, too few samples were collected to take make a firm conclusion, but the highest % of inorganic fractions and the highest fraction of fast settling particles ($v_s > 70\ m/h$) were observed under these conditions.

8.7.2 Modelling of grit chambers

The literature review on grit chamber modelling showed that only very few models exist to describe the behaviour of this unit. Considering this gap on grit chamber modelling, the second objective was pursued and a conceptual model was proposed. It was covered in Chapters 7 (application to a vortex grit chamber) and 8 (application to an aerated grit chamber).

From the sampling campaigns carried out during 2016, 2017, and 2018, it was deduced that the hydraulics of the grit chamber and the settling characteristics of the particles around the unit were key features to be considered for the model. Hence, the model proposed is based on PSVD including the hydraulics behaviour and is inspired by the layered PSVD model for primary clarifiers proposed by Bachis et al. (2015). The novelty of the proposed PSVD model for grit chambers is the use of PSVD curves with a larger range of settling velocities including the fast settling particles (i.e. the particles of interest for grit chamber studies) and the hydraulic configuration of the unit to be modelled.

Vortex grit chamber modelling

First, the PSVD model for grit chambers was developed based on the vortex grit chamber at the Saint-Nicolas WRRF case study because more data were available.

The model was developed to describe the TSS dynamics at the outlet of the grit chamber. Importantly, not only the TSS daily profile was described by the model, the TSS dynamics due to pump activations in the Saint-Nicolas sewer system could also be successfully simulated. Thanks to the developed flow reconstruction model, the inflow dynamics and thus the HRT of the grit chamber, were accurately represented and considered into the model simulations.

The vortex forces causing turbulent mixing in the grit chamber have been represented by a mixing flow with magnitude Q_{mix} between model layers. The Q_{mix} was made inversely proportional to the inlet flow. As a result, a better description of the TSS dynamics at the outlet of the grit chamber was achieved.

Despite the limitations that most of the sampling and characterization were made under dry weather conditions, the model was able to properly describe the TSS concentration dynamics at the outlet of the grit chamber. It not only allowed to successfully calibrate the model under dry weather conditions, but, importantly, the model was also successfully validated under other weather conditions (i.e. dry weather winter conditions and wet weather).

The model is not only able to describe the TSS dynamics at the outlet of the grit chamber, thus giving its removal efficiency, but also to estimate the % removal of each particle class defined. Hence, it allows to evaluate that a higher percentage of fast settling particles is retained by the grit chamber than slow settling particles, as expected.

Despite the good performance of the model (i.e. a Janus of 1.5 for both validation tests performed), a relatively low % removal (around 60 %) of the fast settling particles (class 10) was estimated. This could be explained by the fact that the inlet of the grit chamber was considered homogeneous and since in the model based on the tracer test, 1/3 of the flow is short-circuited without settling, 1/3 of each particle classes will thus never settle into the studied grit chamber. Further analysis of this short-circuit flow should be made.

Aerated grit chamber modelling

To evaluate whether the proposed PSVD model developed and tested on a vortex grit chamber could also be used to describe the TSS removal performance of other grit chambers, the model was applied to an aerated grit chamber where the design and operation are different compared to a vortex grit chamber. In this case, turbulent mixing is induced by the air flow into the grit chamber.

The results of the model showed a good performance (i.e. a Janus coefficient of 2.05 for the validation) describing the overall TSS at the outlet of the aerated grit chamber. It is also able to reproduce the daily dynamics. However, for this case study, the dynamics over a short time could not be well simulated. Due to the limited data available, the reason why could not be identified and the model could not be improved further.

Regardless of the lack of adequate description of the short-term dynamics, the model was successfully calibrated and validated under different weather conditions (i.e. calibrated under dry weather conditions and validated under wet weather conditions). The statistical tests performed, RMSE, bias and difference of the % removal, are similar to the vortex grit chamber case study.

Regarding the % removal of each particle class, it was noticed that the % removal of fast settling particles is higher than slow settling particles, as expected.

To sum up, in this PhD study, a new conceptual model for grit chambers has been proposed based on PSVD, whit the settling characteristics as the model's key feature. Despite the fact that it has previously been shown that the PSVD curves vary with weather conditions, the ensemble of the PSVD curves included in the model for both case studies were only collected under dry weather conditions. Hence, in its current state, the model is not able to distinguish particle settling characteristics under dry weather, wet weather, or snowmelt periods.

The hydraulic behaviour of the unit (i.e. HRT and inlet flow) and the turbulent mixing caused by the forces induced in the system (i.e. vortex forces or air flow) have also been identified to impact the grit removal performance. Despite the fact the the hydraulics has been shown to be an important feature of the grit chamber performance, the hydraulic models for both grit chambers have remained as a conceptual simplification determined from tracer tests.

Despite the limitations of the conceptual model, it has been successfully applied to two different grit chamber configurations: vortex and aerated units. In both cases, the model has been successfully calibrated and validated. Compared to the existing (static) grit chamber models, the proposed dynamic model (applied to a vortex and an aerated grit chambers) allows remarkably good dynamic predictions of TSS concentrations at the outlet of the grit chamber. Also, it shows a good overall removal performance, including under wet weather conditions.

8.7.3 Practical recommendations

Given the important role that grit chambers play to protect the equipment and keeping the performance of the processes downstream, and the lack of knowledge about these units, this PhD study was pursued to meet the expectations of municipalities and industry. From the knowledge acquired during this PhD study, some important insights can be presented. First and foremost, grit has been defined as particles that are a mix of inorganic and organic fractions and are characterized by high settling velocities, i.e. $v_s > 70m/h$.

To rigorously study the performance of grit chambers, proper sampling and characterization of the particles around a treatment unit has to be performed. This requires that:

- The samples at the inlet and at the outlet of the grit chambers has to be representative. Every sampling method and equipment have to be adapted to each case study to cover the entire cross-section of the inlet and outlet channels. This is important because the flows through the channels are heterogeneous.

- If the performance of the grit chamber is studied from grab samples, the hydraulic retention time has to be considered to collect a sample at the outlet of the same water mass that has been sampled at the inlet. It is recommended that several grab samples are taken along the day to evaluate the performance variation of the grit chamber depending on the inlet dynamics.

- If it is desired to evaluate the performance of the grit chamber with samples collected over several hours/days, before to characterize them, two options to collect the sample to be analysed have to be considered:

  1. Grab a sub-sample of the desired volume from the main sample. A good homogenization of the main sample has to be assured to get a representative sample.
  2. Concentrate the sample until the needed volume is obtained. Depending on the method used to reduce the water quantity of the main sample, some particles may be modified or lost.

  In both cases, the original sample is modified, and the sample used for the test may not be totally representative of the original sample or the system. Also, the performance will be estimated globally over the sampling period.

- Sampling, quantification and characterization of the particles collected at the grit bin is an important added value to the unit performance study.

- Do not modify the sample and minimize any sample modification prior to characterization tests so as to avoid changes of the nature of the particles as they exist in the raw wastewater.

- It is preferred to characterize the particles around a grit chamber in terms of particle settling velocity distribution. However, the method used for characterization has to be adapted for fast settling particles, e.g. the 2m-ViCAs column or the applied elutriation test.

- The performance of the grit chamber can be estimated according to different particle classes depending on their settling velocity.

The design of the grit chambers is strongly recommended to be based on particle settling velocities since it is the key parameter of the settling processes on which a grit chamber's operation is based. Designing a grit chamber based on particle size can lead to an underestimation of the treatment unit's size and only particles with higher settling velocities than expected will be able to be removed. This underestimation can be due to the overestimation of the settling velocity from the particle sizes and the overestimation of the density of the particles by assuming they are sand particles.

A dynamic grit chamber model based on particle settling velocity distribution that is properly calibrated and validated, allows describing the grit removal in this treatment unit. Thus, an approximation of the chamber's performance can be determined depending on the operating conditions and the inlet dynamics. Also, a grit chamber model can be used as a tool to design the unit or, being integrated in a WRRF model, simulate a whole plant.

Perspectives and future work

In this PhD thesis, the conceptual dynamic model of grit chambers based on PSVD was shown to be a powerful tool to describe the TSS dynamics at the outlet of the unit and the selective removal of certain settling velocity classes. The characterization of the PSVD was demonstrated to be the key requirement for grit chambers' design and optimization. Despite the fact that the proposed model showed a good performance, representative samples have to be collected and properly characterized.

Based on the findings presented in this PhD thesis, further studies can be carried out to complement and clarify the presented study. Some suggestions can be:

- Perform further tests at other WRRFs to compare sampling devices and strategies. Depending on the WRRF characteristics, the device to be applied or the strategy to be implemented may vary. A rigorous analysis of sampling devices and strategies at different WRRFs may allow developing a standardized sampling protocol. Such protocol should be flexible and adaptable to any WRRF.

- Perform tests with the adapted PSVD characterization methods using synthetic samples with known particles. In this PhD study, both methods were only tested and compared using raw wastewater sampled at the inlet and outlet of the studied grit chambers. However, repeating these tests with a sample with known characteristics should allow validating the methods.

- Specifically for the aerated grit chamber case study at the East Québec City WRRF, more information should be collected for a better understanding of the unit's dynamics, especially regarding the settling characteristics. By including the data into the model, a better performance of the description of the outlet TSS dynamics can be expected.

- Collect more samples under wet weather conditions for both case studies to evaluate the impact of wet weather conditions on the PSVD curves. The presented model only considers PSVD curves under dry weather conditions and it has been noticed that under wet weather conditions the settling characteristics vary. Hence, with PSVD curves under wet weather conditions, one should be able to find a relationship between dry and wet weather curves thus improving the description of the outlet TSS dynamics and the estimation of grit removal.

- Collect a proper data set and perform a deeper study of the PSVD curves during the snowmelt period. Including this information into the model, it should be able to better describe the outlet TSS dynamics and predict grit removal under those conditions. Since in cold regions it is during this period that the largest quantities of grit are collected into the bin and higher inflow is received at a WRRF, grit chambers are struggling and the removal efficiency decreases. In addition, a better knowledge of the operating conditions under snowmelt conditions should allow optimizing the unit's operation and improving the grit removal.

- The impact of the viscosity on the settleability should be studied. In the Québec area, the wastewater temperature varies approximately from 5 to 20 °C between winter and summer. The PSVD curves used for the model were analysed in the lab with sample temperatures around 20 °C which is different than the temperature of the wastewater and may have an impact on the settleability because of the temperature-dependant viscosity.

- Include the vertical heterogeneity of the inlet channel. A better removal performance of fast settling particles should be predicted because CFD studies have shown that the fast settling particles at the inlet are rolling at the bottom of the channel and settle immediately into the grit chamber (*Veolia Water Technologies Canada*, personal communication). This assumption should have a positive impact on the prediction of fast settling particle removal of the vortex grit chamber since 1/3 of the inlet flow is now considered to short-circuit for which no settling was considered. Thus, 1/3 of the particles has no chance to settle, which is not the case for fast settling particles.

- In view of maximizing water resource recovery of organics, ideally, all inorganic particles should settle in a girt chamber while all organic particles should pass through the unit. Hence, the determination of the inorganic/organic fraction removal should be integrated into the model to allow optimizing the fraction's removal. Further tests are needed to determine the inorganic/organic fractions depending on the operating conditions in terms of inflow, TSS dynamics and settling characteristics.

- In view of grit chambers' optimization, the mixing (Q_{mix}) should be estimated depending on the operating conditions, i.e. the paddles rotation speed or the air flow rate. In case of a vortex grit chamber, the estimation of Q_{mix} could be as follows:

$$Q_{mix} = \frac{\alpha_D}{Q_{in}^{\beta_D}} \cdot \left(\frac{v_{rot}}{v_{rot}^{nominal}} \right)^{\gamma_D} \tag{8.3}$$

where v_{rot} is the rotation speed of the paddles to be optimized (RPM), the $v_{rot}^{nominal}$ is the rotation speed of the paddles under the design conditions (RPM), and γ_D is the impact factor of the rotation speed of the paddles on the mixing flow (-).

For an aerated grit chamber, the Q_{mix} could be estimated similarly:

$$Q_{mix} = \frac{\alpha_D}{Q_{in}^{\beta_D}} \cdot \left(\frac{Q_{air}}{Q_{air}^{nominal}} \right)^{\gamma_D} \tag{8.4}$$

where Q_{air} is the air flow to be optimized (m^3/d), and the $Q_{air}^{nominal}$ is the air flow under the design conditions (m^3/d).

Further tests are required under different operation conditions of the paddles rotation speed for vortex grit chambers and air flow for aerated grit chambers to calibrate the model and identify the optimal scenario.

Bibliography

Aiguier, E., G. Chebbo, J.-L. Bertrand-Krajewski, P. Hedgest, and N. Tyack (1996). Methods for determining the settling velocity profiles of solids in storm sewage. *Water Science and Technology 33*(9), 117–125.

Alferes, J., P. Poirier, C. Lamaire-Chad, A. K. Sharma, P. S. Mikkelsen, and P. A. Vanrolleghem (2013). Data quality assurance in monitoring of wastewater quality: Univariate on-line and off-line methods. In *Proceedings 11th IWA conference on instrumentation control and automation, Narbonne, France, September 18-20 2013*.

Alferes, J., S. Tik, J. Copp, and P. A. Vanrolleghem (2013). Advanced monitoring of water systems using in situ measurement stations: data validation and fault detection. *Water Science and Technology 68*(5), 1022–1030.

Alferes, J. and P. A. Vanrolleghem (2016). Efficient automated quality assessment: Dealing with faulty on-line water quality sensors. *AI Communications 29*(6), 701–709.

Andoh, R. and R. Smisson (1996). The practical use of wastewater characterisation in design. *Water Science and Technology 33*(9), 127–134.

Andoh, R. Y. (2015). Grit characterization and optimal grit removal using the HeadCell® device. Hydro International. https://www.hydro-int.com. Accessed: 2016-07-10.

APHA (2012). *Standard Methods for the Examination of Water and Wastewater* (22nd ed.). American Public Health Association, American Water Works Association, Water Environment Federation. Washington, DC, USA.

Ashley, R., J. Bertrand-Krajewski, T. Hvitved-Jacobsen, and M. Verbanck (2005). *Solids in Sewers*. IWA Publishing, London, UK.

ASTM (2014). D4892-14: Standard Test Method for Density of Solid Pitch (Helium Pycnometer Method). Technical report, ASTM International, West Conshohocken, PA, USA.

ASTM (2015a). C128: Standard Test Method for Relative Density (Specific Gravity) and Absorption of Fine Aggregate. Technical report, ASTM International, West Conshohocken, PA, USA.

ASTM (2015b). C136/C136M: Standard Test method for Sieve Analysis of Fine and Coarse Aggregates. Technical report, ASTM International, West Conshohocken, PA, USA.

ASTM (2015c). D5550-14: Standard Test Method for Specific Gravity of Soil Solids by Gas Pycnometer. Technical report, ASTM International, West Conshohocken, PA, USA.

Bachis, G., T. Maruéjouls, S. Tik, Y. Amerlinck, H. Melcer, I. Nopens, P. Lessard, and P. A. Vanrolleghem (2015). Modelling and characterization of primary settlers in view of whole plant and resource recovery modelling. *Water Science and Technology 72*(12), 2251–2261.

Barter, P. and M. Sherony (2011). Grit – you don't know what you're missing! In *5th European Water & Wastewater Management Conference, 26-27 September 2011, London, United Kingdom*.

Bauwens, W., P. Vanrolleghem, and M. Smeets (1996). An evaluation of the efficiency of the combined sewer-wastewater treatment system under transient conditions. *Water Science and Technology 33*(2), 199–208.

Beck, M. (1976). Dynamic modelling and control applications in water quality maintenance. *Water Research 10*(7), 575–595.

Benedetti, L., J. Langeveld, A. Comeau, L. Corominas, G. Daigger, C. Martin, P. S. Mikkelsen, L. Vezzaro, S. Weijers, and P. A. Vanrolleghem (2013). Modelling and monitoring of integrated urban wastewater systems: review on status and perspectives. *Water Science and Technology 68*(6), 1203–1215.

Bennett, N. (1989). Grit - its removal, a new idea. *Water Science and Technology 21*(12), 1767–1770.

Berrouard, E. (2010). Caractérisation de la décantabilité des eaux pluviales. Master's thesis, Université Laval, Québec, QC, Canada.

Black Dog Analytical Lld (2019). Methods on grit sampling and characterization. https://www.blackdoganalytical.com/home-page.html. Accessed: 2019-04-02.

Blain, M., P. Steel, and E. Salenieks (2018). Implementing vortex grit removal the right way. *Environmental Science & Engineering Magazine August 2018*, 18–22.

Box, G. E. P., J. S. Hunter, and W. G. Hunter (2005). *Statistics for Experimenters : Design, Innovation, and Discovery* (2nd ed.). Wiley series in probability and statistics. Hoboken, N.J, USA.

Burbano, M., B. McConnell, C. Knatz, D. Bisson, and B. Tarbuck (2009). Improving grit removal through CFD analysis. In *82nd Water Environment Federation Technical Exhibition and Conference; WEFTEC2009; 10 -14 October, Orlando, FL, USA*, pp. 794–806.

Butler, D., E. Friedler, and K. Gatt (1995). Characterising the quantity and quality of domestic wastewater inflows. *Water Science and Technology 31*(7), 13–24.

Camp, T. R. (1936). A study of the rational design of settling tanks. *Sewage Works Journal 8*(5), 742–758.

Camp, T. R. (1942). Grit chamber design. *Sewage Works Journal 14*(2), 368–381.

Chambers, B. and G. L. Jones (1988). Optimisation and uprating of activated sludge plants by efficient process design. *Water Science and Technology 20*(4-5), 121–132.

Chebbo, G. (1992). *Solides des rejets pluviaux urbains: caractérisation et traitabilité*. Ph. D. thesis, Ecole Nationale des Ponts et Chaussées, Marne-la-Vallée, France.

Chebbo, G. and M.-C. Gromaire (2009). ViCAs—An operating protocol to measure the distributions of suspended solid settling velocities within urban drainage samples. *Journal of Environmental Engineering 135*(9), 768–775.

Chien, M. H., A. Borys, and J. L. Wong (2010). Computational fluid dynamics analysis of a vortex grit removal system. In *83rd Water Environment Federation Technical Exhibition and Conference; WEFTEC2010; 2 - 6 October, New Orleans, LA, USA*.

Couture, M., A. Steele, M. Bruneau, A. Gadbois, and B. Hohman (2009). Achieving greater efficiency for 360 rotational grit removal technology using empirical data and CFD analysis. In *82nd Water Environment Federation Technical Exhibition and Conference; WEFTEC2009; 10 -14 October, Orlando, FL, USA*, pp. 773–783.

Desai, J., J. J. Keane, J. Daily, K. Kennedy, J. Loiacono, R. Sun, and A. Velasco (2014). San Francisco's combined sewer grit management approach at the Southeast plant. In *87th Water Environment Federation Technical Exhibition and Conference; WEFTEC2014; 27 September – 1 October, New Orleans, Louisiana USA*, pp. 3013–3033.

DHI (2019). WEST - Modelling and simulation of wastewater treatment plants. https://www.mikepoweredbydhi.com/. Accessed: 2019-07-10.

Dochain, D. and P. Vanrolleghem (2001). *Dynamical Modelling and Estimation in Wastewater Treatment Processes*. IWA Publishing, London, UK.

Dutta, S., T. E. Tokyay, Y. A. Catano-Lopera, S. Serafino, and M. H. Garcia (2014). Application of computational fluid dynamic modelling to improve flow and grit transport in Terrence J. O'Brien water reclamation plant, Chicago, Illinois. *Journal of Hydraulic Research 52*(6), 759–774.

Environment Canada (2019). Historical climate data. https://weather.gc.ca/. Accessed: 2019-07-17.

Ferrara, R. A. and A. Hildick-Smith (1982). A modeling approach fo storm water quantity and quality control via detention basins. *Journal of the American Water Resources Association 18*(6), 975–981.

Finger, R. E. and J. Parrick (1980). Optimization of grit removal at a wastewater treatment plant. *Journal Water Pollution Control Federation 52*(8), 2106–2116.

Flanagan, E. (2014). Grit removal e identification and removal methods. In *Northeast Biennial WEAT Conference, May 7-8, 2014, Nacogdoches, TX, USA*.

Fradet, O., M. Pleau, and C. Marcoux (2011). Reducing CSOs and giving the river back to the public: innovative combined sewer overflow control and riverbanks restoration of the St Charles River in Quebec City. *Water Science and Technology 63*(2), 331–338.

Frehmann, T., C. Flores, F. Luekewille, T. Mietzel, B. Spengler, and W. Geiger (2005). Modelling of sedimentation and remobilization in in-line storage sewers for stormwater treatment. *Water Science and Technology 52*(5), 151–158.

Gerges, H. (2014). Guidelines for accurate grit sampling evaluation of current sampling techniques. In *87th Water Environment Federation Technical Exhibition and Conference; WEFTEC2014; 28 September - 1 October, New Orleans, LA, USA*, pp. 1840–1849.

Gerges, H. (2016). A guide to grit characterization. In *89th Water Environment Federation Technical Exhibition and Conference; WEFTEC2016; 24 - 28 September, New Orleans, LA, USA*, pp. 6.

Gerges, H., A. Omae, and U. Martinez (2018). An innovative and simple approach to grit evaluation - new settling velocity test replaces sieve analysis. In *91st Water Environment Federation Technical Exhibition and Conference; WEFTEC2018; 29 September - 3 October, New Orleans, LA, USA*, pp. 2692–2698.

Gernaey, K., P. Vanrolleghem, and P. Lessard (2001). Modeling of a reactive primary clarifier. *Water Science and Technology 43*(7), 73–81.

Grit Tech (2019). Grit testing. https://www.grittech.com/. Accessed: 2019-04-02.

Gromaire, M. C., M. Kafi-Benyahia, J. Gasperi, M. Saad, R. Moilleron, and G. Chebbo (2008). Settling velocity of particulate pollutants from combined sewer wet weather discharges. *Water Science and Technology 58*(12), 2453–2465.

Gujer, W. (2008). *Systems Analysis for Water Technology*. Springer. Berlin, Germany.

Gupta, K. and A. J. Saul (1996). Suspended solids in combined sewer flows. *Water Science and Technology 33*(9), 93–99.

Gwinn, A., K. Osei, and R. Andoh (2011). An assessment of a high speed particle imaging technology for measuring particle concentration, size and shape. In *The Surface Water Quality Conference & Exposition (StormCon); August 21-25; Los Angeles, CA, USA,*.

Gwinn, A., K. Osei, J. Fink, and R. Andoh (2013). Development and calibration of a grit settling column. In *86th Water Environment Federation Technical Exhibition and Conference; WEFTEC2013; 5 - 9 October, Chicago, IL, USA*, pp. 2391–2399.

Hadj, I. B. (2013). Caractérisation de la taille des particules et de leur vitesse de chute en décantation primaire. Master's thesis, Université Laval. Québec, QC, Canada. (In French).

He, Q., C. Hu, and Z. Xu (2012). Temporal distribution of grit in the combined sewer system of the typical mountainous city. In *International Symposium on Geomatics for Integrated Water Resources Management (GIWRM), October 19-21, 2012, Lanzhou, China*, pp. 1–4. IEEE.

Hedges, P., F. Becker, and R. Smisson (1998). The application of settling velocity as a parameter for characterising wastewater solids. *Water Science and Technology 37*(1), 45–52.

Hendricks, D. (2016). *Fundamentals of Water Treatment Unit Processes: Physical, Chemical, and Biological.* CRC Press. Boca Raton, FL, USA.

Henze, M., W. Gujer, T. Mino, and M. van Loosdrecht (2000). *Activated Sludge Models ASM1, ASM2, ASM2d and ASM3*, Volume 9. IWA Publishing, London, UK.

Herrick, P., A. Neumayer, and K. Osei (2015). Grit particle settling – refining the approach. *Water Online March*, 1–7.

Herrick, P. and M. Sherony (2017). Plant upgrade optimizes grit removal. *Opflow 43*(9), 22–23.

Hettler, E. N., J. S. Gulliver, and M. Kayhanian (2011). An elutriation device to measure particle settling velocity in urban runoff. *Science of the Total Environment 409*(24), 5444–5453.

Hirschbeck, C. and F. W. Günthert (2015). Vorschlag für ein Prüfverfahren und Prüfsand zur Messung des Abscheidegrads von Sandfängenscher. *KA - Korrespondenz Abwasser, Abfall 7*, 606–614. (In German).

Hoskin Scientific Ltd (2019). Horizontal Van Dorn sampler. https://www.hoskin.ca. Accessed: 25-06-2019.

Hydro International plc (2019). Advanced grit management. https://www.hydro-int.com. Accessed: 2019-09-02.

Jeppsson, U., J. Alex, D. Batstone, L. Benedetti, J. Comas, J. Copp, L. Corominas, X. Flores Alsina, K. Gernaey, I. Nopens, et al. (2013). Benchmark simulation models, quo vadis? *Water Science and Technology 68*(1), 1–15.

Judd, S., M. Khraisheh, K. Al-Jaml, D. Jarman, and T. Jahfer (2017). Influence of composite particle formation on the performance and economics of grit removal. *Water Research 108*, 444 – 450.

Kitching, S. and C. Denton (2012). Characterisation of grit to develop an integrated plant solution. In *85th Water Environment Federation Technical Exhibition and Conference; WEFTEC2012; 29 September - 3 October, New Orleans, LA, USA*, pp. 626–633.

Knatz, C., S. Rafferty, and A. Delescinskis (2015). Optimization of water treatment plant flow distribution with CFD modeling of an influent channel. *Water Quality Research Journal of Canada 50*(1), 72–82.

Krishnappan, B., K. Exall, J. Marsalek, Q. Rochfort, S. Kydd, M. Baker, and R. Stephens (2012). Variability of settling characteristics of solids in dry and wet weather flows in combined sewers: implications for CSO treatment. *Water, Air, & Soil Pollution 223*(6), 3021–3032.

Krishnappan, B. G., J. Marsalek, K. Exall, R. P. Stephens, Q. Rochfort, and P. Seto (2004). A water elutriation apparatus for measuring settling velocity distribution of suspended solids in combined sewer overflows. *Water Quality Research Journal of Canada 39*(4), 432–438.

Laurent, J., R. Samstag, J. M. Ducoste, A. Griborio, I. Nopens, D. J. Batstone, J. Wicks, S. Saunders, and O. Potier (2014). A protocol for the use of computational fluid dynamics as a supportive tool for wastewater treatment plant modelling. *Water Science and Technology 70*(10), 1575–1584.

Le Moullec, Y., C. Gentric, O. Potier, and J. Leclerc (2010). CFD simulation of the hydrodynamics and reactions in an activated sludge channel reactor of wastewater treatment. *Chemical Engineering Science 65*(1), 492–498.

Lemieux, A. and P. Lessard (1993). Détermination statistique de la concentration de matières en suspension décantables d'une eau usée domestique. *Sciences et Techniques de l'Eau 26*(2), 123–128. (In French).

Lessard, P. and M. Beck (1988). Dynamic modeling of primary sedimentation. *Journal of Environmental Engineering 114*(4), 753–769.

Lessard, P. and M. Beck (1991). Dynamic simulation of storm tanks. *Water Research 25*(4), 375 – 391.

Levenspiel, O. (2012). *Tracer Technology: Modeling the Flow of Fluids*. Fluid Mechanics and its Applications. Springer. Berlin, Germany.

Londong, J. (1989). Dimensioning of aerated grit chambers and use as a highly loaded activated sludge process. *Water Science and Technology 21*(4-5), 13–22.

Lucas-Aiguier, E., G. Chebbo, J.-L. Bertrand-Krajewski, B. Gagné, and P. Hedges (1998). Analysis of the methods for determining the settling characteristics of sewage and stormwater solids. *Water Science and Technology 37*(1), 53–60.

Madsen, H., K. Arnbjerg-Nielsen, and P. S. Mikkelsen (2009). Update of regional intensity–duration–frequency curves in Denmark: Tendency towards increased storm intensities. *Atmospheric Research 92*(3), 343–349.

Mansour-Geoffrion, M. (2013). *Trash and grit removal from activated sludge: Evaluating potential for sludge reduction*. Ph. D. thesis, Polytechnique Montréal. Montréal, QC, Canada.

Mansour-Geoffrion, M., P. L. Dold, D. Lamarre, A. Gadbois, S. Déléris, and Y. Comeau (2010). Characterizing hydrocyclone performance for grit removal from wastewater treatment activated sludge plants. *Minerals Engineering 23*(4), 359–364.

Mansour-Geoffrion, M., P. L. Dold, D. Lamarre, A. Gadbois, S. Déléris, and Y. Comeau (2014). Characterization and separation of unbiodegradable matter in WRRFs. In *4th IWA/WEF Wastewater Treatment Modelling Seminar; WWTmod2014; 30 March - 2 April; Spa, Belgium*.

Marsalek, J., B. Krishnappan, K. Exall, Q. Rochfort, and R. Stephens (2006). An elutriation apparatus for assessing settleability of combined sewer overflows (CSOs). *Water Science and Technology 54*(6-7), 223–230.

Maruéjouls, T., P. Lessard, and P. Vanrolleghem (2014). Calibration and validation of a dynamic model for water quality in combined sewer retention tanks. *Urban Water Journal 11*(8), 668–677.

Maruéjouls, T., P. Lessard, and P. A. Vanrolleghem (2015). A particle settling velocity-based integrated model for dry and wet weather wastewater quality modeling. In *WEF Collection Systems Conference; April 20 - 22, Cincinnati, OH, USA*, pp. 19–22.

Maruejouls, T., P. Lessard, B. Wipliez, G. Pelletier, and P. Vanrolleghem (2011). Characterization of the potential impact of retention tank emptying on wastewater primary treatment: a new element for CSO management. *Water Science and Technology 64*(9), 1898–1905.

Maruéjouls, T., P. A. Vanrolleghem, G. Pelletier, and P. Lessard (2012). A phenomenological retention tank model using settling velocity distributions. *Water Research 46*(20), 6857–6867.

Maruéjouls, T., P. A. Vanrolleghem, G. Pelletier, and P. Lessard (2013). Characterisation of retention tank water quality: Particle settling velocity distribution and retention time. *Water Quality Research Journal of Canada 48*(4), 321–332.

McNamara, B., M. Sherony, and P. Herrick (2014). Relative performance of grit removal systems. In *87th Water Environment Federation Technical Exhibition and Conference; WEFTEC2014; 27 September – 1 October, New Orleans, Louisiana USA.*

McNamara, B. F., C. Bott, M. Hyre, D. Kinnear, and J. Layne (2012). How to baffle a vortex. In *85th Water Environment Federation Technical Exhibition and Conference; WEFTEC2012; 29 September - 3 October, New Orleans, LA, USA.*

McNamara, B. F., J. Griffiths, and D. Book (2009). True grit. a grit removal efficiency investigation at five wastewater treatment plants. In *82nd Water Environment Federation Technical Exhibition and Conference; WEFTEC2009; 10 -14 October, Orlando, FL, USA*, pp. 6160–6169.

McNamara, B. F., J. Layne, M. Hyre, D. J. Kinnear, and C. B. Bott (2012). Evaluation of three full-scale grit removal processes using CFD modeling. In *85th Water Environment Federation Technical Exhibition and Conference; WEFTEC2012; 29 September - 3 October, New Orleans, LA, USA.*

Michelbach, S. and C. Wöhrle (1993). Settleable solids in a combined sewer system, settling characteristics, heavy metals, efficiency of storm water tanks. *Water Science and Technology 27*(5-6), 153–164.

modelEAU (2015). *Standard Operating Procedure - Test traceur avec Rhodamine WT* (1 ed.). Université Laval. Québec, QC, Canada. (In French).

Montgomery, D. (2008). *Introduction to Statistical Quality Control* (6 ed.). Wiley. Hoboken, NJ, USA.

Morales, L. and D. Reinhart (1984). Full-scale evaluation of aerated grit chambers. *Journal of the Water Pollution Control Federation 56*(4), 337–343.

Mourad, M. and J.-L. Bertrand-Krajewski (2002). A method for automatic validation of long time series of data in urban hydrology. *Water Science and Technology 45*(4-5), 263–270.

Munoz, A. and S. Young (2009). Two-dimensional model for predicting performance of aerated grit chambers. *Canadian Journal of Civil Engineering 36*(9), 1567–1578.

O'Connor, T. P., D. Fischer, R. Field, J. Cigana, B. Gagné, and M. Couture (2002). Testing solids settling apparatuses for design and operation of wet-weather flow solids-liquids separation processes. Technical report, U.S. Environmental Protection Agency, National Risk

Management Research Laboratory, Office of Research and Development, Cincinnati, OH, USA.

Osei, K. and R. Andoh (2008). Optimal grit removal and control in collection systems and at treatment plants. In *World Environmental and Water Resources Congress, Honolulu, HI, USA*, pp. 12–16.

Osei, K., A. Gwinn, and R. Y. G. Andoh (2012). Development of a column to measure settling velocity of grit. In *World Environmental and Water Resources Congress 2012, Crossing Boundaries; May 20-24, Albuquerque, NM, USA*, pp. 1327–1333. ASCE.

Osei, K., A. Mody, and R. Andoh (2010). Field assessment of grit removal systems. In *World Environmental and Water Resources Congress, Providence, RI, USA*, pp. 12–16.

Otterpohl, R. and M. Freund (1992). Dynamic models for clarifiers of activated sludge plants with dry and wet weather flows. *Water Science and Technology 26*(5-6), 1391–1400.

Pitman, A. (1999). Management of biological nutrient removal plant sludges—change the paradigms? *Water Research 33*(5), 1141–1146.

Plana, Q. (2015). Automated data collection and management at enhanced lagoons for wastewater treatment. Master's thesis, Université Laval. Québec, QC, Canada.

Plana, Q., J. Carpentier, F. Tardif, A. Pauléat, A. Gadbois, P. Lessard, and P. A. Vanrolleghem (2017). Influence of sample pretreatment and weather conditions on grit characteristics. In *90th Water Environment Federation Technical Exhibition and Conference; WEFTEC2017; 30 September - 4 October, Chicago, IL, USA*, pp. 2108–2113.

Plana, Q., J. Carpentier, F. Tardif, A. Pauléat, A. Gadbois, P. Lessard, and P. A. Vanrolleghem (2018). Grit particle characterization: influence of sample pretreatment and sieving method. *Water Science and Technology 78*(6), 1400–1406.

Pretorius, C. F. (2012). A review of vortex grit basin design. In *85th Water Environment Federation Technical Exhibition and Conference; WEFTEC2012; 29 September - 3 October, New Orleans, LA, USA*, pp. 5715–5734.

Primodal (2019). Primodal RSM30. http://primodal.com/. Accessed: 2019-07-08.

Qasim, S. R. (1999). *Wastewater Treatment Plants: Planning, Design, and Operation* (2nd ed.). Routledge. London, UK.

Rasmussen, M. R. and T. Larsen (1996). A method for measuring sludge settling characteristics in turbulent flows. *Water Research 30*(10), 2363–2370.

Rauch, W., J.-L. Bertrand-Krajewski, P. Krebs, O. Mark, W. Schilling, M. Schütze, and P. A. Vanrolleghem (2002). Deterministic modelling of integrated urban drainage systems. *Water Science and Technology 45*(3), 81–94.

Reddy, M. P. and K. Pagilla (2009). Integrated methods for wastewater treatment plant upgrading and optimization. Technical report, Water Environment Research Foundation, Alexandria, VA, USA; and IWA Publishing, London, UK.

Ribes, J., J. Ferrer, A. Bouzas, and A. Seco (2002). Modelling of an activated primary settling tank including the fermentation process and vfa elutriation. *Environmental Technology 23*(10), 1147–1156.

Rieger, L., S. Gillot, G. Langergraber, T. Ohtsuki, A. Shaw, I. Takacs, and S. Winkler (2012). *Guidelines for Using Activated Sludge Models*. Scientific and Technical Report Series. IWA Publishing, London, UK.

Rieger, L. and P. A. Vanrolleghem (2008). monEAU: A platform for water quality monitoring networks. *Water Science and Technology 57*(7), 1079–1086.

Rife, J. C. and L. Botero (2012). Last of the neglected treatment processes: Rewriting the manual of practice No. 8 section on grit removal. In *85th Water Environment Federation Technical Exhibition and Conference; WEFTEC2012; 29 September - 3 October, New Orleans, LA, USA*, pp. 581–587.

Rippon, D., R. R. Higgins, and R. S. Mrkvicka (2010). Grit characterization and the impact on grit removal systems. In *83rd Water Environment Federation Technical Exhibition and Conference; WEFTEC2010; 2 - 6 October, New Orleans, LA, USA*, pp. 5963–5989.

Sawicki, J. M. (2004). Aerated grit chambers hydraulic design equation. *Journal of Environmental Engineering 130*(9), 1050–1058.

s::can (2019). s::can senosrs. https://www.s-can.at/. Accessed: 2019-07-09.

Seifried, C., M. Showalter, and M. Goodin (2013). Aerated grit tank improved using CFD modeling techniques. In *86th Water Environment Federation Technical Exhibition and Conference; WEFTEC2013; 5 - 9 October, Chicago, IL, USA*, pp. 2400–2418.

Sherony, M. and P. Herrick (2015). You don't know what you're missing: Designing a grit removal system that works. *Florida Water Resources Journal January*, 48–53.

Sin, G., D. J. De Pauw, S. Weijers, and P. A. Vanrolleghem (2008). An efficient approach to automate the manual trial and error calibration of activated sludge models. *Biotechnology and Bioengineering 100*(3), 516–528.

Sober, J., A. Gwinn, C. Ortiz, R. Correa, and M. Sherony (2018). Grit settling velocity: A visual comparison of clean sand and wastewater grit. In *91st Water Environment Federation Technical Exhibition and Conference; WEFTEC2018; 29 September - 3 October, New Orleans, LA, USA*, pp. 2692–2698.

Sprenger, J., K. Tondera, and V. Linnemann (2016). Determining fine suspended solids in combined sewer systems: Consequences for laboratory analysis. In *9th Novatech International Conference; June 28 - July 1, 2016; Lyon, France.*

Takács, I., G. G. Patry, and D. Nolasco (1991). A dynamic model of the clarification-thickening process. *Water Research 25*(10), 1263–1271.

Tchobanoglous, G., F. Burton, and H. Stensel (2003). *Wastewater Engineering : Treatment and Reuse* (4th ed.). Metcalf and Eddy. McGraw-Hill Education. New York, NY, USA.

Tchobanoglous, G. and E. Schroeder (1985). *Water Quality: Characteristics, Modeling, Modification.* Addison-Wesley Series on Water Quality Management. Addison-Wesley. Indianapolis, IN, USA.

Tchobanoglous, G., H. D. Stensel, R. Tsuchihashi, F. L. Burton, M. Abu-Orf, G. Bowden, and W. Pfrang (2014). *Wastewater Engineering : Treatment and Resource Recovery* (5th ed.). Metcalf and Eddy. McGraw-Hill Education. New York, NY, USA.

Teefy, S. (1996). *Tracer Studies in Water Treatment Facilities: a Protocol and Case Studies.* American Water Works Association. Denver, CO, USA.

Tik, S. (2019). *Gestion intégrée d'un système d'assainissement urbain: contrôle basé sur la qualité des eaux et strategies tolérantes aux fautes.* Ph. D. thesis, Université Laval, Québec, QC, Canada. In preparation. (In French).

Tik, S., T. Maruéjouls, G. Bachis, B. Vallet, P. Lessard, and P. A. Vanrolleghem (2014). Using particle settling velocity distributions to better model the fate of stormwater TSS throughout the integrated urban wastewater system. *Influents Winter 2014*, 48–52.

Tik, S. and P. A. Vanrolleghem (2017). Chemically enhancing primary clarifiers: Model-based development of a dosing controller and full-scale implementation. *Water Science and Technology 75*(5), 1185–1193.

Tyack, J. and R. Fenner (1999). Computational fluid dynamics modelling of velocity profiles without a hydrodynamic separator. *Water Science and Technology 39*(9), 169–176.

Tyack, J., P. Hedges, and R. Smisson (1993). A device for determining the settling velocity grading of storm sewage. In *Proceedings, 6th International Conference on Urban Storm Drainage, Niagara Falls, ON, Canada*, pp. 1805–1810.

U.S. EPA (2004). Screening and grit removal. Technical report, U.S. Environmental Protection Agency, Washington, DC, USA.

Vallet, B., D. Muschalla, P. Lessard, and P. Vanrolleghem (2014). A new dynamic water quality model for stormwater basins as a tool for urban runoff management: Concept and validation. *Urban Water Journal 11*(3), 211–220.

Vanhooren, H., J. Meirlaen, Y. Amerlinck, F. Claeys, H. Vangheluwe, and P. A. Vanrolleghem (2003). WEST: Modelling biological wastewater treatment. *Journal of Hydroinformatics 5*(1), 27–50.

Verbanck, M. (1995). Variabilité des charges solides en suspension à l'exutoire des réseaux de collecte. *Journée d'etude CB-IAWQ, , 31 May 1995, Liège, Belgium 31.* (In French).

Walling, D. and J. Woodward (1993). Use of a field-based water elutriation system for monitoring the in situ particle size characteristics of fluvial suspended sediment. *Water Research 27*(9), 1413–1421.

WEF (2010). *Design of Municipal Wastewater Treatment Plants: Manual of Practice 8* (5th ed.). WEF Manual of Practice and ASCE Manual and Report on Engineering Practice. McGraw-Hill Education. Alexandria, VA, USA. Water Environment Federation.

WEF (2012). *Clarifier Design. Manual of Practice No. FD-8* (2nd ed.). McGraw-Hill Education. Alexandria, VA, USA. Water Environment Federation.

WEF (2016). *Guidelines of Grit Sampling and Characterization.* Water Environment Federation. Alexandria, VA, USA.

White, F. (2011). *Fluid Mechanics.* McGraw-Hill series in Mechanical Engineering. McGraw Hill. New York, NY, USA.

Wicklein, E., D. J. Batstone, J. Ducoste, J. Laurent, A. Griborio, J. Wicks, S. Saunders, R. Samstag, O. Potier, and I. Nopens (2016). Good modelling practice in applying computational fluid dynamics for WWTP modelling. *Water Science and Technology 73*(5), 969–982.

Wilson, G., G. Tchobanoglous, and J. Griffiths (2007). *The Grit Book.* Hydro International. Hillsboro, OR, USA.

Wong, T. H., T. D. Fletcher, H. P. Duncan, and G. A. Jenkins (2006). Modelling urban stormwater treatment—a unified approach. *Ecological Engineering 27*(1), 58–70.

WTW (2019). WTW sensors. https://www.wtw.com/en/. Accessed: 2019-07-09.

Yoo, C. K., K. Villez, S. W. Van Hulle, and P. A. Vanrolleghem (2008). Enhanced process monitoring for wastewater treatment systems. *Environmetrics 19*(6), 602–617.

Appendix A

Flow reconstruction model

Data required

For the flow reconstruction model, three input files for the same period of time are needed:

- Time series of the hourly inlet flow
- Time series of the on-line temperature measurements every 10 seconds
- Time series of the on-line conductivity measurements every 10 seconds

Also, four model parameters have to be defined. For this case study:

- The pump flow: $Q_{pump} = 810\ m^3/h$
- The time step for the time series of the inlet flow to be generated: $dt = 0.0028\ h = 10\ s$
- Detection limit for the temperature derivation: $L_T = 0.025\ h$
- Detection limit for the conductivity derivation: $L_C = 0.002\ h$

Model description

The procedure followed to simulate the flow at high resolution is:

1. Data set definition of the desired period, i.e. hourly inlet flow, and on-line high frequency data of temperature and conductivity
2. Model parameters definition

3. At each time step, estimate the slope of the temperature (S_T) and conductivity (S_C) data series

4. For each time step (every 10 seconds, same time step as for the temperature and conductivity data), determine when the pump is on or off:

   a) Summer time

      i. When $S_{T,t} \geq L_T$ and $S_{T,t-1} < L_T$, or $S_{C,t} \leq L_C$ and $S_{C,t-1} > L_C$ $\Rightarrow$ The pump turns on

      ii. When $S_{T,t} \leq L_T$ and $S_{T,t-1} > L_T$, or $S_{C,t} \geq L_C$ and $S_{C,t-1} < L_C$ $\Rightarrow$ The pump turns off

   b) Winter time

      i. When $S_{T,t} \geq L_T$ and $S_{T,t-1} < L_T$, or $S_{C,t} \geq L_C$ and $S_{C,t-1} < L_C$ $\Rightarrow$ The pump turns on

      ii. When $S_{T,t} \leq L_T$ and $S_{T,t-1} > L_T$, or $S_{C,t} \leq L_C$ and $S_{C,t-1} > L_C$ $\Rightarrow$ The pump turns off

5. Estimation for how long the pump has been on per hour

$$t_{pumping} = t_{stop} - t_{start} \tag{A.1}$$

6. Estimation of the hourly pumped volume

$$V_{pumped} = Q_{hour} * t_{pumping} \tag{A.2}$$

7. Estimation of the hourly free flow

$$Q_{free} = Q_{hour} * V_{pumped} \tag{A.3}$$

8. Estimation of the pumped flow every 10 seconds:

   a) When the pump is on: $Q_{pumped} = Q_{pump}$

   b) When the pump is off: $Q_{pumped} = 0$

Matlab code for flow reconstruction

```
function [Q1,Q2,Qtot] = Qhor2inst(Qhourly,Temp,Cond,Qpump,dt,L_T,
    L_C)
% INPUTS
% Qhor - Hourly flow measured at the WRRF [m3/h]
```

```
% Qpump - Flow of the pumpt to empty the basin [m3/h]
% Vbasin - Basin volume [m3]
% dt - Desired time step [h]

% Variables definition

thor = Qhourly(:,1);
Qhor = Qhourly(:,2);

t_T = Temp(:,1);
T = Temp(:,2); % Smootherd data for pump activations

t_C = Cond(:,1);
C = Cond(:,2); % Smootherd data for pump activations

% Create a new time series with smaller time step
t_dt = thor(1):dt:thor(end); % Create a new time series according
    to the defined time step, dt
Qhor_dt = interp1(thor,Qhor,t_dt); % Linear interpolation of the
    new data points Q(t) according to the new coordinates t_dt

% Estimate the slope of the T data
slope_T = movingslope(T,10,1);
slope_C = movingslope(C,10,1);

% Upper and Lower limits definition
UL_T = L_T; % Upper limit for T
LL_T = -L_T; % Lower limit for T
UL_C = L_C; % Upper limit for C
LL_C = -L_C; % Lower limit for C

% Calculation of the hourly free flow rate (Q1) and the hourly flow
     rate due to pump activations (Q2)
[Q2_in, Q1] = flowsplitter(thor,Qhor,Qpump,t_T,slope_T,slope_C,UL_T
    ,LL_T,UL_C,LL_C);

% Create a new time series with smaller time step
Q1_dt = interp1(thor(1:end-1),Q1,t_dt); % Linear interpolation of
    the new data points Q(t) according to the new coordinates t_dt
```

```
Q2_in_dt = interp1(thor(1:end-1),Q2_in,t_dt); % Linear
    interpolation of the new data points Q(t) according to the new
    coordinates t_dt

% Estimate inlet and outlet flow of the well (pumping station)
[Q2_out,V, pump_act] = Qin2Qout(t_dt,Q2_in_dt,Qpump,slope_T,slope_C
    ,UL_T,LL_T,UL_C,LL_C);

% Sum of the free flow and the pumped flow
Qtot = Q1_dt+Q2_out;

function [V_pumped, Qfree] = flowsplitter(thor,Qhor,Qpump,t_T,
    slope_T,slope_C,UL_T,LL_T,UL_C,LL_C)
% This functions aims to split the intlet flow coming into a WRRF
% from two different sewer systems:
% 1. flow pumped to the WRRF (Qpumped)
% 2. free flow (Qfree)

pump = [];
onepump = 0;

% Calculation of the free flow (Q1) and the flow due to pump
    activations (Q2)
for i = 2:length(t_T)
%      if ((slope_T(i) >= UL_T) && (slope_T(i-1) < UL_T)) || ((
    slope_C(i) >= UL_C) && (slope_C(i-1) < UL_C)) || (onepump == 1)
    % Winter time
     if (slope_T(i) >= LL_T) && (slope_T(i-1) < LL_T) || ((slope_C(i
         ) <= UL_C) && (slope_C(i-1) > UL_C)) || (onepump == 1) %
         Summer time
          onepump = 1;
     end
%      if (slope_T(i) <= LL_T) && (slope_T(i-1) > LL_T) || (slope_C(
    i) <= LL_C) && (slope_C(i-1) > LL_C) || (onepump == 0) % Winter
    time
     if ((slope_T(i) <= UL_T) && (slope_T(i-1) > UL_T)) || (slope_C(
         i) >= LL_C) && (slope_C(i-1) < LL_C) || (onepump == 0) %
         Summer time
         onepump = 0;
```

```
    end
        pump(i,1) = onepump;
end

h = 1;

for i = 1:length(thor)-1
    p = 1;
    idx_ini = find(round(t_T, 9) == round(thor(i),9));
    idx_fin = find(round(t_T, 9) == round(thor(i+1),9));
    t_p = [];
    t_diff = [];
    for j = idx_ini+1:idx_fin
        if (pump(j) == 1 && pump(j-1) == 0) || ((pump(j) == 1) && (j == idx_ini+1))
            t_p(p,1) = t_T(j); % when pump starts
        elseif (pump(j) == 0 && pump(j-1) == 1) || ((pump(j) == 1) && (j == idx_fin))
            t_p(p,2) = t_T(j); % when pump stops
            t_diff(p,1) = t_p(p,2)-t_p(p,1);
            p = p + 1;
        end
    end
    t_pumped(h,1) = sum(t_diff); % [d]
    h = h + 1;
end

V_pumped = Qpump .*24 .* t_pumped; % [m3 per day]

Qfree = Qhor(1:end-1) - V_pumped;%./24;

end

function [Qout,V, pump] = Qin2Qout(t,Qin,Qpump,slope_T,slope_C,UL_T,LL_T,UL_C,LL_C)
% This function estimates the pumping sequences
% i.e. the pumped flow
n = length(t);
V(1:n) = 0;
```

```
Qout(1:n) = 0;
pump = [];
twopump =0;
onepump = 0;
for i = 2:n
%        if ((slope_T(i) >= UL_T) && (slope_T(i-1) < UL_T)) || ((slope_C(i) >= UL_C) && (slope_C(i-1) < UL_C)) || (onepump == 1) % Winter time
      if (slope_T(i) >= LL_T) && (slope_T(i-1) < LL_T) || ((slope_C(i) <= UL_C) && (slope_C(i-1) > UL_C)) || (onepump == 1) % Summer time
          Qout(i) = Qpump;
          onepump = 1;
          if (Qin(i) > Qout(i)) || twopump == 1 %V(i-1) > V(i-2) || twopump == 1
              Qout(i) = 2*Qpump;
              twopump = 1;
          end
      end
%        if (slope_T(i) <= LL_T) && (slope_T(i-1) > LL_T) || (slope_C(i) <= LL_C) && (slope_C(i-1) > LL_C) % Winter time
      if ((slope_T(i) <= UL_T) && (slope_T(i-1) > UL_T)) || (slope_C(i) >= LL_C) && (slope_C(i-1) < LL_C) % Summer time
         Qout(i) = 0;
         onepump = 0;
         twopump = 0;
      end
          V(i) = V(i-1) + (Qin(i) - Qout(i))* (t(i) - t(i-1));
          pump(i,:) = [onepump twopump];
end

end

end
```

Appendix B

Hydraulic modelling of the vortex grit chamber

As mentioned in Section 7.2.2, two tracer tests were performed to determine the hydraulics behaviour of the full-scale vortex system (i.e. characterization of the mixing and the internal transport processes in the unit). These tracer tests consisted in a pulse injection of the tracer substance (Dirac pulse). About 8 g of a 21.4 % solution of Rhodamine WT were injected into the inlet channel just after the screens (see Figure 3.4). The responses obtained from both tracer tests are presented at Section 7.2.2.

In both tracer tests, a fast response of the system is observed together with a slow response. This fast response suggests that there may be a short-circuit into the unit and suggests that there are two flow tracks through the grit chamber. From this idea, a hydraulic model was proposed after testing several configurations in terms of number of tanks in series for both flow tracks, the volume of the tanks and the fraction of the short-circuited flow. The configuration ultimately retained is presented in Figure B.1, where the fast track corresponds to the six tanks in series with a volume of 0.3 m^3 each and carrying 30% of the flow. The other 70% is passing through a a completely mix tank of 15 m^3 coinciding with the average occupied volume.

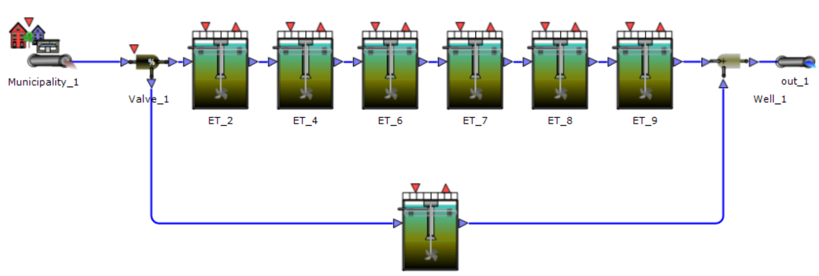

Figure B.1: Hydraulic model of the vortex grit chamber.

With the configuration presented in Figure B.1, the tracer concentration at the outlet was simulated for both tracer tests (see Figures B.2 and B.3). For the first tracer test, an averaged flow from the measured flows at the beginning and at the end of the test was considered for the simulation. In case of the second tracer test, the detailed recorded inflow during the test was used for it.

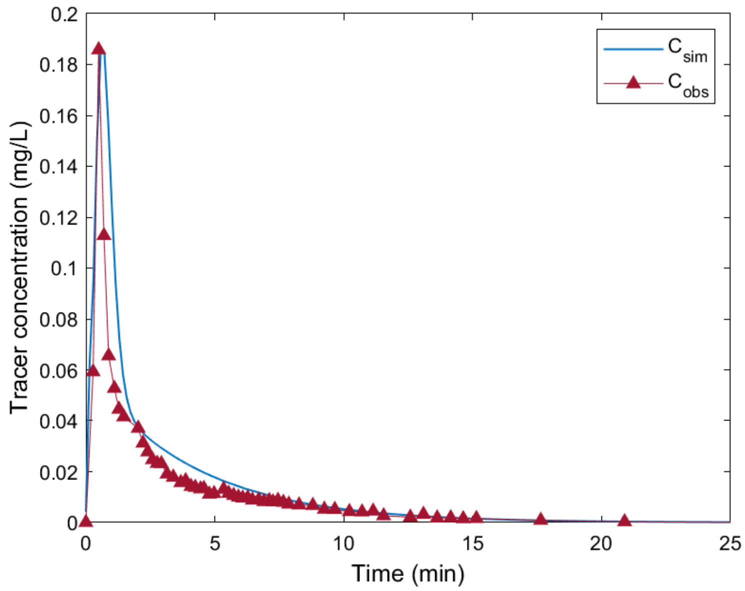

Figure B.2: Simulated and observed tracer concentrations for the first tracer test.

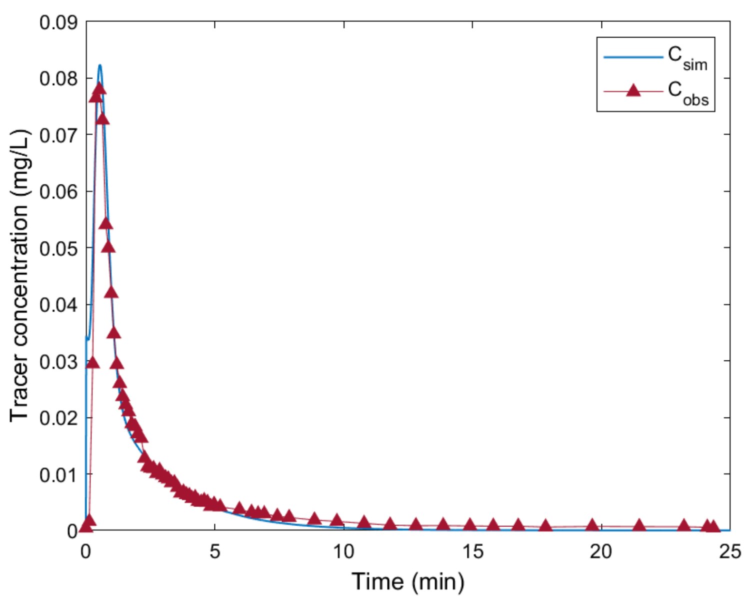

Figure B.3: Simulated and observed tracer concentrations for the second tracer test.

Since the simulated tracer concentration fits nicely to the observed data for both tracer tests, the presented hydraulic configuration was accepted. Hence, this hydraulic model was coupled to the PSVD model and recalibrated with the second tracer test as presented in Section 7.3.3.